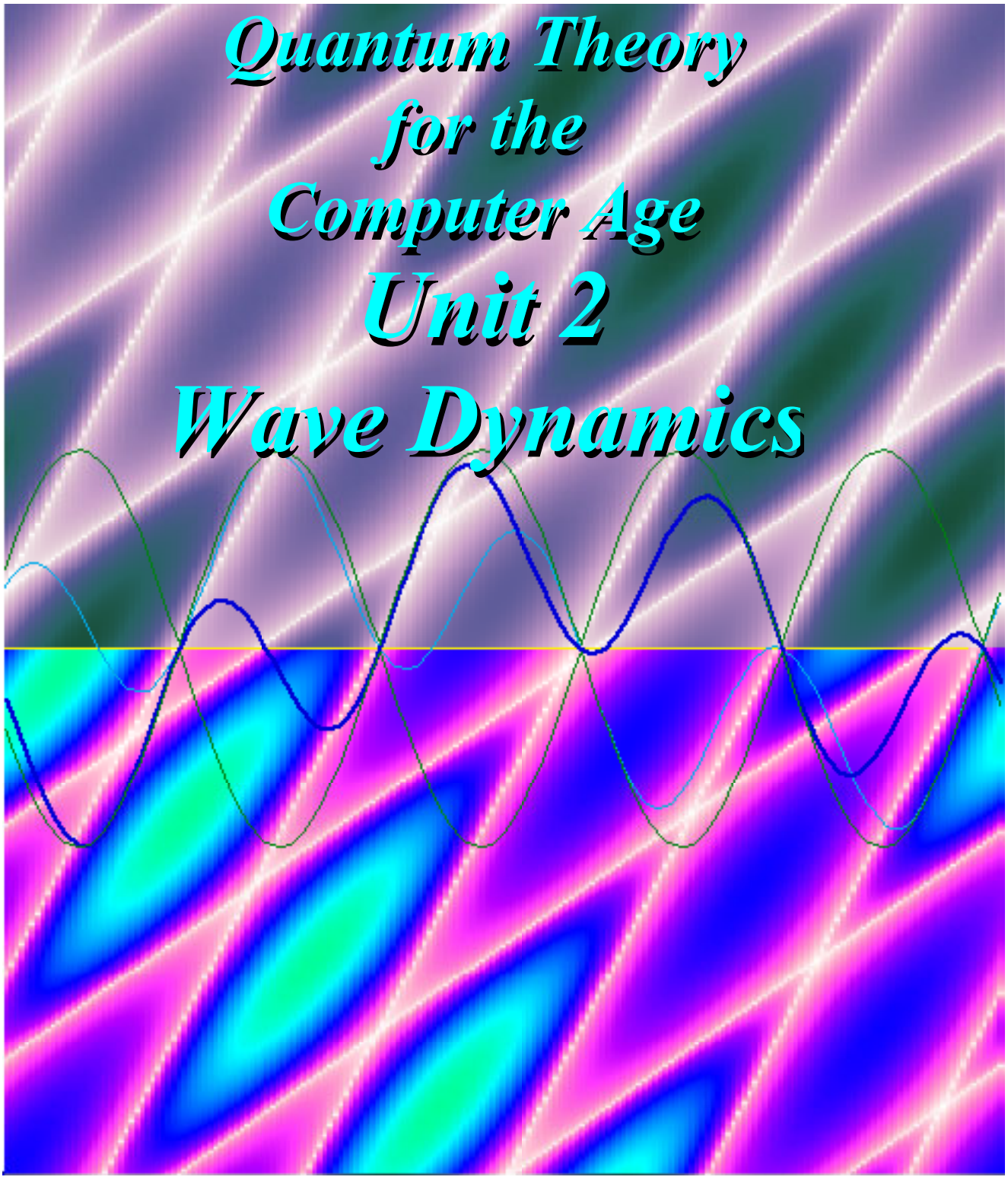
Quantum Theory
for the
Computer Age
Unit 2
Wave Dynamics

Unit 2 Wave Dynamics

Unit 1 used the two states of electromagnetic wave polarization as an introduction to quantum theory but did not consider the propagation of such a wave through space. In Unit 2, wave phase properties in space and time (spacetime) are examined by combining spacetime with wavevector and frequency (per-spacetime) pictures.
A clear understanding of interference properties of light (or γ-waves) leads to simple geometric and algebraic derivations of the special theory of relativity for spacetime and per-spacetime in Chapter 4. In Chapter 5, the per-spacetime theory leads to similar derivations of the dispersion properties of "matter waves" (or μ-waves) and to fundamental ideas of relativistic and non-relativistic quantum theory. Concepts of energy, momentum, mass, acceleration and inertia are seen to arise from quite simple quantum wave interference effects. Wave propagation and modes in two or three dimensions are examined in Chapter 6.

W. G. Harter
Department of Physics
University of Arkansas
Fayetteville

Hardware and Software by

HARTER-*Soft*
Elegant Educational Tools Since 2001

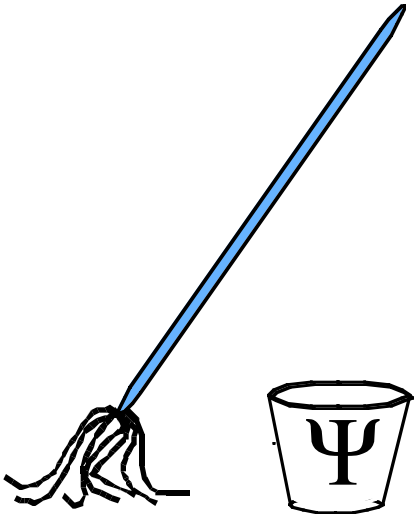

QM for AMOP

Chapter 4
Waves in Space and Time

W. G. Harter

Wave propagation along a line is analyzed using complex functions, phasors, and space-time diagrams for waves having only one or two frequency components and a single dimension of amplitude. (For em-waves: only a single polarization plane.) Ch. 4 includes a derivation of phase velocity, group velocity, standing-wave-ratio, Doppler shift (for em-waves) and the Lorentz transformation theory of special relativity as a result of wave interference. With only two frequency components, a waves-on-line-system is effectively a two-state system and analogous to the 2-state systems introduced in Unit 1. A further analogy, which will be exploited many times in this book, is introduced between optical polarization and waves-on-a-ring

UNIT 2 WAVE DYNAMICS 1

CHAPTER 4. WAVES IN SPACE AND TIME 1

4.1 Discrete vs. Continuous: Function Space 3
(a) State vectors vs. wavefunctions: Dirac delta functions 4
(b) Probability and count rates for continuum states 5

4.2 Wavefunctions, Wave Velocity, and Wave Visualization 6
(a) Complex amplitudes and phasor clocks 6
What are we in for? (We really don't know waves at all.) 7
(b) Wave antomy: Expo-trig identites 8
Visualizing Complex Wave Amplitudes and Phasors by WaveIt 8
Phase velocity 11
Group velocity 13
Wave lattice paths in space and time 13
Particle or pulse lattice paths in space and time 15
Spacetime lattices collapse for co-propagating optical waves 15

4.3 When Lightwaves Collide: Relativity of Spacetime 17
(a) The colorful relativity axiom: Using Occam's razor 17
Relativity by interfering counter-propagating laser waves 18
(b) How'd we get relativity so quickly? Follow the zeros! 21
Phase invariance: Keep the phase! 21
Colorful Relativitistic logic: Simpler or not? 23
(c) Phase invariance in spacetime (x,ct) or per-spacetime (ck,ω) plots 23
(d) Pulsed Wave (PW) and "particle" paths *versus* Continuous Wave (CW) laser 27
The "Now" line(s) 27

4.4 Geometry and Invariance in Lorentz transformations 28
(a) Geometric construction of relativistic variables 30
Lorentz contraction and aberration angle 31
Lorentz-Einstein factors 31
Doppler factors 31
Coordinate lines and invariants for waves or pulses: Baseball diamond geometry 33
(b) Comparing Circular and Hyperbolic Functions 35

4.5. When Lightwaves Dance: Superluminal phase 37
(a) Galloping waves and Standing Wave Ratio (SWR) 37
(b) Kepler's Law for galloping 39
Analogy with polarization ellipsometry 39
(c) SWR algebra and geometry 41
Analogy between complex waves and polarization: Stadium circumference waves 41

4.6 When Lightwaves Go Crazy: Spacetime switchbacks 45
(a) Wobbly and switchback waves 45

4.7 Co-vs.-Counter propagating waves: Modulation and Beats 47
(a). Time modulation: Beats 49
Analogy with Faraday polarization rotation 50
(b). Group velocity for continuous waves 51
(c). Counter-versus-co propagating waves 51

Problems for Chapter 4 53

.

Unit 2 Wave Dynamics
Chapter 4. Waves in Space and Time

Having introduced quantum amplitudes in Unit 1 using mostly two-state systems, we now introduce infinite-state wave systems. Quite a jump! It would be nice if we could just take our *(n=2)*-state quantum mechanics and gradually increase *n* to infinity ($n \to \infty$) and hope to see the limiting case. What makes this particularly difficult is that mathematics has two kinds of infinities; there is the comparatively tame *discrete or denumerable infinity* and then there is the much wilder *continuous or non-denumerable infinity*.

It is the latter that has been used by physicists since the development of differential and integral calculus. It provides us with the tools of real analysis, complex variables, and modern functional analysis. The idea of a real variable *x* or complex variable *z* that can assume arbitrary floating-point values (as opposed to only integer values) is so ingrained in our mathematical physics that few can carry on an intelligent conversation without using these continuum concepts.

The object of the next two units is to show how infinite-state quantum systems, even the continuously infinite state systems can be managed using the same sort of Dirac bra-ket and operator mathematics introduced in Unit 1. This accomplishes two things. First, it allows the vast literature base of quantum mechanics to be more easily read and understood. Second, it points out several approaches to numerical simulations of quantum systems on digital computers.

Before beginning this discussion, a word of caution is offered. It is entirely possible that two or three hundred years of continuum mathematics is, for the physicist, like a kind of drug that has hampered us from seeing nature as it really is. The idea that space-time is continuous without limit down to arbitrarily small sizes is being seriously challenged by various grand-unification schemes. The notion of the "point-particle" is also questioned. It is proposed that "elementary" particles are tiny vibrating "strings." Such speculation still lack evidence but the questioning is by itself encouraging.

Also, on a more practical note, no digital computer is capable of truly simulating a continuum, or, for that matter, any kind of infinity. Even floating point numbers are stored as discrete binary integers whose size of mantissa and exponent is limited by size of registers. Also, time simulations and space-time plots are series of discrete steps and pixels that only appear to be continuous because the machinery has become so fast and fine. It might be hoped that analog computers are better realizations of a continuum (forgetting for a moment that their currents and voltages are quantized) but, unfortunately, analog accuracy is far less than digital precision because of thermal noise. So called "quantum computers" have been imagined, but it remains to be seen what form and function these will take.

It helps to approach any comparison of continuous functional analysis and discrete vector analysis by imagining that we need to simulate and store the various mathematical objects as realistically as possible on a standard digital computer. Continuum calculus and analysis have been and will probably always continue to be wonderful tools for discovering certain model approximations, but an increasing number of problems require computer synthesis in order to make consistently accurate predictions.

A Time and Frequency Hero – Ken Evenson (1932-2002)

When US soldiers punch up their GPS coordinates they may owe their lives to an under sung hero and his students who toiled 18-hour days deep inside labs lit only by the purest light in the universe.

Let me introduce an "Indiana Jones" of modern physics. While he may never have been called "Montana Ken," such a name would describe a real life hero from Boseman, MT, whose accomplishments far surpass, in many ways, the fictional character in *Raiders of the Lost Arc* and other cinematic thrillers.

Indeed, I know of a real life moment shared by his wife Vera, when Ken was in a canoe literally inches from the hundred-foot drop-off of Brazil's largest waterfall. But, such outdoor exploits, of which Ken had many, pale in the light of an in-the-lab brilliance and courage that profoundly enriched the world.

Ken is one of few, if not the only physicist to be listed twice in the *Guinness Book of Records*. It was not for jungle exploits but for the highest frequency measurements and speed of light determination that made quantum optics many times more precise.

The meter-kilogram-second (mks) system of units underwent a redefinition largely because of Ken's efforts. Thereafter c was defined as $299,792,458$ and the meter was defined in terms of c, instead of the other way around. Time and frequency precision trumped that of distance. Without such resonance precision, the Global Positioning System (GPS) would be impossible.

Ken's courage and persistence at the Time and Frequency Division of the Boulder Laboratories in the National Bureau of Standards (now the National Institute of Standards and Technology or NIST) are legendary as are his railings against boneheaded administrators trying to thwart his efforts. By painstakingly exploiting the resonance properties of metal-insulator diodes, Ken's lab succeeded in literally counting the waves of 200 THz near-infrared radiation and eventually, visible light itself.

4.1 Discrete vs. Continuous: Function Space

Let us first compare a finite *discrete* and *bounded* *n*-state system (the easiest of all possible mathematical worlds!) to an ∞-state system of the worst kind, which is a *continuous* and *unbounded* system. The discrete and bounded system is indexed by state *index* numbers *a = 1, 2, 3, ..., n,* which are discrete ("quantized") and bounded by a lowest number (*1*) and a highest number (*n*). Meanwhile, the continuous (shall we say "indiscreet") and unbounded system is indexed by a real variable *x* which ranges from *x* = -∞ to *x* = + ∞,and isn't bounded at all as sketched in the upper part of Fig. 4.1.1.

Imagine that the real variable *x* stands for a "particle" position coordinate on the *x*-axis. (The ubiquitous quantum "particle" concept arises again. You are free to substitute the words "electron" or "photon" if that helps any.) The idea is that you could install particle counters at arbitrary x-positions and wait for counts. Clearly, we cannot afford an infinite number of counters, much less an unbounded continuum of them; we're probably lucky just to have one or two left over from our 2-state experiments. So it appears this theory is already in hot water before we even get started. But, let's proceed anyway.

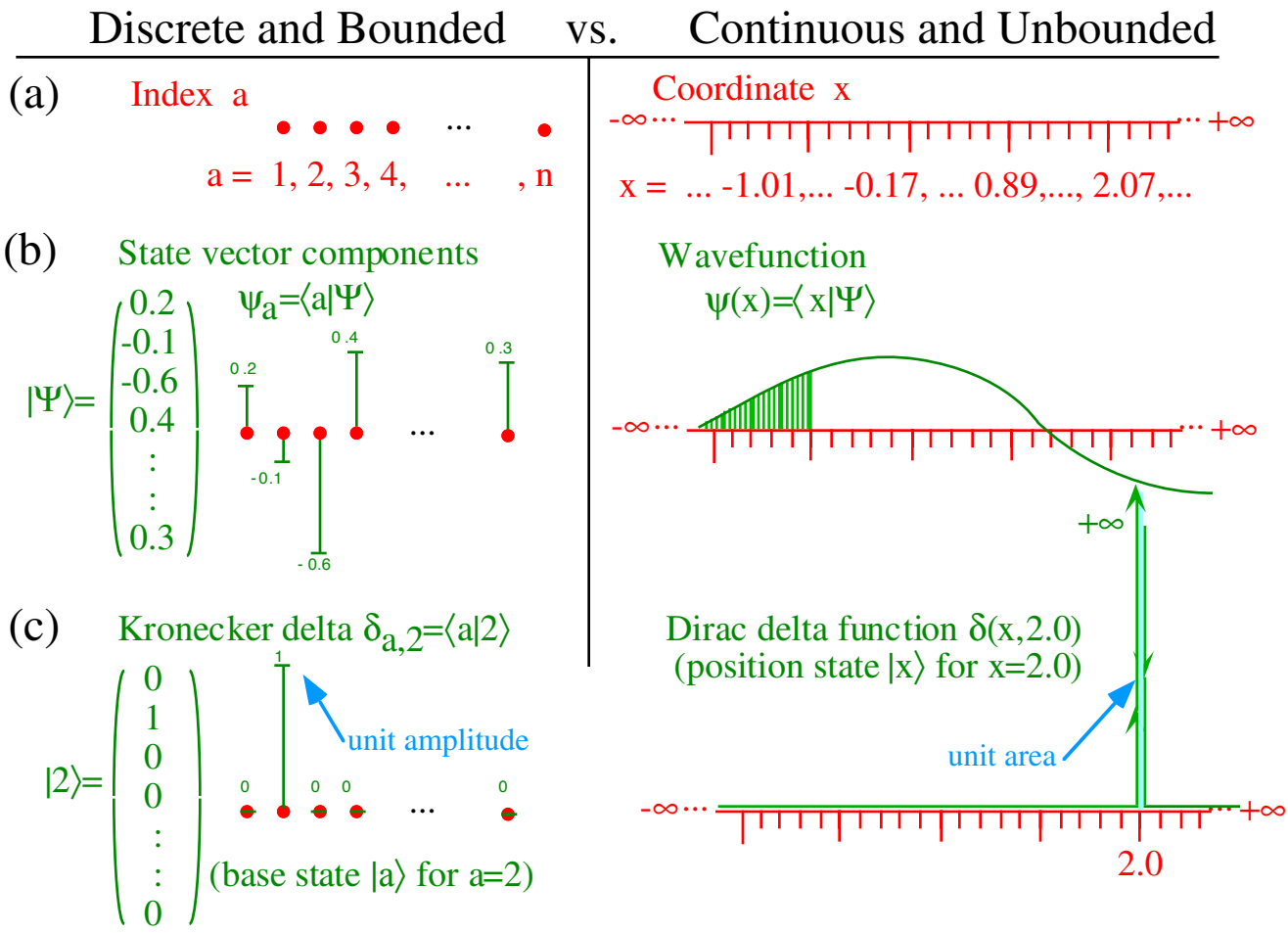

Fig. 4.1.1 Comparison of discrete state space versus continuum wavefunction

(a) State vectors vs. wavefunctions: Dirac delta functions

Fig. 4.1.1 sketches the relation between state vectors in discrete n-state systems and wavefunctions in continuous ∞-state systems. A discrete state $|\Psi\rangle$ is defined by a list of n-numbers $\langle a|\Psi\rangle$ called *amplitudes*, one for each value $a = 1, 2, ..., n$ of an *index*. A continuous state $|\Psi\rangle$ is defined by an infinite list of numbers $\langle x|\Psi\rangle$ called a *wavefunction* $\psi(x)=\langle x|\Psi\rangle$, one for each value $-\infty<x<\infty$ of a *coordinate* x. Of course, if you plot a wavefunction on a computer (as is done in Fig. 4.2.1(b-right)) it will also be a finite list of points; at whatever *resolution* you choose.

As shown in Chapter 1 (Sec. 1.4(b)) each amplitude $\langle a|\Psi\rangle$ is written as a scalar product of the state $|\Psi\rangle$ vector with base bra $\langle a|$. By axiom-2 and 4 we may write

$$\langle a|\Psi\rangle = \sum_{b=1}^{n} \langle a|b\rangle\langle b|\Psi\rangle = \sum_{b=1}^{n} \delta_{ab}\langle b|\Psi\rangle. \tag{4.1.1a}$$

This is a sum involving the *Kronecker delta symbol* $\delta_{a,b}$.

$$\langle a|b\rangle = \delta_{ab} = \begin{Bmatrix} 1 \text{ if: } a = b \\ 0 \text{ if: } a \neq b \end{Bmatrix} \tag{4.1.1b}$$

A common shorthand notation for the sum is the following.

$$\Psi_a = \sum_{b=1}^{n} \delta_{ab}\Psi_b \tag{4.1.1c}$$

Now a similar construction is defined for continuous systems, only each sum is replaced by an integral so (4.1.1a) becomes

$$\langle x|\Psi\rangle = \int_{-\infty}^{\infty} dy\langle x|y\rangle\langle y|\Psi\rangle = \int_{-\infty}^{\infty} dy\,\delta(x,y)\langle y|\Psi\rangle \tag{4.1.2a}$$

This integral involves the *Dirac delta function* $\delta(x,y)=\delta(x-y)$.

$$\langle x|y\rangle = \delta(x,y) = \begin{Bmatrix} \infty \text{ if: } x = y \\ 0 \text{ if: } x \neq y \end{Bmatrix} = \delta(x-y) = \delta(y-x) \tag{4.1.2b}$$

A common shorthand notation for the integral is the following.

$$\Psi(x) = \int_{-\infty}^{\infty} dy\,\delta(x-y)\Psi(y) \tag{4.1.2c}$$

An attempt to plot the Dirac delta function is shown in Fig. 4.1.1(c-right) by showing a "spike" function with unit area, zero base and infinite height. This is a tall order, indeed. It is based upon the requirement that expansion (4.1.2c) be valid for a unit function $\Psi(x) = 1$.

$$1 = \int_{-\infty}^{\infty} dy\,\delta(x-y)\cdot 1 = \int_{-\infty}^{\infty} dx\,\delta(x-y)\cdot 1 \tag{4.1.3}$$

The comparable discrete version is much easier to picture.

$$1 = \sum_{b=1}^{n} \delta_{ab}\cdot 1 = \sum_{a=1}^{n} \delta_{ab}\cdot 1 \tag{4.1.4}$$

A Kronecker delta, like $\delta_{a,2}$ represents a particular base state, in this case, the state $|2\rangle$ for which the probability is 100% certain that the system will be found in state-2 if forced to choose from its basis of n-states $\{|1\rangle,|2\rangle,...,|n\rangle\}$. By analogy, a Dirac delta, such as $\delta(x-2.0)$ represent a coordinate base state $|x\rangle=|2.0\rangle$ for which the probability is 100% certain that the particle is exactly $x=2.0$.

(b) Probability and count rates for continuum states

Does a $|x\rangle$-position state exist? Only in theory. (Here is one more case where "theory" gets a bad name!) In fact, we shall see that it would cost more than all the energy in the universe to put a single electron at *exactly* $x=2$. Such precision is hardly worth the price. For less than *15 eV* (*1eV = 1.6E-19 J.*) you can locate an electron with a precision of one-tenth of a billionth of a meter. (A tenth of a nanometer or one *Angstrom (= 10^{-10} m)* is roughly the diameter of the hydrogen atom.)

A coordinate base state $|x\rangle$ with its Dirac delta representation (4.1.2b) is not a physically realizable state. This is unlike the discrete states of electron or optical polarization which achieve 100% occupation of a $|\uparrow\rangle$ or $|y'\rangle$ base state by just passing through a filter. There is a price of doing calculus with wavefunctions $\Psi(x)$ defined on a continuum. First, you have to deal with infinitesimals and limits and infinite or *unbounded norms* such as the $\langle x|y\rangle = \delta(x-y)$ in (4.1.2b).

Also, probability definitions must be made more flexible with continuum states. For discrete states, the norm of a state never exceeds $\langle\Psi|\Psi\rangle = 1$ which corresponds to 100% probability. Norms like $\langle x|x\rangle = \infty$ of continuum states are unbounded. Probability $\langle\Psi|\Psi\rangle$ easily exceeds 100% unless the definition of axiom-1 is rescaled to avoid this unphysical situation. A common solution to this problem is to let $|\Psi(x)|^2$ be the probability of finding a particle in a given unit of length, area, or volume so that the measured count rate R is given by a definite integral over the length, area, or volume of a counter.

$$R_{Line\,L} = \int_L dx|\Psi(x)|^2, \quad R_{Area\,A} = \iint_A dxdy|\Psi(x.y)|^2, \quad R_{Volume\,V} = \iiint_V dxdydz|\Psi(x,y,z)|^2. \quad (4.1.5)$$

Recall that time is regarded as a continuum, too. Even the simple 2-state experiments we mentioned in Ch. 1 have implicit time limits. (We can't wait forever for those counts!) The implicit per-unit-time is always part of any probability calculation for a quantum system, be it discrete or continuous. So the probability for getting one count or the expected number of counts in a piece of laboratory apparatus will be proportional to a space-time integral such as

$$P = \int_T dt \iiint_V dxdydz|\Psi|^2. \quad (4.1.6)$$

When calculus fails to produce analytic integrals we resort to computational approximations. For numerical calculations we must *coursegrain* or *discretize* the entire space (or space-time) occupied by a wavefunction. We imagine the space filled with hundreds, or thousands, or even millions of "bins" or "eyelets" each behaving as a discrete section of a very complex but perfect "do-nothing" analyzer. Then the simulated experiments begin. Each experiment corresponds to replacing one or more of the "eyelets" with counters or more subtle apparatus that responds to (and affects) the phase or amplitude in each bin. In this way, any system is reduced to one that is discrete and bounded, as infinite integrals become finite sums. Part of the artistry of quantum theory and experiment involves relating apparently infinite continua to finite and discrete lattices that may serve as practical approximations to the world.

4.2 Wavefunctions, Wave Velocity, and Wave Visualization

Complex numbers and functions are indispensable computational tools and visualization aids for the physics of waves and particularly for quantum wavefunctions. Some of these ideas are introduced.

(a) Complex amplitudes and phasor clocks

As we mentioned in Ch. 1 (Sec. 1.2(b)), an amplitude is a complex number in modern quantum theory. In the very simplest cases, which involve systems with a single (monochromatic) energy ε or frequency ω, these complex amplitudes have a Planck phase factor.

$$e^{-i\omega t} = \cos\omega t - i\sin\omega t \qquad (4.2.1)$$

The angular frequency $\omega=2\pi\nu$ or frequency ν is related by *Planck's constant* $h=2\pi\hbar=6.63E\text{-}34Js$

$$\varepsilon = h\nu = \hbar\omega\,, \qquad (4.2.2)$$

to the energy ε of a quantum state. Here, we will view these amplitudes as *phasors* or *quantum clocks* sketched in Fig. 4.2.1-4.2.2. Each of these quantum clocks rotates clockwise as time advances.

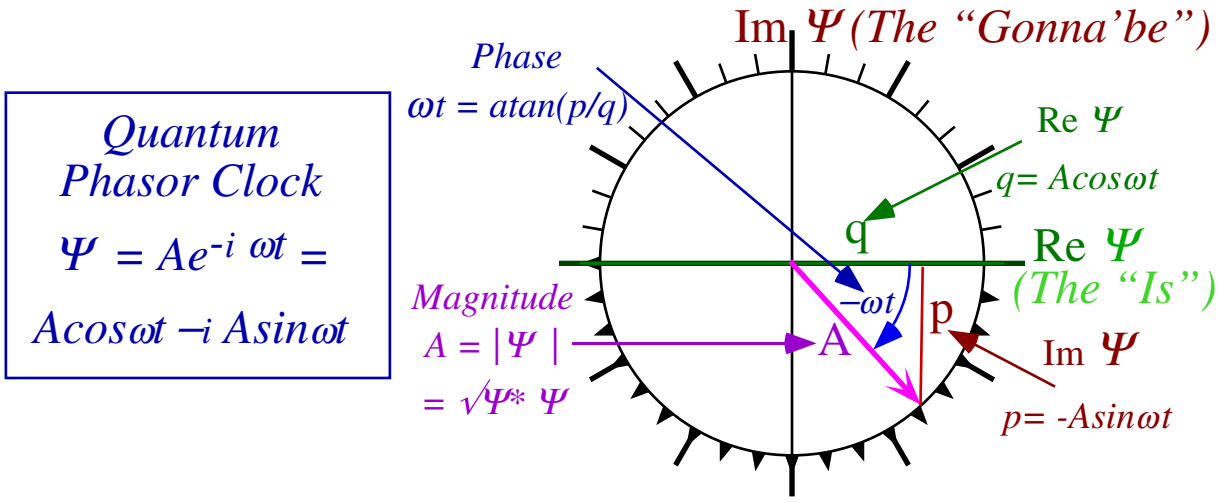

Fig. 4.2.1 Geometry of quantum phasor clock $\Psi=q+ip=Ae^{-i\omega t}=A\cos\omega t - iA\sin\omega t$

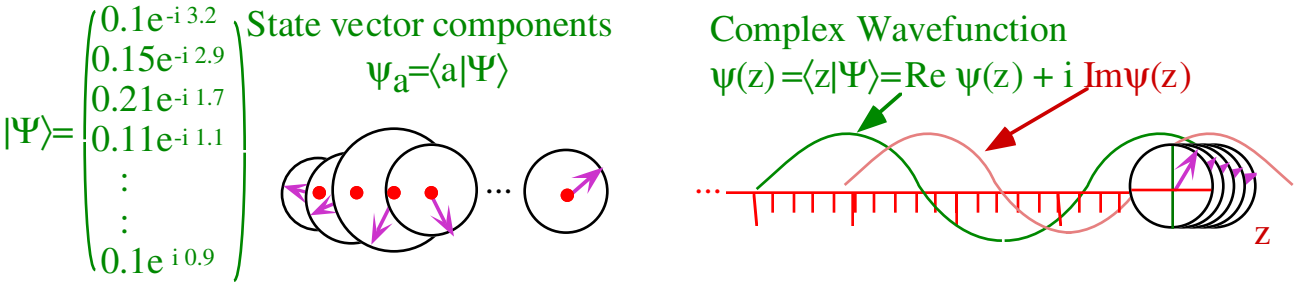

Fig. 4.2.2 Discrete set of complex amplitudes versus complex wavefunction

Complex numbers help to visualize one-dimensional oscillation as a two-dimensional process with an *amplitude* (A) and a *phase* ($-\omega t$) or else *real* ($q=Re\,\Psi$) and *imaginary* ($p=Im\Psi$) parts, which are like oscillator *phase variables* of coordinate (q) and momentum (p). The $e^{-i\omega t}$ amplitude in Fig. 4.2.1 has a negative ($-\omega t$) time-phase so the q-axis and p-axis make right-handed phase space with clockwise circulation. We shall name q and p the *"is"* and *"gonna' be"* variables since $q=Re\,\Psi(z)$ is where the wave

is and $p=Im\ \Psi(z)$ is where the wave is gonna' be in *1/4*-cycle. (See Fig. 4.2.2.)A mnemonic helps: "Imagination precedes reality." The imaginary wave always precedes the real wave in examples below.

Please Note: Never NEVER imagine that the phasor "velocity" or "momentum" p =ImΨ has any *direct* connection with an actual classical particle velocity, or that the phasor "coordinate" q =ReΨ has any direct connection with a particle's location in space or time. The quantum phasors (or wavefunctions they represent) seem to be *behind-the-scenes* objects. (Some will say they're mere theoretical constructions!) In fact, the phasors are so far behind the scene that generally they're not directly observable! Only probability $|\Psi|^2$ is readily observable (but needs millions of irreversible counts to be very useful.)

A complex wavefunction $\psi(z)$ defined over a continuum can be viewed as two overlapping real functions *Re* $\psi(z)$ and *Im* $\psi(z)$ or as a continuous set of phasor clocks as shown in Fig. 4.2.2 (right). Obviously, a continuum of clocks is impossible. So once again, we will settle for a coursegrained picture as indicated in the figure. Only enough clocks to resolve a quarter wavelength, or so, are actually needed.

This Sec. 4.2 has examples of complex wavefunctions and phasor clocks to help analyze quantum waves and wave dynamics in general. These are powerful visual aids as well as computational tools. Note, that the beams we used to begin quantum analysis in Ch. 1 are actually composed of waves of the kind we are introducing here. Every *n*-state beam is described at every point in the *z*-continuum along the beam by a discrete set of *n*-phasors, or equivalently, *n* complex wavefunctions $\{\psi_1(z), \psi_2(z),...,\psi_n(z)\}$.

The 2-state systems such as the optical polarization states of lightbeams, require two phasors to describe the light at any point *z* on a beam. This involves a bit of a notation hassle. In Ch. 1 the letters x and y were used as state indices; they denoted directions of polarization. In this chapter the same letters *x*, *y*, and also *z* are used to designate a continuum coordinate, usually along a beam direction. Be careful to distinguish this nomenclature. Perhaps, *z* should replace *x* everywhere in this chapter.

If x and y-polarization is normal to the beam propagation direction *z*, the notation is not so confusing. An x-phasor describes the x-polarization amplitude $\psi_x(z)=\langle x|\Psi(z)\rangle$ while another y-phasor describes the y-polarization amplitude $\psi_y(z)=\langle y|\Psi(z)\rangle$ at each *z*-point. When a beam gets split by a sorter or analyzer, then each sub-beam also has two phasors (An *n*-state beam has *n*-phasors).

What are we in for? (We really don't know waves at all.)

A word of caution about this unit: It is hoped that you are going to learn things about waves and spacetime that are quite astounding. Most courses that introduce waves do not prepare for this. There is so much to learn about waves. A refrain from a song *Clouds* by Joni Mitchell comes to mind. Here we put "waves" in place of "clouds" in her song in an attempt to describe what is to follow.

"...I've looked at waves from both sides now ...
up and down and all around.... still it's waves' illusions I recall...
...I really don't know waves at all " *Joni Mitchell 1974*

Fig. 4.2.3

(b) Wave anatomy: Expo-trig identities

Two key identities, the *expo-cosine* and *expo-sine* relations, let us easily combine two complex waves.

$$\psi_+ = e^{ia} + e^{ib} \quad (expo-cos) \qquad \psi_- = e^{ia} - e^{ib} \quad (expo-sin)$$

$$= e^{i\frac{a+b}{2}}\left(e^{i\frac{a-b}{2}} + e^{-i\frac{a-b}{2}} \right) \qquad = e^{i\frac{a+b}{2}}\left(e^{i\frac{a-b}{2}} - e^{-i\frac{a-b}{2}} \right)$$

$$= 2e^{i\frac{a+b}{2}} \cos\frac{a-b}{2} \quad (4.2.3a) \qquad = 2ie^{i\frac{a+b}{2}} \sin\frac{a-b}{2} \quad (4.2.3b)$$

Each of these identities extracts a wave's *modulus MOD* or *group envelope* embodied by the cosine or sine MOD factor that defines the wave's outside "skin" as sketched in Fig. 4.2.4(a).

$$MOD(\psi_\pm) = |\psi_\pm| = \sqrt{\psi_\pm^* \psi_\pm} = \begin{cases} \cos\left(\frac{a-b}{2}\right) & \text{for } \psi_+ \\ \sin\left(\frac{a-b}{2}\right) & \text{for } \psi_- \end{cases} \quad (4.2.4a)$$

The wave's *argument ARG* or *overall phase* in the exponential factor $e^{i(a+b)/2}$ define its "insides" or "guts" including its real part $\mathrm{Re}\psi$ and its imaginary part $\mathrm{Re}\psi$ sketched in Fig. 4.2.4(b).

$$ARG(\psi_\pm) = ATN\frac{\mathrm{Im}\psi_\pm}{\mathrm{Re}\psi_\pm} = \begin{cases} \left(\frac{a+b}{2}\right) & \text{for } \psi_+ \\ \left(\frac{a+b}{2} + \frac{\pi}{2}\right) & \text{for } \psi_- \end{cases} \quad (4.2.4b)$$

(To some the wave looks like a boa constrictor that has swallowed some very live prey.)

The speed of the outside $MOD(\psi_\pm)$ wave factor is called *group velocity*. The external "skin" of the wave is the only part visible to probability or intensity measurements of $\psi^*\psi$. The speed of exponential phase factor inside the envelope is called *mean phase velocity* or just plain *phase velocity*. The internal phase "guts" of the wave is the part measured by (difficult) phase-sensitive detection schemes. One may think of such "intra-gut" observation as "surgery" for which patient survival is not always possible!

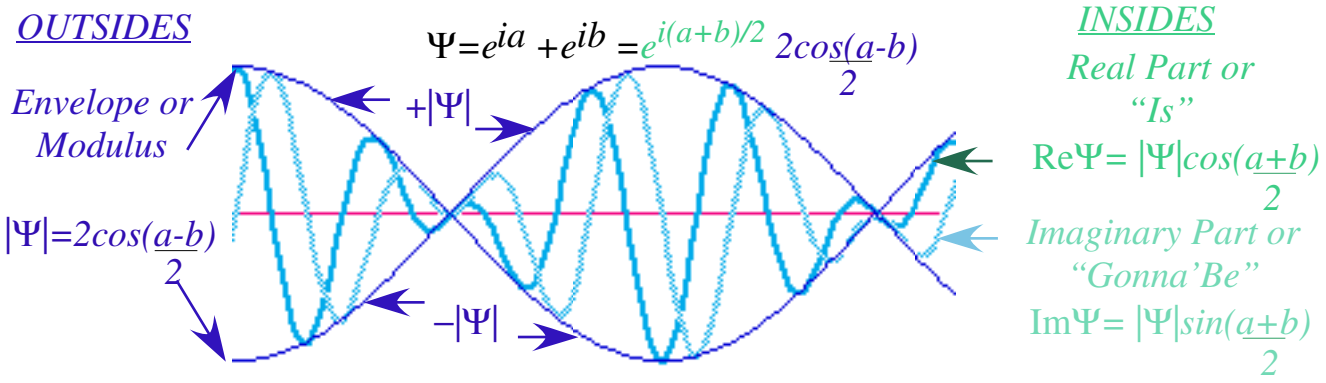

Fig. 4.2.4 Anatomy of a wave combination of two wave components e^{ia} and e^{ib}.
Visualizing Complex Wave Amplitudes and Phasors by WaveIt

Visualization of complex wavefunctions is an important part of being able to work with them. Complex analysis provides powerful techniques, but it is difficult to apply it to physical problems

without some intuition. An ability to run fast is of dubious value if you can't see where you're going. Phasor clocks provide a visual representation of complex wavefunctions Ψ. Few 20th century EM and QM texts mention this visual aid in spite of the fact that some 19th century ones did do so. 21st century cyber-animation (Here it's *WaveIt.*) makes phasor animation revealing as well as practical.

The two axes or components of a phasor are the real (x=ReΨ) and the imaginary (y=ImΨ) as in Fig. 4.2.5. When plotting *transverse* waves it helps to rotate the phasor xy-axes *90°* so the real part or x-axis points up in the transverse (+)-direction of the wave amplitude as shown in the figure below.

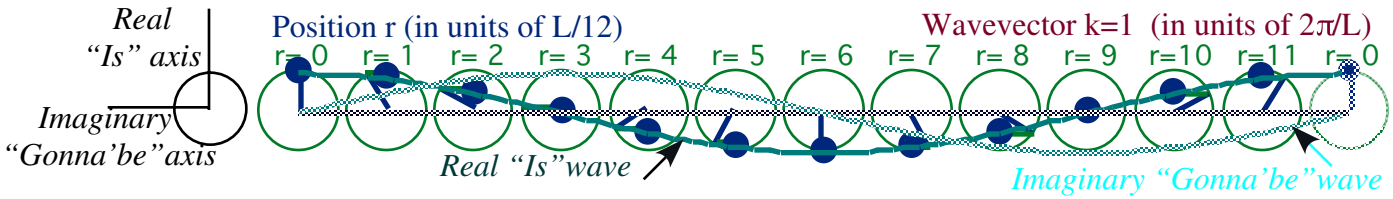

Fig. 4.2.5 Right-moving (Positive k=1) transverse wave $\Psi_{\rightarrow} = e^{i(kr - \omega t)}$ *at time t=0.*

The phasor at position r=0, 1, 2,..., 10, 11 is set to 12, 11, 10, 9,..., 2, 1 o'clock, respectively. As the clocks turn clockwise at angular frequency ω, the transverse "high-noon" peak moves from r=0 to r=1 to r=2 ...in much the same way as solar time settings of global clocks (or temperature above mean T) advance around the world. The real part ReΨ tells what the amplitude "is" while the ImΨ or imaginary part gives its rate of change in ω-units and so tells what it is "gonna' be" 1/4-hour later

When plotting *longitudinal* or *density* waves we place the phasor xy-axes so the real part or x-axis points rightward in the longitudinal direction of (+)-wave amplitude as shown in the figure below. Now the real part "is" the density ρ while the imaginary part gives velocity flow or current ι and thereby predicts what the density (above mean ρ_0) is "gonna' be" 1/4-hour later

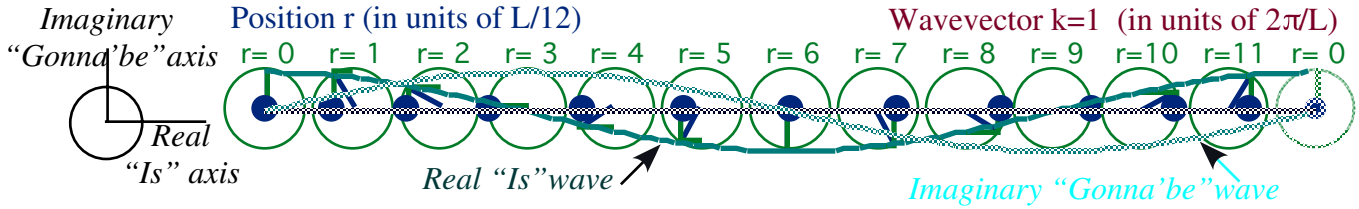

Fig. 4.2.6 Right-moving (Positive k=1) longitudinal $\rho_{\rightarrow} = e^{i(kr - \omega t)}$ *at time t=0.*

An East-to-West or left-moving transverse wave is shown in Fig. 4.2.7. (Here North is up.) The phasors at r=0, 1, 2,..., 10, 11 are set to 1, 2, 3, 4,..., 10, 11 o'clock, respectively. A phasor that is ahead of a neighbor pushes or pulls that neighbor while being pulled or pushed by the neighbor on the other side that is behind in phase. Here the effects of push and pull are equal so no phasor ever changes size.

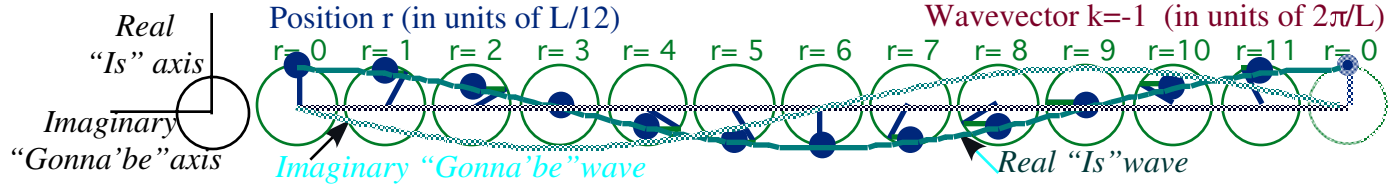

Fig. 4.2.7 Left-moving (Negative k=-1) transverse $\Psi_{\leftarrow} = e^{i(-|k|r - \omega t)}$ *at time t=0. (.)*

Vector addition of phasors in Fig. 4.2.5 and Fig. 4.2.7 gives a *standing wave* shown in Fig. 4.2.8-9. Each phasor rotates clockwise synchronously so relative phase difference is constant in time. Position r=6 adds in-phase to give an *anti-node*. Other places like r=10 near *nodes* do not match in phase and cancel.

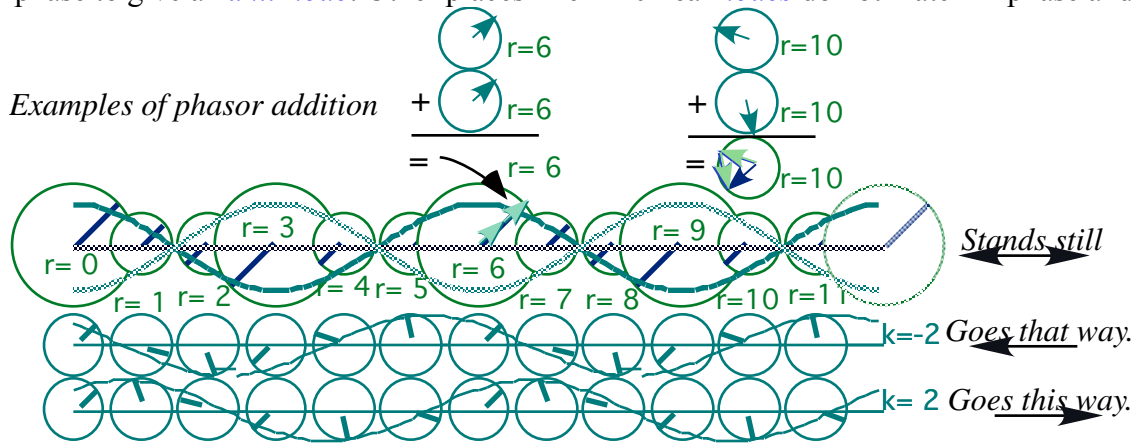

Fig. 4.2.8 Standing wave made by summing phasors of left-and-right moving waves.

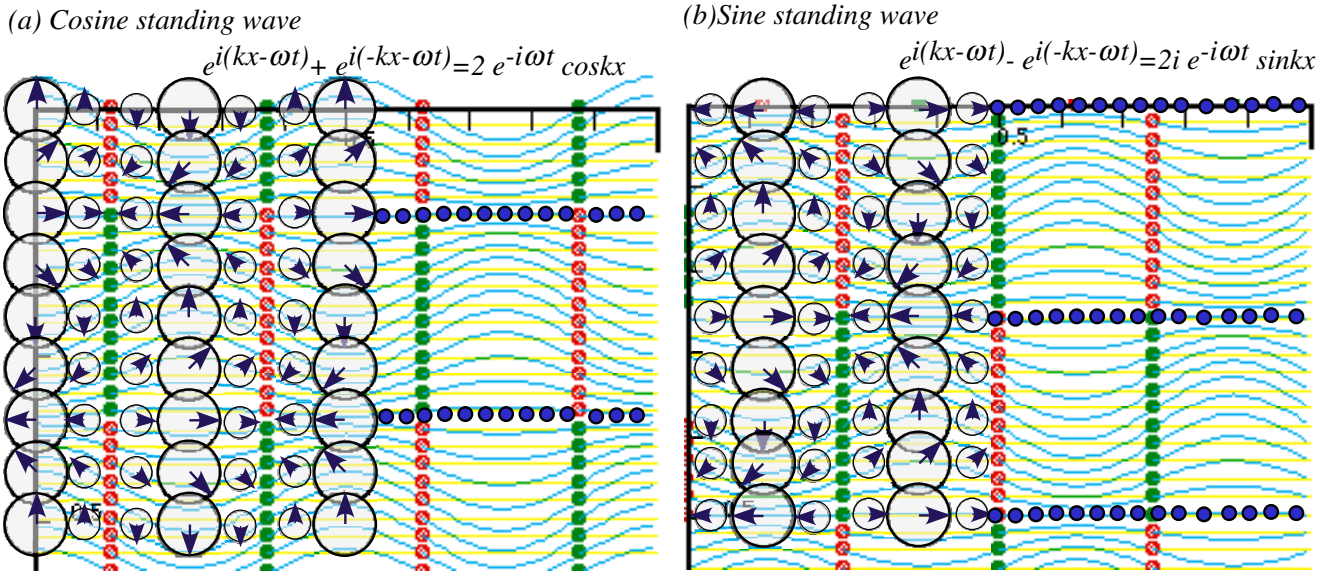

Fig. 4.2.9 Space-time phasor plots. (a) Standing cosine wave Ψ_c *and (b) i-sine wave* Ψ_s *(*$\omega = 2c = k\,c$*)*

Note that each time, all standing-wave phasors are either in phase or else *180°* (π) out of phase with all the others. Also, the size of the phasor dials, while constant in time, varies sinusoidally with the spatial coordinate *x*. That size is determined by the envelope or *MOD* function of (4.2.4).

(c) When Lightwaves Interfere: Phase and Group Velocity

The standard units of time *t* and space *x* are *seconds* and *meters*. Pure waves are labeled by inverse units that count waves *per-time* or *frequency ν*, which is *per-second* or *Hertz (1Hz=1 s^{-1})* and waves *per-meter* that is called *wavenumber κ* whose units are *Kaiser (1 K=1 cm^{-1}=100 m^{-1})*. Inverting back gives the *period τ=1/ν* or *time for one wave* and *wavelength λ=1/κ* or the *space occupied by one wave*.

Physicists prefer angular or radian quantities of *radian-per-second* or *angular frequency ω=2πν* and *radian-per-meter* or *wavevector k=2πκ* as used, for example, in a plane wavefunction.

$$\langle k,\omega\,|\,x,t\rangle = \psi_{k,\omega}(x,t) = e^{i(kx-\omega t)} = \cos(kx-\omega t) + i\sin(kx-\omega t), \qquad (4.2.5)$$

The sine and cosine are functions of wave *phase (kx-ω t)* given in radians. An extra 2π is needed.

$$\tau = \frac{2\pi}{\omega} = \frac{1}{\nu} \qquad (4.2.6a) \qquad\qquad \lambda = \frac{2\pi}{k} = \frac{1}{\kappa} \qquad (4.2.6b)$$

Theses are the relations between time and space and *per*-time and *per*-space wave parameters.

Phase velocity

Spacetime plots of the real field $\mathrm{Re}\psi_{k,\omega}(x,t)$ for moving laser light waves are shown in Fig. 4.2.10. The left-to-right moving wave $e^{i(kx-\omega t)}$ in Fig. 4.2.10(a) has a positive wavevector *k* while *k* is negative for right-to-left moving wave $e^{i(-|k|x-\omega t)}$ in Fig. 4.2.10(b). Light and dark lines mark time paths of crests, zeros, and troughs of $\mathrm{Re}\psi_{k,\omega}(x,t)$. A peak for the zero-phase line is where *kx-ω t* is zero, that is,

$$kx-\omega t = 0\,, \quad \text{or:} \quad \frac{x}{t} = V_{phase} = \frac{\omega}{k} = \nu\lambda \qquad (4.2.7)$$

Each white line in Fig. 4.2.10 has a phase is an odd multiple *(N=1,3,...)* of *π/2* and marks a *λ/2*-interval.

$$kx-\omega t = \pm N\frac{\pi}{2}\,, \quad \text{or:} \quad x = V_{phase}t \pm N\frac{\pi}{2k} = V_{phase}t \pm N\frac{\lambda}{4} \qquad (4.2.8)$$

The slope or *phase velocity* V_{phase} of optical phase line is a universal constant *c=299,792,548ms*$^{-1}$ for light waves. (Recall tribute to Ken Evenson earlier.) Velocity is a ratio of space to time *(x/t)* or a ratio of per-time to per-space *(ν/κ)* or *(ω/k)*, or a product of per-time and space *(νλ)*. The concept of light speed is a deep one and it will be introduced in the *Colorful Relativity* axiom at the beginning of Sec. 4.3.

The standard wave quantities of (4.2.6) are labeled for a long wavelength example (infrared light) in the lower part of Fig. 4.2.10. Note that the $\mathrm{Im}\psi_{k,\omega}(x,t)$ wave precedes the $\mathrm{Re}\psi_{k,\omega}(x,t)$ wave. Recall the mnemonic, "Imagination precedes reality." It also applies to combined waves treated in the following sections and later chapters.

Fig. 4.2.10 Phasor and spacetime (BohrIt) plots of moving laser waves. (a) Left-to-right. (b) Right-to-left.

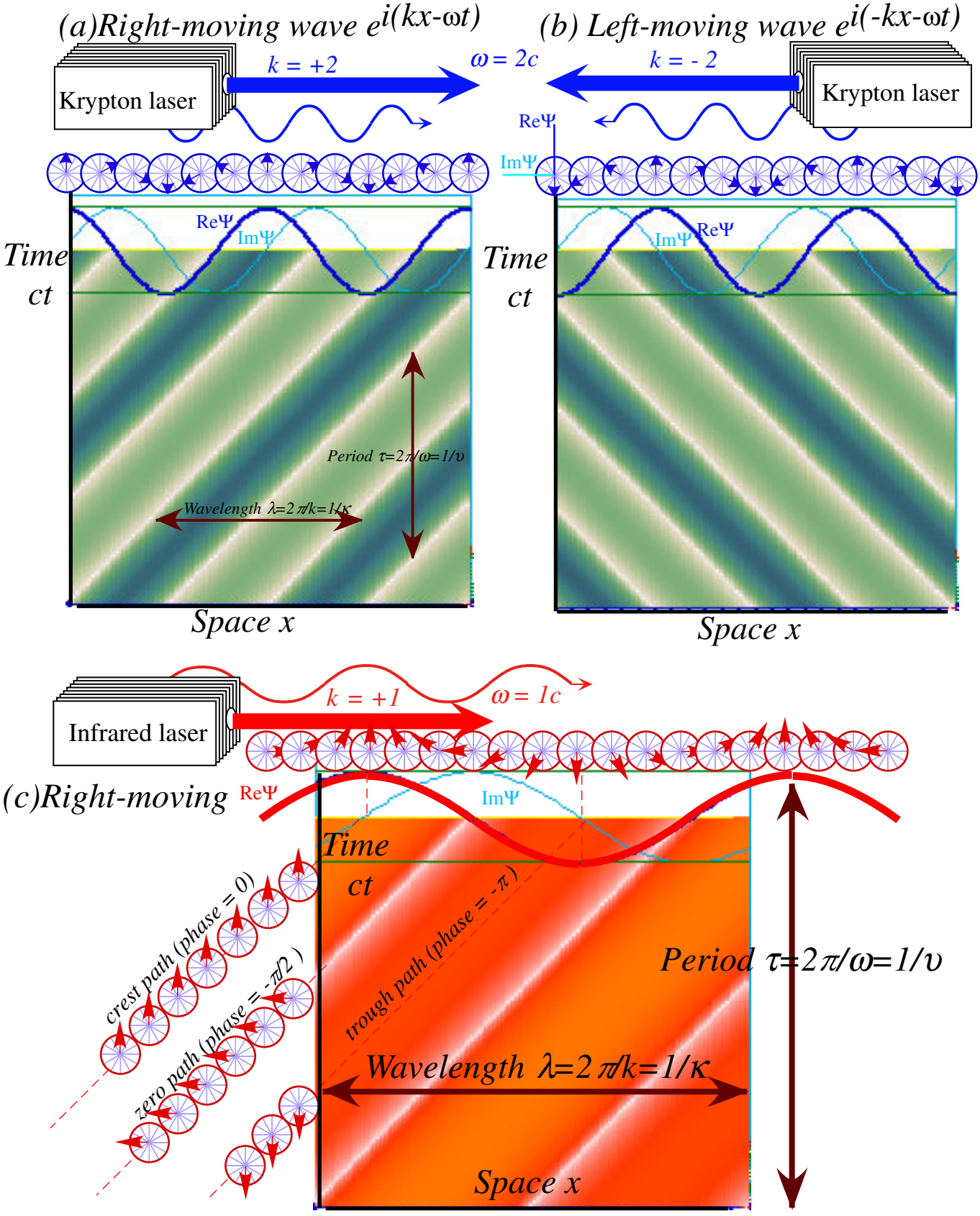

Group velocity

Group velocity is not seen unless at least two different moving waves are combined, and to define it we need waves quite unlike light. Fig. 4.2.11 shows a pair of "non-light" wave sources. The first *source-2* puts out a "red" wave of wavevector-frequency $(k_2,\omega_2)=(1,2)$ while the other *source-4* puts out a "blue" wave of wavevector-frequency $(k_4,\omega_4)=(4,4)$. The "non-light" waves are *Bohr-Schrodinger matter waves* or *μ-waves* (derived later) for an atom of rest mass $(M=2)$ in natural (k,ω) units. But, the following applies to a general wave. You may pick four random numbers for *source-2* (k_2,ω_2) and *source-4* (k_4,ω_4) and the formulas (4.2.9) and (4.2.10) below will still apply.

Given any wavevector-frequencies $\mathbf{K}_2=(k_2,\omega_2)$ and $\mathbf{K}_4=(k_4,\omega_4)$ the *e-cos* relation (4.2.3a) applies.

$$\Psi_{4+2}=e^{i(k_2x-\omega_2t)}+e^{i(k_4x-\omega_4t)}=2e^{i\left(\frac{k_4+k_2}{2}x-\frac{\omega_4+\omega_2}{2}t\right)}\cos\left(\frac{k_4-k_2}{2}x-\frac{\omega_4-\omega_2}{2}t\right) \qquad (4.2.9)$$

In *phase factor* $e^{i()}$ and *group factor* $\cos()$ is a sum $\mathbf{K}_{phase}=(\mathbf{K}_4+\mathbf{K}_2)/2$ or difference $\mathbf{K}_{group}=(\mathbf{K}_4-\mathbf{K}_2)/2$.

$$\mathbf{K}_{phase}=\frac{\mathbf{K}_4+\mathbf{K}_2}{2}=\frac{1}{2}\begin{pmatrix}\omega_4+\omega_2\\ k_4+k_2\end{pmatrix}=\frac{1}{2}\begin{pmatrix}4+1\\ 4+2\end{pmatrix}=\begin{pmatrix}2.5\\ 3.0\end{pmatrix} \qquad (4.2.10a)$$

$$\mathbf{K}_{group}=\frac{\mathbf{K}_4-\mathbf{K}_2}{2}=\frac{1}{2}\begin{pmatrix}\omega_4-\omega_2\\ k_4-k_2\end{pmatrix}=\frac{1}{2}\begin{pmatrix}4-1\\ 4-2\end{pmatrix}=\begin{pmatrix}1.5\\ 1.0\end{pmatrix} \qquad (4.2.10b)$$

The vectors $\mathbf{K}_2$, $\mathbf{K}_4$, $\mathbf{K}_{phase}$ and $\mathbf{K}_{group}$ are drawn in Fig. 4.2.11(b). Each slope is a *wave velocity*.

$$V_4=\frac{\omega_4}{k_4}=\frac{4}{4}=1 \qquad (4.2.10c)$$

$$V_2=\frac{\omega_2}{k_2}=\frac{1}{2}=0.5 \qquad (4.2.10d)$$

$$V_{phase}=\frac{\omega_4+\omega_2}{k_4+k_2}=\frac{5}{6}=0.83 \qquad (4.2.10e)$$

$$V_{group}=\frac{\omega_4-\omega_2}{k_4-k_2}=\frac{3}{2}=1.5 \qquad (4.2.10f)$$

The spacetime plot of wave zeros of $\mathrm{Re}\Psi$ in Fig. 4.2.11(a) shows a *group velocity* nearly twice the *mean phase velocity* as given by (4.2.10e-f). This is a peculiarity of Bohr matter waves that is explained later.

Wave lattice paths in space and time

Fig. 4.2.11 is actually a single plot that combines *spacetime (x,t)* with Fourier space or *per-spacetime (ω,k)*. It relates localized pulses ("particle-like" waves) to continuous "coherent" waves by a latticework of $\mathrm{Re}\Psi$ wave-zero paths in Fig. 4.2.11(a). On wave *phase-zero paths* the real part of phase factor $e^{i(k_px-\omega_pt)}$ in (4.1.5a) is zero: $k_px-\omega_pt=n_p=N_p\pi/2\ (N_p=\pm1,\pm3...)$. *Group-zero paths* have zero group factor $\cos(k_gx-\omega_gt)$ or: $k_gx-\omega_gt=n_g=N_g\pi/2$. At *wave lattice points (x,t) both* factors are zero.

$$\begin{pmatrix}k_p & -\omega_p\\ k_g & -\omega_g\end{pmatrix}\begin{pmatrix}x\\ t\end{pmatrix}=\begin{pmatrix}n_p\\ n_g\end{pmatrix}\ \text{where: }\mathbf{K}_{phase}=\begin{pmatrix}\omega_p\\ k_p\end{pmatrix}=\frac{1}{2}\begin{pmatrix}\omega_4+\omega_2\\ k_4+k_2\end{pmatrix},\ \mathbf{K}_{group}=\begin{pmatrix}\omega_g\\ k_g\end{pmatrix}=\frac{1}{2}\begin{pmatrix}\omega_4-\omega_2\\ k_4-k_2\end{pmatrix} \qquad (4.2.11a)$$

Solving this shows that the *wavevector*-vectors $\mathbf{K}_{phase}$ and $\mathbf{K}_{group}$ define *spacetime (x,t)* zero-paths.

$$\begin{pmatrix}x\\ t\end{pmatrix}=\frac{\begin{pmatrix}-\omega_g & \omega_p\\ -k_g & k_p\end{pmatrix}\begin{pmatrix}n_p\\ n_g\end{pmatrix}}{\omega_pk_g-\omega_gk_p}=\frac{-n_p\begin{pmatrix}\omega_g\\ k_g\end{pmatrix}+n_g\begin{pmatrix}\omega_p\\ k_p\end{pmatrix}}{\omega_pk_g-\omega_gk_p}=-\frac{n_p}{D}\mathbf{K}_{group}+\frac{n_g}{D}\mathbf{K}_{phase}\ \text{where: }\begin{pmatrix}n_p\\ n_g\end{pmatrix}=\begin{pmatrix}N_p\\ N_g\end{pmatrix}\frac{\pi}{2} \qquad (4.2.11b)$$

The phase zeros follow $\mathbf{K}_{phase}$ at V_{phase} while the envelope zeros go along $\mathbf{K}_{group}$ at a higher speed V_{group}. Anti-nodes occupy an "in-between" lattice with even integer $(N_p,N_g=0,\pm2,\pm4...)$.

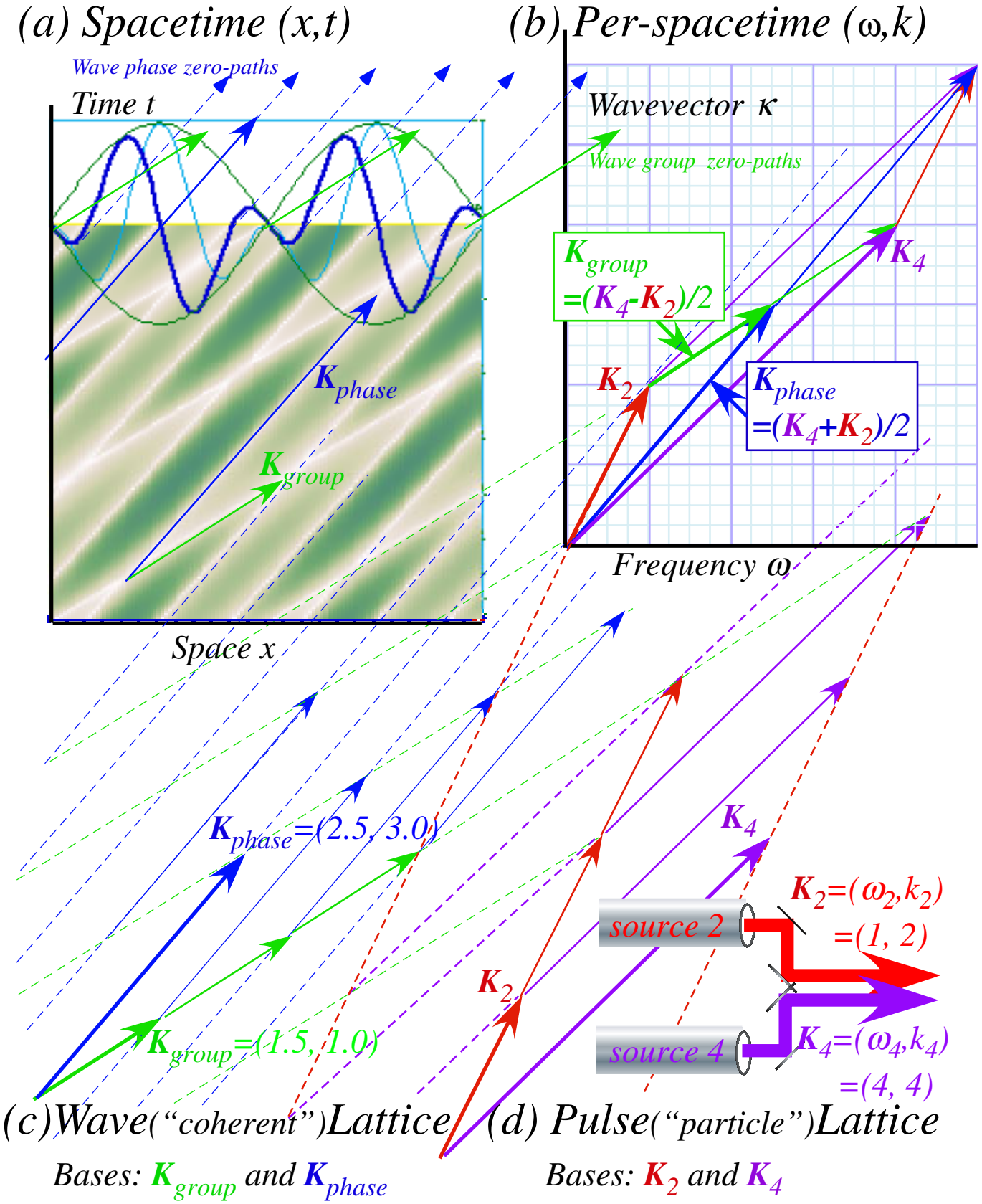

Fig. 4.2.11 Wave paths in spacetime (x,t) and Fourier per-spacetime (ω,k). (a-b) Wave zero paths along group and phase wavevectors. (c-d) Wave lattices with and without coherence.

It should be noted that the joining of a per-spacetime Fourier plot with a spacetime plot is unusual, and requires some care. First, if t is plotted versus x then (4.2.11b) requires that we plot the wavevector k versus the frequency ω instead of the other way around. (The usual dispersion functions $\omega(k)$ are plotted ω against k as will be done in later figures.) Also, we rescale the k-v*ersus*-ω plot by the determinant $D=\omega_p k_g-\omega_g k_p$ in (4.2.11b) so its lattice in Fig. 4.2.11(b,d) matches the x-v*ersus*-t wave-zero lattice in Fig. 4.2.11(a).

When that is done, the two plots may use exactly the same lattice vectors $\mathbf{K}_2$, $\mathbf{K}_4$, $\mathbf{K}_{phase}$ and $\mathbf{K}_{group}$ to define unit cells in either plot. While the $\mathbf{K}_2$ and $\mathbf{K}_4$ vectors define a primitive cell in the pulse plot of Fig. 4.2.11(d) discussed below, they also define the diagonals of the phase and group wave-zero cells spanned by $\mathbf{K}_{phase}$ and $\mathbf{K}_{group}$ in Fig. 4.2.11 (a-c). Also, the vectors $\mathbf{K}_{phase}$ and $\mathbf{K}_{group}$ define the diagonals of the primitive $\mathbf{K}_2$ and $\mathbf{K}_4$ cells as required by the vector sum relations in (4.2.10) and Fig. 4.2.11(b).

Particle or pulse lattice paths in space and time

A discussion of the paths of wave packet or pulses for the individual sources completes the picture. Suppose the output of the two sources could not interfere and behaved like Newtonian corpuscles or particles emitted each at their assigned frequency $\omega_2=1$ or $\omega_4=4$ to go along vectors $\mathbf{K}_2$ and $\mathbf{K}_4$ at their assigned phase velocities $V_2 = 0.5$ for *source-2* particles or $V_4 =1.0$ for *source-4* particles as given by (4.2.10c) and (4.2.10d). That is, four times as many $\mathbf{K}_4$ lattice lines as $\mathbf{K}_2$ lines cross the t-axis (or k-axis) but only twice as many $\mathbf{K}_4$ lines as $\mathbf{K}_2$ lines ($k_4/k_2=2$) are found at one time along the x-axis (or ω-axis). In other words, *source-4* goes *"patooey, patooey, patooey, patooey,…"* while *source-2* only spits half as fast, *"patooey,……, patooey,…"*.

If a pulse-counter at origin $x=0$ could distinguish the "red" $\mathbf{K}_2$ from the "blue" $\mathbf{K}_4$ then it would register four times as many "blue" counts as "red" ones. All this assumes that the pulses or particles have non-dispersing Fourier components with the same phase velocity c, that is, linear dispersion $\omega=ck$, as does light. But, $\mathbf{K}_2$ and $\mathbf{K}_4$ are not on a line through origin in Fig. 4.2.11. Their dispersion is *not* linear, and as will be shown later, extraordinary interference effects arise from non-linear dispersion.

Spacetime lattices collapse for co-propagating optical waves

Fig. 4.2.12 shows the same vectors as Fig. 4.2.11 but for the combination (4.2.9) of optical or laser waves. Both V_2 for *source-2* photons and V_4 for *source-4* photons as given by (4.2.10c-d) now equal c as required by the *Colorful Relativity* axiom that starts the following Sec. 4.3. Then, the phase and group velocities are c by (4.2.10e-f), as well, and scale denominator $D=\omega_p k_g-\omega_g k_p$ in (4.2.11b) is zero. So all the vectors $\mathbf{K}_2$, $\mathbf{K}_4$, $\mathbf{K}_{phase}$ and $\mathbf{K}_{group}$ collapse onto the $45°$ line that holds both phase velocities and group velocities since they all have the speed of light only.

So, the optical co-propagation lattice collapses. To make a spacetime lattice with light requires *counter*-propagating waves. This leads to a simple derivation of the theory of relativity in the following Sec. 4.3 and the basic theory of relativistic quantum mechanics in Chapter 5.

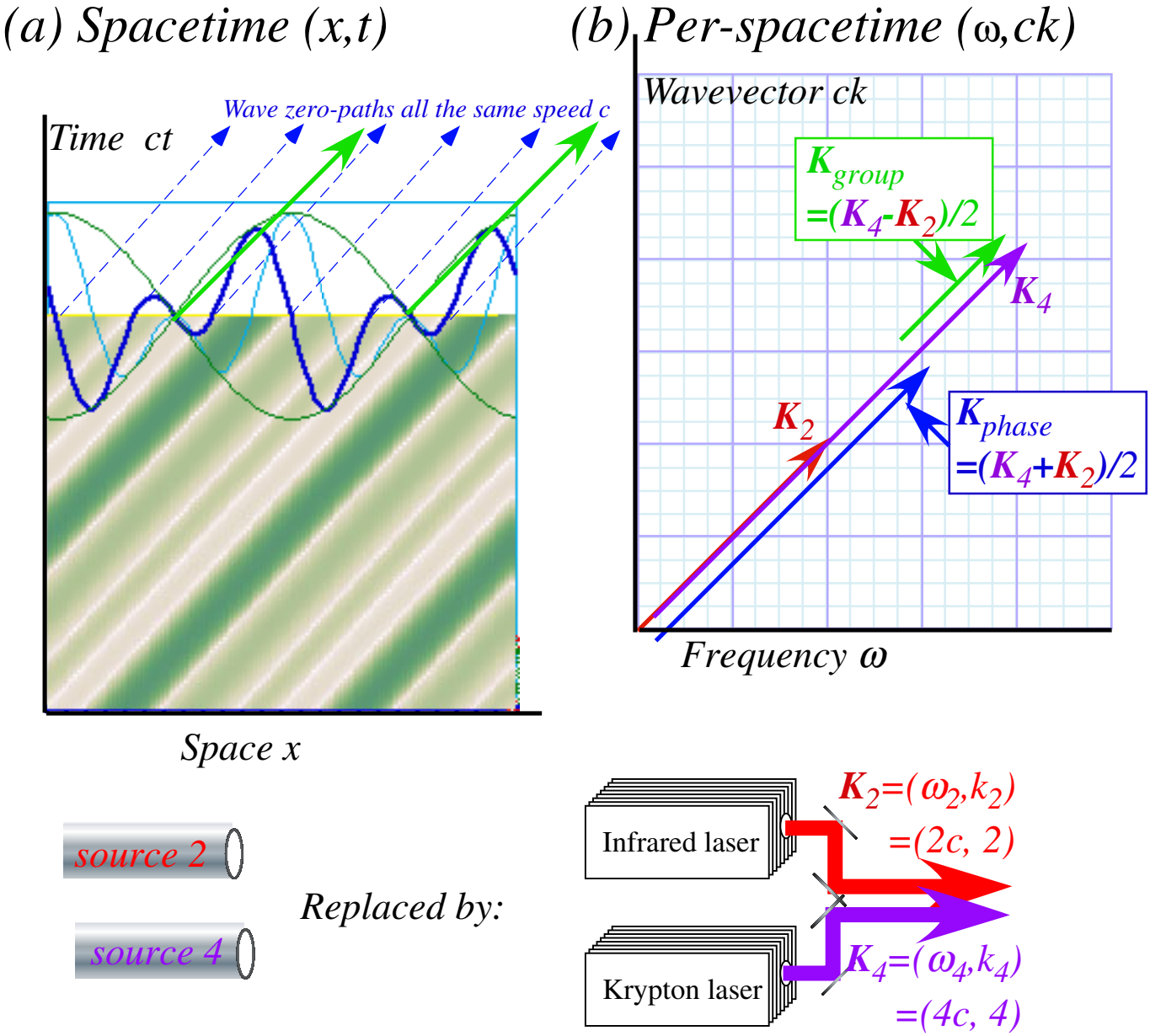

Fig. 4.2.12 Simplified wave dynamics for co-propagating optical sources.

The preceding constructions have managed to put Fourier or wave-like (per-spacetime) properties on the same page, so to speak, with Newtonian or particle-like (spacetime) ones. This is analogous to what is done in X-ray crystallographic analysis in which a real atomic position vector lattice is described using an inverse or reciprocal wavevector lattice.

In either case, the scaling in one is the inverse of the other. A larger wavevector means smaller spacing between waves in position space and *vice-versa*. The scale denominator $D=\omega_p k_g - \omega_g k_p$ in (4.2.11b) takes care of the connection of spacetime and per-spacetime plots *for that particular pair of waves only.* Another pair will generally have a different scale, but you're only allowed one scale factor per plot. Use caution when plotting *three* (or more) waves!

4.3 When Lightwaves Collide: Relativity of Spacetime

The waves combined in Fig. 4.2.12 have positive "kink-vectors" k_m so they both had positive phase velocity $V_{phase}(m)=\omega_m/k_m$. Such waves are *co-propagating* waves. Angular frequency ω_m or "wiggle rate" is positive by a convention so that phasors $e^{-i\omega t}$ always turn clockwise but k_m may have either sign. Now we look at *counter-propagating* waves, in particular, counter propagating green laser beams whose *k*-vectors and phase velocities have opposite sign as shown in Fig. 4.3.1(a).

If these were water waves going at ±*3 meters per second (mps)*, a boat going *-4 mps* adds *4* to each wave velocity. It goes against the *+3mps*-waves at *3+4=7mps* while catching and passing *-3mps*-waves at *–3+4=+1 mps*, and so, relative to the boat, those waves become co-propagating at *+7* and *+1*.

Can the same trick be done with light? Apparently not, as Fig. 4.3.1(b) shows what is seen by an atom "boat" attempting, by going left relative to lasers, to catch and pass a *–3 Hundred Million meter per second* light wave having *k*-vector $k_{\leftarrow}=-2$ and frequency $\omega_{\leftarrow}=2c$. (The atom sees lasers going right.)

The atom can never catch the green light from the right hand laser, but it does see a Doppler-red-shift down to a lesser *k*-vector $k'_{\leftarrow}=-1$ and frequency $\omega'_{\leftarrow}=1c$ for *infrared* light from a laser receding at *180 Million meter per second* or *3c/5*. This is derived easily below in (4.3.5b) as is the perceived *blue*-shifted output of the left hand laser coming *toward* the atom at *3c/5*. Its green light of *k*-vector $k_{\rightarrow}=+2$ and frequency $\omega_{\rightarrow}=2c$ is Doppler blue-shifted up to *ultraviolet* light of *k*-vector $k'_{\rightarrow}=+4$ and frequency $\omega'_{\rightarrow}=4c$. (Green wavelength is λ=0.5μm. Its *k*-vector is $k_{\rightarrow}=2\pi/\lambda$ so the length unit for Fig. 4.3.1 is 2π *microns*. Lightspeed is now *exactly c=2.99792458E8m/s* following ultra-accurate time and frequency determination by Ken Evenson's group that gave rise to the 1980 meter redefinition.)

Atoms will always fail to catch light waves and profoundly so. Even if they go fast enough to Doppler shift a green *600 THz* laser beam to below *1 Hz*, they still face a fundamental axiom or postulate that precludes ever catching a light wave. According to this, we never see light speed slow down *at all*!

(a) The colorful relativity axiom: Using Occam's razor

The Colorful Relativity Axiom: En vacuo, all colors go the same speed $c=\omega/k$ (4.3.1)

Light has *linear dispersion* $\omega=ck$. Otherwise stellar images would arrive color dispersed as if viewed through cheap binoculars, and each color would come in infinite variety. There would be green light from a stationary laser, green light made by an approaching red laser, and green light made by a receding blue laser, all presumably the same frequency but differing somehow in wavelength and speed. An invariant dispersion function wouldn't exist. Such fickle light would interfere itself to **blackness**. The colorful coherent continuous wave (CCCW) axiom is an Occam razor cut of the usual pulse wave (PW) axiom.

Examining the night sky or, better, a Hubble space telescope image, shows that all colors do indeed arrive in step even after billions of years of unimaginably perilous travel. To have even a tiny deviation from linear dispersion would make our night sky into a kaleidoscope of smeared color. Larger deviations would leave us wandering virtually blind in a colorful fog. (See discussion at the end of this section.)

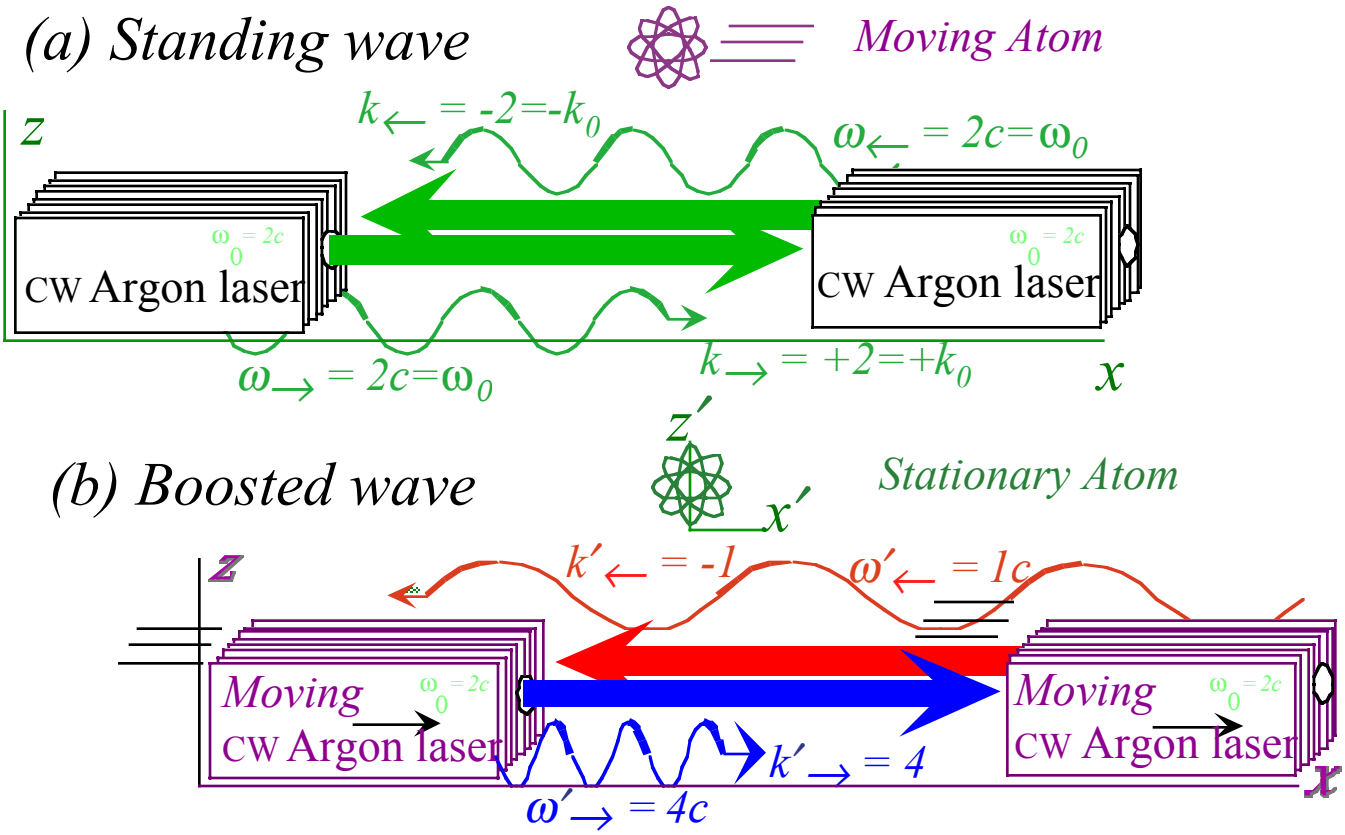

Fig. 4.3.1 Atom in Lasers. (a) Laser frame sees left-moving atom. (b) Atom sees right moving lasers.

Relativity by interfering counter-propagating laser waves

The wave in the laser frame of Fig. 4.3.1(a) is a *standing cosine wave* like Fig. 4.2.9(a).

$$e^{i(k_{\rightarrow}x-\omega_{\rightarrow}t)} + e^{i(k_{\leftarrow}x-\omega_{\leftarrow}t)} = 2e^{i\left(\frac{k_{\rightarrow}+k_{\leftarrow}}{2}x-\frac{\omega_{\rightarrow}+\omega_{\leftarrow}}{2}t\right)}\cos\left(\frac{k_{\rightarrow}-k_{\leftarrow}}{2}x-\frac{\omega_{\rightarrow}-\omega_{\leftarrow}}{2}t\right)$$
$$= 2e^{i(0x-\omega_0 t)}\cos\left(k_0 x-\frac{0}{2}t\right) = 2e^{-i\omega_0 t}\cos k_0 x \quad \text{where: } \begin{cases} k_{\rightarrow} = k_0 = -k_{\leftarrow} \\ \omega_{\rightarrow} = \omega_0 = \omega_{\leftarrow} \end{cases} \tag{4.3.2a}$$

Its group or envelope velocity is zero by (4.2.10f), but by (4.2.10e) its mean phase velocity is *infinite*.

$$V_{group} = \frac{\omega_{\rightarrow}-\omega_{\leftarrow}}{k_{\rightarrow}-k_{\leftarrow}} = 0 \quad (4.3.2b) \qquad V_{mean\ phase} = \frac{\omega_{\rightarrow}+\omega_{\leftarrow}}{k_{\rightarrow}+k_{\leftarrow}} = \infty, \text{ where: } \begin{cases} k_{\rightarrow} = k_0 = -k_{\leftarrow} \\ \omega_{\rightarrow} = \omega_0 = \omega_{\leftarrow} \end{cases} \tag{4.3.2c}$$

V_{group} is represented by a zero slope arrow connecting the $(k_{\rightarrow}, \omega_{\rightarrow})$ and $(k_{\leftarrow}, \omega_{\leftarrow})$ vectors in Fig. 4.3.2(a) and $V_{mean\ phase}$ is represented by a ∞-slope vector sum of the $(k_{\rightarrow}, \omega_{\rightarrow})$ and $(k_{\leftarrow}, \omega_{\leftarrow})$. V_{group} is zero since standing wave zeros don't move in the laser frame except when the wave is zero everywhere. (Then they jump at infinite $V_{mean\ phase}$ as seen later!) Now consider what the atom going velocity $-u$ sees in Fig. 4.3.2(b).

The atom sees a laser and attached zeros go by at velocity $+u$ in Fig. 4.3.2(b). What wave does the atom see? Frequency $\omega'_{\rightarrow} = b\omega_0$ is blue-shifted by factor b and $\omega'_{\leftarrow} = (1/b)\,\omega_0$ is red shifted by a factor $1/b$ that is *inverse* by time-reversal symmetry. (A receiver tuned to $\omega'_{\rightarrow} = b\,\omega_0$, to hear an ω_0-tuned transmitter approaching at speed u, keeps the same frequency $\omega'_{\rightarrow}$ to *transmit* to an $\omega_0 = (1/b)\,\omega'_{\rightarrow}$ tuned receiver *departing* at speed $-u$. Speedy spacemen must listen and talk on different channels. "Roger and over!")

Now the power of Occam's razor is seen. The colorful axiom (4.3.1) demands that all light waves, regardless of color shifts or direction, have the same phase speed c.

$$\omega'_{\rightarrow} / k'_{\rightarrow} = \omega_0 / k_0 = \omega'_{\leftarrow} / k'_{\leftarrow} = \pm c \qquad (4.3.3)$$

So k-vectors use the same Doppler factors b or $1/b$ as frequency (but with a (-)-sign if headed left).

$$\omega'_{\rightarrow} = b\omega_0 \quad (4.3.4a) \qquad \omega'_{\leftarrow} = (1/b)\omega_0 \quad (4.3.4b)$$

$$k'_{\rightarrow} = b\, k_0 \quad (4.3.4c) \qquad k'_{\leftarrow} = -(1/b)\, k_0 \quad (4.3.4d)$$

Now the standing wave (4.3.2a) in the laser frame $(x, y,..)$ is a *boosted wave* in the atom frame $(x', y',..)$.

$$\begin{aligned} e^{i(k'_{\rightarrow}x' - \omega'_{\rightarrow}t')} + e^{i(k'_{\leftarrow}x' - \omega'_{\leftarrow}t')} &= 2e^{i\left(\frac{k'_{\rightarrow}+k'_{\leftarrow}}{2}x' - \frac{\omega'_{\rightarrow}+\omega'_{\leftarrow}}{2}t'\right)} \cos\left(\frac{k'_{\rightarrow}-k'_{\leftarrow}}{2}x' - \frac{\omega'_{\rightarrow}-\omega'_{\leftarrow}}{2}t'\right) \\ &= 2e^{i\left(\frac{b-1/b}{2}k_0x' - \frac{b+1/b}{2}\omega_0t'\right)} \cos\left(\frac{b+1/b}{2}k_0x' - \frac{b-1/b}{2}\omega_0t'\right) \end{aligned} \qquad (4.3.4e)$$

Implicit is Einstein's idea: an atom has its own space*time* (x', t') frame. So, it sees different group velocity $V'_{group} = \frac{x'}{t'}$ where the new V'_{group} must be velocity u of wave envelope fixed to the laser frame by (4.3.2).

$$V'_{group} = \frac{\omega'_{\rightarrow}-\omega'_{\leftarrow}}{k'_{\rightarrow}-k'_{\leftarrow}} = \frac{b-1/b}{b+1/b}\frac{\omega_0}{k_0} = u\,, \qquad V'_{mean\ phase} = \frac{\omega_{\rightarrow}+\omega_{\leftarrow}}{k_{\rightarrow}+k_{\leftarrow}} = \frac{b+1/b}{b-1/b}\frac{\omega_0}{k_0},$$

$$\frac{V'_{group}}{c} = \frac{b^2-1}{b^2+1} = \frac{u}{c}\,, \qquad \frac{V'_{mean\ phase}}{c} = \frac{b^2+1}{b^2-1} = \frac{c}{u}\,. \qquad (4.3.5a)$$

Then the new $V'_{mean\ phase}$ (in c units) is *inverse c/u*. We solve for *relativistic Doppler blue shift* or b-factor.

$$b^2 - 1 = \frac{u}{c}b^2 + \frac{u}{c}, \quad \text{or:} \quad b^2 = \frac{1+\frac{u}{c}}{1-\frac{u}{c}}, \quad \text{or:} \quad b = \sqrt{\frac{1+\frac{u}{c}}{1-\frac{u}{c}}}\ (Blue\ shift), \quad \frac{1}{b} = \sqrt{\frac{1-\frac{u}{c}}{1+\frac{u}{c}}}\ (Red\ shift), \qquad (4.3.5b)$$

The wave function (4.3.4e) has *Lorentz factors* $\left(b \pm \frac{1}{b}\right)/2$ that depend on the *relativity speed ratio*: $\beta = \frac{u}{c}$.

$$\frac{b+\frac{1}{b}}{2} = \frac{1}{\sqrt{1-\frac{u^2}{c^2}}} = \frac{1}{\sqrt{1-\beta^2}}, \qquad \frac{b-\frac{1}{b}}{2} = \frac{\frac{u}{c}}{\sqrt{1-\frac{u^2}{c^2}}} = \frac{\beta}{\sqrt{1-\beta^2}}, \quad \text{where: } \beta = \frac{u}{c}. \qquad (4.3.5c)$$

Finally, we equate the wave phases of (4.3.4e) to those of (4.3.2a). (This step needs further discussion!)

$$e^{i\left(\frac{b-1/b}{2}k_0x' - \frac{b+1/b}{2}\omega_0t'\right)} \cos\left(\frac{b+1/b}{2}k_0x' - \frac{b-1/b}{2}\omega_0t'\right) = e^{i\left(\frac{\beta}{\sqrt{1-\beta^2}}k_0x' - \frac{1}{\sqrt{1-\beta^2}}\omega_0t'\right)} \cos\left(\frac{1}{\sqrt{1-\beta^2}}k_0x' - \frac{\beta}{\sqrt{1-\beta^2}}\omega_0t'\right)$$

(Equate mean phases, and equate group phases) :: $e^{-i\omega_0 t}$ $\cos k_0 x$ (4.3.5d)

The result is the entire *Lorentz-Einstein transformation* of *special relativity* derived in so few steps!

$$k_0x = \frac{1}{\sqrt{1-\beta^2}}k_0x' - \frac{\beta}{\sqrt{1-\beta^2}}\omega_0t', \qquad \text{or:} \quad x = \frac{1}{\sqrt{1-\beta^2}}x' - \frac{\beta}{\sqrt{1-\beta^2}}ct',$$

$$-\omega_0t = \frac{\beta}{\sqrt{1-\beta^2}}k_0x' - \frac{1}{\sqrt{1-\beta^2}}\omega_0t', \qquad \text{or:} \quad ct = \frac{-\beta}{\sqrt{1-\beta^2}}x' + \frac{1}{\sqrt{1-\beta^2}}ct'. \qquad (4.3.5e)$$

The atom's spacetime (x', ct')-axes are based, as in Fig. 4.2.11, on per-spacetime vectors $\mathbf{K}'_{group}$ and $\mathbf{K}'_{phase}$.

$$\mathbf{K}'_{phase} = (k'_p, \omega'_p) = ((k'_{\rightarrow}+k'_{\leftarrow})/2,\ (\omega'_{\rightarrow}+\omega'_{\leftarrow})/2) \qquad \mathbf{K}'_{group} = ((k'_{\rightarrow}-k'_{\leftarrow})/2,\ (\omega'_{\rightarrow}-\omega'_{\leftarrow})/2))$$

(See Fig. 4.3.2(b).) So, relativity is a natural consequence of very basic wave interference phenomena.

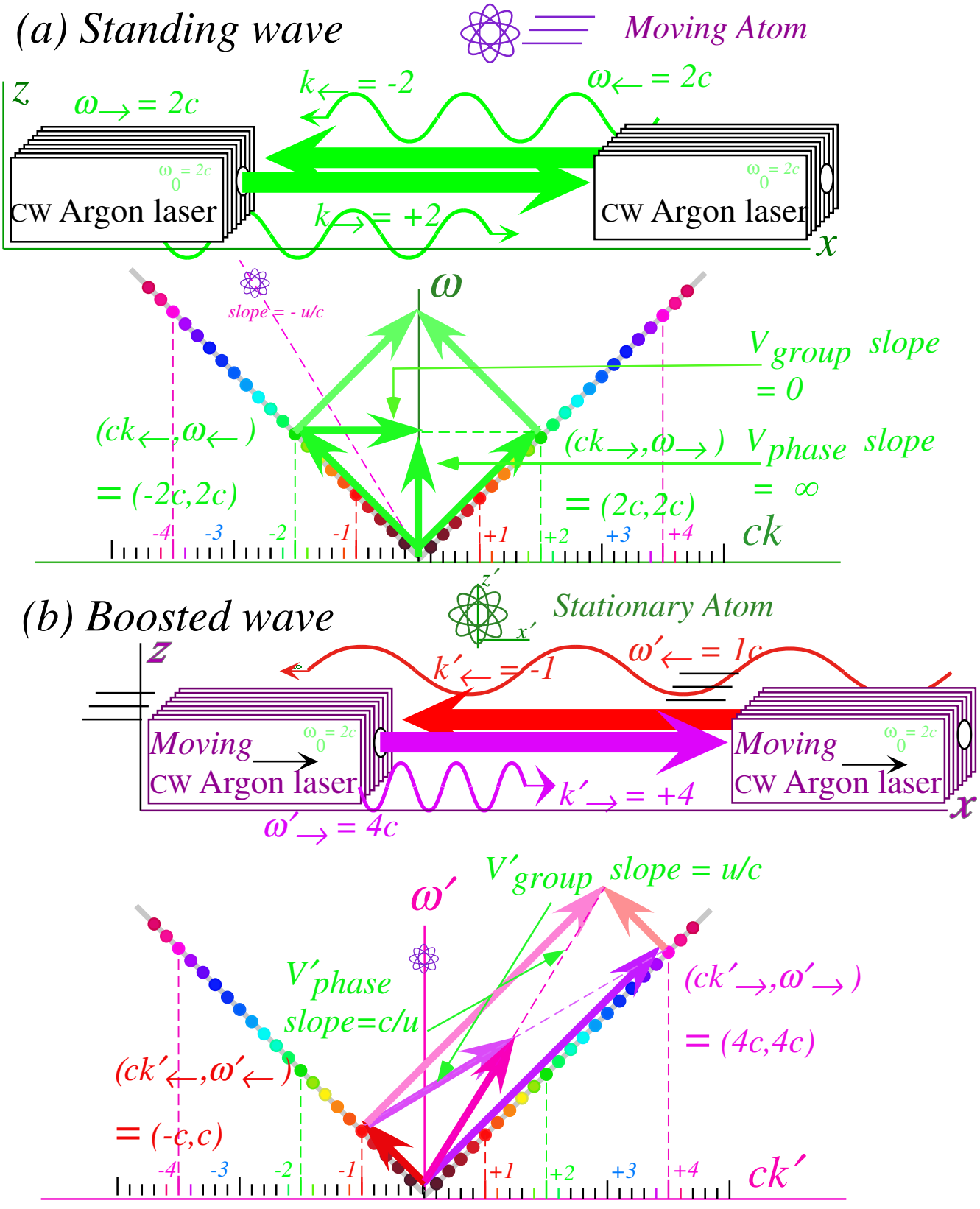

Fig. 4.3.2 Wave (ck-omega)-vector analysis of laser wave group and mean phase velocity.

(b) How'd we get relativity so quickly? Follow the zeros!

Let us look at spacetime plots (by *BohrIt*) of the waves as seen by the lasers that are making them in their own frame, and compare that to the plot of the wave seen by the atom. The first plot, a laser view, is shown in Fig. 4.3.3(a). Notice an orderly square space-time graph grid made by the zeros of the real part of the wave (4.3.2). The imaginary part can be used just as well. (In fact, that's the one plotted to get a zero going through origin $x=0$ at time $t=0$. A sine-envelope wave is needed to do that.)

Here the time or *ct-axis* is vertical as are its companion grid lines representing the stationary-in-laser-frame envelope nodes. Those lines have zero group velocity and zero *x-versus-ct* slopes.

On the other hand, the space or *x-axis* and its parallel companions are horizontal and represent brief moments when the mean phase is zero and the real wave (electric field) is zero everywhere. The space axis lines have infinite mean phase velocity and infinite *x-versus-ct* slope.

The zeros and infinities go away according to the atom in a frame made of a bent-egg-crate of grid lines in Fig. 4.3.3(b). The Cartesian grid in Fig. 4.3.3(a) is replaced by lines running with the slope of the wave group velocity including the new *atomic time* ct'*-axis* crossing the new *atomic space* x'*-axis* whose slope is the mean phase velocity. This is the Lorentz-Minkowski spacetime coordinate grid given by (4.3.5e). End of story! Well, not quite. Such a view opens up a *lot* of questions.

The first is, "Where are Einstein's meter rods and cuckoo clocks?" They're in a museum and good riddance! They never worked very well. The *Global Positioning System (GPS)* uses waves and is trillions of times more precise. Waves are more accurate and intuitive spacetime meter rods and clocks. The key is wave phase invariance of the "readings" on real *vs.* imaginary wave phasor clocks in Fig. 4.2.10. Since about 1960, all CW lasers have had precise Einstein-Minkowski wave coordinates hidden in them.
Phase invariance: Keep the phase!

Wave nodes and zeros are key indicators and measuring tools in physics, optics, and electrical engineering. The white regions that define the grid lines in Fig. 4.3.3 are regions of low or zero electric field where the real part $\mathrm{Re}\Psi \sim \mathrm{Re}E$ of the wave is small. Zero-$\mathrm{Re}\Psi$ means phase is zero modulo $\pi/2$, and the Ψ–phasor clock has struck *12 o'clock* or *6 o'clock* while $\mathrm{Re}\Psi$ is changing its *(±)*-sign.

Each strike of the phasor clock, indeed any tick, can be regarded as a relativistic *event*. It could be arranged that each zeroing of field resulted in a tiny "pop" with the clock's reading, say, $\Phi = 1012\pi$ printed out at that point. Each "pop" and its *phase* reading is a *proper invariant* whose existence and value must be agreed upon by all competent observers though they may disagree about time and spatial location of it. Traveling at high speed alters space *(x meters)*, time *(t sec.)*, *k*-vector *(k per meter)*, and frequency *(ω per-second)* but cannot cause a piece of silicon stamped 1012π to read 2101π or 1012.1π instead!

If there is a simpler or more powerful axiom than the *Colorful Relativity Axiom* (4.3.1) then it would probably be an axiom of phase invariance. We shall take up this idea shortly.

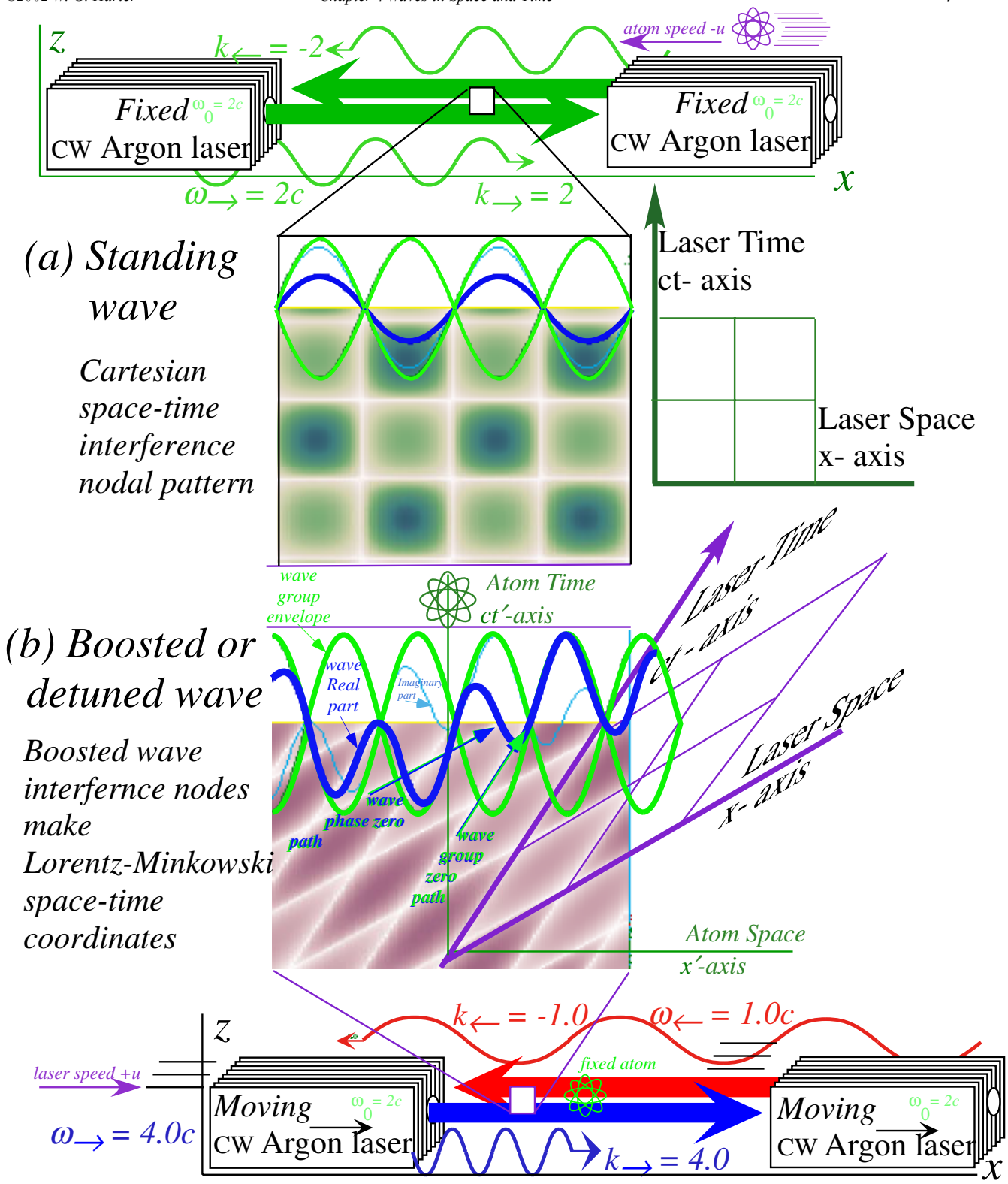

Fig. 4.3.3 Lasers do Cartesian (x,ct)-wave frame for themselves but Minkowski (x′,ct′)-frame for atom. (a) (x,ct) frame: fixed lasers, atom goes –u=-3c/5. (b) (x′,ct′)-frame: lasers go +u=3c/5, atom fixed .

Colorful Relativitistic logic: Simpler or not?

A postulate of relativity for a continuous wave (CW) theory is stated in (4.3.1). Simply put, it says, "*All colors go the same speed c*." The usual relativity postulate uses light flashes or optical pulse trains (OPT) which all go the same speed. The two axioms are equivalent, but a CW approach, with just two frequencies, has a power and simplicity that an OPT approach, with innumerable frequencies, lacks.

The idea that a light pulse appears to have the same speed for all observers, be they fast or slow, is counter-intuitive. Invariant light pulses that can't be approached seem mythical. Instead, we propose a more intuitive idea that a continuous 200THz light wave has different frequency (*color*) for different speeds, say, 400Thz approaching and 100Thz going away. Indeed, the Doppler shift, in one form or another, has been taught since Christian Doppler introduced it in the 1600's.

Still, electromagnetic waves have a unique but simple property: CW radiation of, say, 400Thz is the same as 400Thz light made by an approaching 200Thz source, or by you approaching that source, or by a fixed source tuned up to 400Thz, or by a slowly approaching 399THz source, and so on. In contrast, sound waves of, say, 400Hz heard coming from a car horn approaching is not the same as another 400Hz wave heard while approaching that fixed source. The wavelength and speed of one 400Hz sound wave will differ from the other because the speed of a sound wave depends on the relative speed of a mechanical medium (wind, liquid, or solid) carrying it. Not so for light in a vacuum. It seems not to have anything to help "blow it along."

So while the speed c and wavelength λ of a given frequency-ν sound wave might vary between, say, $c = \lambda\nu$ and $c' = \lambda'\nu$, a ν=400THz red light will always be seen to possess the same speed c and wave length λ by any observer as it beams through a vacuum devoid of interfering mechanical media. That is part of a CW relativistic postulate: allowing only one wavelength $\lambda(\nu)$ for each frequency ν, or stated conversely, only one frequency $\nu(\lambda)$ for each wavelength λ. That is simpler and less surprising than the alternative, having different "kinds" of light for each ν, a much more complicated situation.

It turns out that quantum matter waves also have a definite frequency $\nu(\lambda)$ assigned to each λ by a function called a *dispersion function*. Dispersion functions $\nu(\lambda)$ or $\omega(k)$ are the end-all-be-all for any wave theory; $\omega(k)$ determines how a wave pulse disperses or spreads as it propagates. The optical dispersion function is simplest of all, a linear relation $\omega(k)=ck$, or equivalently, a single wave speed $c = \lambda\nu = \lambda'\nu'$ for all frequencies or wavelengths $(c = \lambda\nu = constant = 2.99792458E8 ms\text{-}1)$.

Constant c completes the CW postulate: *All colors go the same speed in a vacuum for any observer*. It is simple, less surprising, and in accordance with the best frequency experiments showing non-dispersal of vacuum light pulses. But, the CW postulate, however logical or conventional it might now seem, still appears to imply a mythical invariant pulse having an unapproachable speed c. In fact, this *is* a myth that needs closer examination as will be done in the following chapters.

(c) Phase invariance in spacetime (x,ct) or per-spacetime (ck,ω) plots

The colorful axiom (4.3.1) says light phase velocity is invariant. We now argue that each plane $e^{i(kx-\omega t)}$-wave has an *invariant phase* $\Phi = kx-\omega t$. No matter who sees different (Doppler shifted) values $[(ck,\omega),(ck',\omega'),(ck'',\omega''),\ldots]$ for k-vector (or wavelength $\lambda=2\pi/k$) and frequency (or period $\tau=2\pi/\omega$) and Lorentz transformed values $[(x,ct),(x',ct'),(x'',ct''),\ldots]$ of space and time, they must come up with the same value for each "strike" Φ on a wave phase clock. (Otherwise they're ruled incompetent!)

$$\Phi = kx - \omega t = k'x' - \omega' t' = k''x'' - \omega'' t'' = \ldots \qquad (4.3.6a)$$

Does this axiom hold for any given wave at all its spacetime points? Suppose we ask, "How fast goes the 12 o'clock *(phase* $\Phi=0$*)* strike?" If phase Φ is invariant, each observer answers, in turn,

$$\Phi = 0 = kx - \omega t = k'x' - \omega' t' = k''x'' - \omega'' t'' \ldots \quad \text{or :} \quad \frac{x}{t} = \frac{\omega}{k}, \quad \frac{x'}{t'} = \frac{\omega'}{k'}, \quad \frac{x''}{t''} = \frac{\omega''}{k''}, \ \ldots \qquad (4.3.6b)$$

That would just be their readings of the wave's phase velocity. For a lightwave they all say, *"c!"* Phase-invariance axiom (4.3.6a) is consistent with *"All colors go c"*-axiom (4.3.1) or (4.3.3), but, it is much deeper. It applies to the mean phases and group phases in (4.3.5d). Indeed, it applies to *all* waves and *all combinations of all waves* including quantum matter waves of which we are made! How can this be?

This requires linearity of Lorentz transformation (4.3.5e) and its inverse *(β→–β or ρ→–ρ)*

$$\begin{aligned} x &= x'\cosh\rho - ct'\sinh\rho \\ ct &= -x'\sinh\rho + ct'\cosh\rho \end{aligned} \quad (4.3.7a) \qquad \begin{aligned} x' &= x\cosh\rho + ct\sinh\rho \\ ct' &= x\sinh\rho + ct\cosh\rho \end{aligned} \quad (4.3.7b)$$

Modern notation uses hyperbolic functions of *relativistic rapidity* ρ. (The geometry of the rapidity "angle" ρ is clarified in Sec. 4.4 (b). Here it's just a shorthand notation based on an identity $\cosh^2\rho - \sinh^2\rho = 1$.)

$$\cosh\rho = \frac{1}{\sqrt{1-\beta^2}} \quad (4.3.7c) \qquad \sinh\rho = \frac{\beta}{\sqrt{1-\beta^2}} \quad (4.3.7d) \qquad \tanh\rho = \beta = \frac{u}{c} \quad (4.3.7e)$$

The laser frame *x*-unit *(x=1, ct=0)* transforms by (4.3.7b) to an atom-frame point *(x′=coshρ, ct′=sinhρ)*.

$$x' = x\cosh\rho + ct\sinh\rho = \cosh\rho \qquad ct' = x\sinh\rho + ct\cosh\rho = \sinh\rho. \quad (4.3.7f)$$

Phase invariance (4.3.6a) applies to *any* *k*-vector-frequency pair *(k,ω/c)* or spacetime *(x,ct)* pair. Let us take a pair *(x,ct)=(1,0)* that implies *(x′=coshρ, ct′=sinhρ)* and a pair *(x,ct)=(0,1)* that implies *(x′=sinhρ, ct′=coshρ)*

$$k = kx - \omega t = k'x' - \omega' t' = k'\cosh\rho - \frac{\omega'}{c}\sinh\rho \quad \text{for: } x = 1 \text{ and: } ct = 0. \quad (4.3.8)$$

$$-\frac{\omega}{c} = kx - \omega t = k'x' - \omega' t' = k'\sinh\rho - \frac{\omega'}{c}\cosh\rho \quad \text{for: } x = 0 \text{ and: } ct = 1. \quad (4.3.9)$$

So, relations (4.3.7b) make each *(ck,ω)*-per-spacetime pair transform just like spacetime *(x,ct)*.

$$\begin{aligned} ck &= ck'\cosh\rho - \omega'\sinh\rho \\ \omega &= -ck'\sinh\rho + \omega'\cosh\rho \end{aligned} \quad (4.3.10a) \qquad \begin{aligned} ck' &= ck\cosh\rho + \omega\sinh\rho \\ \omega' &= ck\sinh\rho + \omega\cosh\rho \end{aligned} \quad (4.3.10b)$$

So does a sum $(ck_{phase}, \omega_{phase}) = \big((ck_1 + ck_2), (\omega_1 + \omega_2)\big)/2$ for a wave of speed $V_{phase} = (\omega_1 + \omega_2)/(k_1 + k_2)$ or a difference $(ck_{group}, \omega_{group}) = \big((ck_1 - ck_2), (\omega_1 - \omega_2)\big)/2$ for a wave of speed $V_{group} = (\omega_1 - \omega_2)/(k_1 - k_2)$. In fact, any linear combination $(ck_{12}, \omega_{12}) = A(ck_1, \omega_1) + B(ck_2, \omega_2)$ of optical *(ck,ω)*-pairs transforms this way.

$$\begin{aligned} ck_{12} &= ck'_{12}\cosh\rho - \omega'_{12}\sinh\rho \\ \omega_{12} &= -ck'_{12}\sinh\rho + \omega'_{12}\cosh\rho \end{aligned} \quad (4.3.10c) \qquad \begin{aligned} ck'_{12} &= ck_{12}\cosh\rho + \omega_{12}\sinh\rho \\ \omega'_{12} &= ck_{12}\sinh\rho + \omega_{12}\cosh\rho \end{aligned} \quad (4.3.10d)$$

Pair (ck_{12}, ω_{12}) may lie on ±*c*-lightcone line or else on *hyperbolic invariant* curves above or below them.

$$\omega_{12}^2 - (ck_{12})^2 = \omega'^2_{12} - (ck'_{12})^2 = (2AB)\,\frac{D}{c} \quad (4.3.11a)$$

Locus of (ck_{12}, ω_{12}) depends on an invariant *wave-propagation discriminant* D. (Recall also (4.2.11).)

$$D = \mathbf{K_1} \times \mathbf{K}_2 = \omega_1 ck_2 - \omega_2 ck_1 = \omega'_1 ck'_2 - \omega'_2 ck' = \begin{cases} 2c\omega_1\omega_2 = 2c\omega_0^2 & (\text{Counter - propagate}) \\ 0 & (\text{Co - propagate}) \end{cases} \quad (4.3.11b)$$

Co-propagation ($\omega_1/k_1 = \omega_2/k_2 = \pm c$) has *D=0* in (4.3.11) so wave lattices collapse onto ±*45°* lines $\omega_{12} = \pm c\, k_{12}$ as in Fig. 4.2.12. Counter-propagation ($\omega_1/k_1 = -\omega_2/k_2 = \pm c$) turns a wave lattice in Fig. 4.2.11 into a Lorentz grid of Fig. 4.3.4. (4.3.11a) is a hyperbola that crosses ω-axis at $\pm\omega_1$ for *(A=1/2=B)* or *ck*-axis for *(A=1/2=-B)*.

$$\omega_{12}^2 - (ck_{12})^2 = \begin{cases} +\omega_0^2 & \mathbf{K}_{\text{phase}} \text{ wave: } (A = 1/2 = +B) \\ -\omega_0^2 & \mathbf{K}_{\text{group}} \text{ wave: } (A = 1/2 = -B) \end{cases} \quad (4.3.12)$$

Recall that the Doppler relations (4.3.3), by time reversal, give blue shift $\omega_1 = b\omega_0$ inverse to red shift $\omega_2 = 1/b\omega_0$ so the product $\omega_1\omega_2 = \omega_0^2 = \omega'_1\omega'_2$ is frame-invariant. Area $D = \mathbf{K}_1 \times \mathbf{K}_2$ is thus invariant.

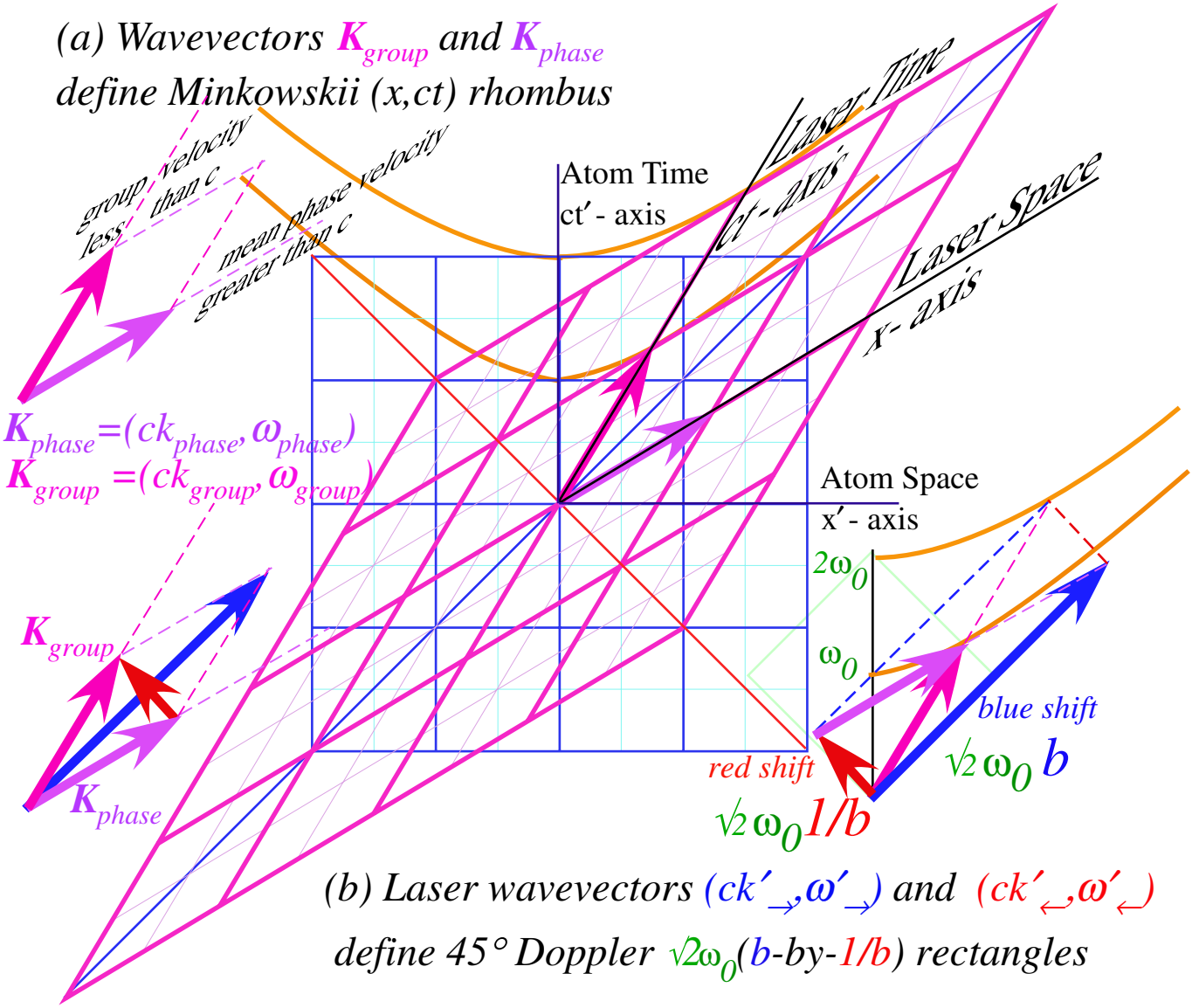

Fig. 4.3.4 Spacetime paths of laser standing wave zeros using (a) V_{group} and V_{phase}. (b) Doppler shifts.

Rhombic spacetime wave lattice paths shown above in Fig. 4.3.4 reconstruct the ones in Fig. 4.3.3(b). Fig. 4.3.4(a) shows the V_{group} and $V_{mean\ phase}$ slopes u/c and c/u (V_{group} is slower than c and $V_{mean\ phase}$ is faster than c) of a rhombic (x,ct)-lattice based on $(ck'_{group}, \omega'_{group})$ and $(ck'_{phase}, \omega'_{phase})$ vectors. These are half-diagonals of 45°-tipped rectangles shown in Fig. 4.3.4(b). Each rectangle has a longer side of length $b\sqrt{2}\omega_0$ that is the blue shifted laser wave vector $(ck'_{\rightarrow}, \omega'_{\rightarrow})$ and a shorter side of length $1/b\ \sqrt{2}\omega_0$ that is the red shifted wave vector $(ck'_{\leftarrow}, \omega'_{\leftarrow})$ of the oppositely moving laser. (Here, $b=2$ again.) Rhombic cell vectors frame an invariant area ω_0^2 and lie on hyperbolas of radius ω_I as given by (4.3.12). The rhombic cells have half the area ($2\omega_0^2$) of their enclosing $b\sqrt{2}\omega_0$-by-$1/b\ \sqrt{2}\omega_0$ rectangle whose diagonal lies on an invariant hyperbola of double-radius $2\omega_I$, twice that of the rhombic half-diagonal's hyperbola.

Fig. 4.3.4 emphasizes continuous wave (CW) phase paths. The following Fig. 4.3.5 shows pulsed wave (PW) paths that we might see if the lasers just spat out Newtonian corpuscles or incoherent pulses.

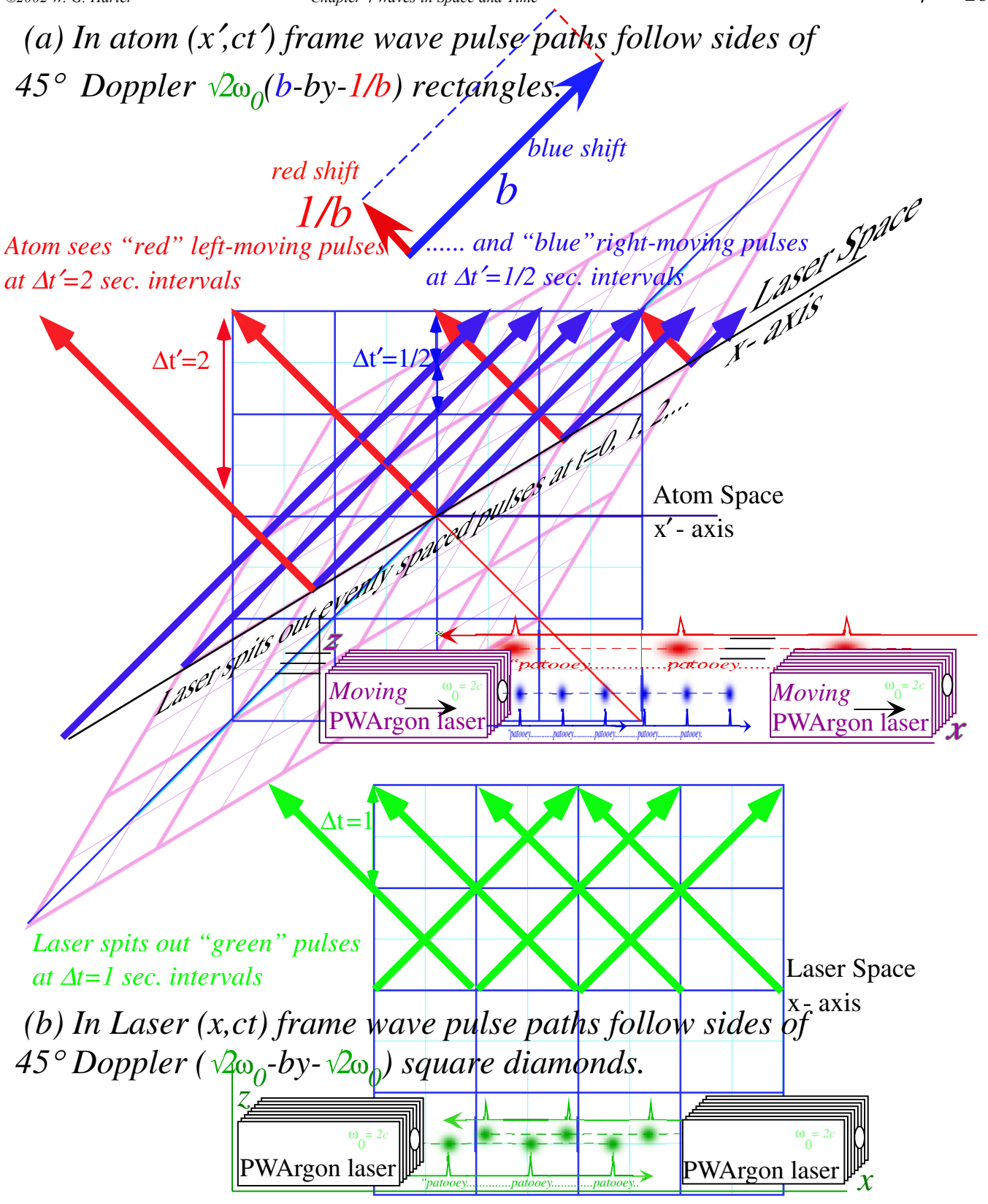

Fig. 4.3.5 Spacetime paths of laser pulses or "particles" as seen by (a) Atom frame. (b) Laser frame.

(d) Pulsed Wave (PW) and "particle" paths *versus* Continuous Wave (CW) laser

If the lasers in the preceding figures were to spit out pulses at *1 sec*. intervals, then the Minkowski wave interference grid of Fig. 4.3.3 and Fig. 4.3.4 is replaced by a latticework of *45°* rectangles that may be thought of as pulse or particle paths as noted in Fig. 4.2.11. Rectangle aspect ratio is that of the Doppler *b*-shift squared, that is, $b^2=4$ or *4-to-1* in the case shown in Fig. 4.3.5(a).

Such paths result from the lasers emitting pulses at *1 sec.* intervals in both directions as shown in Fig. 4.3.5(b). Newton viewed light as a beam of "corpuscles" that occasionally has "fits" (his term for what later was seen as wave interference.) The "corpuscles" of modern quantum theory are called *photons* but are not simply wave pulses. Nevertheless, we may imagine photons follow pulse paths.

The atom frame sees Doppler shifted rates of pulse production just as it saw the color frequencies shifted by the same *b*-factor of *2* on the "blue" side and *1/2* on the "red" side. The quotes around the color names are to remind us that very sharp pulses are "white" combinations of many colors interfering all at once as will be explained later. Fig. 4.3.5 shows broad pulses, say $\Delta t \sim 10^{-2}$ second, plotted once a second on a length scale of light-seconds. Such broad pulses do not compromise their "color" significantly as shown in simulations of Fig. 5.3.2 in the following Chapter 5.

The "Now" line(s)

At each instant of time in each frame there is a line of points that the frame calls *NOW*. For the atom *(x′,ct′)*-frame in Fig. 4.3.5(a) the *NOW* line for *(x′,ct′=0)* is the horizontal *x′*–axis. Meanwhile, for the laser *(x,ct)*-frame in Fig. 4.3.5(a), the *NOW* line for *(x,ct=0)* is the *x*–axis which is tipped up at the velocity slope *u/c*. The laser would prefer to plot its frame as shown in Fig. 4.3.5(b) with its *NOW* line horizontal. Then the atom *NOW* line for *(x′,ct′=0)* and *x′*–axis would tip *down* at slope *–u/c*.

If the laser spits out pulses at equal space intervals along its *(t=0)-NOW* line as shown in Fig. 4.3.5(b) then the pulses go off at speed *±c* and are seen to pass any space point at equal time intervals regardless of direction of travel. Not so, according to the atom frame as plotted in Fig. 4.3.5(a). The atom faults the laser for not releasing those pulses on a *NOW* line belonging to the atom and thereby causing the right-moving blue pulses to "pile-up" and hit rapidly like "*clink, clink, clink, clink, clink,…*" while the left moving red pulses spread out and hit less often like "*clunk,…., clunk,….*"

The delay of the "clunkers" is made worse for the atom by the fact that their release locations are stretched out from, say, laser point *(x=1,ct=0)* to atom point *(x′=cosh β, ct′=sinh β)* as given by (4.3.7f). In order to appreciate the ways that time definition may seem out-of-whack, we need to explore further the geometry of the wave and pulse path coordinate systems. This is addressed in the following section.

4.4 Geometry and Invariance in Lorentz transformations

The Lorentz transformations (4.3.7) relate the two coordinate systems in Fig. 4.3.3 and Fig. 4.3.5. To check (4.3.7a) note that the time axis $x= 0 = x'-\beta ct'$ gives a line $x'=\beta ct'=ut'$ consistent with the figures having a laser traveling positively at velocity $u=\beta c$. Fig. 4.4.1 shows a close-up view of the *(+,+)* quadrant including the geometry of the well-known *Einstein time dilation* Δt (which is *125%* for $\beta=3/5$)

$$\Delta t'/t' = \frac{1}{\sqrt{1-\beta^2}} = cosh\rho \approx 1+\frac{\rho^2}{2} \quad (\text{for } \rho \approx \beta << 1), \tag{4.4.1a}$$

and the well known *Lorentz-Fitzgerald length contraction* ΔL (which is *80%* for $\beta=3/5$).

$$\Delta L'/L' = \sqrt{1-\beta^2} = sech\rho \approx 1-\frac{\rho^2}{2} \quad (\text{for } \rho \approx \beta << 1) \tag{4.4.1b}$$

These are each second order effects for small velocity while the *Doppler shift* $\Delta\omega$ is a *first* order one.

$$\Delta\omega'/\omega' = \frac{\sqrt{1+\beta}}{\sqrt{1-\beta}} = \frac{1+\beta}{\sqrt{1-\beta^2}} = e^{\rho} \approx 1+\rho \quad (\text{for } \rho \approx \beta << 1) \tag{4.4.2}$$

While Lorentz length contraction and Einstein time dilation are the first topics in most old-fashioned relativity treatments, the Doppler shifts are far greater effects. Also, Doppler is the primary concept for wave relativity. Its derivation (4.3.5) is comparatively clear and simple. Anyone who has gotten a speeding ticket from a Doppler meter-yielding cop has felt its effects. To feel the second-order dilation or contraction effects would involve, at the very least, an astronomical speeding ticket!

As discussed in Sec. 4.3.(c), $\beta = 3/5$ Doppler blue and red shifts correspond to *(+,+)* diagonal expansion of *200%* and *(+,–)*-diagonal foreshortening of *50%* , respectively. As shown in Fig. 4.4.1, the quantities $\Delta L'$ and $\Delta t'$ correspond, respectively to only *80%* and *125%* Minkowski graph projections from the unit grid markers *(x=1.0) and (ct=1.0)* in the laser frame onto the atom's *(x') or (ct')* axes.

The atom says, "Laser's unit length has contracted to *0.8*, but his unit time has dilated to *1.25*!" However, projections from *(x'=1.0,ct'=1.0)* in the atom frame to the laser's *(x,ct)* axes tell a seemingly contradictory story. The laser says, "No! It's the atom's unit length which has contracted to *0.8*, and it's the atom's unit time that has dilated to *1.25*!" It gets to be a serious argument because *they are both right*!

The resolution of this paradox centers on the definition of *now* or *simultaneity.* The projections in Fig. 4.4.1 respect the *NOW*-line of the atom that is always parallel to his horizontal *x'*-axis in this graph. He asks, "Along what horizontal now-line is the laser tick *ct=1.0*?" (At atom now-line *ct'=1.25*.)And, "What is the distance between the laser's rear *(x=0)* and front *(x=1.0)* along my *ct'=0* now-line?" (The distance is $\Delta L=0.8$ along any of the atom's now-lines.)

However, the laser's now-line is always parallel to his *x*-axis so it slopes up by *3/5* in Fig. 4.4.1. (Presumably, *x* would be horizontal if you asked laser people to draw the graph, but, then the atom's *x'*-axis would tip down.) So the laser's projections also show a *1.25* time dilation and a *0.8* length contraction, just like those claimed by the atom in Fig. 4.4.1. (The space and time grid markers follow invariant hyperbolas (4.3.12) shown in the figure. Invariants are discussed at length in the following chapter.)

Perhaps, it is surprising that old-fashioned texts do not mention the reverse of the Lorentz length contraction and Einstein time dilation. Just as real and present in Fig. 4.4.1 are *length dilation* and *time contraction* effects which the atom frame records for a speeding laser system.

Dropping a perpendicular (not shown in Fig. 4.4.1) from the laser point *(x=1.0, ct=0.0)* to the atom's *x′*-axis shows that the laser unit length at its zero-time *(ct=0)* has dilated by *125%* to *x′=1.25* at atom time *ct′=0.75*. (By that time the laser origin has moved to *x′=(3/4)(4/5)=0.45* leaving the old Lorentz contracted length of exactly *1.25-0.45=0.8*. But, whom are you going to believe here?)

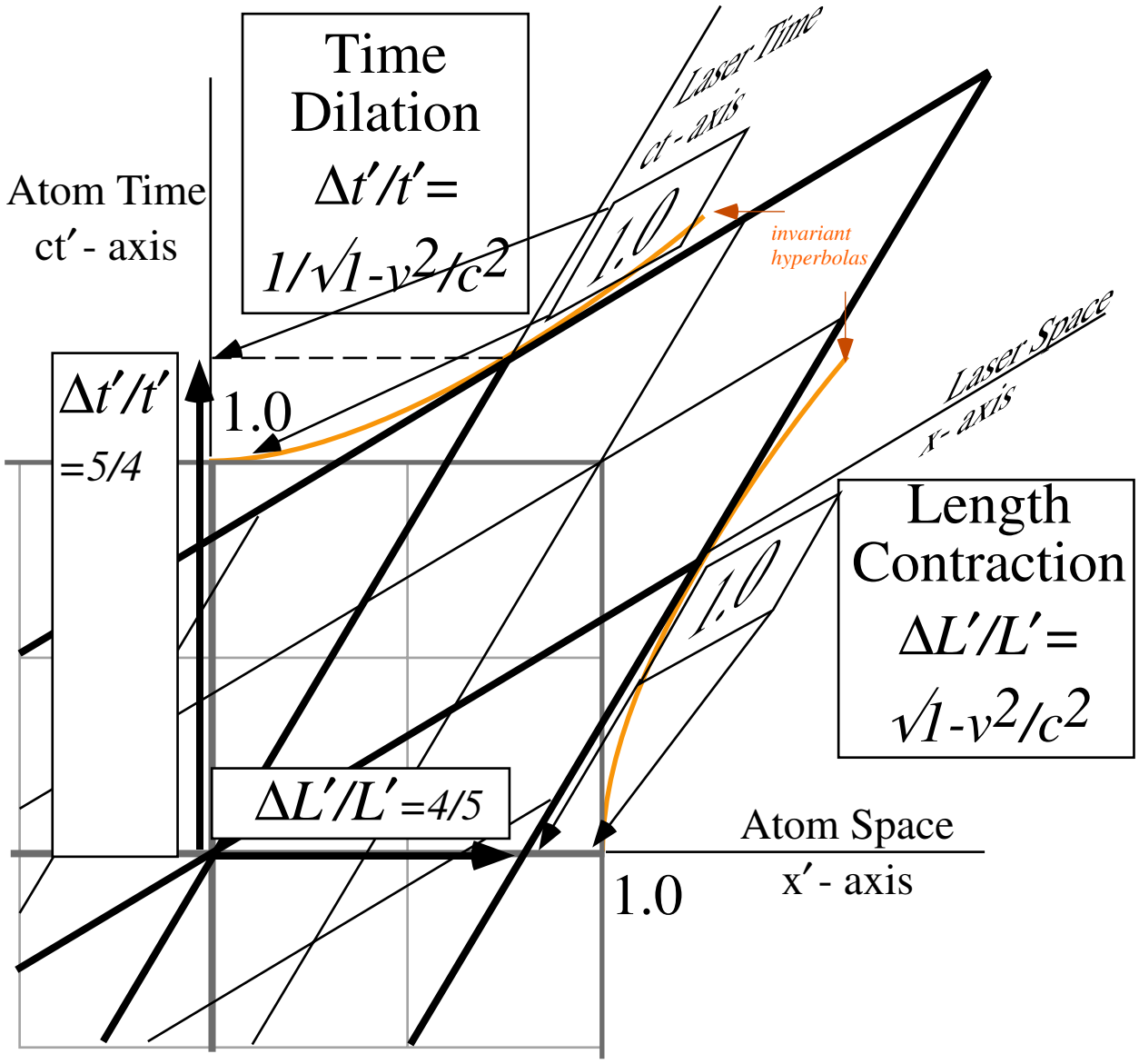

Fig. 4.4.1 Minkowski plot showing time dilation and Lorentz contraction effects at u=3c/5.

Time contraction is relevant to the atom who asks, "When do I experience a laser phasor ticking its unit time *ct′=1.00* ?" That time point at the atom's origin *(x=0)* is a "contracted" time of *ct=0.8*. But, the laser *origin* doesn't tick *1 o'clock* until the old dilated atom time of *ct=1.25*. It's all relative!

(a) Geometric construction of relativistic variables and invariants

Fig. 4.4.2 shows a geometric construction of relativistic quantities in the order that they are normally introduced in conventional algebraic treatments starting with velocity u/c in Fig. 4.4.2(a) then followed by Lorentz contraction factor $\sqrt{1-u^2/c^2}$ and *stellar aberration angle* σ in Fig. 4.4.2(b).

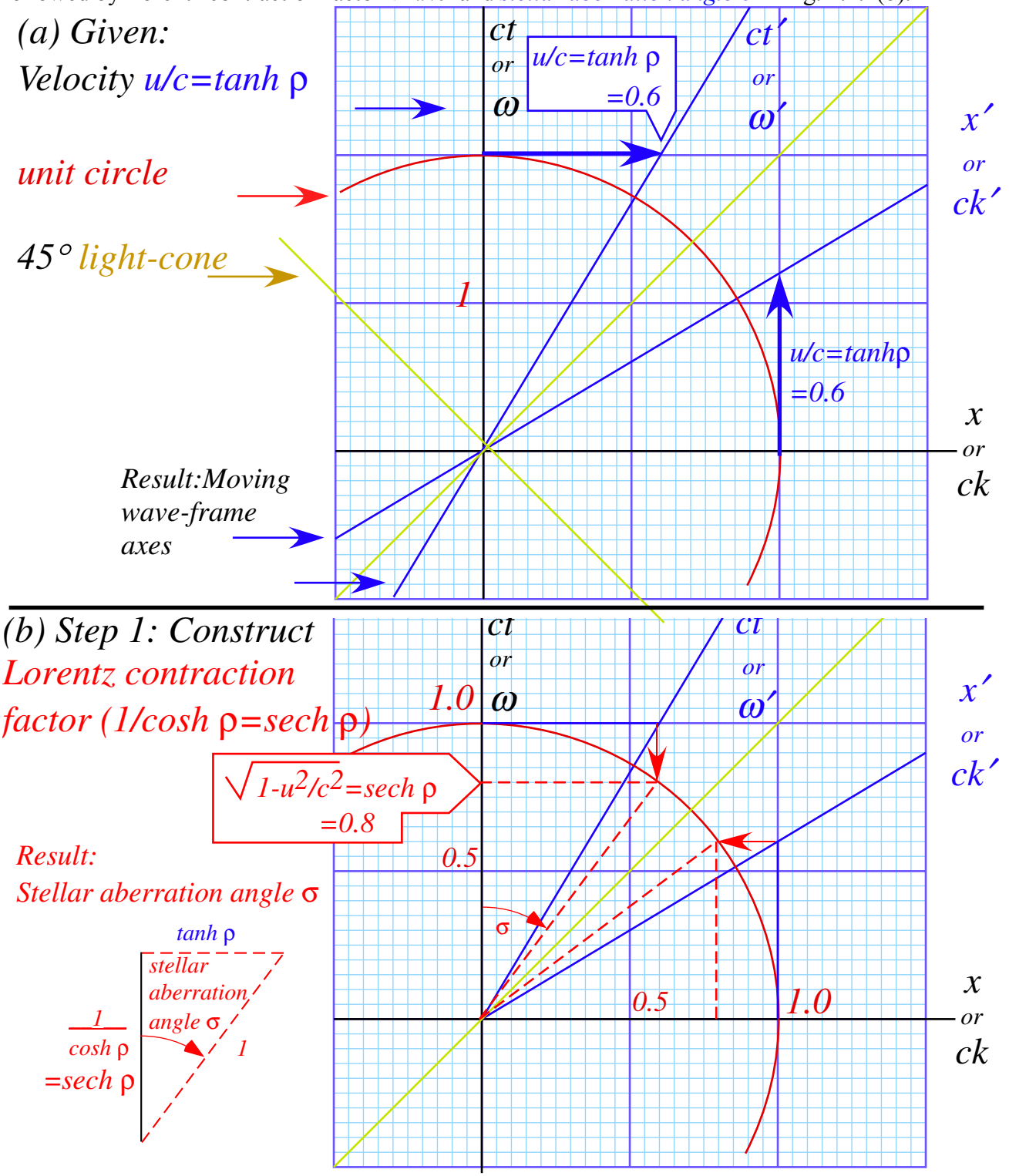

Fig. 4.4.2 Geometry of relativistic quantities. (a) Velocity u/c=3/5. (b) Related Lorentz contraction.

Lorentz contraction and aberration angle

The *stellar aberration angle* ($\sigma=atan(sinh\ \rho)$) is the angle a telescope must tip to catch starlight coming in normal to the telescope's direction of motion. This is discussed more fully in the development of three-dimensional space and four-dimensional wave coordinates. (See Chapter 6.)

The physical significance of *Lorentz contraction factor* $sech\ \rho$ has been noted in the discussion of Fig. 4.4.1. Here in Fig. 4.4.2(b) the plane geometric construction starts by dropping a perpendicular from the unit abscissa (or ordinate) toward the unit circle. The intercept is the altitude (or base) of the stellar aberration triangle whose hypotenuse is unity and base (or altitude) is the Lorentz contraction factor.

Lorentz-Einstein factors

Lorentz-Einstein *asimultaneity factor* $sinh\ \rho$ and *time-dilation factor* $cosh\ \rho$ are obtained geometrically in Fig. 4.4.2(c). Asimultaneity coefficient $sinh\ \rho$ is found by extending the stellar-aberration hypotenuse from the unit circle back to the unit abscissa (or ordinate) where the intercept distance is $sinh\ \rho$. Finally, a line perpendicular to the unit line intercepts the space (or time) axis at a point whose coordinates ($sinh\ \rho$, $cosh\ \rho$) (or ($cosh\ \rho$, $sinh\ \rho$)) include the time-dilation $cosh\ \rho$, as well.

Both coefficients $sinh\ \rho$ and $cosh\ \rho$ approach half-exponential functions $e^{+\rho}/_2$ for large ρ, with dilation $cosh\ \rho$ bigger than asimultaniety $sinh\ \rho$ by $e^{-\rho}$, the red-shift. So, the $(sinh\ \rho\ ,\ cosh\ \rho)$-triangle slope can only approach the $45°$ or unit slope that represents the speed-of-light horizon. However, only zero and ±infinity limit the slope of the stellar-aberration hypotenuse. As speed approaches c, stars appear to swing in front arbitrarily close to the direction of travel.

In the non-relativistic limit of low speeds $(u<<c)$, the asimultaneity factor $sinh\ \rho$ is first order in velocity u or rapidity ρ while the time-dilation factor $cosh\ \rho$ remains equal to 1 and grows only by second order term $(u/c)^2/_2$. Having $cosh\ \rho \sim 1$ and $sinh\ \rho \sim \rho \sim u/c$ simplifies the construction in Fig. 4.4.2(c). In this limit the stellar aberration $(tanh\ \rho\ ,\ 1)$-triangle reduces to a $(u/c,1)$-triangle and becomes equal to the coordinate $(sinh\ \rho\ ,\ cosh\ \rho)$-triangle that reduces to a $(u/c,1)$-triangle, too.

For speeds low enough to ignore time dilation, there is only one pair of triangles: a $(u/c,1)$-triangle defining the time axis and a $(1,\ u/c)$-triangle defining the space axis. The non-relativistic limit is *not* the same as the so-called Galilean limit that has no asimultaneity factor $sinh\ \rho$ at all and would fail to tip the space axis $(1,\ u/c)$. The asimultaneity factor is a *first* order one giving $sinh\ \rho \sim u/c$ and *not* zero.

Doppler factors

Both Doppler factors $b=e^{+\rho}$ and $b^{-1}=e^{-\rho}$ are first order in u and are fundamental to the wave based development stated by (3.2.5). Here $e^{+\rho}$ and $e^{-\rho}$ are the last to appear in the construction ending with Fig. 4.4.2(d). This last step simply strikes an arc of radius $sinh\ \rho$ from the time dilation point $cosh\ \rho$ so as to locate the sum $e^{+\rho}= cosh\ \rho+sinh\ \rho$ and difference $e^{-\rho}= cosh\ \rho–sinh\ \rho$ that are the Doppler factors.

The construction is quite straightforward as presented by Fig. 4.4.2(a-d), but it is even simpler if the Doppler factor b is given first. A lattice of b-by-b^{-1} rectangles defines the Doppler pulse-paths in Fig. 4.4.2(d). Then the rectangle diagonals give the $(sinh\ \rho\ ,\ cosh\ \rho)$-triangles directly and the rest follows.

(c)

Step 2: Construct Lorentz factors (sinh ρ , cosh ρ)

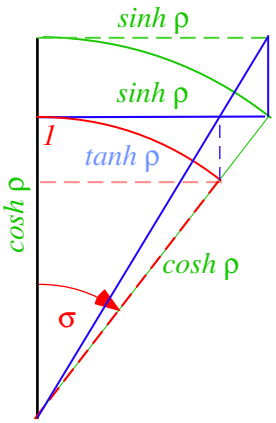

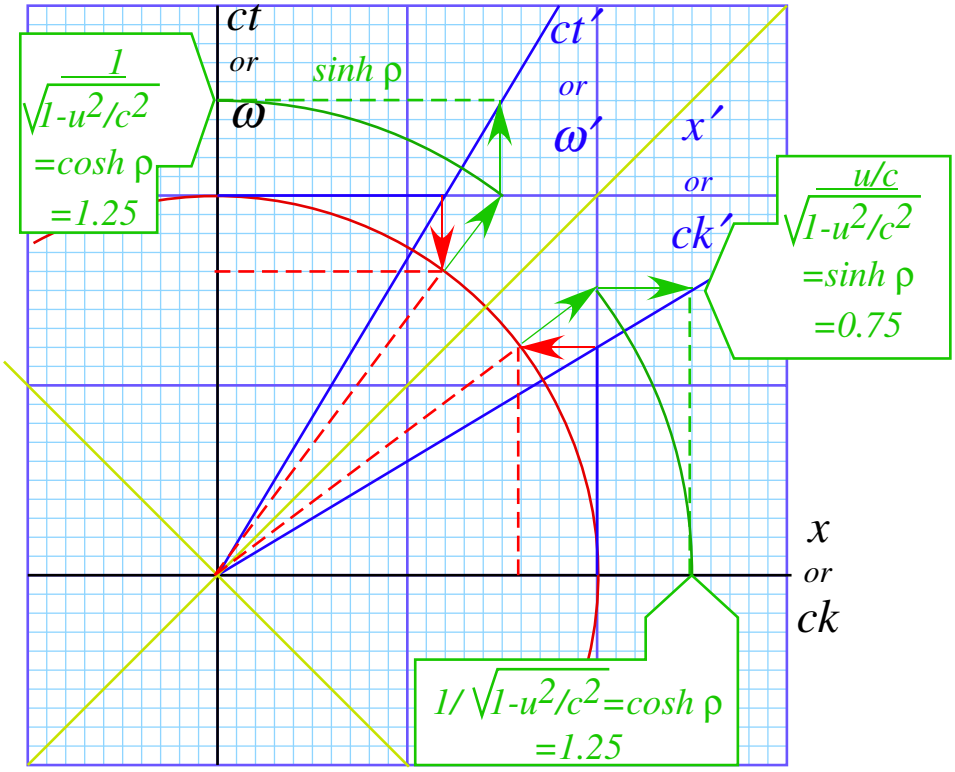

(d)

Step 3: Construct Doppler factors ($e^{+\rho}$, $e^{-\rho}$) and paths.

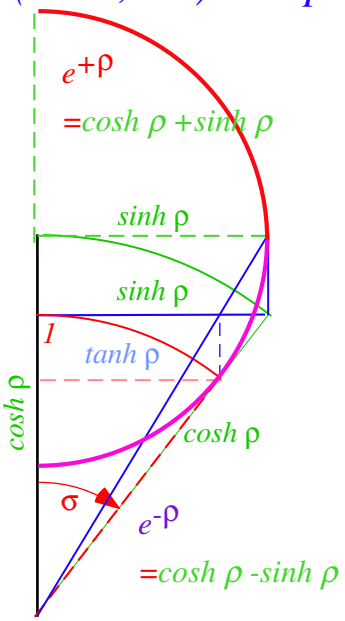

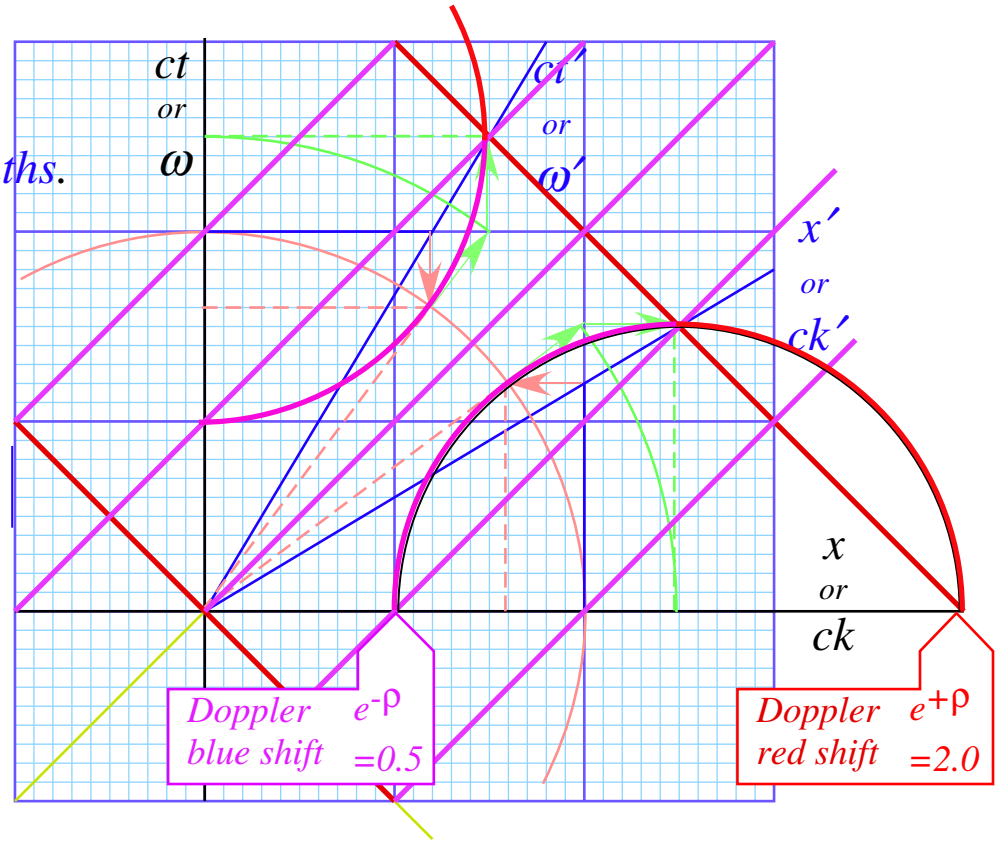

Fig. 4.4.2 (contd.) *(c) Einstein-Lorentz time-dilation and asimultaniety factors.*
(d) Doppler shift factors and particle-pulse paths.

Coordinate lines and invariants for waves or pulses: Baseball diamond geometry

Both the geometric construction and algebraic development of relativity and quantum wave mechanics is simplified and clarified by starting with wave Doppler factors. As shown in Fig. 4.4.2(d) (also in Fig. 4.3.5), the Doppler factors b and b^{-1} are the intercept intervals of the $\pm 45°$ trajectories of optical pulses in a moving frame. (In all cases illustrated, the Doppler factor is $b=2.0$ for a frame is moving at $u=3c/5$.)

The fundamental geometry of b-by- b^{-1} Doppler rectangles given in Fig. 4.4.2(d) is repeated in Fig. 4.4.3(a) that also shows the rectangle diagonals defining space and time axes and grid lines. Each figure has an inset sketch of its fundamental geometry. The inset in Fig. 4.4.3(a) is the simpler of the two because it is based on the b-by- b^{-1} Doppler rectangle. If there is a single geometric construction that represents modern physics as we currently understand it, then this must be the one. It is a "slide rule" for relativistic spacetime and quantum wave mechanics based entirely upon properties of light.

The Doppler rectangle is a distortion of a square diamond quite like a baseball diamond. It starts out with equal right and left arms (the "first" and "third" baselines) of length $\omega_0\sqrt{2}$ intersecting at origin or "home plate" at the bottom. The diamond center $(0, \omega_0)$ is the "pitcher's mound." At the top $(0, 2\omega_0)$ of the diamond shaped "infield" is the "2nd base" vector that is the sum of the "1st " and "3rd " base vectors.

Doppler blue shift b causes the home-to-first baseline to stretch by b, but it must remain on the $+45°$ right "foul-ball-line" by the rule of the *Colorful Axiom* (3.3.1) that demands constant lightspeed. The time reversal axiom then requires that the home-to-third baseline to shrink to $1/b$ (the Doppler red-shift factor) while staying on the $-45°$ left "foul-ball-line" according (3.3.1). The central pitcher mound and the second base vector lie on the sum of 1st and 3rd base vectors that tips as blue shift b increases.

When b is only slightly greater than one, the distance from home to the pitcher's mound or to 2nd base grows only to *2nd order*. (This is the non-relativistic limit mentioned earlier.) However, as b grows without limit so do the distances to 1st and 2nd base as 2nd base follows a mass-shell hyperbola that brings it ever closer to 1st base but takes both of them deep into the "outfield" near the foul-ball-line.

Finally, the distance $1/b$ between 1st and 2nd base (and between home and 3rd) shrinks to a tiny value. This is known as the *ultra-relativistic limit*. Then the mass-shell point (2nd base) is quite like the right-moving photon point (1st base) and both have huge frequency and wavevector. Meanwhile, the left-moving photon wave (3rd base) has lost practically all its frequency and wavevector.

At this point, you may wish to skip to the beginning of Chapter 5 where it is seen that this "baseball diamond" also describes relativistic energy-momentum relations. The horizontal hyperbolas in Fig. 4.3.5(b) are called "mass shells" and vertical hyperbolas are constant-acceleration trajectories. Indeed, this little baseball diamond jewel of a construction is a Rosetta stone for the foundation of all of classical and quantum mechanics. What a simple rule-and-compass derivation of spacetime wave mechanics!

This is not to say the rest of Chapter 4 may be ignored. It contains important details about this wave based approach, and as Freeman Dyson is supposed to have said, "The devil is in the details!"

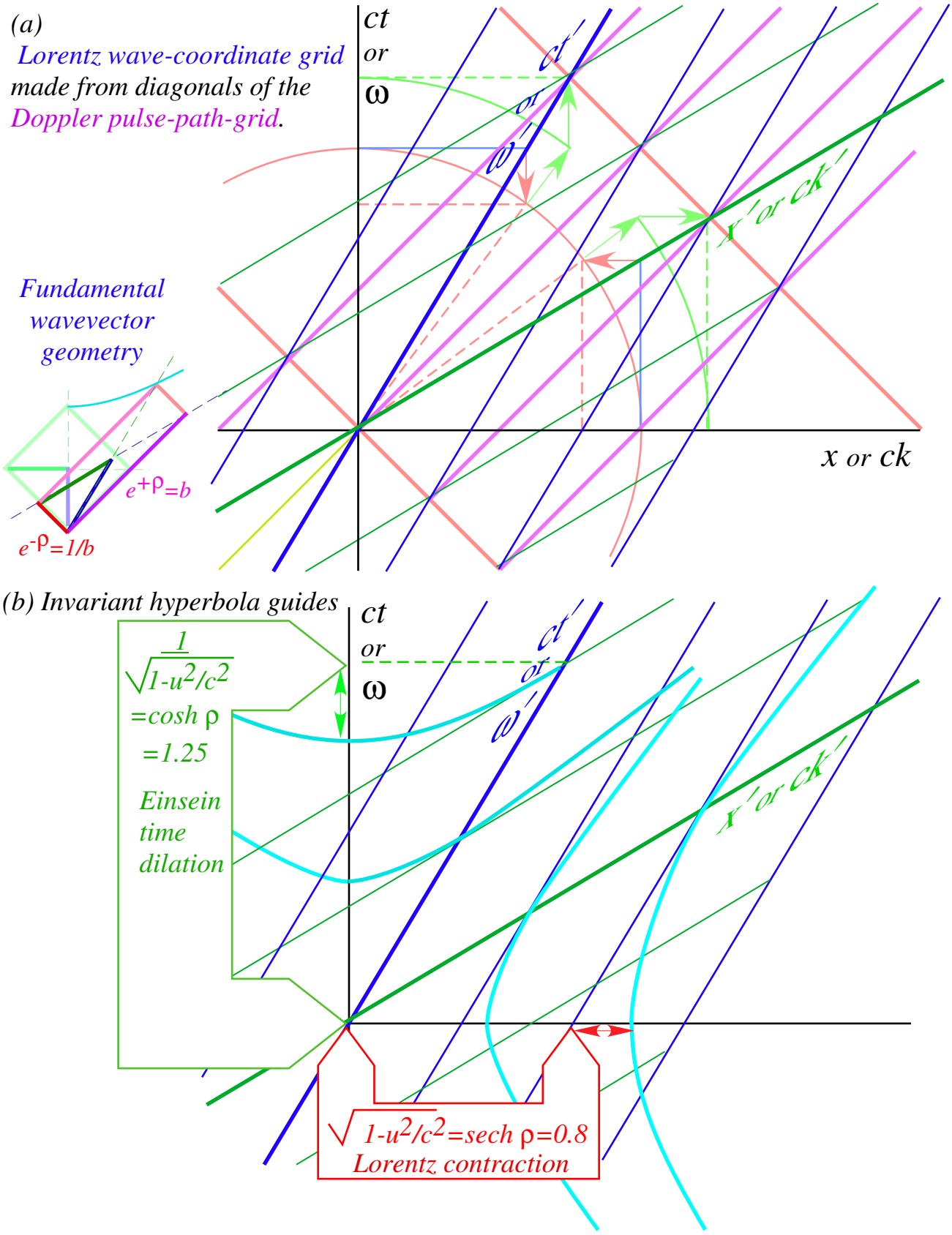

Fig. 4.4.3 Geometry of (a) Lorentz coordinates and (b) invariant hyperbolas

(b) Comparing Circular and Hyperbolic Functions

Quantum theory and relativity make frequent use of trigonometric circular functions ($\sin\phi$, $\cos\phi$, etc.) and hyperbolic functions ($\sinh\phi$, $\cosh\phi$, etc.), and so it helps to be familiar with some tricks and definitions. To aid this, Fig. 4.4.3 presents a comparison of the circular and hyperbolic geometric ϕ definitions. First, it should be noted that both types of function are defined in terms of an area ϕ subtended by a rotating diameter, the gray area ϕ in Fig. 4.4.4 (a-b). (Note it is twice that subtended by the radius.) For circular functions, ϕ is also the usual rotational polar angle in radians ($-\pi<\phi<\pi$), but no such simple equivalent exists for hyperbolic ϕ geometry. As derived below, the area ϕ swept by a hyperbolic diameter is the rapidity ρ of Lorentz transformation (4.3.7a) or (4.3.7b).

A key idea here is that areas can be added to combine transformations. Transformation by ϕ_{AB} from frame *A* to *B* followed by a transformation by ϕ_{BC} from frame *B* to *C* equals a transformation by

$$\phi_{AC} = \phi_{AB} + \phi_{BC} \tag{4.4.3a}$$

from frame *A directly* to *C*. Relativistic velocities $u/c = \beta = \tanh\phi$ add through hyper-tangents.

$$\tanh(\phi_{AB}+\phi_{BC}) = \frac{\tanh(\phi_{AB})+\tanh(\phi_{BC})}{1+\tanh(\phi_{AB})\cdot\tanh(\phi_{BC})} \quad \text{implies:} \quad \beta_{AC} = \frac{\beta_{AB}+\beta_{BC}}{1+\beta_{AB}\cdot\beta_{BC}} \tag{4.4.3b}$$

Adding angles is well known; but "slope-addition" is not an easy way to combine rotations! Adding velocities like (4.4.3b) takes some getting used to, too. Before relativity came along, we thought like Galileo that adding velocities directly ($u_{AC} = u_{AB} + u_{BC}$) was the way to transform them, and for small velocities, this is what (4.4.3b) gives. But, simple rapidity summing using (4.4.3a) is safe at any speed.

Let us prove that area ϕ swept by hyperbolic diameter *(x=cosh ρ, y=sinh ρ)* in Fig. 4.4.4(b) is ρ. By symmetry, the radially swept area in just one hyperbolic quadrant of $y = +\sqrt{1-x^2}$ is half that value.

$$\begin{aligned}\frac{\phi}{2} = \begin{matrix}\text{triangle}\\ \text{area}\end{matrix} - \begin{matrix}\text{area under}\\ \text{hyperbola}\end{matrix} &= \frac{1}{2}x\cdot y - \int_{x=1}^{x} y\cdot dx = \frac{1}{2}\sinh\rho\cdot\cosh\rho - \int_{\rho=0}^{\rho}\sinh\rho\cdot d(\cosh\rho)\\ &= \frac{1}{4}\sinh 2\rho - \int_{\rho=0}^{\rho}\sinh^2\rho\cdot d\rho\end{aligned} \tag{4.4.4a}$$

Using $\sinh^2\rho = \left(e^{\rho}-e^{-\rho}\right)^2/4 = \left(\cosh 2\rho - 1\right)/2$ shows the equality of ϕ and ρ.

$$\frac{\phi}{2} = \frac{1}{4}\sinh 2\rho - \int_{\rho=0}^{\rho}\frac{1}{2}\left(\cosh 2\rho - 1\right)\cdot d\rho = \frac{\rho}{2} \tag{4.4.4b}$$

The ϕ–area or rapidity $\rho = \ln b$ is unlimited. There is an infinite amount of area in a hyperbola's asymptote. For example, at $\beta=0.99999999$ the blue Doppler factor $b=e^{\rho}$ and ϕ are approximated easily.

$$b = \sqrt{\frac{1+\beta}{1-\beta}} \xrightarrow[\beta\to 1]{} \sqrt{\frac{2}{1-\beta}} = \sqrt{\frac{2}{10^{-8}}} = 10^4\sqrt{2}, \qquad \phi = \ln b \cong \ln\sqrt{\frac{2}{1-\beta}} = \ln\left(10^4\sqrt{2}\right) = 9.6 \tag{4.4.5}$$

But, the hyperbolic area ϕ grows slowly with *b* or β, roughly as the number of 9's in β. It shows that approaching the speed of light is like approaching an out of reach horizon.

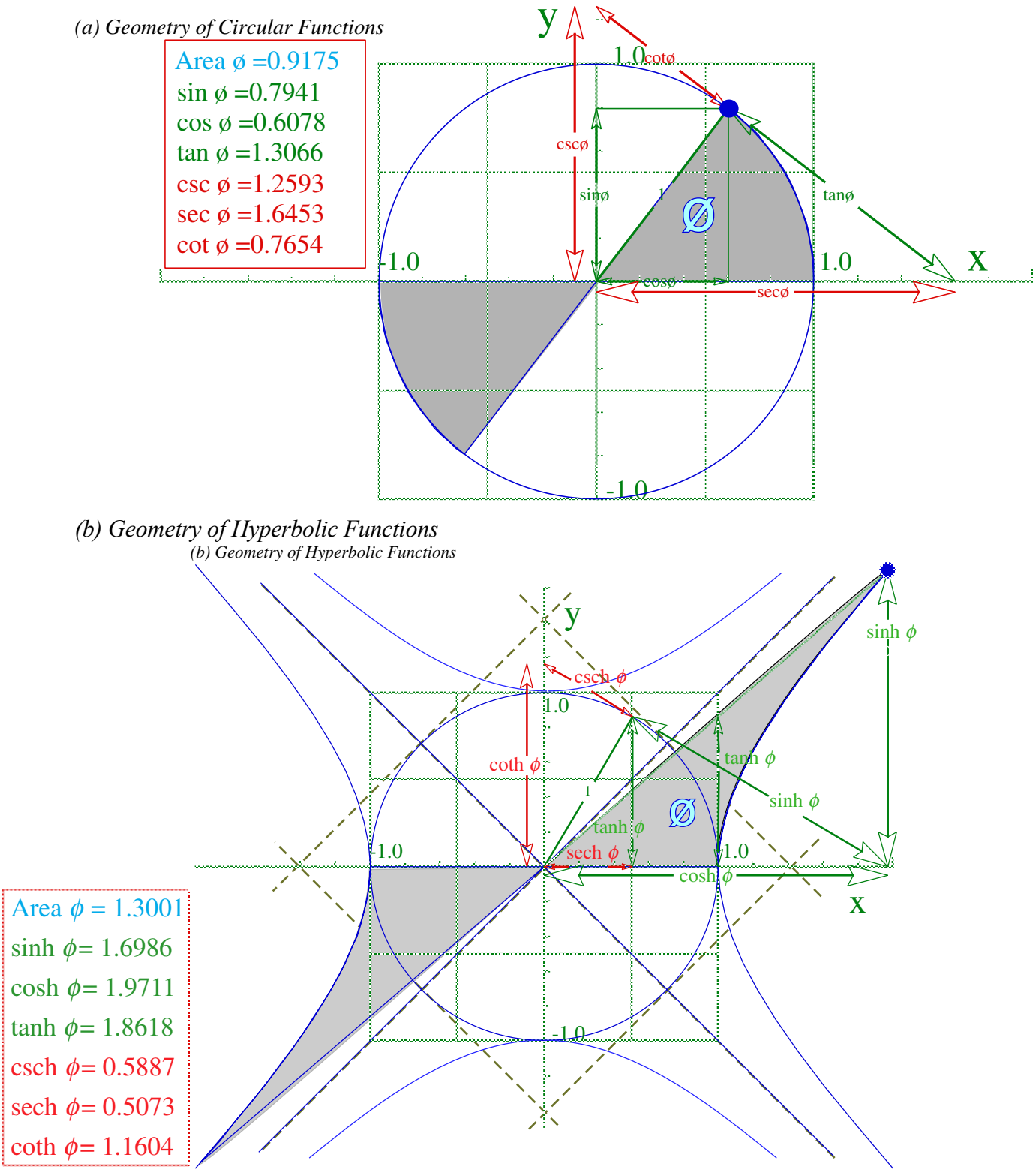

Fig. 4.4.4 Geometry and trigonometry of exp() functions (a)Circular and (b)Hyperbolic.(From RelativIt*)*

4.5. When Lightwaves Dance: Superluminal phase

The preceding relativistic quantum wave development was actually discovered in connection with a little known but quite striking wave interference phenomenon called *galloping*. The spacetime wave-zero coordinates displayed in the laser trap of Fig. 4.3.3 are each due to an extreme form of galloping in which phase velocity repeatedly or persistently exceeds the speed of light. Galloping is not restricted to γ-waves (light) but appears in virtually all wave phenomena including the μ-waves (matter) derived in Chapter 5.

A related but more complex wave phenomena called *revivals* is another striking interference effect that occurs in matter waves or in light confined by a waveguide. Revivals are most prevalent and persistent if the dispersion function is purely quadratic as it is for a DeBroglie-Bohr-Schrodinger wave described by the low-*k*-vector μ-wave case outlined in Chapter 5.

(a) Galloping waves and Standing Wave Ratio (SWR)

For counter-propagating laser beams such as in Fig. 4.3.3(a), galloping waves are the rule rather than the exception. In fact the only way to squelch galloping is to turn off one of the lasers! Turning off the right laser gives a pure *right-moving wave* $e^{i(kx-\omega t)}$ that traces *45°* wave zero lines going at a constant lightspeed *c* as shown in the spacetime plot of Fig. 4.5.1(a). Turning on even a small amount of *left-moving wave* $e^{i(-kx-\omega t)}$ results in galloping paths as shown in Fig. 4.5.1(b-e). The real part $Re\Psi$ of the wave gallops faster than light once each half-cycle just *1/4*-cycle behind a similarly galloping $Im\Psi$.

As the relative amount of left moving wave increases, galloping becomes more pronounced, and then, for equal left and right amplitudes, the zeros of the real standing wave gallop infinitely fast at each moment $Re\Psi$ is zero everywhere. (Being everywhere is tantamount to going infinitely fast!) This is the special case that gives a Cartesian *(x,ct)* grid shown in Fig. 4.3.3(a). Finally, for dominant left-moving amplitudes, the galloping reverses sign and subsides as in Fig. 4.5.1(e-f).

Counter-propagating laser waves in Fig. 4.5.1 have the following wave zeros of $Re\Psi$.

$$0 = \mathrm{Re}\,\Psi(x,t) = \mathrm{Re}\left[A_{\rightarrow}e^{i(k_0x-\omega_0t)} + A_{\leftarrow}e^{i(-k_0x-\omega_0t)}\right]$$
$$= A_{\rightarrow}\left[\cos k_0x\ \cos\omega_0t + \sin k_0x\,\sin\omega_0t\right] + A_{\leftarrow}\left[\cos k_0x\ \cos\omega_0t - \sin k_0x\,\sin\omega_0t\right]$$
$$= \left(A_{\rightarrow} + A_{\leftarrow}\right)\left[\cos k_0x\ \cos\omega_0t\right] + \left(A_{\rightarrow} - A_{\leftarrow}\right)\left[\sin k_0x\,\sin\omega_0t\right]$$

Galloping varies according to a *Standing Wave Quotient SWQ* or its inverse *Standing Wave Ratio SWR*.

$$\tan k_0x = -SWQ\cdot\cot\omega_0t \quad (4.5.1a) \qquad \text{where: } SWQ = \frac{A_{\rightarrow}+A_{\leftarrow}}{A_{\rightarrow}-A_{\leftarrow}} = \frac{1}{SWR} \quad (4.5.1b)$$

The time derivative gives upper and lower speed limits in terms of $V_{phase} = \frac{\omega_0}{k_0} = c$ and *SWQ* or *SWR*.

$$\frac{dx}{dt} = c\cdot SWQ\frac{\csc^2\omega_0t}{\sec^2k_0x} = \frac{c\cdot SWQ}{\sin^2\omega_0t + SWQ^2\cdot\cos^2\omega_0t} = \begin{cases} c\cdot SWR & \text{for: } t = 0,\ \pi,\ 2\pi... \\ c\cdot SWQ & t = \pi/2,\ 3\pi/2,... \end{cases} \quad (4.5.1c)$$

The functional dependency (4.5.1) might have been a familiar one to Galileo and Kepler who analyzed orbits of swinging lamps and planets using elliptical geometry sketched in Fig. 4.5.2. This analogy is examined in the following section.

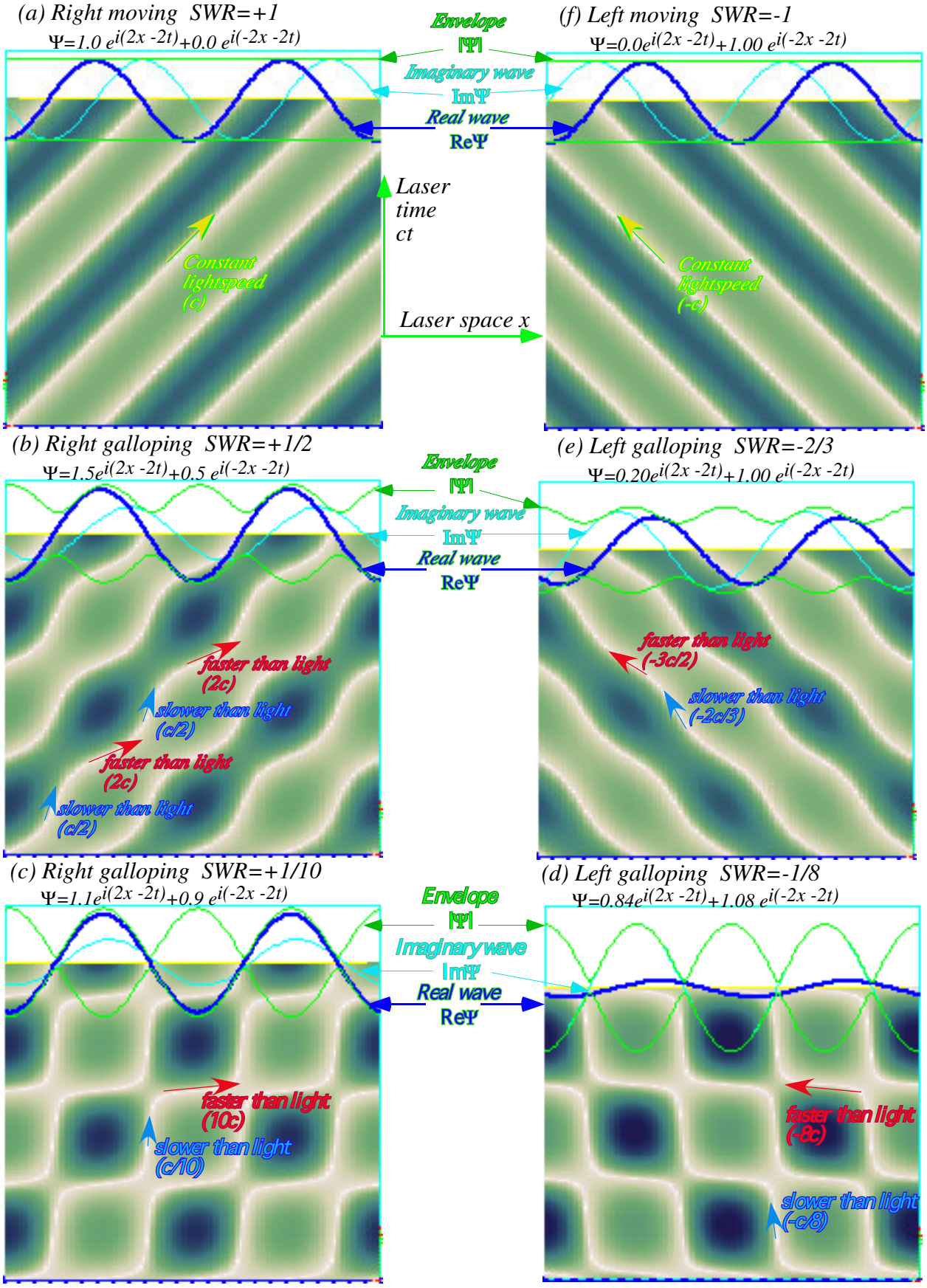

Fig. 4.5.1 Spacetime plots of monochromatic waves of varying Standing Wave Ratio (SWR).

(b) Kepler's Law for galloping

Galloping wave velocity (4.5.1c) is directly related to Kepler's Law for isotropic force field orbits, such as in a 2D oscillator orbit constructed by Fig. 4.5.2. (Recall also Fig. 1.3.6.) If polar angle $\phi(t)$ of ellipse-orbiting point $P=(x=a\sin\omega t,\ y=a\cos\omega t)$ is read clockwise like orbital phase ωt, then they relate by

$$\tan\phi(t)=\frac{y}{x}=-\frac{b}{a}\cdot\cot\omega t\ . \qquad (4.5.2)$$

This resembles the galloping wave equation (4.5.1a) with the ellipse aspect ratio b/a replacing a standing wave ratio. To conserve orbital angular momentum $\mathbf{r}\times\mathbf{v}$ in the absence of torque, the orbital velocity $v(r)$ gallops to a faster $v(b)$ at perigee $(r=b)$ and a slower $v(a)$ at apogee $(r=a)$. In the same way waves in Fig. 4.5.1 gallop faster through smaller parts of their envelope and slow down as their amplitudes grow.

Analogy of laser wave dynamics (4.5.1) to classical orbital mechanics (4.5.2) has physical as well as historical use. Wave galloping shown in Fig. 4.5.1 happens equally in systems with open or infinite boundaries as it does in closed or periodic (ring laser or Bohr-ring) systems. In fact, Fig. 4.5.2 are pictures of 2nd lowest $(k_m=\pm2)$-modes of a micro-ring-laser or the 2nd excited Schrodinger $(m=\pm2)$-waves on a Bohr-ring. Exactly two wavelengths fit in each space frame and two periods fit in each time frame. (While Bohr dispersion $\omega_m=Bm^2$ in Fig. 4.5.1(b) differs from optical dispersion $\omega_m=|ck_m|$, that does not affect Fig. 4.5.1. Right and left moving waves have the same frequency in either case, and time is scaled accordingly.)

Analogy with polarization ellipsometry

If a frame in Fig. 4.5.1 were drawn instead for 1st or fundamental $(m=\pm1)$-waves or $(k_m=\pm1)$-modes of either ring system it would just be a *1/4*-area square section with only one sine wave per frame. (Recall Fig. 4.2.10(c).) Such a wave has an average dipole moment $\mathbf{p}=\langle p\rangle$ that orbits an ellipse like radius $\mathbf{r}$ in Fig. 4.5.2 and is analogous to a polarization figures used to depict states in optical ellipsometry.

In the polarization analogy, purely right-moving $(m=+1)$ or purely left-moving $(m=-1)$ wave states e^{+ikx} and e^{-ikx} are analogous, respectively, to right or left circular polarization states. Equal combinations $e^{+ikx}+e^{-ikx}=2\cos kx$ or $e^{+ikx}-e^{-ikx}=2i\sin kx$ are analogous, respectively, to x-plane or y-plane polarization. Most arbitrary combinations $ae^{+ikx}+be^{-ikx}$ are analogous to elliptical polarization. A polarization vector for elliptic states enjoys the same Kepler galloping described by Fig. 4.5.2.

Perhaps the simplest explanation of wave galloping in Fig. 4.5.1 uses an analogy with the elliptical polarization states as in Fig. 4.5.3. The uniformly spaced ticks on the circular polarization circles are crowded into a traffic jam at the long axes of their elliptic orbits as the aspect ratio b/a or SWR approaches zero. The ticks near the short axes maintain their spacing in the Kepler geometry. Like a uniformly turning lighthouse beacon viewed edge-on, the beam is seen to gallop by quickly and then slow to a crawl as it swings perpendicular to the line of sight.

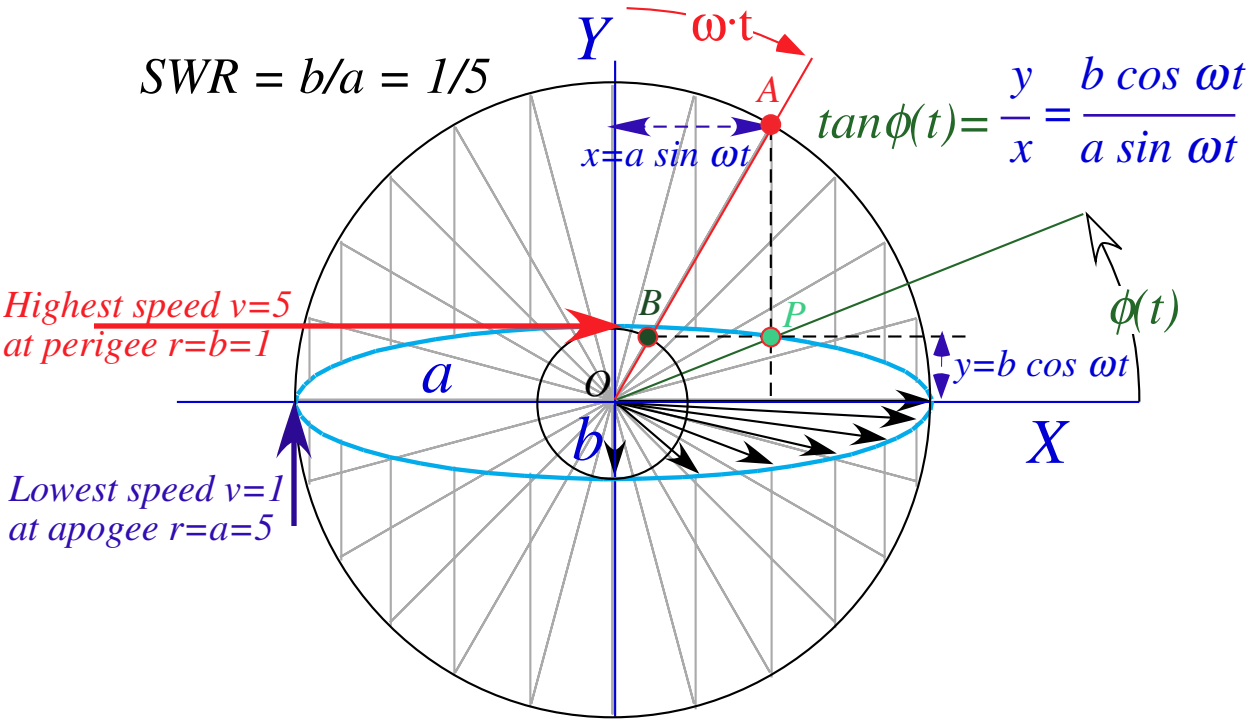

Fig. 4.5.2 Elliptical oscillator orbit and a Kepler construction

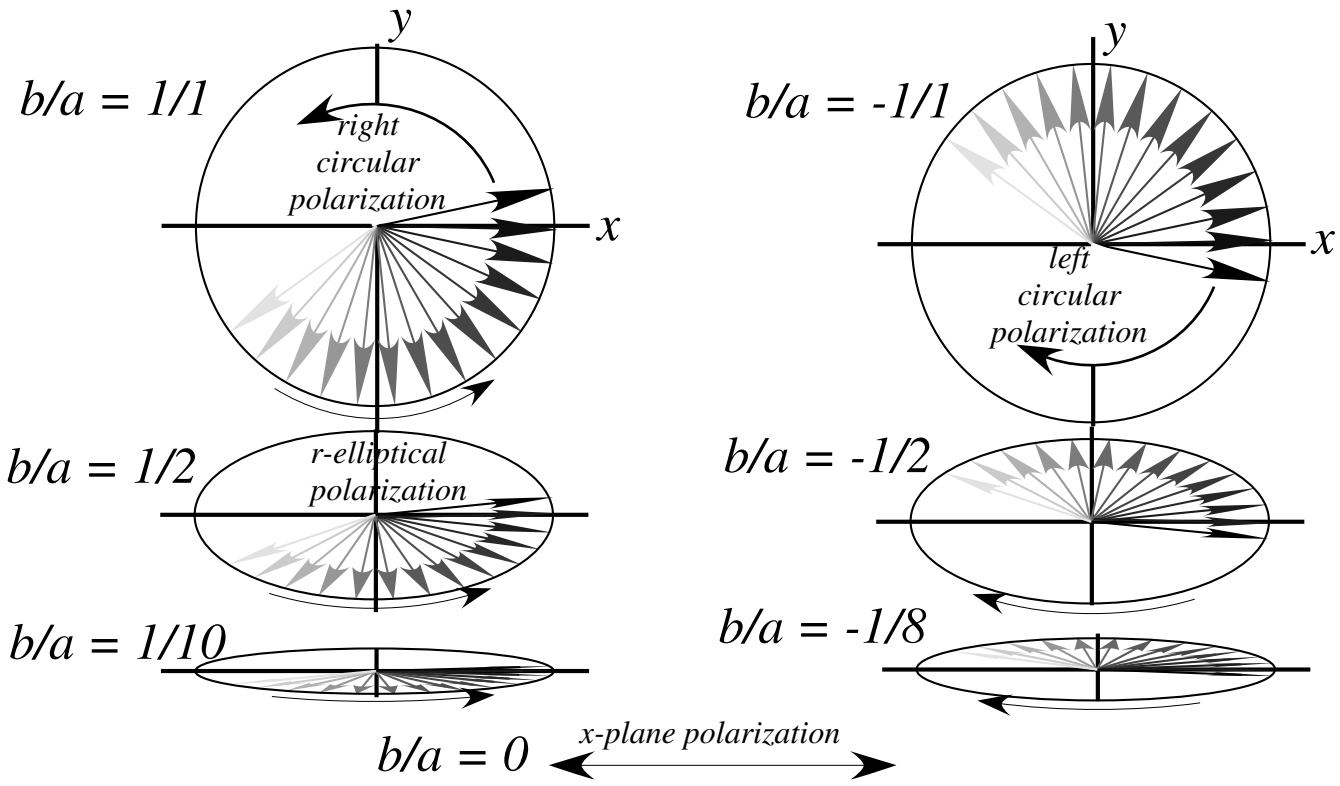

Fig. 4.5.3 Elliptical polarization states of varying aspect ratio a/b or standing wave ratio SWR. This figure is analogous to Fig. 4.5.1 according to the Keplerian geometry of Fig. 4.5.2.

(c) SWR algebra and geometry

The galloping waves $Re\Psi(x,t)$ and $Im\Psi(x,t)$ in Fig. 4.5.4(b-e) are speeding or galloping inside stationary envelopes $e=\pm|\Psi|=\pm\sqrt{(\Psi^*\Psi)}$ that serve as the "skin" of the wave. The bounding skin $\pm|\Psi|$ is a pair of square roots of the probability function $\Psi^*\Psi$ for a general galloping wavefunction

$$\Psi\left(A_{\rightarrow},\omega_{\rightarrow},k_{\rightarrow};A_{\leftarrow},\omega_{\leftarrow},k_{\leftarrow}\right)=A_{\rightarrow}e^{i\left(k_{\rightarrow}x-\omega_{\rightarrow}t\right)}+A_{\leftarrow}e^{i\left(k_{\leftarrow}x-\omega_{\leftarrow}t\right)}. \qquad (4.5.3)$$

The envelope function is worked out below assuming real amplitudes $A_{\leftarrow}{}^*=A_{\leftarrow}$ and $A_{\rightarrow}{}^*=A_{\rightarrow}$.

$$e(x,t)=\left|\Psi\left(A_{\rightarrow},\omega_{\rightarrow},k_{\rightarrow};A_{\leftarrow},\omega_{\leftarrow},k_{\leftarrow}\right)\right|=\sqrt{\Psi^*\Psi}$$

$$=\sqrt{\left(A_{\rightarrow}^*e^{-i\left(k_{\rightarrow}x-\omega_{\rightarrow}t\right)}+A_{\leftarrow}^*e^{-i\left(k_{\leftarrow}x-\omega_{\leftarrow}t\right)}\right)\left(A_{\rightarrow}e^{i\left(k_{\rightarrow}x-\omega_{\rightarrow}t\right)}+A_{\leftarrow}e^{i\left(k_{\leftarrow}x-\omega_{\leftarrow}t\right)}\right)}$$

$$=\sqrt{A_{\rightarrow}^*A_{\rightarrow}+A_{\leftarrow}^*A_{\leftarrow}+A_{\leftarrow}^*A_{\rightarrow}e^{i\left[\left(k_{\rightarrow}-k_{\leftarrow}\right)x-\left(\omega_{\rightarrow}-\omega_{\leftarrow}\right)t\right]}+A_{\leftarrow}A_{\rightarrow}^*e^{-i\left[\left(k_{\rightarrow}-k_{\leftarrow}\right)x-\left(\omega_{\rightarrow}-\omega_{\leftarrow}\right)t\right]}} \qquad (4.5.4a)$$

$$=\sqrt{A_{\rightarrow}{}^2+A_{\leftarrow}{}^2+2A_{\rightarrow}A_{\leftarrow}\cos\left[\left(k_{\rightarrow}-k_{\leftarrow}\right)x-\left(\omega_{\rightarrow}-\omega_{\leftarrow}\right)t\right]} \quad \text{(for real } A_{\rightarrow} \text{ and } A_{\leftarrow}\text{)} \qquad (4.5.4b)$$

$$=\sqrt{A_{\rightarrow}{}^2+A_{\leftarrow}{}^2+2A_{\rightarrow}A_{\leftarrow}\cos[2kx]} \quad \text{(for: } k_{\rightarrow}=k=-k_{\leftarrow} \text{ and: } \omega_{\rightarrow}=\omega=\omega_{\leftarrow}\text{)} \qquad (4.5.4c)$$

For monochromatic $(\omega_{\leftarrow}=\omega_{\rightarrow})$ counter-propagating $(k_{\leftarrow}=-k_{\rightarrow})$ waves, the envelope is a stationary or standing wave pattern. The envelope is a *two-component quantum interference function* similar to one first introduced in (1.3.10). Its min-max values give the amplitude peaks and valleys in Fig. 4.5.4a.

$$e_{MIN}=\sqrt{|A_{\rightarrow}|^2+|A_{\leftarrow}|^2-2|A_{\rightarrow}||A_{\leftarrow}|}=|A_{\rightarrow}|-|A_{\leftarrow}|$$
$$|e_{MAX}|=\sqrt{|A_{\rightarrow}|^2+|A_{\leftarrow}|^2+2|A_{\rightarrow}||A_{\leftarrow}|}=|A_{\rightarrow}|+|A_{\leftarrow}| \qquad (4.5.5)$$

The ratio of interference maxima (where amplitudes $A_{\rightarrow}$ and $A_{\leftarrow}$ add constructively) to minima (where they subtract or interfere destructively) is called the *standing wave ratio (SWR)*.

$$-1\le SWR=\frac{e_{MIN}}{e_{MAX}}=\frac{|A_{\rightarrow}|-|A_{\leftarrow}|}{|A_{\rightarrow}|+|A_{\leftarrow}|}\le 1 \qquad (4.5.6)$$

Let us pause to reconsider the simple analogy between galloping waves and optical polarization. This analogy is related to a crowd behavior of American football fans. Whoopee. (Or Woo-pig-sooee.)

Analogy between complex waves and polarization: Stadium circumference waves

Imagine a single-kink *(k=1)* wave wrapped around a ring like a "football stadium wave" in Fig. 4.5.4. As fans take turns standing up, a "stand-up" wave rotates clockwise around the stadium from $+x$-axis on North side (*r=0* or *12 o'clock*) to $-y$-axis on East side (*r=3* or *3 o'clock*) and so on.

The imaginary ("gonna' be standing-up") wave rotates *90°* ahead from the $-y$-axis in the figure down to the $-x$-axis (*r=6* or *6 o'clock*). This wave is analogous to a left-circular (clockwise) polarization state: $|L\rangle=|x\rangle - i|y\rangle$ which evolves in time according to $|L(t)\rangle=|L\rangle e^{-i\omega t}$. The real ("is") part of $|L(t)\rangle$ is $\mathrm{Re}|L(t)\rangle=\cos\omega t|x\rangle-\sin\omega t|y\rangle$, the dark arrows rotating clockwise from $|x\rangle$ at *r=0* or *12 o'clock* toward minus $|y\rangle$ at *r=3* or *3 o'clock* in the figure above. The blue-gray arrows rotating clockwise from minus $|y\rangle$ at *r=3* or *3 o'clock* toward minus $|x\rangle$ at *r=6* or *6 o'clock* depict the imaginary ("gonna'be") part of $|L(t)\rangle$, that is: $\mathrm{Im}|L(t)\rangle=-\sin\omega t|x\rangle-\cos\omega t|y\rangle$.

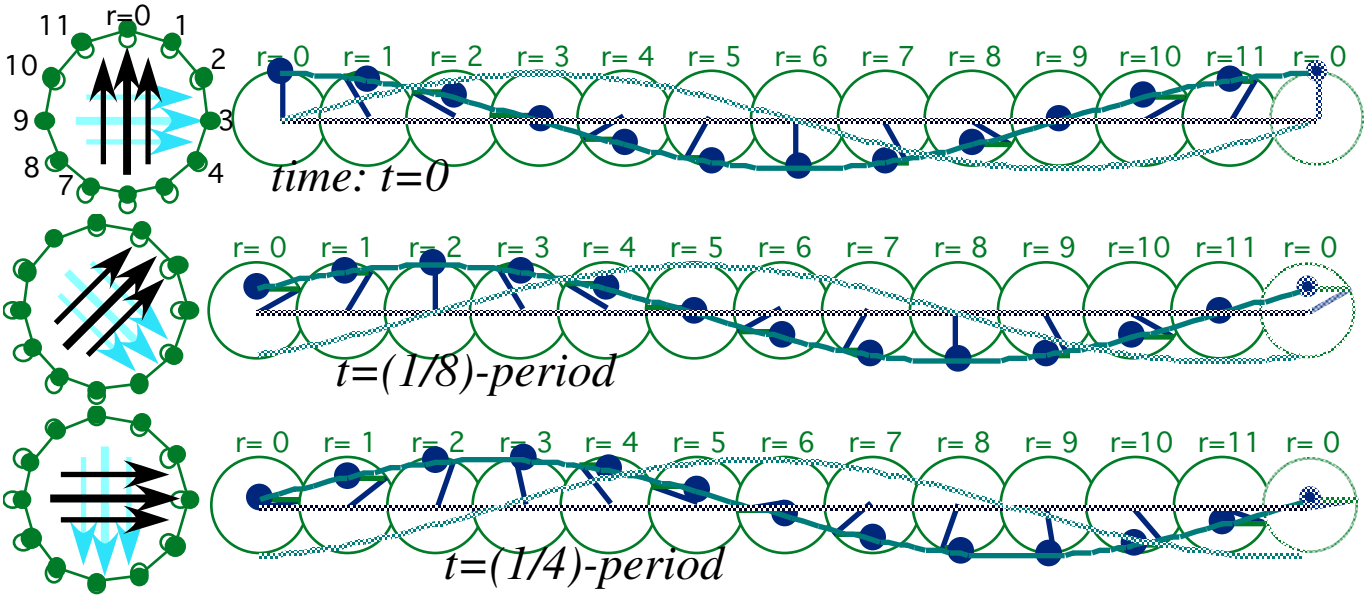

Fig. 4.5.4 Left-polarization state $|L(t)\rangle=(|x\rangle-i|y\rangle)e^{-i\omega t}$ is like a (k=1) right-moving wave $\Psi_{\rightarrow}= e^{i(kr-\omega t)}$

Next imagine a *negative*-single-kink *(k=-1)* "football stadium wave" going *anti*-clockwise in Fig. 4.5.5. This is *left*-moving wave $\Psi_{\leftarrow}= e^{i(-|k|r-\omega t)}$ or *right*-hand circular polarization state $|R\rangle=|x\rangle+i|y\rangle$. Because, human hands curl naturally inward (unlike reptiles) the *right* hand tends to point *left*-over-the-top.

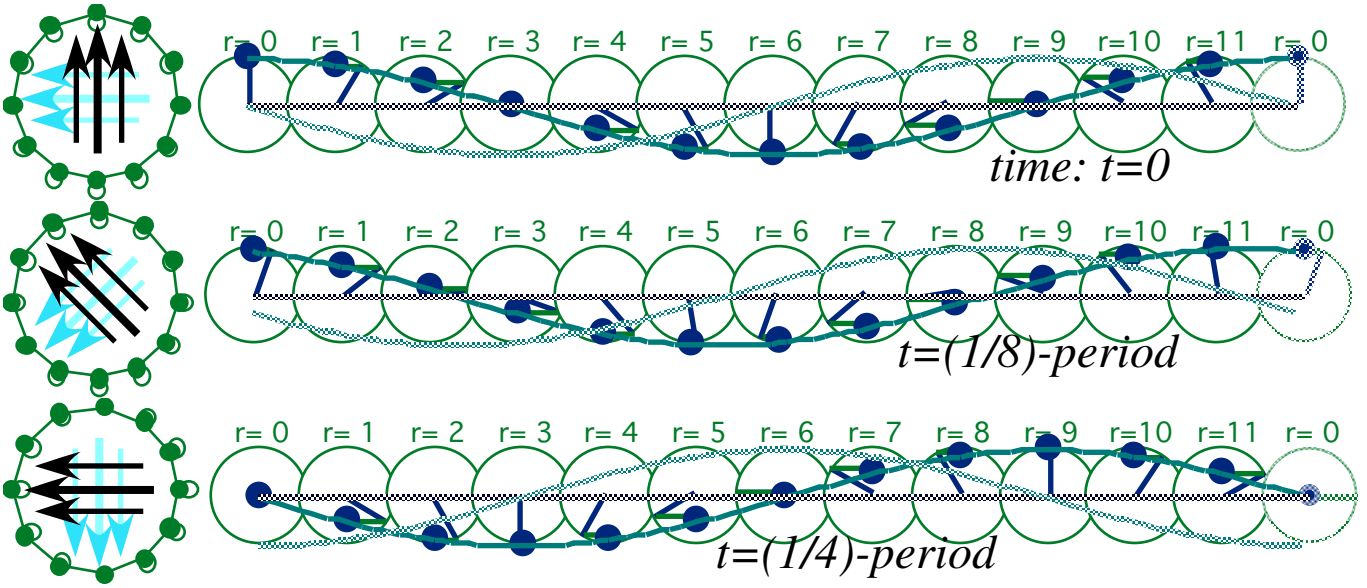

Fig. 4.5.5 Right-polarization state $|R(t)\rangle=(|x\rangle+i|y\rangle)e^{-i\omega t}$ is like left-moving wave $\Psi_{\leftarrow}= e^{i(-|k|r-\omega t)}$.

Now consider a 50-50 combination the right-handed and left-handed states.

$(|L\rangle+|R\rangle)/2 = (|x\rangle - i|y\rangle + |x\rangle + i|y\rangle)/2 = |x\rangle$ $\qquad$ $(\Psi_{\rightarrow}+\Psi_{\leftarrow})/2 = (e^{i(kr-\omega t)}+e^{i(-kr-\omega t)})/2 = e^{-i\omega t}\cos kr$

The result is clearly *x*-polarization or a *cosine standing wave* as shown below in Fig. 4.5.6. Notice that it starts out with a zero imaginary or "gonna'be" part. This predicts (correctly) that the real part is going to die. Notice that it does perish 1/4-cycle later when the real wave "is" zero everywhere. Let this be a lesson to ye of little or no imagination! In this case, however, hope springs eternal; then the "gonna'be" wave predicts a revival in the nether regions (with dubious anthropomorphic implications, however!).

Another 50-50 combination of right-handed and left-handed states is a difference instead of a sum.

$(|L\rangle - |R\rangle)/2 = (|x\rangle - i|y\rangle - |x\rangle - i|y\rangle)/2 = -i|y\rangle$ $\qquad$ $(\Psi_{\rightarrow}-\Psi_{\leftarrow})/2 = (e^{i(kr-\omega t)}-e^{i(-kr-\omega t)})/2 = e^{-i\omega t}i\sin kr$

The result is clearly *y*-polarization and a *sine standing wave* as seen in Fig. 4.5.7, but it starts *90°* behind in phase. (Notice the "*i*" factor.)

The moving $\Psi_{\rightarrow}$ or $|L\rangle$ waves in Fig. 4.5.4 and $\Psi_{\leftarrow}$ or $|R\rangle$ waves in Fig. 4.5.5 represent one extreme while the cosine or *x*-standing waves in Fig. 4.5.6 and sine or *y*-standing waves in Fig. 4.5.7 represent another. In between these cases lie the general galloping or elliptic wave states of Fig. 4.5.1(b-d) with polarization that traces elliptical paths of the form sketched in Fig. 4.5.1 and Fig. 4.5.3.

Now we confront a familiar question, "Which came first, the chicken or the egg?" Should we think of plane-polarized states as being made of circular ones, or are circular-polarized states being made from plane old $|x\rangle$ and $|y\rangle$? We have emphasized the latter so far, but the answer is *both* (and which ever you find more convenient). Clearly, other plane polarized states such as θ=*45°* polarization bases $|x'\rangle = \cos\theta\,|x\rangle + \sin\theta\,|y\rangle$ and its orthonormal partner $|y'\rangle = -\sin\theta\,|x\rangle + \cos\theta\,|y\rangle$ are best described by good old plain old $|x\rangle$ and $|y\rangle$.

Perhaps, the more general elliptical polarization states and galloping waves beg to be described by circular polarization bases $|L\rangle$ and $|R\rangle$ and moving waves $\Psi_{\rightarrow}$ and $\Psi_{\leftarrow}$.. Nevertheless, all orthonormal and complete bases, including any valid elliptical pair, provide (as the name implies) a complete description according to Axioms 2 through 4, and are themselves completely described by any complete set of bases. It's all relative!

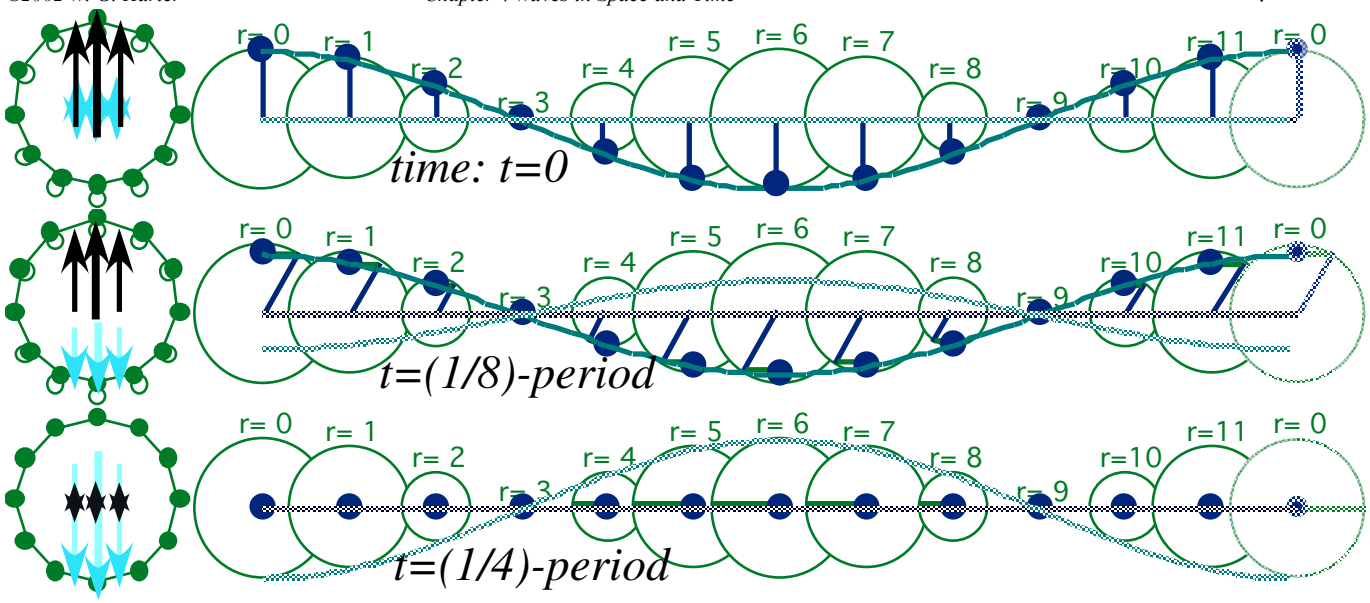

Fig. 4.5.6 x-polarization state $|x\rangle$ is like a (k=1) cosine standing wave $(\Psi_{\rightarrow}+\Psi_{\leftarrow})/2 = = e^{-i\omega t}\cos kr$.

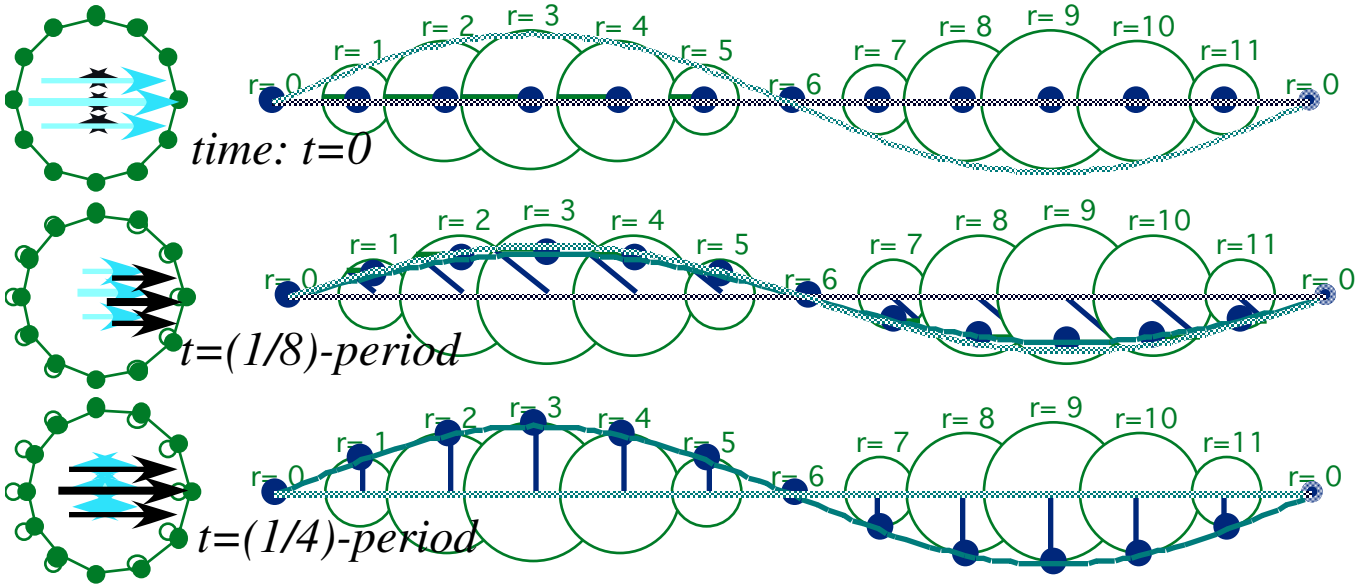

Fig. 4.5.7 y-polarization state $|y\rangle$ is like a (k=1) (i)sine standing wave $(\Psi_{\rightarrow}-\Psi_{\leftarrow})/2 = = e^{-i\omega t} i\sin kr$.

4.6 When Lightwaves Go Crazy: Spacetime switchbacks

For most of the waves discussed so far and particularly for the wave coordinates in Fig. 4.5.2 there is phase velocity or "speed of zeros" that exceeds the speed of light. A conventional aphorism, "Nothing can go faster than light." needs a more positive version, "Nothing *CAN* go faster than light!"

Still, as Feynman pointed out, there are consequences (a cosmic speeding ticket, if you will) for having the temerity and the "right stuff" (that is, *NO* stuff) to break this law. The consequences are to be seen undergoing pair creation and then annihilation while following a zigzag spacetime trajectory called a *Feynman-Wheeler switchback*. That is, you are reported to be simultaneously at three or more places!

(a) Wobbly and switchback waves

Each part in Fig. 4.6.1 is an atom-frame view of a corresponding part of Fig. 4.5.2. Recall from Fig. 4.3.3 that atom sees the approaching green laser blue shifted from $\omega_0=2$ to $\omega'_{\rightarrow}=4=2\omega_0$ as in Fig. 4.6.1(a) while the receding laser is seen red-shifted to $\omega'_{\leftarrow}=1=(1/2)\omega_0$ as in Fig. 4.6.1(f). Fig. 4.6.1(b) has a small amount of red light added to the blue *(SWR=1/2)*. The effect is just a small velocity wobble. But, if *SWR* is reduced to almost zero as in Fig. 4.6.1(c), the Minkowski coordinate lines of Fig. 4.3.3(b) emerge.

Each wave in Fig. 4.6.1 (b-e) with non-zero *SWR* has a simple wavefunction.

$$\Psi_{wobbly}= A_{\Rightarrow}\,\Psi_{\Rightarrow}+ A_{\Leftarrow}\Psi_{\Leftarrow} \qquad = A_{\Rightarrow}\, e^{\,i\,4x\,-\,i4ct} + A_{\Leftarrow}\, e^{-i\,1x\,-\,i\,1ct} \qquad (4.6.1)$$

For example, the wave in Fig. 4.6.1(c) with *SWR=0.1* has the following *wobbly wavefunction*.

$$\Psi_{wobbly}= 1.1\,\Psi_{\Rightarrow}+0.9\,\Psi_{\Leftarrow} \qquad = 1.1\, e^{\,i\,4x\,-\,i4ct} + 0.9\, e^{-i\,1x\,-\,i\,1ct} \qquad (4.6.2)$$

A *Minkowski wavefunction* (Recall Fig. 4.3.3(b) where *SWR=0.*) lies between the cases of Fig. 4.6.1 (c-d).

$$\Psi_{Minkowski}= 1.0\,\Psi_{\Rightarrow}+1.0\,\Psi_{\Leftarrow} \qquad = 1.0\, e^{\,i\,4x\,-\,i4ct} + 1.0\, e^{-i\,1x\,-\,i\,1ct} \qquad (4.6.3a)$$

$$= 2.0\, e^{i(4-1)x/2-i(4+1)ct/2}\, cos((4+1)x/2 - (4-1)\, ct/2) \qquad (4.6.3b)$$

If *SWR* is negative the low-frequency ($\omega'_{\leftarrow}=1$)-light dominates as in Fig. 4.6.1 (d-e). Then zigzag wave-zero switchback curves appear. The following is a *switchback wavefunction* with *SWR=-0.1*.

$$\Psi_{switch}= 0.9\,\Psi_{\Rightarrow}+1.1\,\Psi_{\Leftarrow} \qquad = 0.9\, e^{\,i\,4x\,-\,i4ct} + 1.1\, e^{-i\,1x\,-\,i\,1ct} \qquad (4.6.4)$$

Wave-zero-creation is seen each time a minimum point of $\mathrm{Re}\Psi$ dips below the space axis. Creation is followed by wave-zero-annihilation as the faster of the wave-zeros run ahead to annihilate neighboring slow-moving zeros. Later, the slower moving zeros meet the same fate when caught from behind by faster moving zeros to their left. Faster-moving zeros are "anti-zeros" going back in time. Examples of annihilation and creation points are indicated in the upper part of Fig. 4.6.1(d).

An alternative view of the fast-moving zero is that it belongs to a triplet consisting of its "creator" to the left and its "killer" to the right. The triplet is all the same zero, *located three places at one time*. This is sketched in the lower part of Fig. 4.6.1(d).

Waves do things that defy classical intuition. Since the world, as seen by relativity of γ-waves and the quantum theory of μ-waves described in the following Chapter 5, is composed entirely of waves, it may be wise to replace our old "natural" classical intuition with a new and more natural wave-savvy one.

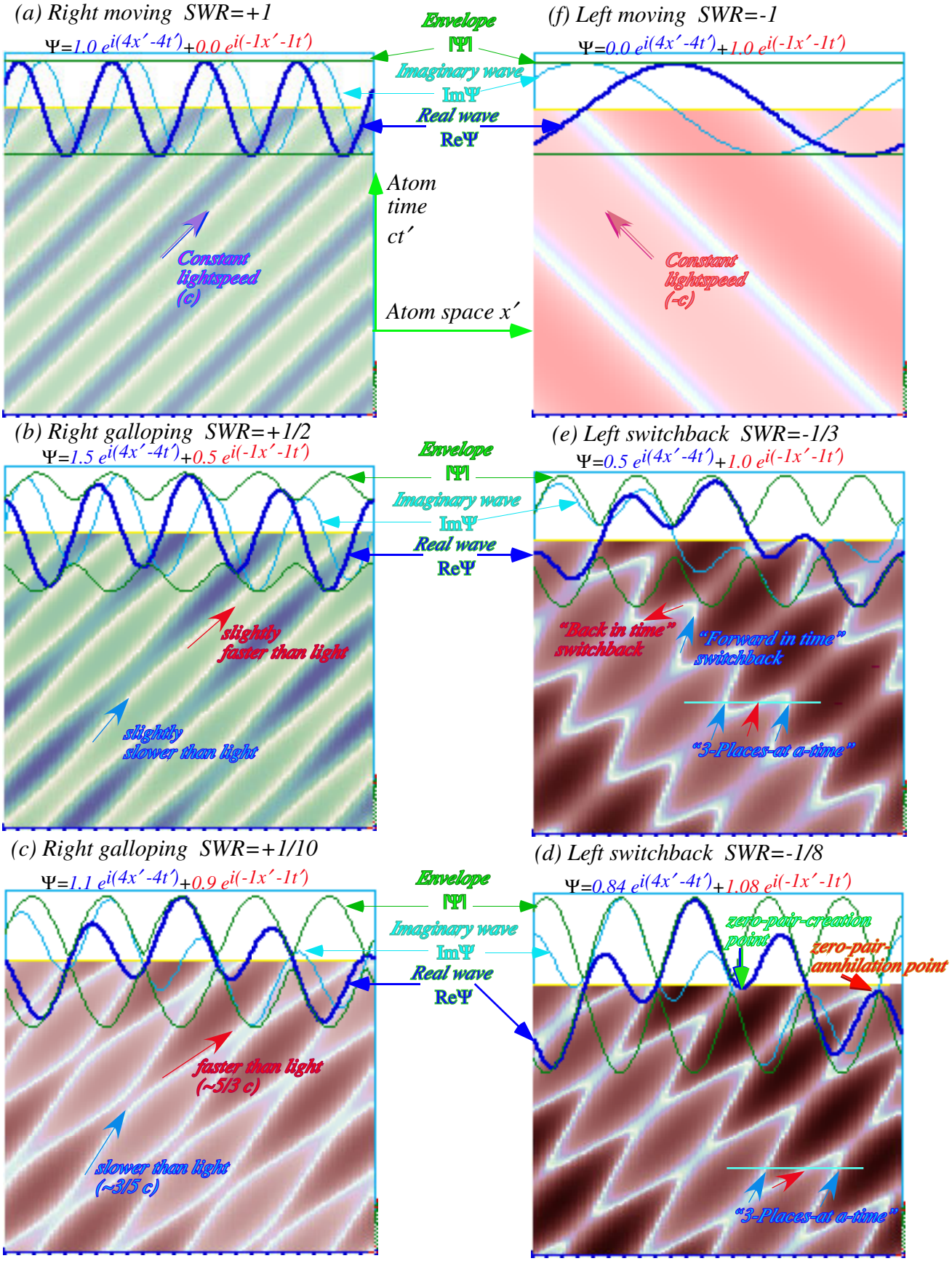

Fig. 4.6.1 Switchback waves (Atom spacetime (x,ct)-view of various galloping waves in Fig. 4.5.1.)

4.7 Co-vs.-Counter propagating waves: Modulation and Beats

Switchback and Minkowski waves (4.6.1) contain *counter-propagating* waves as opposed to *co-propagating* waves in which wavevectors k_1 and k_2 have the same sign as, for example, light waves with $(k_1=1,\ \omega_1= c)$ and $(k_2=4,\ \omega_2= 4c)$. In Fig. 4.7.1 k and ω are the same as in Ψ_{switch} (4.6.4) except k_1 is positive so the red wave goes in the *same* direction as the blue k_2 wave. A *group wave* results.

$$\Psi_{group} = 1.1\, e^{\,i\,(k_1 x - \omega_1 ct)} + 0.9\, e^{i\,(k_2 x - \omega_2 ct)}$$
$$= 1.1\, e^{\,i\,(x - ct)} + 0.9\, e^{i\,(4x - 4ct)} = 1.1\,\Psi_{1\Rightarrow} + 0.9\,\Psi_{4\Rightarrow} \qquad (4.7.1a)$$

Time snapshots of the group wave Ψ_{group} shown in Fig. 4.7.1 below may be compared to those of the switchback waves Ψ_{switch} in Fig. 4.6.1. In Fig. 4.7.2 are higher wave frequency values $(k_1=7,\ \omega_1= 7c)$ and $(k_2=10,\ \omega_2= 10c)$ giving more waves inside each group, but the envelope in Fig. 4.7.2 is the same.

$$\Psi_{group} = 1.1\, e^{\,i\,(7x - 7ct)} + 0.9\, e^{i\,(10x - 10ct)} = 1.1\,\Psi_{7\Rightarrow} + 0.9\,\Psi_{10\Rightarrow} \qquad (4.7.1b)$$

Let us derive the *amplitude modulation (AM) envelope* $|\Psi_{group}|$ or modulus of a group wave.

$$|\Psi group| = \sqrt{\Psi^{*}\Psi} = \sqrt{\left(A_1 e^{-i(k_1 x-\omega_1 t)} + A_2 e^{-i(k_2 x-\omega_2 t)}\right)\left(A_1 e^{i(k_1 x-\omega_1 t)} + A_2 e^{i(k_2 x-\omega_2 t)}\right)}$$
$$= \sqrt{A_1^{\,2} + A_2^{\,2} + 2A_1A_2\cos\left[(k_1-k_2)x-(\omega_1-\omega_2)t\right]} \quad (\text{for real } A_1 \text{ and } A_2) \qquad (4.7.1c)$$

The $|\Psi_{group}|$ envelope formula is the same as that of a $|\Psi_{switch}|$ envelope (4.5.4a). Also, Ψ_{group} has the same group velocity V_{group} and phase velocity V_{phase} formulas as (4.3.2) for switchback waves.

$$V_{group} = \frac{\omega_1-\omega_2}{k_1-k_2} = V_{envelope} \qquad (4.7.2a) \qquad V_{phase} = \frac{\omega_1+\omega_2}{k_1+k_2} = V_{carrier} \qquad (4.7.2b)$$

As before, V_{group} is the *probability distribution velocity* since probability Ψ*Ψ is the square $|\Psi_{group}|^2$.

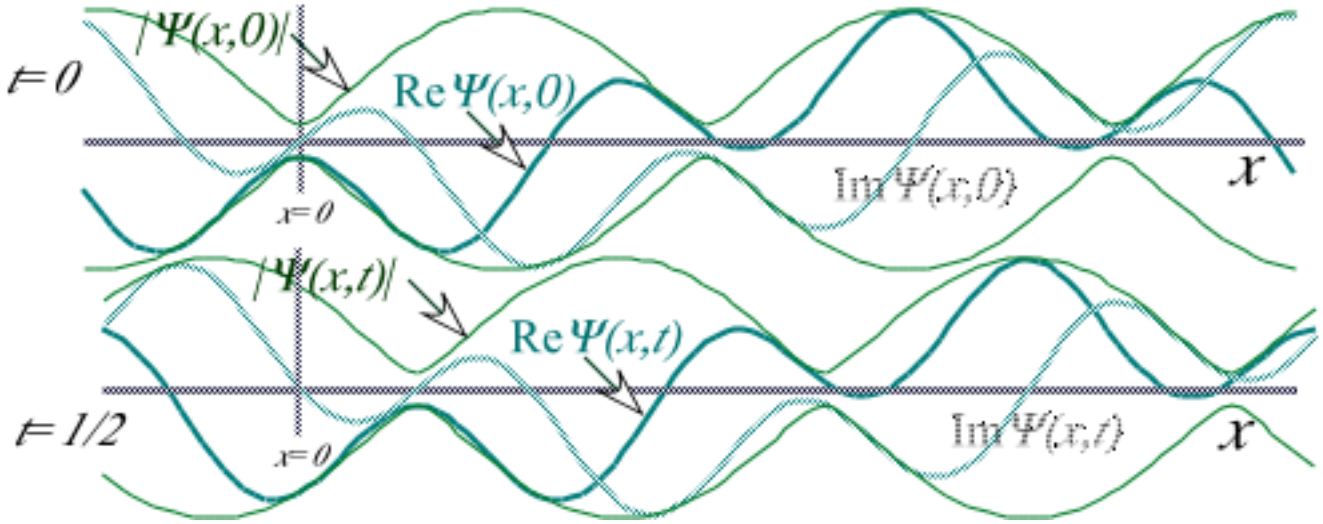

Fig. 4.7.1 Time snapshots of group wave moving in step with its envelope. $(k_1=1,\ \omega_1= c,\ k_2=4,\ \omega_2= 4c)$

However, co-propagating light waves satisfy $\omega_1 = ck_1$ and $\omega_2 = ck_2$ with wavevectors k of the same sign (unlike $k_{\leftarrow}$ for Ψ_{switch} in (4.3.20b)), so group and phase velocity both equal the velocity of light.

$$V_{group} = c = V_{phase} \quad (\text{for light in vacuum})$$

So Ψ_{group} light waves and envelopes march together in lock step at the speed of light for all frequencies ω_1 and ω_2 and amplitudes A_1 and A_2 . No negative k is here to cause galloping or SWR dependence.

Recall that Ψ_{switch} is "tamed" by setting *50-50* amplitudes ($|A_1|=|A_2|$) to get (4.6.3b). The same may be done to Ψ_{group} in Fig. 4.7.2(a) as shown in Fig. 4.7.2(b) where the envelope is "pinched" closed. This is derived algebraically by using an expo-cosine identity (4.2.3a) or (4.3.5a).

$$\Psi_{50\text{-}50group} = 0.5\, e^{i(7x - 7ct)} + 0.5\, e^{i(10x - 10ct)} \qquad (4.7.3a)$$

$$= A_1 e^{i(k_1 x - \omega_1 ct)} + A_2\, e^{i(k_2 x - \omega_2 ct)} \qquad (4.7.3b)$$

$$\left(\text{for: } A_1 = \frac{1}{2}, A_2 = \frac{1}{2}\right) \quad = ie^{i\left[\frac{k_1+k_2}{2}x - \frac{\omega_1+\omega_2}{2}ct\right]} \cos\left[\frac{k_1-k_2}{2}x - \frac{\omega_1-\omega_2}{2}ct\right] \qquad (4.7.3c)$$

The cosine factor in (4.7.3c) replaces the root-cosine in (4.7.1). Note the sine arguments are half as large as the arguments of the root-cosine. This is due to the half-angle identity: $\cos\frac{a}{2} = \sqrt{\frac{1+\cos a}{2}}$.

$$\sqrt{A_1^2 + A_2^2 + 2A_1A_2\cos\left[(k_1-k_2)x - (\omega_1-\omega_2)t\right]} = \frac{\sqrt{1+\cos\left[(k_1-k_2)x-(\omega_1-\omega_2)t\right]}}{2} \qquad (4.7.4)$$

$$\left(\text{for: } A_1 = \frac{1}{2}, A_2 = \frac{1}{2}\right) \qquad = \cos\left[\frac{k_1-k_2}{2}x - \frac{\omega_1-\omega_2}{2}ct\right]$$

The kinky root-cosine function in Fig. 4.7.2(a) is "tamed" into a cosine envelope that appears to smoothly cross the *x*-axis in Fig. 4.7.2(b). The root-cosine *x*-factor $|k_1 - k_2|=3$ implies that the number of groups is $|10-7|=3$ (per 2π distance across Fig. 4.7.2 frame), but the cosine *x*-factor $|k_1 - k_2|/2=1.5$ indicates half as many or $|10-7|/2=1.5$ groups in the same interval. This is correct since the cosine-groups are exactly twice as long as the root-cosine groups.

Meanwhile, the phase factor $|k_1 + k_2|/2$ in (4.7.3c) indicates the number of half-waves (per 2π frame) being modulated by group envelope is $|10 + 7|/2=17/2$. Note 16 or 17 half-waves in Fig. 4.7.2 lie inside 3 "lumps" or groups that (for Fig. 4.7.2(b)) are 1.5 sine-envelope wavelengths.

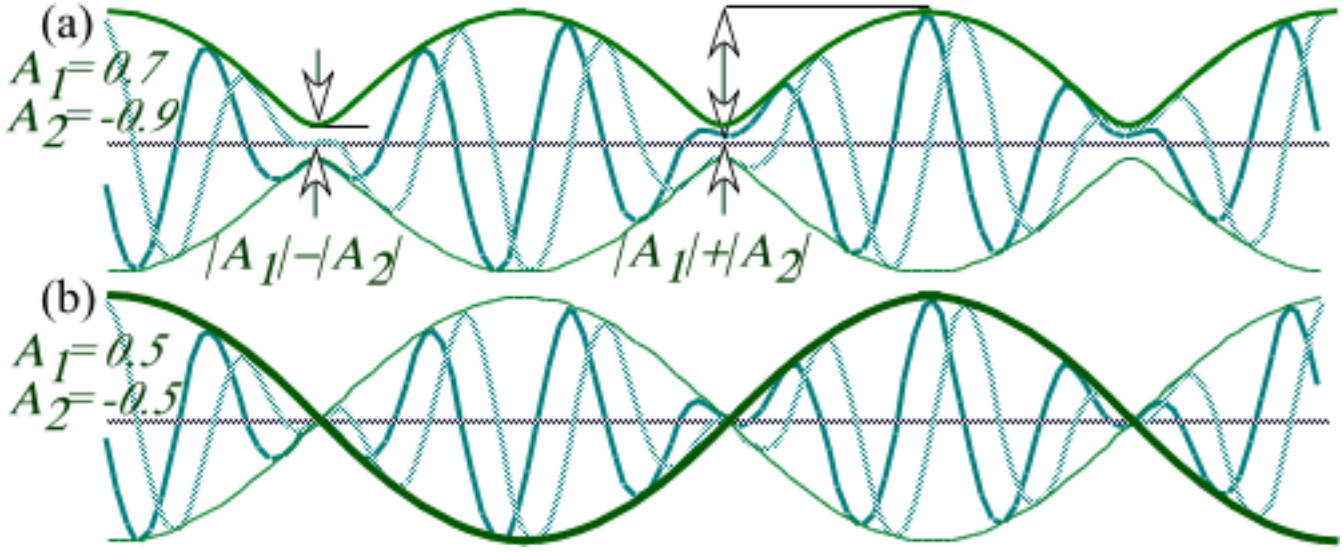

Fig. 4.7.2 Group waves and envelopes.($k_1=7$, $\omega_1= 7c$, $k_2=10$, $\omega_2= 10$ (a) Group wave (b) 50-50 group.

Light waves *en-vacuo* discussed so far are *non-dispersive*, that is, all colors or frequencies travel at the same phase velocity $\omega/k = c$. Most waves (including light waves in many situations) are not so simple. Whenever the velocity $\omega_1/k_1 = v_1$ for one component differs from the velocity $\omega_2/k_2 = v_2$ of its

traveling companion, there will be "sparks" between them as one "rubs" by the other at relative velocity $v_2 - v_1$. (Recall the galloping wave components had the same speed but opposite *velocity*.) Then the phase velocity V_{phase} in (4.7.2b) will also differ from the V_{group} in (4.7.2b). Furthermore, dispersive phase velocity will be guaranteed a constant value V_{phase} only for a 50-50 wave such as (4.7.3) and not for general group waves such as given by (4.7.1).

(a). Time and space modulation: Beats and bumps

Plots in Fig. 4.4.2 of two-ω-component light waves look the same plotted vs. distance *x* or plotted vs. time *ct* because, for photons: $\omega = kc$. Time amplitude modulation groups are called *beats*. By (4.7.2) the number of *beats* or groups per 2π-time unit is $|\omega_2 - \omega_1| = 3$c, and the number of *carrier* waves inside the group envelope is $|\omega_2 + \omega_1|/2 = 17c/2$ (per 2π-time unit). This is old AM radio jargon. Radio 'messages' (music, voice, gunshots, etc.) are "carried" in the modulation of the amplitude of a fundamental carrier wave running at an assigned radio frequency much higher than that of the message. Ratios of the AM peak amplitudes to the AM valleys, as in Fig. 4.7.2 are for radio an important figure of merit (or lack of merit if it's excessive and results in FCC fines!).The ratio is called an *Amplitude Modulation Ratio (AMR)* or an *Amplitude Modulation Quotient (AMQ)* depending on whether you prefer to deal with a ratio in the range -*1* to +*1* or its inverse outside that range.

$$AMR = \frac{|A_1| - |A_2|}{|A_1| + |A_2|}, \qquad AMQ = \frac{|A_1| + |A_2|}{|A_1| - |A_2|} \tag{4.7.5a}$$

These are analogous to the *Standing Wave Ratio (SWR)* or a *Standing Wave Quotient (SWQ)* for galloping waves that label a pure standing wave with zero *(SWR = 0)* or infinity ($SWQ = \infty$).

$$SWR = \frac{|A_{\rightarrow}| - |A_{\leftarrow}|}{|A_{\rightarrow}| + |A_{\leftarrow}|}, \qquad SWQ = \frac{|A_{\rightarrow}| + |A_{\leftarrow}|}{|A_{\rightarrow}| - |A_{\leftarrow}|} \tag{4.7.5b}$$

For quantum waves, the message or beats are the only thing we can see directly in a Ψ∗Ψ counting experiment as seen by (4.7.1). The phase carrier velocity (4.7.2b) is hidden from our view. Furthermore, the message will be "audible" only if the amplitudes $|A_1|$ and $|A_2|$ are both non-zero. Ψ∗Ψ in (4.7.1) is constant if amplitude product A_1A_2 is zero but is "loudest" for 50-50 amplitudes ($A_1 = A_2$).

The frequency beats or AMR modulation in time of co-propagating waves are analogous to the spatial bumps or SWR groups in space that cause galloping of mono-chromatic (single frequency ω_0) counter-propagating waves as discussed in Sec. 4.5. Two frequency counter-propagating waves such as in Sec. 4.6 may have both beats and moving bumps as may the co-propagating waves here described.

A key quantum principle emerges.

> *The probability distribution* $\Psi^*\Psi$ *for quantum wave composed of two frequencies* ω_1 *and* ω_2 *(or energies* $\hbar\omega_1$ *and* $\hbar\omega_2$*) will oscillate at the beat frequency* $|\omega_1 - \omega_2|$ *with an amplitude that is greatest when the two amplitudes are equal and zero if either one is zero.*

An important corollary of this is due to the Planck factor $e^{-i\omega t}$ being killed in a $\Psi^*\Psi$ product.

> *The probability distribution* $\Psi^*\Psi$ *for quantum wave composed of a single frequency (or energy) is motionless.*

Single-energy states are called *stationary-states*. They are dead as a doornail, so far as a stationary observer can tell. Galloping motion and phase velocity are not directly observable. Counts come randomly according to the probability $\Psi^*\Psi$ but the statistics stays the same. Phase motion is observable only when there is an interference between two systems, and many many quantum counts are needed to see that.

A common electrical or optical engineering diagnosis is to send a monochromatic input wave of amplitude $A_1 = A_{\rightarrow}$ down a transmission line and measure the amplitude $A_2 = A_{\leftarrow}$ that 'echoes' and gallops back using the interference highs and lows whose ratio is the *SWR* in (4.7.5b). This is just what we will be doing with simulated quantum waves later on. The quantum theory of scattering begins by analyzing just such a galloping wave interference problem.

Analogy with Faraday polarization rotation

The complicated motion of atom frame waves in Fig. 4.6.1 has an optical polarization and 2D-oscillator analogy that extends the analogy given for laser frame waves in Fig. 4.5.1. The difference between the two figures is that right and left-moving waves in Fig. 4.6.1 differ in frequency $\omega'_{\rightarrow} = 4$ and $\omega'_{\leftarrow} = 1$. So mixtures of them will undergo a quantum beat at their difference frequency $\omega'_{\rightarrow} - \omega'_{\leftarrow} = 3$.

The group envelope will rotate around the ring at this beat frequency with velocity u given first in (4.3.5a). That rotation is analogous to what a polarization ellipse undergoes in circular dichroism or *Faraday rotation* due to a difference in frequency of left and right polarization states.

A 2-level or spin-$^1/_2$ or U(2) system has quantum beats and Rabi-like rotation that is maximum at saturation *(SWR=0)*. Galloping and switchback waves are perhaps the oldest *U(2)* systems (~1650) and polarization activity may be the next oldest (~1860). Such analogies serve long and well and should be exploited whenever possible. This is taken up in Chapter 10.

Using (4.7.1) you should be able to show how the shape and location of the *SWR* envelope gives the *complex* echo amplitude $A_{\leftarrow} = |A_{\leftarrow}|e^{i\phi}$, that is, *both* its magnitude $|A_{\leftarrow}|$ and its phase ϕ relative to $A_{\rightarrow}$.. Note again that monochromatic galloping light speeds range from *(SWR)c* to *(SWQ)c* by (4.5.1).

(b). Group velocity for continuous waves

We may approximate the formula (4.7.2a) for group velocity by a derivative relation if the angular frequency ω and wavevector k form a continuum and are related by a continuous function $\omega(k)$ or $k(\omega)$. An $\omega(k)$ relation is called a *dispersion relation* because it tells how wave velocities vary with frequency or color and tells how color components "disperse" in a general multi-component light pulse. So far, we have mainly considered photons or vacuum optics for which $\omega = kc$. This is the case of constant wave velocity that suffers no dispersion.

The continuum approximation to (4.7.2a) is the following derivative formula.

$$v_{group} = \frac{\omega_1 - \omega_2}{k_1 - k_2} = \frac{\Delta\omega}{\Delta k} \rightarrow v_{group} = \frac{d\omega}{dk}, \text{ as: } \Delta k \rightarrow 0 \qquad (4.7.6a)$$

For vacuum optics the derivative relation for group velocity always gives speed of light c.

$$v_{group} = \frac{d\omega}{dk} = c, \text{ for: } \omega = kc \qquad (4.7.6b)$$

This is the same as the continuum formula for phase velocity that follows from (4.7.2b).

$$v_{phase} = \frac{\omega}{k} = c \qquad (4.7.7)$$

Without dispersion, velocity V_{group} and V_{phase} are the same as was shown in Fig. 4.2.12.

(c). Counter-versus-co propagating waves

The formula (4.7.6a) for group velocity assumes a continuum of possible ω-values of frequency and k-values of wavevector in order to define a derivative $d\omega/dk$. Quantum mechanics often disallows this because, as we will see in later chapters, these quantities are usually quantized and discrete. Also, a derivative is meaningless for the counter-propagating wave groups since the interfering k-values are of opposite sign so cannot be infinitesimally close. Hence, we must use our discrete algebraic sum and difference formulas (4.1.5f) and (4.1.5g) for V_{group} and V_{phase}. Here a quadratic dispersion $\omega(k) = k^2$ is assumed. (Later, this turns out to be an approximate form for the dispersion of quantum matter waves.)

$$V_{group} = \frac{\omega_2 - \omega_1}{k_2 - k_1} \qquad (4.\ 1.5f) \qquad V_{phase} = \frac{\omega_2 + \omega_1}{k_2 + k_1} \qquad (4.\ 1.5g)$$

As an example compare a co-propagating pair of $k_1=8$ and $k_2=9$ waves with wave velocities

$$V_{group} = \frac{\omega_9 - \omega_8}{9 - 8} = \frac{9^2 - 8^2}{9 - 8} = 17 \qquad (4.7.8a)$$

$$V_{phase} = \frac{\omega_9 + \omega_8}{9 + 8} = \frac{9^2 + 8^2}{9 + 8} = 8.53 \qquad (4.7.8b)$$

with a counter-propagating pair of $k_1=-8$ and $k_2=9$ waves with wave velocities

$$V_{group} = \frac{\omega_9 - \omega_8}{9 + 8} = \frac{9^2 - 8^2}{9 + 8} = 1 \qquad (4.7.9a)$$

$$V_{phase} = \frac{\omega_9 + \omega_8}{9 - 8} = \frac{9^2 + 8^2}{9 - 8} = 145 \qquad (4.7.9b)$$

The resulting waves are rendered into spacetime plots by the following Fig. 4.7.3. These *BohrIt* plots were introduced in Fig. 4.2.11 and Fig. 4.3.3.

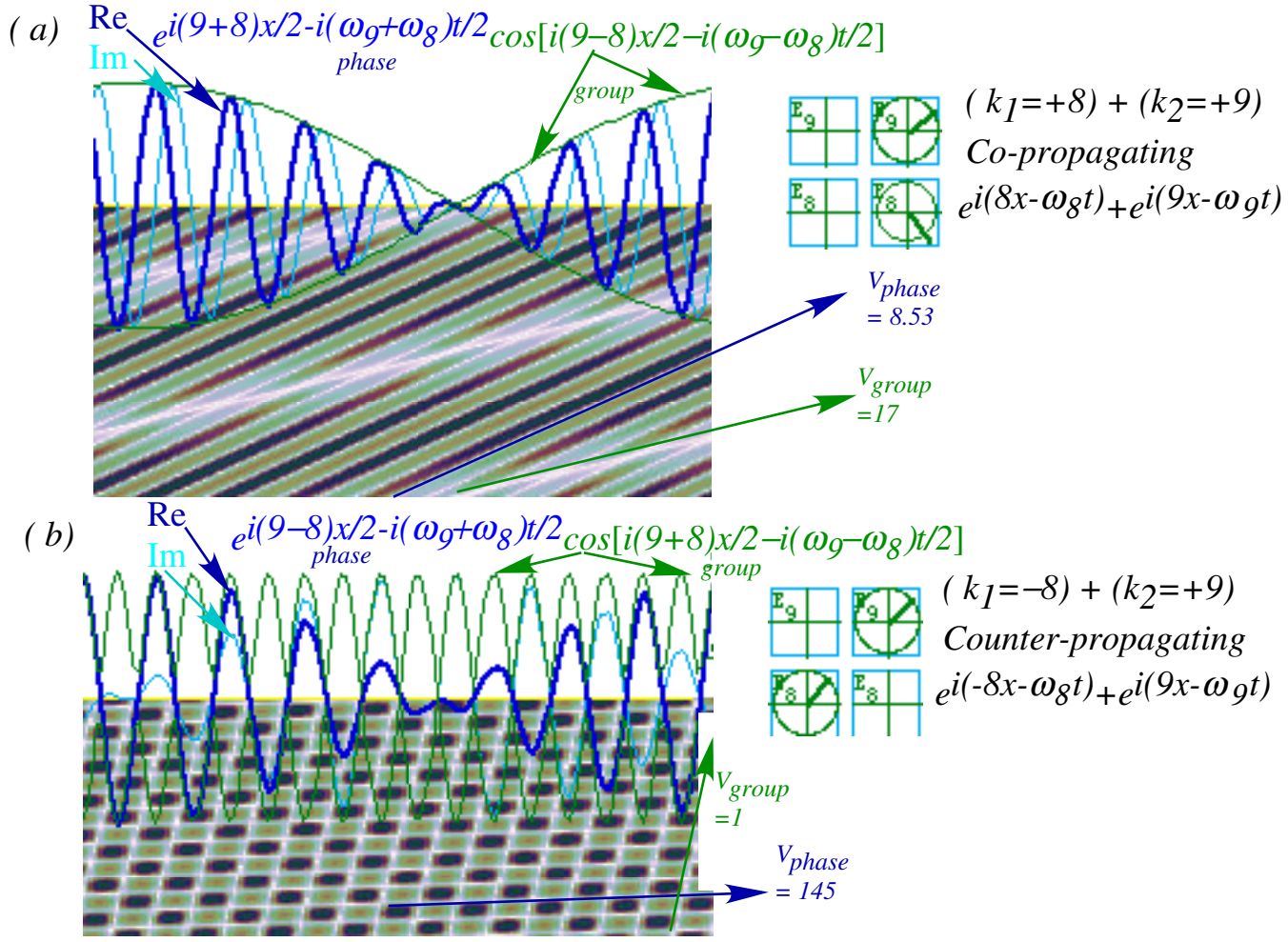

Fig. 4.7.3 Waves for $\omega=k^2$ dispersion (a) Co-propagating and (b) Counter-propagating. (BohrIt plot)

What a difference a ±-sign in k makes! The co-propagating wave in Fig. 4.7.3(a) has a $(k_2-k_1)=1$-half-wave envelope containing $(k_2+k_1)=17$-half waves of phase carrier. For the counter-propagating wave in Fig. 4.7.3 (b) it's vice-versa: a $(k_2-k_1)=17$-half-wave envelope containing a single ($(k_2+k_1)=1$) half wave of phase that looks like more waves because it's constrained by a very kinky envelope.

Furthermore the speeds of the four different wave parts vary greatly between (4.7.8) and (4.7.9). The phase part of the counter-propagating wave in Fig. 4.7.3 (b) zips along at 145 units by (4.7.9b), while the group envelope only creeps by at 1 unit by (4.7.9a). In contrast, the co-propagating group speed 17 is a little less than twice the phase speed 8.53 in Fig. 4.7.3(a) according to (4.7.8a-b).

The real and imaginary parts of the co-propagating phase in Fig. 4.7.3(a) have much the same shape as their counter-propagating counterparts in Fig. 4.7.3(b). But the huge speed 145 of the counter-propagating phase in Fig. 4.7.3(b) makes its imaginary wave pattern march 17 times further ahead of its real part than it does in the co-propagating phase above it in Fig. 4.7.3 (a).

As we will see later, the two wave functions in Fig. 4.7.3 have the same value of energy. Looks and shape can be both deceiving and telling in the quantum wave world!

Problems for Chapter 4

Not casting dispersion

4.2.1. Using 4x4 minor-per-major engineering graph paper with ruler and compass you should be able to easily construct 12-phasor wave diagrams like Fig. 4.2.5-8 with 12 tangent phasors per fundamental (k=1) wavelength L. Use this scheme to render the following wavefunctions. Label&check with complex algebra. Let $\omega=ck$ where c=1 fundamental length L per second.

(a) Fundamental left-to-right moving (k=+1) wave $\psi = e^{i(kx-\omega t)}$ at t=0 and t=(1/4)(2π/ω) or 1/4-period.
(b) Fundamental right-to-left moving (k=-1) wave $\psi = e^{i(kx-\omega t)}$ at t=0 and t=(1/4)(2π/ω) or 1/4-period.
(c) 2nd harmonic left-to-right moving (k=+2) wave $\psi = e^{i(kx-\omega t)}$ at t=0 and t=(1/4)(2π/ω) or 1/4-period.
(d) Half the sum of (b) and (a) at t=0 and t=(1/4)(2π/1) or 1/4-period of fundamental.
(e) Half the sum of (c) and (a) at t=0 and t=(1/4)(2π/1) or 1/4-period of fundamental.
(f) Half the sum of (c) and (b) at t=0 and t=(1/4)(2π/1) or 1/4-period of fundamental.
(g) Half the sum of (a) and a "do-nothing-wave" (k=0) at t=0 and t=(1/4)(2π/1) or 1/4-period of fundamental.

Casting dispersion

4.2.2. Using 4x4 minor-per-major engineering graph paper with ruler and compass you should be able to easily construct 12-phasor wave diagrams like Fig. 4.2.5-8 with 12 tangent phasors per fundamental (k=1) wavelength L. Use this scheme to render the following wavefunctions. Label&check with complex algebra. Let $\omega=ck^2$ where c=1 fundamental length L per second.

(a) Fundamental left-to-right moving (k=+1) wave $\psi = e^{i(kx-\omega t)}$ at t=0 and t=(1/4)(2π/ω) or 1/4-period.
(b) Fundamental right-to-left moving (k=-1) wave $\psi = e^{i(kx-\omega t)}$ at t=0 and t=(1/4)(2π/ω) or 1/4-period.
(c) 2nd harmonic left-to-right moving (k=+2) wave $\psi = e^{i(kx-\omega t)}$ at t=0 and t=(1/4)(2π/ω) or 1/4-period.
(d) Half the sum of (b) and (a) at t=0 and t=(1/4)(2π/1) or 1/4-period of fundamental.
(e) Half the sum of (c) and (a) at t=0 and t=(1/4)(2π/1) or 1/4-period of fundamental.
(f) Half the sum of (c) and (b) at t=0 and t=(1/4)(2π/1) or 1/4-period of fundamental.

Mastering dispersion

4.2.3. Using engineering graph paper with ruler and compass you should be able to easily construct per-spacetime and spacetime diagrams like Fig. 4.2.11(a-b). Construct vector lattice diagrams for the following wavefunction combinations taken from preceding problems 4.2.1-2. Label&check with algebraic formulas for all relevant wave velocities and how waves moved in problems 4.2.1-2. Note denominator scale D for each.

From Problem 4.2.1 Letting $\omega=ck$ where c=1 fundamental length L per second.

(a) Half the sum of (b) and (a).
(b) Half the sum of (c) and (a).
(c) Half the sum of (c) and (b).

From Problem 4.2.2 Letting $\omega=ck^2$ where c=1 fundamental length L per second.

(d) Half the sum of (b) and (a).
(e) Half the sum of (c) and (a).
(f) Half the sum of (c) and (b).

Lorentz's Own-Bra

4.4.1. (a) Derive eigenbras and eigenkets of the Lorentz transformation matrix L_{mn} in (4.3.5e) and discuss the physical interpretation of its eigenvalues and eigenvectors.

(b) Use geometry to construct accurate u = $\pm^3/_5$c and u = $\pm^4/_5$c graph paper using the simplest steps with a rule&compass. For Prob. 4.4.2 it will help to have t range from +5 to +5 sec. , and x between ±3 litesec. Hint: An easy relabeling converts u = +(whatever)-graph paper into u = -(whatever)-graph paper. How?

Spacetime Terrorism

4.4.2 (a) Complete the following happening tables using the Lorentz transformation between ship space-time coordinates (x',ct') and lighthouse coordinates (x,ct) given that the ship is traveling from right to left at a speed of $^3/_5$c and passes the lighthouse at t=0=t'. Calculate and then use a $^{\pm 3}/_5$c graph (preceding exercise) to check the results.

Ship emits light	Explosion #1	Explosion #2	Explosion #3
x = 3 litesec. t = -5 sec.	x = t =	x = -1 litesec. t = -1 sec.	x = t = 1 sec.
x' = t' =	x' = -1 litesec. t' = -3 sec.	x' = t' =	x' = -3 litesec. t' =

(b) Draw the space-time paths of light waves emitted right and left from explosions #1 and #2 on the space-time graph and answer the following questions.

(a) When does light from explosion #1 hit the lighthouse? _____(Lighthouse time)
(b) When does light from explosion #1 hit the lighthouse? _____(Ship time)
(c) When does light from explosion #2 hit the lighthouse? _____(Lighthouse time)
(d) When does light from explosion #2 hit the lighthouse? _____(Ship time)
(e) Draw the space-time paths of fragments going left and right away from explosions #1 and #2 assuming that each fragment has a speed c/2 or -c/2 relative to the ship.

B.I.G.A.N.N. Investigates

4.4.3 The explosions in problem 4.4.2 lead to an investigation by B.I.G.A.N.N. (Bureau of Intergalactic Aids to Navigation at Night) headed by Rolla H. Ann Hoover (doubly illegitimate granddaughter of J. Edgar Hoover).

(a) When does the first fragment from explosion #1 hit the lighthouse? _____(Lighthouse time)
(b) When does a second fragment from explosion #1 hit the lighthouse? _____(Lighthouse time)
(c) When does a fragment from explosion #1 hit the ship? _____(Ship time)
(d) When does a fragment from explosion #2 hit the ship? _____(Ship time)
(e) When does a fragment from explosion #2 hit the Lighthouse? _____(Lighthouse time)
(f) How fast would the lighthouse say the first fragment was going?_____c (Get sign right.) Does this check with velocity addition formula (4.4.3)?
(g) How fast would the lighthouse say the second fragment was going?_____c (Get sign right.) Does this check with velocity addition formula (4.4.3)?
(h) The authorities of BIGANN have spotted a causal (as opposed to acausal) connection between all the explosions. To whom does it point?

Galloping Into the Sunset

4.5.1. The ReΨ zeros of the real part of a general monochromatic light wave

$$\Psi_{gallop} = A_{\Rightarrow}\Psi_{\Rightarrow} + A_{\Leftarrow}\Psi_{\Leftarrow} = A_{\Rightarrow}e^{i(kx-\omega t)} + A_{\Leftarrow}e^{i(-kx-\omega t)}$$

follow a curved "galloping" trajectory such as shown in Fig. 4.5.1.

(a) Derive an equation *x=x(ct)* for one of the curves in Fig. 4.5.1(d) and plot it for that case.
(b) Give a formula for the max and min speeds of the zeros and apply it to Fig. 4.5.1.
(c) Do similar max/min apply to zeros of ImΨ? What about zeros of $|\Psi|$? Are there any?
(d) Discuss limiting cases of (a) to (b) when amplitudes are equal.($A_{\Rightarrow} = A_{\Leftarrow}$)

Hopalong Kepler

4.5.2. The Kepler orbit of an isotropic 2D-oscillator exhibits a kind of galloping motion similar to that of interfering waves. How similar? Compare eccentric anomaly time behavior $\phi(t)$ with wave phase velocity derived in preceding exercise 4.5.1.

Nothing Going Nowhere Fast

4.6.1. The ReΨ zeros of a general counter-propagating dichromatic light wave

$$\Psi_{switch} = A_1 \Psi_{\Rightarrow} + A_2 \Psi_{\Leftarrow} = A_1 e^{i(k_1 x - \omega_1 t)} + A_2 e^{i(-k_2 x - \omega_2 t)}$$

follow a curved "switchback" trajectory such as shown in Fig. 4.6.1(d).

(a) Derive equation(*s)* for one of these curves and plot it for the case in Fig. 4.6.1(d). Hint: Implicit functions are OK. Doppler and Lorentz formulas discussed in section 4.3 may make this a lot easier.

(b) Discuss the zero-speeds at the points near where zeros are created or annihilated in Fig. 4.6.1(d). Apply to your discussion the velocity addition formulas (4.4.3) of Sec. 4.4.

(c) Similar to (b), discuss the maximum and minimum and inflection zero-speeds in Fig. 4.6.1(d).

(c) Discuss limiting cases when amplitudes are equal ($A_{\Rightarrow} = A_{\Leftarrow}$) as it applies to Fig. 4.6.1.

Counterfeit and Cofeit

4.7.1. The ReΨ zeros of an equi-amplitude (A_1=A_2) dichromatic Bohr-matter wave (dispersion: ω=k^2)

$$\Psi_{group\ \text{matter}} = A_1 e^{i(k_1 x - \omega_1 t)} + A_2 e^{i(k_2 x - \omega_2 t)}$$

follow a grid of spacetime trajectories such as is shown in Fig. 4.7.3(a) for co-propagating (k_1k_2>0) and in Fig. 4.7.3(b) for counter-propagating (k_1k_2<0) cases.

(a) Using the k-values given for each figure (a) and (b) derive the wave lattice (4.2.11) for each case and plot as in Fig. 4.2.11. Indicate “particle paths” as well as wave-zero paths.

(b) The imaginary part ImΨ is hidden more in Fig. 4.7.3(b) than in Fig. 4.7.3(a). Where is it? Derive and/or sketch. Does the counter-propagating ImΨ look at all like its co-propagating cousin?

WaveIt Quiz (You should be able to do this in 10 minutes or less.)

Write down the expo-cosine identity: $(e^{ia}+e^{ib})/2$ = _____

NO CALCULATORS! Many of the answers are in units of *c*. Just write, say, *8c* not *2.4E9* etc.

$\Psi(x,t)$ =	Does Ψ have a constant phase velocity?	Does Ψ have a constant group velocity?	Does ReΨ wave speed "gallop" continuously.	Does Ψ wave represent a stationary state?
$3e^{i(2x-2ct)}$ $+2e^{i(4x-4ct)}$	Yes__? or No__? If Yes give value _____	Yes__? or No__? If Yes give value _____	Yes__? or No__? If Yes give range of speed:_____ to:_____	Yes__? or No__? If No give beat frequency(ies) :_____ :_____
$2e^{i(2x-2ct)}$ $+2e^{i(-2x-2ct)}$	Yes__? or No__? If Yes give value _____	Yes__? or No__? If Yes give value _____	Yes__? or No__? If Yes give range of speed:_____ to:_____	Yes__? or No__? If No give beat frequency(ies) :_____ :_____
$3e^{i(2x-2ct)}$ $+2e^{i(-2x-2ct)}$	Yes__? or No__? If Yes give value _____	Yes__? or No__? If Yes give value _____	Yes__? or No__? If Yes give range of speed:_____ to:_____	Yes__? or No__? If No give beat frequency(ies) :_____ :_____
$3e^{i(2x-2ct)}$ $+3e^{i(-4x-4ct)}$	Yes__? or No__? If Yes give value _____	Yes__? or No__? If Yes give value _____	Yes__? or No__? If Yes give range of speed:_____ to:_____	Yes__? or No__? If No give beat frequency(ies) :_____ :_____

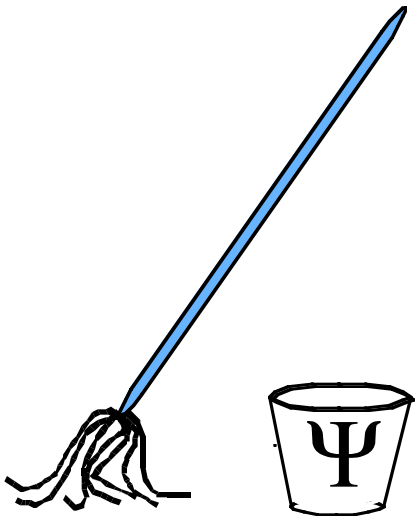

QM for AMOP

Chapter 5
Waves in Per-Spacetime: (k,ω)-Dispersion

W. G. Harter

A fundamental axiom of wave-phase invariance leads to a logical development of the principles of quantum theory and relativistic dynamics that are the current foundations of modern physics. Careful examination of wavevector and frequency leads to their relativistic properties that mirror those of space and time developed in the preceding chapters. The Planck's axiom $E=h\nu$ then leads directly to momentum-energy , rest energy Mc^2, and other key ideas such as a wave dispersion interpretation of inertial mass and classical dynamics. The Schrodinger equation is seen as an approximation and it limitations are discussed. Relativistic accelerative dynamics are introduced from both classical and quantum points of view.

CHAPTER 5. WAVES IN PER-SPACETIME: (K,W)-DISPERSION 1

5.1 Relativistic invariant hyperbolas 1
(a) Hyperbolic wavevector geometry: "baseball diamond" invariants 1
(b) Spacetime invariants: Proper time 3
(c) Per-spacetime invariants: Proper frequency 3
Proper time versus frequency: γ-waves never age! 4
But, μ-waves do age! 5
γ-waves versus μ-waves 5

5.2. CW relativistic energy-momentum: Quantum theory 7
(a) To catch a μ-wave…(or "particle") 7
Lab view of a μ-wave 7
(b) Planck-DeBroglie-Einstein relations 8
(c) Quantum dispersion relations 8
Non-relativistic (Schrodinger-Bohr) dispersion 10
(d) Quantum count rates suffer Doppler shifts, too 10
Relativistic Fourier amplitude shifts 10
Broadcasting optical coordinates: SWR transforms like velocity 11
(e) Imprisoned light ages (And gets heavier) 12
But, why twice as heavy? 13
(f) Effective mass 15
(g) Two photons for every mass: Compton recoil 17

5.3. Pulse Wave (PW) Dynamics :Wave-Particle Duality 19
(a) Taming the phase: Wavepackets and pulse trains 19
(b) Continuous Wave (CW) vs. Pulsed Wave (PW): colorful versus colorless 21
Wave ringing: m_{Max}-term cutoff effects 23
Ringing suppressed: m_{Max}-term Gaussian packets 23
Are these pulses photons? 23
(c) PW switchbacks and "anomalous" dispersion 25
Abnormal relativistic dispersion 25
Abnormal laboratory dispersion 25

5.4. Quantum-Classical Relationships 27
(a) Deep classical mechanics: Poincare's invariant 27
(b) Classical versus quantum dynamics 28
A crummy (but quick!) derivation of Schrodinger's equation 28
(c) A slightly improved derivation of Schrodinger's equation 29
Schrodinger difficulties 30
Classical relativistic Lagrangian derived by quantum theory 31

5.5 Relativistic acceleration: Newton's invariants 33
(a) Classical particle and PW theory of acceleration 33
Proper length: Gentlemen start your engines! 35
(b) Wave interference and CW theory of acceleration 39
Per-spacetime diamond geometry 44
Acceleration by Compton scattering 45

5.6 Bohr-Orbitals and Higher Energy Physics 47
(a) Dirac's anti-matter 47
(b) Numerology: Bohr electron radii and Compton wavelength 48
(c) Bohr matter-wave PW revivals: When μ-waves party! 51
Bohr-Schrodinger dispersion and group velocity 51
Bohr μ-wave quantum speed limits 53
Follow the zeros! 53
Bohr μ-wave pulse train dephasing and revival 55

Problems for Chapter 5. 57

Chapter 5. Waves in Per-Spacetime: (k,ω)-Dispersion

5.1 Relativistic invariant hyperbolas

So much of physics held dear in Newtonian theory seems to soften in relativity and quantum wave theory. As modern physics mixes time and space or per-time (frequency ω) and per-space (k-vector), the hard and precise classical world might seem to be melting into shifting sands as wave relativism trumps cherished absolutes. However, any idea that classical measurement may have absolute precision is a myth.

In fact, modern coherent wave and pulse optics has achieved a precision that puts any classical "hard edge" meter rods to shame. Imagine building a Global Positioning System out of steel girders even for a *1 km* asteroid! Without optically aided stabilization, such a frame would be next to useless.

Optics owes much of its tremendous precision to *invariants* that are constant for all observers. Lightspeed in (4.3.1) is one invariant and *wave phase* in (4.3.6) is another. Other invariants, including the hyperbolic geometry introduced in Sec. 4.4 and reviewed below, are related to these. Any and all invariants are welcome and useful additions to spacetime wave theory. A port, any port, in a storm!

(a) Hyperbolic wavevector geometry: "baseball diamond" invariants

The "baseball-diamond" geometry of counter-propagating laser waves introduced in Fig. 4.3.2 and Fig. 4.4.3 is repeated again in the following Fig. 5.1.1. This has per-spacetime plots or frequency-ω-*versus*-wavevector-*ck* graphs of the interfering output waves between a pair dueling lasers of identical frequency $\omega_0=2c$ and opposite wavevectors $ck_0=\pm 2c$. (*1c* unit is 300 THz.) Fig. 5.1.1(a) displays green light *ck*-wavevectors pointing in opposite directions at 600 THz, as seen by the lasers. Fig. 5.1.1(b), is the view of an atom traveling right to left in the frame where it sees the right-moving laser beam Doppler blue shifted up to 1200 THz while the left-moving wave is red shifted down to 300THz.

The color-invariant lightspeed axiom (4.3.1) confines laser *(ck,ω)* vectors to the *±45°* baselines or "foul ball lines" while the time-reversal axiom demands that Doppler red shift $r=e^{-\rho}$ be inverse to the blue shift $b=e^{\rho}$ in (4.3.5b). The right baseline stretches by *b=2* while the left baseline shrinks by *1/b*. So a product of foul-line hypotenuses $\sqrt{2}\omega_0 b$ and $\sqrt{2}\omega_0 r$ must be a constant $2\omega_0^2$. So, the diagonal of the $\sqrt{2}\omega_0 b$–by–$\sqrt{2}\omega_0 r$ rectangle follows a hyperbola of radius $2\omega_0$ traced by "2nd base" in Fig. 5.1.1(b) as blue shift *b* or relativistic speed $\beta=u/c$ of the atom increases.

Baseball diamond half-diagonals follows a hyperbola of radius ω_0, on which lies the "pitcher's mound" at diamond center. Half-diagonal vectors $\mathbf{K'}_{phase}=(\mathbf{K'}_{\rightarrow}+\mathbf{K'}_{\leftarrow})/2$ and $\mathbf{K'}_{group}=(\mathbf{K'}_{\rightarrow}-\mathbf{K'}_{\leftarrow})/2$ are half-sum (difference) of laser vectors $\mathbf{K'}_{\rightarrow}$ and $\mathbf{K'}_{\leftarrow}$. They define phase and group waves in (4.2.10) or (4.3.4).

$$\mathbf{K'}_{phase}=((k'_{\rightarrow}+k'_{\leftarrow})/2,\ (\omega'_{\rightarrow}+\omega'_{\leftarrow})/2) \quad (5.1.1a) \qquad \mathbf{K'}_{group}=((k'_{\rightarrow}-k'_{\leftarrow})/2,\ (\omega'_{\rightarrow}-\omega'_{\leftarrow})/2)) \quad (5.1.1b)$$

Vectors $\mathbf{K'}_{phase}$ and $\mathbf{K'}_{group}$ define a Lorentz-Einstein-Minkowski coordinate grid in *both* spacetime (4.3.5e) *and* per-spacetime (4.3.10). A wave-produced spacetime grid is shown in Fig. 4.3.3(a) for the lasers and in Fig. 4.3.3(b) for the atom speeding through the laser field at $\beta=u/c=-3/5$. Per-spacetime grid vectors for lasers in Fig. 5.1.1(a) and for the atom in Fig. 5.1.1(b) are shown along with invariant hyperbolic curves.

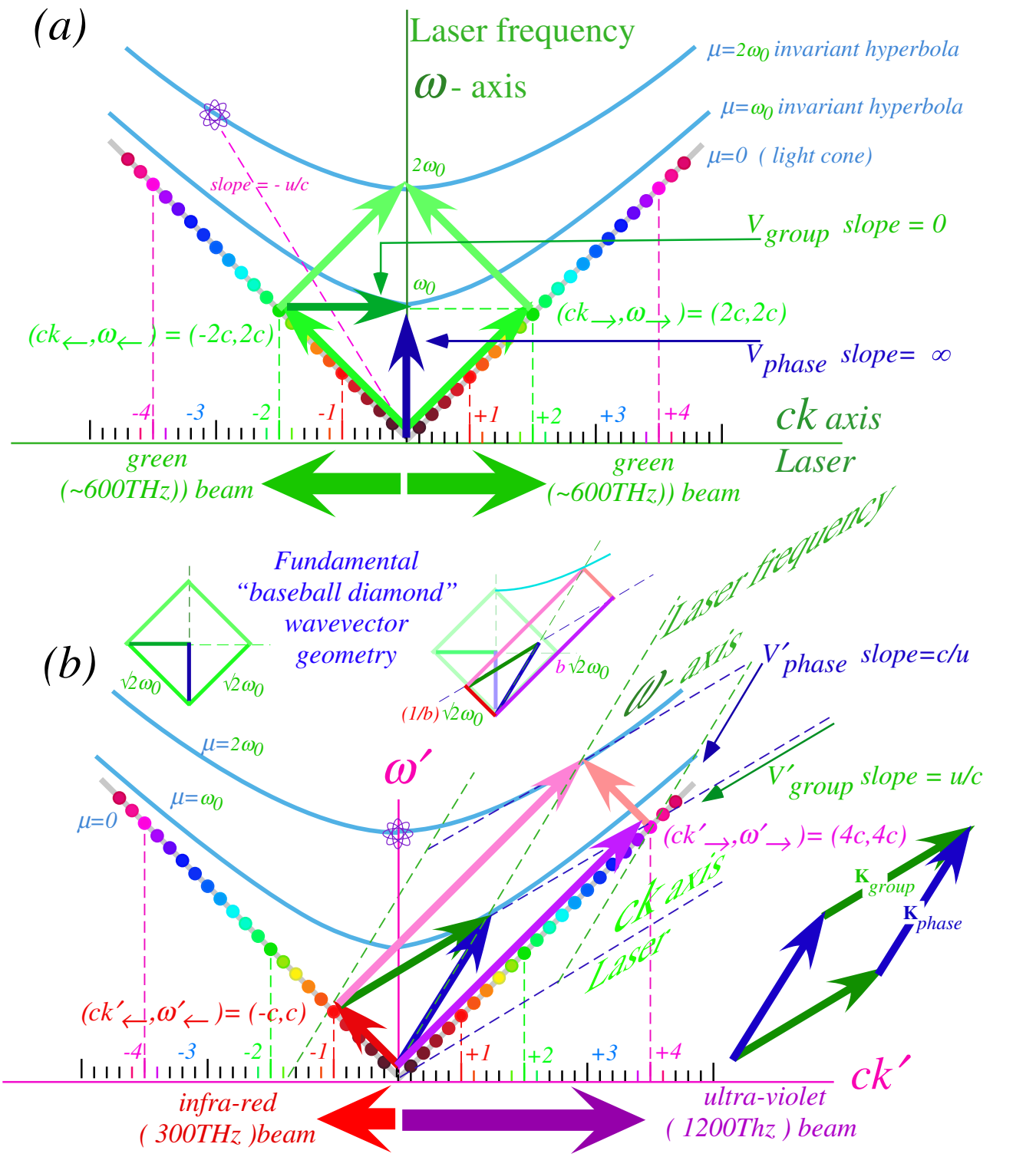

Fig. 5.1.1 Baseball wavevector geometry. (a) Laser view with atom at velocity u=-3c/5. (b) Atom view.

The hyperbolas, derived in (4.3.11), look the same in either atom (ck',ω') or laser (ck,ω) coordinates.

$$\omega^2{}_{12}-\left(ck_{12}\right)^2=\omega'^2{}_{12}-\left(ck'_{12}\right)^2=\mu^2=0,\pm\omega_0^2,\pm 2\omega_0^2,\ldots \tag{5.1.2}$$

Each hyperbolic radius $\mu=0,\ \omega_0,\ 2\omega_0,\ \ldots$ is the *invariant* or *proper frequency* of that hyperbola.

Proper or invariant quantities are key descriptors of physical objects or waves that do not depend upon the reference frame or coordinates used to define the object. Below is a discussion of a spacetime invariant called *proper time* τ. Later it is compared with proper frequency μ defined above.

Any quantity, invariant or otherwise, defined in spacetime, has a similar quantity defined in per-spacetime with an inverse physical interpretation. Particle velocity has units of x/t (*meters*)-per-(*second*), while wave velocity has the units ω/k (*per-second*)-per-(*per-meter*). A time t *vs.* space x plot in Fig. 4.2.11(a) keeps the same slope-velocity correspondence as a per-space k *vs.* per-time ω plot of Fig. 4.2.11(b) by switching ck and ω axes. Note also that phase velocity and group velocity (4.3.5a) are inverses of each other so our ω *vs.* ck per-spacetime plots have $\mathbf{K}_{phase}$ and $\mathbf{K}_{group}$ define ω and ck axes, respectively, but they switch roles in spacetime plots where $\mathbf{K}_{group}$ and $\mathbf{K}_{phase}$ define the t and x-axis.

(b) Spacetime invariants: Proper time

The area of a unit rectangular *(b)-by-(1/b)* cell in Fig. 5.1.2(a) is *1* for any speed u of the atom. The Lorentz rhombic graph in Fig. 5.1.2(a) is just a square graph stretched by a Doppler factor of b along the x-ct or $+45°$ diagonal and compressed by the inverse factor $1/b$ along the other diagonal so its area stays the same. As speed u varies, all grid points trace hyperbolas with UV=constant where $U=x+ct$ and $V=x-ct$ are $\pm 45°$ diagonal coordinates that might be used in Fig. 5.1.2(a) in place of x and ct.

It is easy to check that the product UV is unchanged by Lorentz transformation (4.3.5e).

$$-UV = -(x+ct)(x-ct) = (ct)^2 - (x)^2 = (ct')^2 - (x')^2 \qquad (5.1.3)$$

For an atom who carries its origin $x=0$ this quantity is called its *proper time* τ or *own-time* or *age*.

$$c^2\tau^2 = (ct)^2 - (x)^2 = (ct')^2 - (x')^2 \qquad (5.1.4)$$

Except for light, these are equations of hyperbolas in spacetime. Light has $\tau=0$ on straight $\pm 45°$ lines called the *light cone* where age τ is forever zero. *Light never ages.* It just can't grow up! If you could accompany light along the $45°$ path in Fig. 4.2.10(c) then you, too, would see all phasors frozen at one time.

Grids and invariants are plotted in Fig. 5.1.2. Notice how the hyperbolas serve as grid markers for both the square unsqueezed diamond as well as any squeezed or Lorentz-transformed rhombus.

(c) Per-spacetime invariants: Proper frequency

The per-spacetime invariant (5.1.2) is called *proper frequency* μ or *own frequency*.

$$\mu^2 = (\omega)^2 - (ck)^2 = (\omega')^2 - (ck')^2 \qquad (5.1.5a)$$

Proper frequency is the flip side of proper time (5.1.4), that is, if τ is an *age*, then μ is the *rate* of aging. Light never ages, so its proper frequency μ is identically zero. Having $\mu=0$ implies a constant-c speed.

$$(\omega)^2-(kc)^2 = (\omega')^2-(k'c)^2 = 0 \text{ implies:} \qquad c=|\omega/k|=|\omega'/k'|. \qquad (5.1.5b)$$

The *null-invariant* $\mu=0$ or *light cone* in (kc,ω)-per-spacetime is the $\pm 45°$ "X" in Fig. 5.1.2 (b) as is $\tau=0$ for (x,ct)-spacetime in Fig. 5.1.2(a). Non-zero-μ-invariant hyperbolas in Fig. 5.1.2(b) serve as grid markers in per-spacetime just as do τ-invariant hyperbolas in spacetime of Fig. 5.1.2(a).

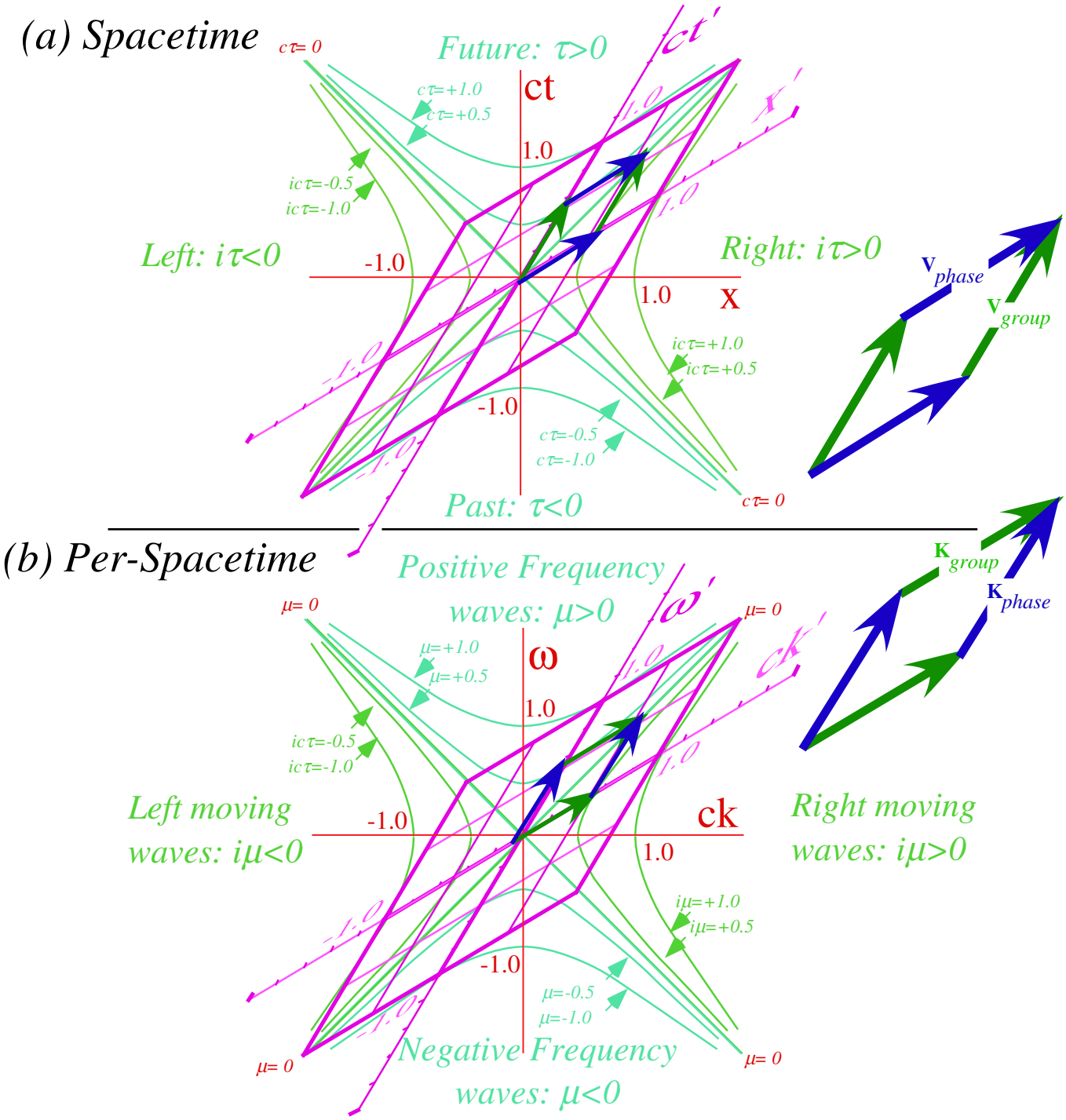

Fig. 5.1.2(a) Space-time grid plot with proper time invariant hyperbolas $c\tau^2=ct^2-x^2 = 0, \pm 0.5, \pm 1.0,..$

Fig. 5.1.2(b) Wavevector-frequency plot with proper frequency invariants $\mu^2=\omega^2-(ck)^2 = 0, \pm 0.5, \pm 1.0,..$

Proper time versus frequency: γ-waves never age!

Non-degenerate τ-hyperbolas with real τ such that $c^2\tau^2=1,4,...$ serve to mark temporal grid points $ct'=\pm 1, \pm 2,...$ for any ct'-axis. Imaginary τ such as $c^2\tau^2=-1,-4,...$ serve to mark spatial axis grid points $x'=\pm 1, \pm 2,...$ As shown in Fig. 5.1.2(a), real proper time τ values demark time in the past or future while

imaginary $\tau=ix$ demark distance to the right or left. Proper time τ means "own" time or "eigen" time. τ is an "age" $\tau=t'$ or $\tau=t''$ of any object that is holding its "own" origin $x'=0$ or $x''=0$, respectively.

Light cone residents always have zero proper time in (5.1.3b). It is as though they never age. Free photons or γ-waves, from below radio frequency to ExaHertz and above, are all forever young!

But, μ-waves do age!

However, we seem to be made of other "stuff" than simple γ-waves. Unfortunately, for those of us who would like to live forever, our "stuff" ages. The μ-waves, which we call *matter*, have intrinsic τ-clocks running at a *non*-zero proper frequency μ. This allows μ-waves to have any speed *but* the speed c of light. In contrast, a light wave (γ-wave) travels at only its speed c but with internal clocks frozen like an $x=ct$ line of phasors in Fig. 4.2.10(c). Having zero proper frequency $\mu=0$, means you just don't tick!

The μ-hyperbolas with real μ such that $\mu^2=1, 4,...$ serve to mark frequency grids at points $,\omega'=\pm1, \pm2,...$ for an observant atom in a general $(k'c,\omega')$-frame of Fig. 5.1.2(b). The positive frequency side ages normally while those on the negative frequency side un-age, that is, appear to *go back in time*! (We will have more to say about such *anti-matter* behavior later.)

The μ-hyperbolas with imaginary μ with $\mu^2=-1, -4,...$ mark points $,ck'=\pm1, \pm2,...$ on the wavevector axis of the $(k'c,\omega')$-frame with $\pm k$ labeling right or left-moving waves. Imaginary-μ-waves correspond to faster-than-light or so-called *tachyonic* waves. For example, phase waves with $\mathbf{K}_{phase}$ in (5.1.1a) have to go faster-than-light in order to trace the x-coordinate grids or *NOW*-lines in Fig. 4.3.3(b).

γ-waves versus μ-waves

Since all colors go c, a rocket ship cannot ever catch-up to a light or γ-wave. As shown in Fig. 5.1.3 below, an ever-faster rocket may only Doppler shift the light more and more to the red, but it never can achieve exactly zero for either the frequency ω of a γ-wave or for a γ-wave's wavevector k.

However, a rocket ship may catch-up and even pass a matter or μ-wave as sketched in Fig. 5.1.4. A μ-wave has $\mathbf{K}_{phase}=(ck_p,\omega_p)$ on a hyperbola of radius $\omega_0=\mu=2c$ that tracks the center "pitcher's mound" of the "baseball diamond" in Fig. 5.1.1.

As the rocket speeds up, it sees k_p swing from $k_p=1.5$ (Fig. 5.1.4(a)) through zero (Fig. 5.1.4(b)) to a negative value $k_p=-1.5$ (Fig. 5.1.4(c)) while the frequency ω_p dips from $\omega_p=2.5c$ to a minimum $\omega_p=\mu=2$ (Fig. 5.1.4(b)) and then back to $\omega_p=2.5c$. This makes the phase velocity $V_{phase}=\omega_p/k_p$ go from $5c/3$ to infinity, then to minus infinity and finally to a fast negative value $V_{phase}=-5c/3$ in the final frame of Fig. 5.1.4(c).

Meanwhile, group velocity $V_{group}=\omega_g/k_g$ simply goes from $3c/5$ to zero in Fig. 5.1.4(b) to $-3c/5$ in Fig. 5.1.4(c). This group wave dynamics is more like what one sees when passing a classical object of matter. But, group *and* phase dynamics underlie all waves that make our world, light or matter.

Wave behavior is, perhaps, one of the deepest and most fundamentally unifying ideas in all of modern physics. Indeed, with 20-20 hindsight, we find beginnings of the idea of matter-as-waves going back centuries to works of Huygens, Hamilton, and Poincare′ as discussed later in Sec. 5.4. In order to understand and derive quantum theory, the concept of phase invariance and its related *Colorful Relativity* axiom (4.3.1) is essential and fundamental. Now, let us put these concepts to work!

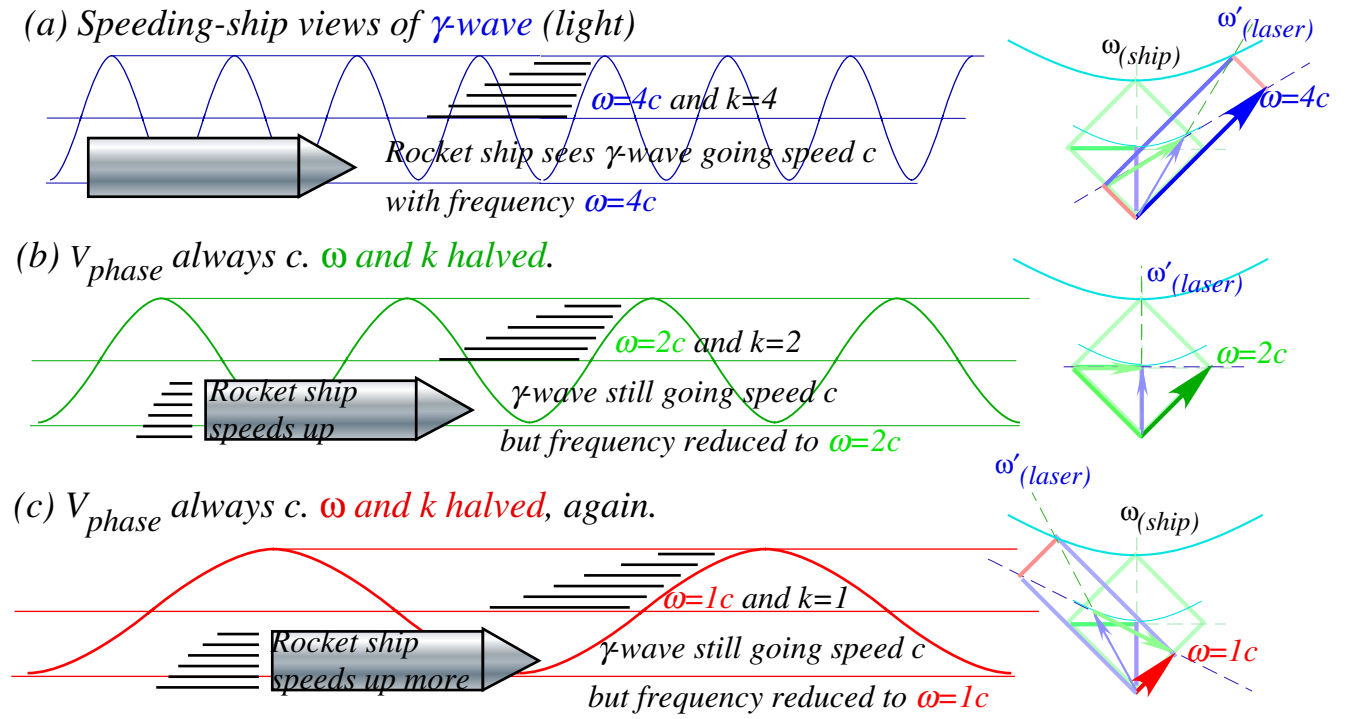

Fig. 5.1.3 Light γ-wave cannot be passed by rocket but ω may appear Doppler-shifted (almost) to zero.

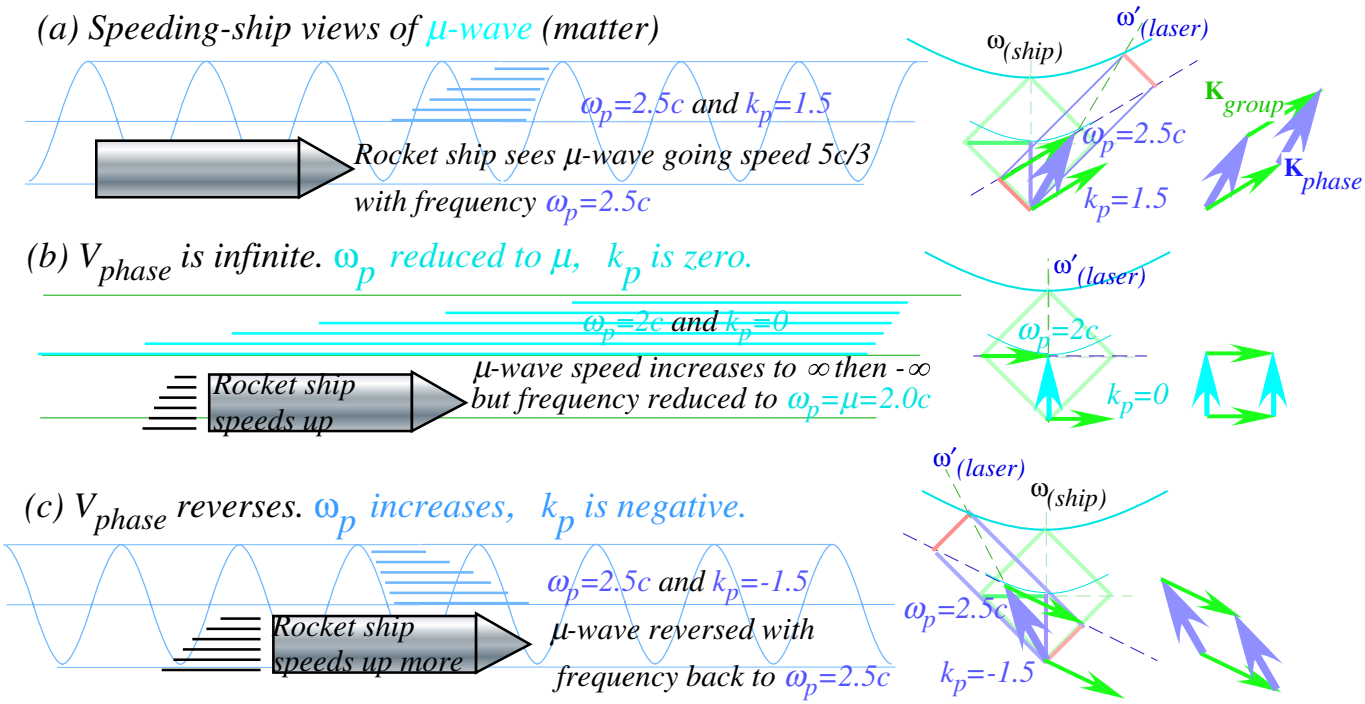

Fig. 5.1.4 Matter μ-wave is caught (b) and passed (c) by rocket but ω_p cannot be Doppler-shifted below μ.

5.2. CW relativistic energy-momentum: Quantum theory

This section is an important one. It derives fundamental quantum dynamics using the continuous wave (CW) theory of just two "colors" developed so far. As seen in the following Sec. 5.3, pulse wave (PW) or optical pulse train (OPT) dynamics require many frequencies. So, CW theory is simpler. Also, it is not predjudiciously encumbered by ideas of Newtonian "particles" of matter or "corpuscles" of light.

(a) To catch a μ-wave...(or "particle")

Relativistic symmetry of the continuous wave (CW) development is based on invariance of phase Φ (4.3.6) and proper frequency μ (5.1.5). This applies to *matter* or *μ-waves* as well as to light or γ-waves. Matter waves age at some invariant proper frequency μ that, unlike that of light, is *non*-zero. Lab frequency ω of a *μ-wave* lies on a non-degenerate hyperbola (5.1.5) in (ck,ω)-per-spacetime.

$$(\omega)^2-(kc)^2 =(\omega')^2-(k'c)^2 = \mu^2 >0 \qquad (5.2.1)$$

Consider a wave that has positive real proper frequency, say, the $(\mu=1)$-hyperbola in Fig. 5.1.2(b). Each point (ck,ω) on the $(\mu=1)$-hyperbola corresponds to one wave state of $(\mu=1)$-"stuff" with a wavevector k and a frequency ω. That point also defines another frame such as the tilted one labeled $(k'c,\omega')$ in Fig. 5.1.2(b). In the $(k'c,\omega')$-frame the wavevector k' is zero and frequency ω' is μ, that is, $(k'c,\omega')=(0,\mu)$ by (5.2.1). It looks like the rocket-view sketched in Fig. 5.1.4(b): a "kinkless" wave with infinite phase speed.

That wave point (kc,ω) also defines a space-time (x',ct')-frame of speed $u=\beta c$ such as the one in Fig. 5.1.2(a) that has exactly the same velocity tilt $\beta=u/c$ as the frame in Fig. 5.1.2(b). (They both have our familiar $\beta=3/5$.) It is a *rest-frame* of the matter wave or "particle" defined by having the wavevector k "Doppler-shifted" to zero as in Fig. 5.1.4(b) $(k'c,\omega')=(0,\mu)$.Any (kc,ω)-state is a "kinkless" $(k'=0)$-wave in the one frame that has "caught up" with it by going the velocity u that is a special velocity for the wave, namely its group velocity V_{group} (4.3.2). That u is the classical Newtonian "particle" or matter velocity.

Lab view of a μ-wave

The frequency ω' in atom frame where $k'=0$ is the *proper frequency* $\mu=\omega'$ by (5.2.1). Lorentz equations (4.3.10a) then give lab values (k,ω) of the $((k',\omega')=(0,\mu))$-wave that "has" velocity u in the lab.

$$ck = \frac{ck'+\beta\omega'}{\sqrt{1-\beta^2}} = \frac{0+\mu u/c}{\sqrt{1-(u/c)^2}} \cong \mu\frac{u}{c}-\frac{1}{2}\mu\left(\frac{u}{c}\right)^3+\ldots \qquad (5.2.2)$$

$$\omega = \frac{\beta ck'+\omega'}{\sqrt{1-\beta^2}} = \frac{0+\mu}{\sqrt{1-(u/c)^2}} \cong \mu+\frac{1}{2}\mu\left(\frac{u}{c}\right)^2+\ldots \qquad (5.2.3)$$

Binomial expansion $(1-x)^{-1/2}\sim 1+x/2+...$ approximates waves of low group velocity ($u<<c$).

Our difficult work is now done and it is only necessary to apply *Planck's axiom* $(E=\hbar\omega)$ of quantum theory. This, however, is a step far less trivial than it might seem. Indeed, Planck proposed $E=\hbar\omega$ or its Hertz equivalent, $E=h\nu$, as a "trick" to solve vexing cold-blackbody radiation problems. But, upon reconsideration, he actually sought to discard it. Taking Planck's axiom $(E=\hbar\omega)$ seriously demands the *equivalence of energy and frequency*. Energy IS some ω wiggle rate! So, what's wiggling? That's the hard

question. Is it space time itself? That $E=\hbar\omega$ seemed wacky to Planck. Energy of a classical oscillator goes as frequency *squared*. ($E_{HO}=k\omega^2$) We now use of his curious $E=\hbar\omega$, but we do not just take it lightly!

(b) Planck-DeBroglie-Einstein relations

Planck's axiom *($E=\hbar\omega$)* of energy-frequency equivalence is applied to (5.2.3).

$$E=\hbar\omega=\frac{\hbar\mu}{\sqrt{1-(u/c)^2}}\cong\hbar\mu+\frac{1}{2}\hbar\mu\left(\frac{u}{c}\right)^2+\ldots \qquad (5.2.4)$$

Energy E rises quadratically in velocity u *($E\sim[\hbar\mu/c^2]u^2$)* as should kinetic energy $^1/_2Mu^2$ for a classical mass M. Setting M to the coefficient $\hbar\mu/c^2$ in (5.2.4) fixes the invariant proper frequency constant μ.

$$\hbar\mu=Mc^2 \qquad (5.2.5a)$$

So, $\hbar\mu$ is *Einstein rest energy* Mc^2, the first term in an expansion of exact *total relativistic energy* E.

$$E=\hbar\omega=\frac{Mc^2}{\sqrt{1-(u/c)^2}}\cong Mc^2+\frac{1}{2}Mu^2+\ldots \qquad (5.2.5b)$$

Classical kinetic energy $^1/_2Mu^2$ is the lowest order u-term in $\hbar\omega$. Now by (5.2.2) the lowest order u-term in $\hbar k$ is classical *momentum* Mu (using $\mu=Mc^2/\hbar$). So, $\hbar k=p$ is the exact *relativistic momentum*.

$$p=\hbar k=\frac{Mu}{\sqrt{1-(u/c)^2}}\cong Mu+\frac{1}{2}Mc^2\left(\frac{u}{c}\right)^3+\ldots \qquad (5.2.5c)$$

Momentum, or *impego* as Galileo called it, falls out as the *DeBroglie momentum-wavevector equivalence*: momentum *IS* so many kinks in space. It is analogous to the Planck energy-frequency equivalence: energy *IS* so many wiggles in time. Perhaps, Planck's axiom isn't so wacky, after all!

(c) Quantum dispersion relations

Einstein and DeBroglie energy and momentum relations (5.2.5) follow directly from the continuous wave (CW) phase invariance axiom (5.2.1) and Planck's frequency-energy equivalence axiom *($E=\hbar\omega$)*. Next we derive the quantum matter or μ-wave dispersion relation that governs the world's dynamics.

Energy and momentum equations (5.2.5b-c) each solve for wave group velocity u or slope $\beta=u/c$.

$$\frac{u}{c}=\frac{\sqrt{E^2-(Mc^2)^2}}{E}=\frac{cp}{E}=\frac{cp}{\sqrt{(Mc^2)^2+(cp)^2}} \qquad (5.2.6)$$

The preceding uses an energy-momentum μ-invariant (5.2.1) or they come directly from (5.2.5b-c).

$$E^2-(cp)^2=(Mc^2)^2=\mu^2\hbar^2 \qquad (5.2.7)$$

Solving for energy $E=\hbar\omega$ gives a *relativistic matter-energy dispersion function $\omega(k)$* plotted in Fig. 5.2.1a.

$$E=\hbar\omega=\sqrt{(Mc^2)^2+(cp)^2}=\sqrt{(Mc^2)^2+(c\hbar k)^2}\cong Mc^2+\frac{p^2}{2M}+\ldots \qquad (5.2.8)$$

The dispersion function $\omega(k)$ gives wave velocities. Here V_{phase} formula (4.3.2c) is used with equal same sign wavevectors *($k_1=k=k_2$)* and equal frequency ($\omega_1=\omega=\omega_2$) to give the conventional *(ω/k)*-formula for phase velocity. It checks with the value derived before in (4.3.5a).

$$V_{phase} = \lim \frac{\omega_1 + \omega_2}{k_1 + k_2}\bigg|_{(k_1)=k=(k_2)} = \frac{\omega}{k} = \frac{E}{p} = \frac{c^2}{u} \tag{5.2.9a}$$

Using (4.2.12) with k_1 *approaching* k_2 gives the conventional group velocity or "particle" velocity u.

$$V_{group} = \lim \frac{\omega_1 - \omega_2}{k_1 - k_2}\bigg|_{(k_1)\to(k_2)} = \frac{d\omega}{dk} = \frac{dE}{dp} = \frac{c^2 p}{E} = u \tag{5.2.9b}$$

The conventional definition of group velocity is a slope of a tangent to a dispersion function. Fig. 5.2.1(a) shows an $E'=1$ line tangent to an $Mc^2=1$ dispersion. Its slope of $u/c=-3/5$ is that of the p'-axis for a frame moving from right to left at $u=-3c/5$. As in Fig. 5.1.2, a μ-hyperbola crosses the ω'-axis at $\omega'=\mu$.

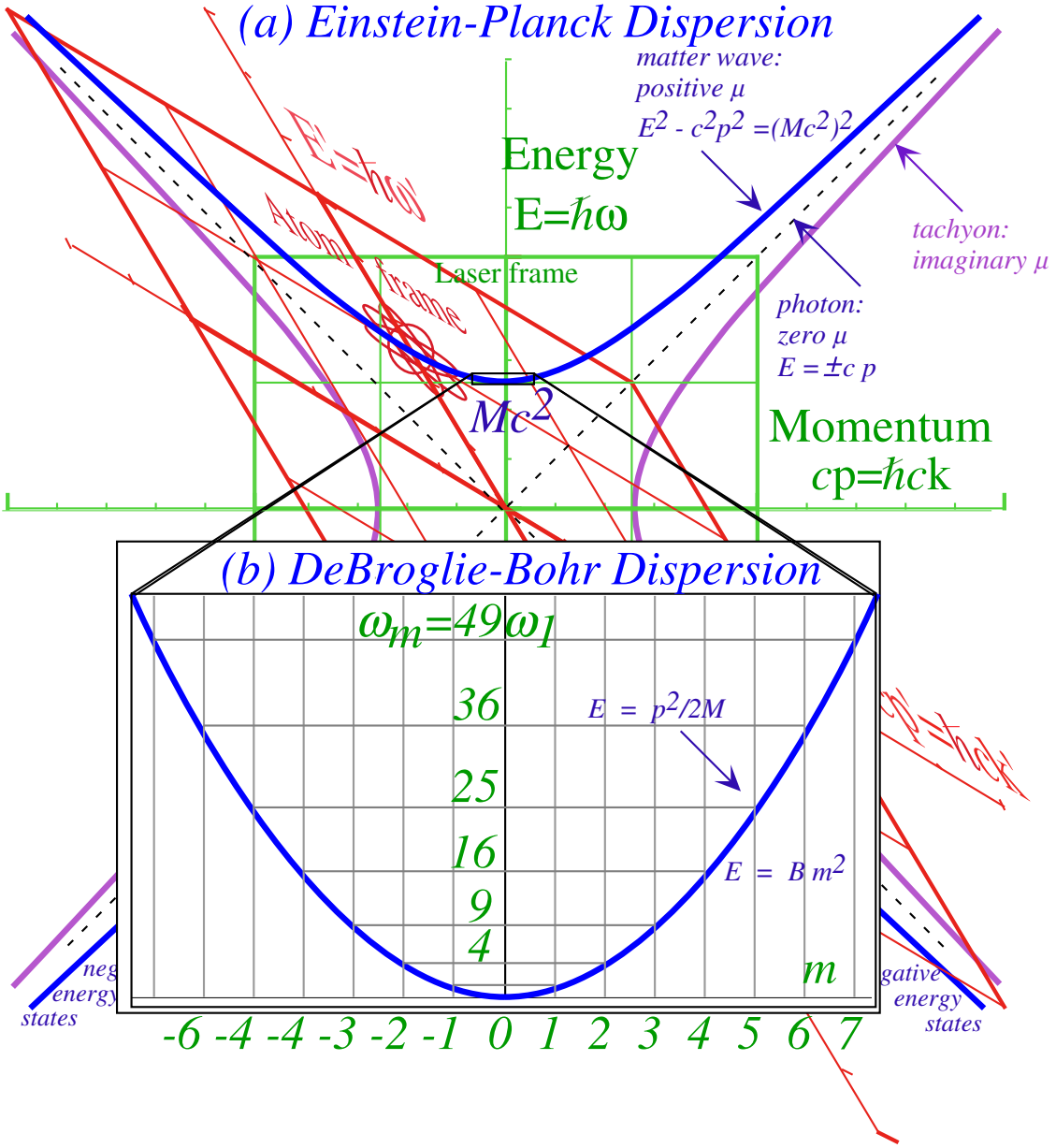

Fig. 5.2.1 Energy vs. momentum dispersion functions including mass M, photon, and tachyon.
(a) Relativistic (Einstein-Planck) case: $(Mc^2)^2=E^2-(cp)^2 = 1$ *or* $\mu^2=\omega^2-(ck)^2 = 1/\hbar^2$.
(b) Non-relativistic (Schrodinger-DeBroglie-Bohr) case: $E=-(1/2M)p^2$ *or* $\omega=\hbar k^2/2M$

Feynman showed energy and momentum arise from transformation of a *(k=0)* wave. That is, energy-momentum states are boosts of zero-momentum "particles" by *(cp,E)*-Lorentz relations.

$$cp = \frac{cp' + \beta E'}{\sqrt{1-\beta^2}} = cp' \cosh\theta + E' \sinh\theta \qquad (5.2.10a)$$

$$E = \frac{\beta cp' + E'}{\sqrt{1-\beta^2}} = cp' \sinh\theta + E' \cosh\theta \qquad (5.2.10b)$$

Energy-momentum relations are simply *(ck,ω)*-relations (4.3.10) or (5.2.2) multiplied by $\hbar$. It's an easy derivation of such important equations if based on CW states having well defined energy-momentum.

Non-relativistic (Schrodinger-Bohr) dispersion

In the non-relativistic limit *(u<<c)*, approximations of energy, such as (5.2.8) or Fig. 5.2.1b, usually drop the Mc^2 term since neither absolute energy nor absolute phase are physically observable. Only energy *difference* is physically important for classical mechanics, and only *relative* phase and phase velocity is observed in quantum mechanics. Neglecting a constant term like Mc^2 in energy expression (5.2.5b) does not change the group velocity $d\omega/dk = u$ or any wave behavior given by a probability envelope $\Psi^*\Psi$. The envelope $\Psi^*\Psi$ always has group velocity *u* according to equations (4.7.2).

On the other hand, phase velocity ω/k, is reduced by neglecting Mc^2 and changes from an enormous value c^2/u to a value near $u/2$ that is quite small in the non-relativistic limit *(u<<c)*, indeed, it is about half of the group velocity as in (4.7.8) and Fig. 4.7.3. This, however, is not inconsistent with classical physics or experiments based on observing $\Psi^*\Psi$ since the phase cancels out of $\Psi^*\Psi$. Phase velocity is more easily detectible for light, but then for $Mc^2=0$, all velocities are *c*, anyway.

(d) Quantum count rates suffer Doppler shifts, too

Doppler shifts, galloping waves, and electromagnetic wave coordinates made by CW lasers have been the basis of the development of relativity in Chapter 4 and of quantum theory in the present Chapter 5. A discussion of wave coordinates seen by arbitrarily moving sources and observers is given now. The discussion revolves around the question, *"Can a laser-pair in a frame-A produce the Minkowski coordinate grid of a frame B suitable for viewing by a third observer in a frame-C?"*

A simpler question is, "Can the laser-pair in frame *A* produce a grid for a moving observer's frame *B* so that it is seen by *B* as a Cartesian space-time grid?" This would seem easy. Simply tune up the laser shining along *B*'s velocity $u=\beta c$ by Doppler factor $b=\sqrt{(1+\beta)}/\sqrt{(1-\beta)}$ to frequency $\omega_{\rightarrow} = (b)\omega_0$ and de-tune the oppositely moving wave to $\omega_{\leftarrow} = (1/b)\omega_0$. However, we must also adjust laser wave *amplitudes* as well as frequencies in order that the intended observer *B* sees a standing wave like Fig. 4.3.3(a) and not a galloping one like Fig. 4.5.1 or Fig. 4.6.1. The same applies to the more complex *A*, *B*, and *C* question.

Relativistic Fourier amplitude shifts

Spacetime simulations in Fig. 4.3.3 and particularly those in Fig. 4.3.3(b) show that Lorentz-Minkowski wave coordinate lines are obtained from balanced Fourier combinations of plane waves. In Fig. 4.3.3, the amplitude $E_{\rightarrow}$ of the left-to-right wave must equal the amplitude $E_{\leftarrow}$ of the right-to-left wave. Otherwise, wave galloping arises as shown in Fig. 4.5.1 and Fig. 4.6.1.

However, balanced amplitudes in the laser lab frame do *not* translate into balanced amplitudes in a boosted atom frame or *vice-versa*. Both the frequencies *and the amplitudes* are affected by Lorentz transformation. Surprisingly, it turns out that amplitudes of light waves transform in the same way as their frequency, that is, by a Doppler blue-shift factor $b=e^{\rho}$ (or red-shift *1/b*) of (4.3.5b) repeated here.

$$\omega_{\leftarrow} = \sqrt{\frac{1-\beta}{1+\beta}}\omega_0 = e^{-\rho}\omega_0\,, \qquad \omega_{\rightarrow} = \sqrt{\frac{1+\beta}{1-\beta}}\omega_0 = e^{+\rho}\omega_0\,, \tag{5.2.11}$$

Relativistic tensor analysis [AJP **53** 671(1985)] of electromagnetic plane wave amplitudes gives the following.

$$E_{\leftarrow} = \sqrt{\frac{1-\beta}{1+\beta}}E_0 = e^{-\rho}E_0\,, \qquad E_{\rightarrow} = \sqrt{\frac{1+\beta}{1-\beta}}E_0 = e^{+\rho}E_0\,. \tag{5.2.12}$$

But, *E*-amplitude shifts (5.2.12) can be derived more easily by revisiting the Doppler shift while imagining light corpuscles or "photons." Pulse rates and photon count rates transform in the same way as any frequency. Doppler formulas (5.2.11) determine the atom's photon or pulse count rate $N_{\leftarrow}$ of right-to-left (red) photons and $N_{\rightarrow}$ of left-to-right (blue) photons, if N_0 (green) photons per second are emitted by each PW laser in Fig. 5.2.2(a) boosted to velocity $u=\beta c=3c/5$ in Fig. 5.2.2(b).

$$N_{\leftarrow} = \sqrt{\frac{1-\beta}{1+\beta}}N_0 = e^{-\rho}N_0\,, \qquad N_{\rightarrow} = \sqrt{\frac{1+\beta}{1-\beta}}N_0 = e^{+\rho}N_0\,, \tag{5.2.13}$$

Recall Fig. 4.2.5 where $N_0 = 1.0Hz$ lasers hit the atom with "red" at $N_{\leftarrow} = 0.5Hz$ and "blue" at $N_{\rightarrow} = 2.0Hz$.

The quantum count rate N is related to Poynting flux S or electromagnetic field energy density U.

$$S = |\mathbf{E}\times\mathbf{B}| = cU \;\; [Joule/(m^2 s)]$$

The e.m. field energy $U[Jm^{-3}]$ is product of photon number $N\,[m^{-3}]$ and Planck's energy $\hbar\omega$ per photon

$$U = \varepsilon_0|E|^2 = N\hbar\omega \;\; [Joule/(m^3)], \tag{5.2.14a}$$

where N is the expected photon number

$$N = |\Psi|^2\,. \tag{5.2.14b}$$

This relates the classical electric field E to a quantum field or wave probability amplitude Ψ.

$$E = \sqrt{\frac{\hbar\omega}{\varepsilon_0}}\Psi \tag{5.2.14c}$$

Since the energy density $|E|^2$ is a product of N and ω which each shift factor by Doppler factor b, the E-field also shifts by b for a moving observer as in (5.2.12) while the energy density shifts by b^2.

$$U_{\leftarrow} = \frac{1-\beta}{1+\beta}U_0\,, \qquad U_{\rightarrow} = \frac{1+\beta}{1-\beta}U_0 \tag{5.2.15}$$

Broadcasting optical coordinates: SWR transforms like velocity

It is interesting to derive the amplitude settings that are needed to broadcast a 50-50 Minkowski wave (4.6.3) to a moving atom so it sees a laser space-time coordinate system as a Minkowski grid like Fig. 4.3.3(b). A 50-50 wave in one frame has unit ratio of left and right moving amplitudes. The amplitude ratio in a β-moving frame is the square of a Doppler shift factor given by (5.2.12).

$$\frac{E_{\leftarrow}}{E_{\rightarrow}} = \frac{1-\beta}{1+\beta}. \tag{5.2.16}$$

Solving for $\beta=u/c$ shows that the relativity parameter β is just the *SWR* (4.5.1b) in the broadcasting frame.

$$\beta = \frac{E_{\leftarrow} - E_{\rightarrow}}{E_{\leftarrow} + E_{\rightarrow}} = SWR_{broadcast}\,. \tag{5.2.17}$$

This shows that the broadcaster must match the minimum galloping wave speed (4.5.1c), that is, its *SWR*, to the speed of the frame containing the intended recipient.

The optical *SWR* has a transformation relation based on (5.2.12).

$$E'_{\leftarrow} = \sqrt{\frac{1-\beta}{1+\beta}}E_{\leftarrow}\,, \qquad E'_{\rightarrow} = \sqrt{\frac{1+\beta}{1-\beta}}E_{\rightarrow}\,. \tag{5.2.18a}$$

$$SWR' = \frac{E'_{\rightarrow} - E'_{\leftarrow}}{E'_{\rightarrow} - E'_{\leftarrow}} = \frac{SWR + \beta}{1 + SWR\cdot\beta}\,. \tag{5.2.18b}$$

So *SWR* transforms like velocity $\beta_0 = u_0/c$ in (4.4.3b) as it must since velocity is determined by *SWR*.

$$\beta_0' = \frac{\beta_0 + \beta}{1 + \beta_0\cdot\beta} \tag{5.2.19}$$

All this shows that perfect standing waves *(SWR=0)* and linear wave coordinates are possible in only one Lorentz frame at a time. For the atom's waves to look like Fig. 4.3.3(b), lasers must tune the *SWR* to the atom's β-value of *–3/5*. Then the lasers have galloping waves like Fig. 4.5.1(e) and not Fig. 4.3.3(a) where *SWR=0*. If the lasers leave their *SWR* at zero, then the atom sees *SWR′=3/5* with galloping waves like Fig. 4.6.1(b) and not a perfect Minkowski grid. (But, the atom could recover a perfect grid by simply attenuating the blue-shifted UV beam by *b=2*.)

By detuning frequencies as well as *SWR*, the lasers can present the speeding atom with its own Cartesian coordinate frame. An ultraviolet laser on the right with twice the argon frequency and twice the amplitude meeting an infrared beam with half the frequency and half the amplitude would make a square green grid like Fig. 4.3.3(a) *for the atom*. The result is the same as the atom would see if it had its own pair of argon lasers. In the original laser frame the atom's lasers would yield an intense UV beam counter-propagating right-to-left with a weak IR beam going left-to-right, just the reverse of Fig. 4.3.3(b). That results in a coordinate grid like the one labeled "*Atom Frame*" in Fig. 5.2.2(a).

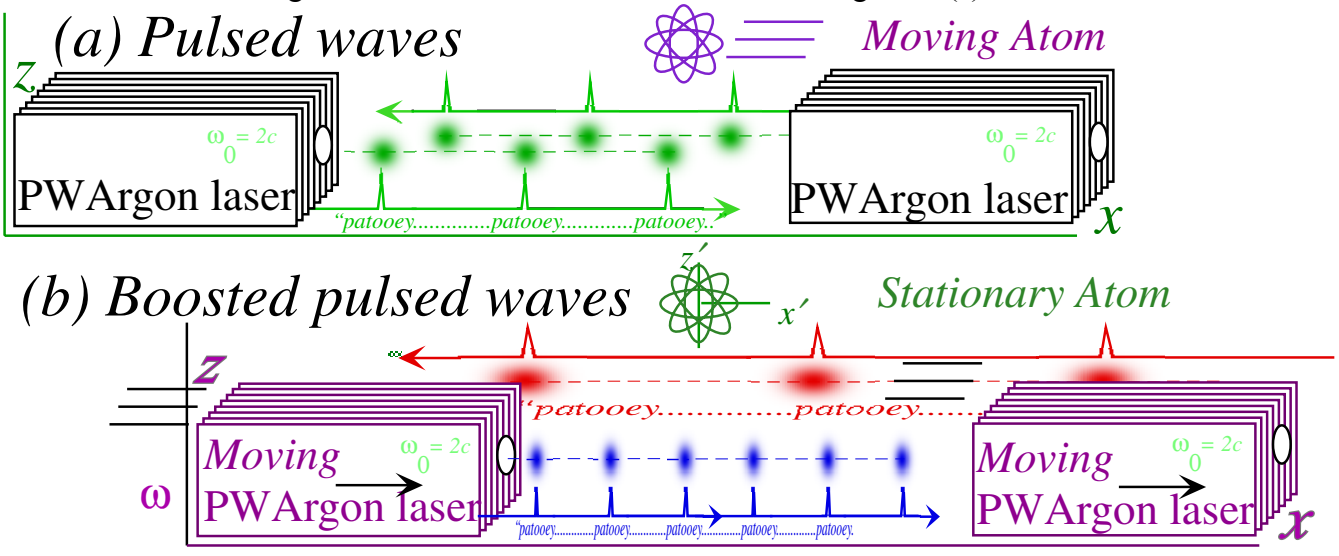

Fig. 5.2.2 Doppler shifting pulsed wave (PW) output. (a) Laser view. (b) Atom view.

(e) Imprisoned light ages (And gets heavier)

Each two-laser field depicted so far may be replaced by single inter-cavity laser field or, in principle, by a field between a pair of perfect mirrors. When a pair of counter-propagating waves add

together as they do inside a cavity the resultant (ck,ω)-vector $\mathbf{K}_+ = \mathbf{K}_\rightarrow + \mathbf{K}_\leftarrow$ points to a positive frequency hyperbola as in Fig. 5.2.3, which is a copy of Fig. 5.2.1 with cavity mirrors added.

Shown also are the hyperbolas associated with the difference vector $\mathbf{K}_- = \mathbf{K}_\rightarrow - \mathbf{K}_\leftarrow$ and the group and phase vectors $\mathbf{K}_{group} = (\mathbf{K}_\rightarrow - \mathbf{K}_\leftarrow)/2$ and $\mathbf{K}_{phase} = (\mathbf{K}_\rightarrow + \mathbf{K}_\leftarrow)/2$ whose sum and difference are the original primitive $\mathbf{K}_\rightarrow$ and $\mathbf{K}_\leftarrow$ laser source vectors.

Other observers such as the atom see the vectors $\mathbf{K}_{group}$, $\mathbf{K}_{phase}$, $\mathbf{K}_+$ and $\mathbf{K}_-$ differently, but always on their respective hyperbolas ($\mathbf{K}_\rightarrow$ and $\mathbf{K}_\leftarrow$ stick to $\pm 45°$ light cones) as shown in Fig. 5.2.1(b). The atom-viewed vectors $\mathbf{K}'_\rightarrow$ and $\mathbf{K}'_\leftarrow$ define particle paths as in Fig. 4.2.11(b) while $\mathbf{K}'_{group}$ and $\mathbf{K}'_{phase}$ span a wave coordinate lattice as in Fig. 4.2.11(a). Fig. 5.2.3(b) shows the Lorentz-Minkowski lattice of Fig. 4.3.3(b) or energy-momentum wave lattices of Fig. 5.2.1 or Fig. 5.1.1 in a cavity that is Lorentz-contracted and time skewed to fit the waves it contains (as well as the matter-waves that make its box).

This brings the (continuous wave) CW development of relativistic quantum theory full circle and shows that a combination of two γ-waves having **K**-vectors $\mathbf{K}_\rightarrow = (ck_0,\omega_0)$ and $\mathbf{K}_\leftarrow = (-ck_0,\omega_0)$ is like a μ-wave with proper frequency $\mu = 2\omega_0$. In fact, combinations in a box are μ-waves with many of the wave properties of a massive "particles." Trapped light acquires a non-zero proper frequency $\mu = 2\omega_0$ and that is the same as acquiring mass according to (5.2.5b). "Light-plus-Light" acts like "matter."

But, why twice as heavy?

To accelerate the box to a small velocity *u* requires momentum associated with twice the photon frequency ω_0 since it has to be turned around and bounced forward. So a proper frequency $\mu = 2\omega_0$ gives the correct rest mass $M_{rest} = \hbar\mu/c^2 = 2\hbar\omega_0/c^2$ of this arrangement.

Still, it seems that a laser cavity operating at the frequency ω_0 should only have proper frequency ω_0 and not twice that. Adding up two waves of frequency ω_0 is still just frequency ω_0.

The trick is to note that this must be (at least) a *two*-photon state involving *products* of the two wave states in a correlated or "entangled" sum in order to make this heavier "light-particle" box which responds with increased inertia. A product $\psi_{K\rightarrow}\psi_{K\leftarrow}$ of the two plane wave states gives a state with the K-vector $\mathbf{K}_+ = \mathbf{K}_\rightarrow + \mathbf{K}_\leftarrow$ that has proper frequency $\mu = 2\omega_0$. Exciting more photons means more wave or state factors and a heavier box. Frequency is energy is mass is (for a moving observer) momentum.

Several things are missing that prevent us from giving a precise discussion of trapped photons. First, the one-dimensional cavity sketched in Fig. 5.2.3 lacks another pair of walls with floor and ceiling. It's not maximum-security incarceration! Two and 3-dimensional box modes will be discussed in Chapter 6. Second, we need the quantum mechanics of wave products or "multi-particle" states to be introduced in Chapter 21. Finally, theory of quantum states of radiation, that is, "multi-photon" states, will be taken up in Chapter 22. We've got a ways to go. Newton's corpuscles aren't entirely dead yet!

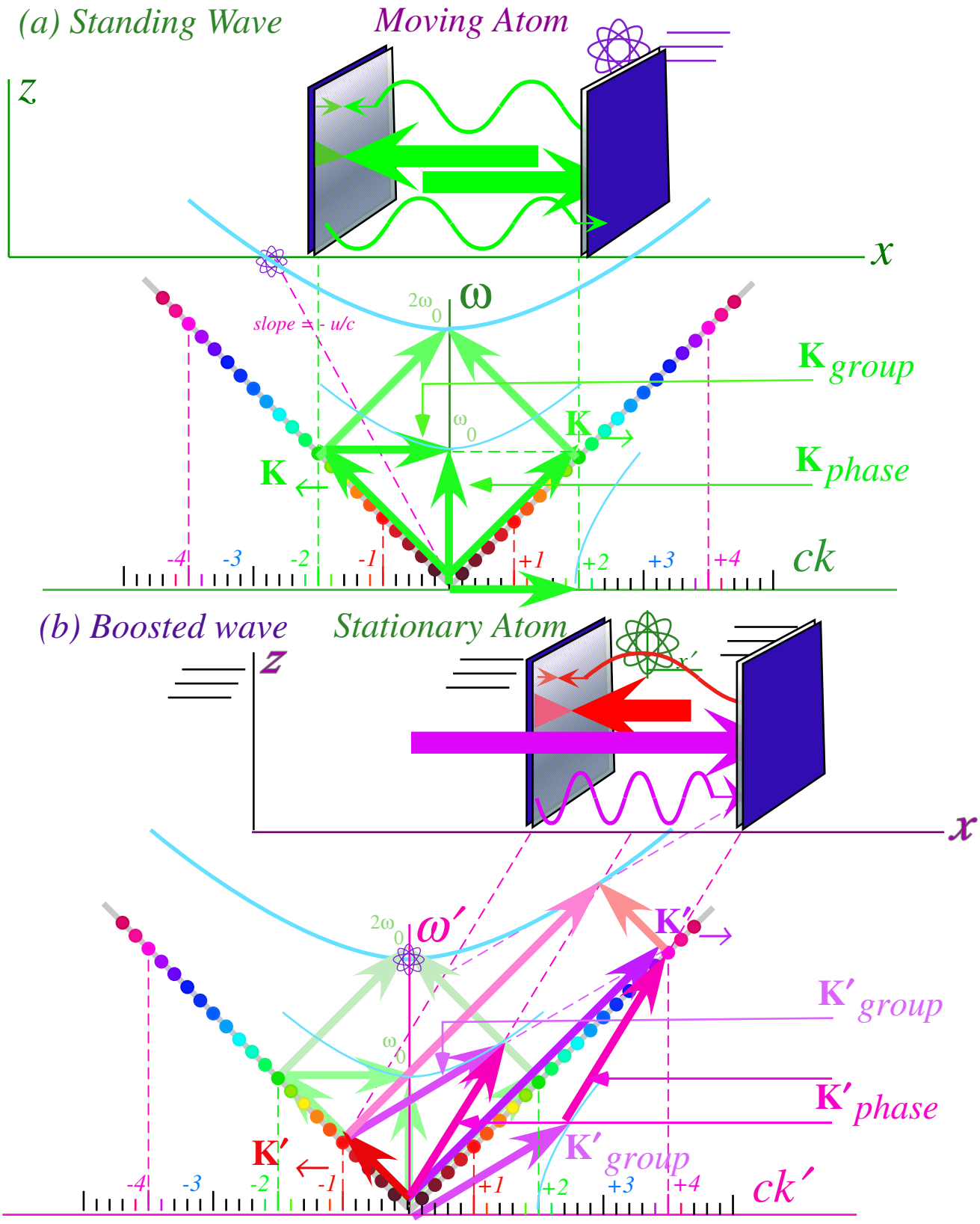

Fig. 5.2.3 Different views of a "photon(s)-in-a-box" and atom. (a) Box view. (b) Atom view.

(f) Effective mass

Classical mechanics is concerned with particle velocity u and momentum p that, in the non-relativistic limit *($u<<c$)*, are directly proportional to the wave group velocity (5.2.9b). (Relativistic phase velocity c^2/u (5.2.9a) is *inversely* proportional to group velocity u.) Classical dynamics equates rate of change of momentum ($\dot{p} = \hbar\dot{k}$) to a force F introduced by Newton's Second Law $F=ma$. This "law" or axiom (It used to be taught in high school.) introduces inertial mass m as a ratio F/a of force to acceleration. How is this mass m related to wave proper-frequency μ or rest-mass $M=\hbar\mu/c^2$ in (5.2.5a)?

Effective mass M_{eff} is the ratio of wave force $F = \hbar\dot{k}$ (or $\dot{p}$) and wave group acceleration $a = \dot{V}_{group} = \dot{u}$. Then M_{eff} is inversely proportional to the curvature of the dispersion function (5.2.8).

$$M_{eff} = \frac{F}{a} = \frac{\hbar\dot{k}}{\left(\frac{dV_{group}}{dt}\right)} = \frac{\hbar\dot{k}}{\left(\frac{dV_{group}}{dk}\frac{dk}{dt}\right)} = \frac{\hbar}{\left(\frac{d^2\omega}{dk^2}\right)} \qquad (5.2.20a)$$

The relativistic quantum dispersion (5.2.8) gives M_{eff}, for low velocity, as approaching the rest mass M.

$$M_{eff} = \frac{F}{a} = \frac{1}{\left(\frac{d^2E}{dp^2}\right)} = \frac{M}{\left(1-\beta^2\right)^{3/2}} \xrightarrow[\beta\approx 0]{} M \qquad (5.2.20b)$$

These results may seem paradoxical in light of the observation that a photon dispersion function is a straight line ($\omega = c|k|$). So, is photon effective mass really infinite? Yes! Pure photon group and phase velocity never change no matter what "force" is encountered. ("Pure" means no μ-waves combining with γ-waves to change dispersion (5.2.8).) γ-wave effective mass is indeed infinite. Effective mass of a massive particle (μ-waves) also approaches infinity as it nears the speed of light *($\beta\rightarrow 1$)*. Here mass means inertia.

The invariant mass M of a particle is its *rest mass*, that is, its effective mass at zero wavevector. This means inertial mass is due to a *($k=0$)* wave wiggle rate: the proper frequency $\mu = Mc^2/\hbar$ from (5.2.5a). Waves that wiggle faster are harder to accelerate, except for photons whose proper frequency is zero. The photon dispersion function ($\omega = c|k|$) in Fig. 5.2.1 has a *90°* "corner" with infinite curvature at the origin. So its rest mass, according to the equation (5.2.20a), is indeed zero.

It may be difficult to tell the difference between a very "light" particle and light itself. The dispersion function of a low-μ matter wave differs from that of light only near the origin ($k=0$) as sketched in Fig. 5.2.4. Elsewhere, the dispersion function hugs the light cone so closely that a light particle might as well be light.

It may help to visualize a *($k=0$)*-photon as a nearly uniform ("kinkless" like the wave in Fig. 5.1.4(b)) electric field oscillating at a very low frequency $\mu=\omega_0$. A boost of such a system (or of an observer viewing this system) results in a finite wavevector because of the asimultaneity effect. For small ω_0, a small change in k makes a wave with speed near c. It is as though a very tiny mass briefly underwent an enormous acceleration to near c. Then the electric rest-wave acquires near-light speed and "recovers" its

near-infinite inertia so it can no longer accelerate. Further acceleration causes little further change in apparent wavespeed c since $(k'c,\omega')$ is so close to the light-cone-asymptote of the dispersion hyperbola.

However, no observer can get into a true photon's $(k=0)$ frame without going at exactly the speed c of light, while, as shown in Fig. 5.1.4, one can catch up with a matter μ-wave. In fact, we do it every day whenever you pass somebody! As we have noted, the lightspeed "horizon" may be approached but never reached. In Sec. 5.6 we will see what happens if we to approach it with enormous acceleration.

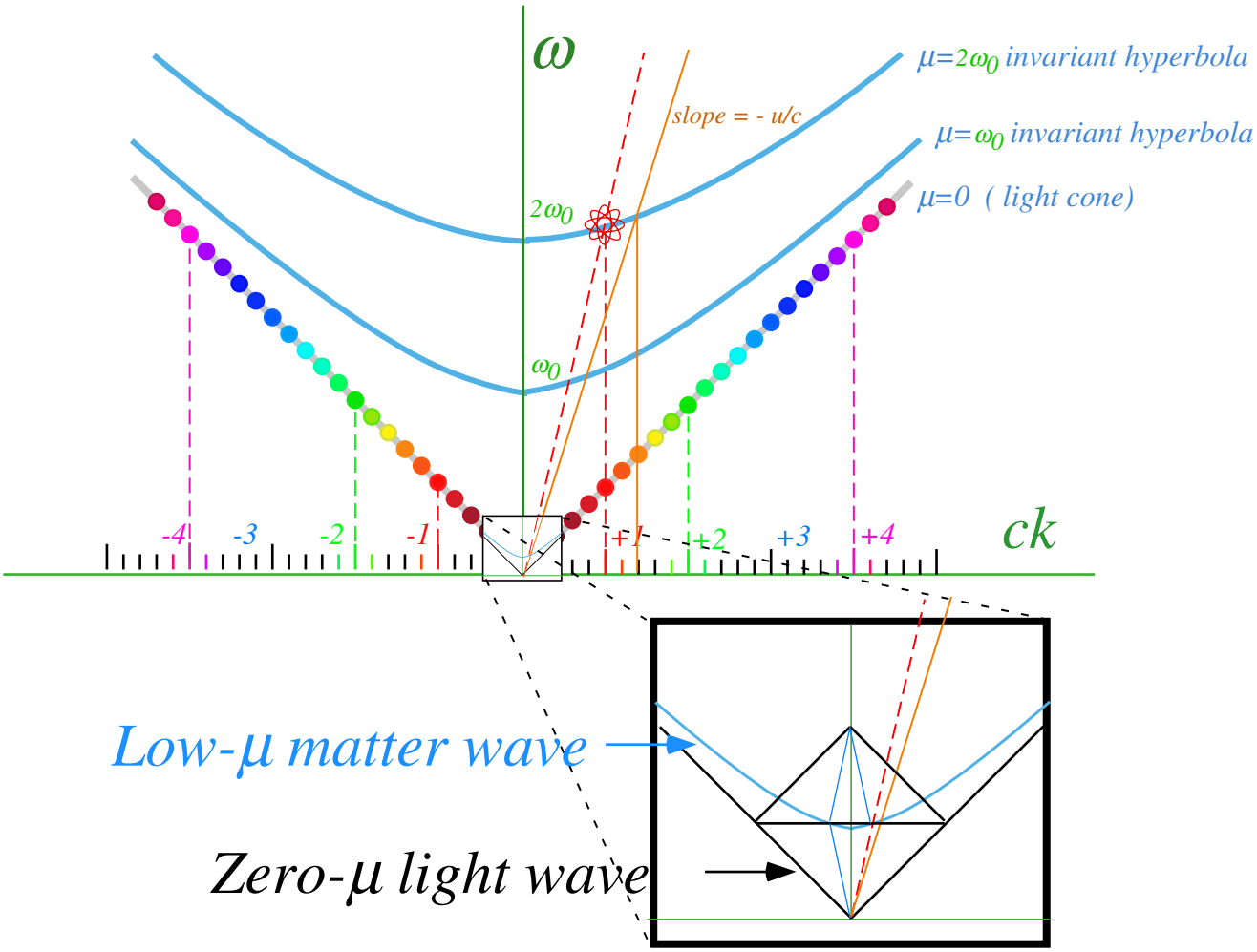

Fig. 5.2.4 Comparing light and very light matter.

(g) Two photons for every mass: Compton recoil

An optical cavity sketched in Fig. 5.2.3 decays to a lower energy (frequency) states by emitting light and is an analogy for a molecular, atomic, or nuclear *photoemission process* sketched in Fig. 5.2.5.

Feynman tells of a question his father asked him when he visited home after completing a (pricey) education at MIT. Feynman's father had heard that an atom can emit a photon and wanted to know where that photon was before it "came out." Feynman said he was sorry he didn't have a good answer for his father who had funded his MIT tuition for many years. Standard answers seemed unsatisfying. One such answer is that photons are "manufactured" by an atom occupying at once states $E_1=\hbar\mu_1$ and $E_0=\hbar\mu_0$ so its charge cloud "beats" at the difference frequency $\Delta=\mu_1-\mu_0$ thus broadcasting light at this frequency.

Feynman's father's question has a Newtonian flavor, but it can be answered nicely by the wave "baseball diamond" geometry developed in this chapter. This also gives a more precise photoemission frequency $\omega_\gamma(final)$ that is shifted from Δ by a relativistic *Compton recoil shift* $\delta\omega$ that we derive now.

The trick is to imagine the excited μ_1 atom is "made" of two monstrous counter-propagating photon waves represented by big $\mathbf{K}_\rightarrow(\mu_1)$ and $\mathbf{K}_\leftarrow(\mu_1)$ vectors each taking up length $\mu_1/\sqrt{2}$ along the baselines of the diamond in Fig. 5.2.6(a). By "monstrous" we mean $E_1=\hbar\mu_1=M_1c^2$ or trillions of *Volts (TeV)*.

Similarly, the de-excited μ_0 atom is "made" of two smaller (but still monstrous) photons having $\mathbf{K}_\rightarrow(\mu_0)$ and $\mathbf{K}_\leftarrow(\mu_0)$ vectors in Fig. 5.2.6(b-c). In contrast, typical atomic photoemission is tiny $\mathbf{K}(\omega_\gamma)$, a few *eV*, or so. That would be too small to draw in Fig. 5.2.6 so instead we imagine a nuclear or high-energy process with a big $\mathbf{K}(\omega_\gamma)$. Then, relativistic shifts are comparable to the energy values themselves.

The emission $\mathbf{K}(\omega_\gamma)$ is the difference between the sum of the excited and de-excited atom vectors according to a *phase conservation* rule requiring equality of **K**-vector sums before and after emission.

$$\mathbf{K}(initial\ total)=\mathbf{K}_\rightarrow(\mu_1)+\mathbf{K}_\leftarrow(\mu_1)=\mathbf{K}_\rightarrow(\mu_0)+\mathbf{K}_\leftarrow(\mu_0)+\mathbf{K}\ (\omega_\gamma)=\mathbf{K}(final\ total) \qquad (5.2.21)$$

That is equivalent to conservation of *both* total energy (frequency) *and* momentum (wavevector) and so represents fundamental axioms of Newtonian mechanics. However, as will be shown later, (5.2.21) is an *approximate* consequence of wave interference. (Reducing **K**-vector uncertainty nearer to CW limit makes it a better approximation.) Quantum theory "proves" Newtonian axioms, but only *approximate*ly.

To make the final total-**K** match the initial one, we Doppler lengthen the 1st baseline $\mathbf{K}_\rightarrow(\mu_0)$ vector (length $\mu_0/\sqrt{2}$) by a factor $b=e^\rho$ so as to equal the length $\mu_1/\sqrt{2}$ of initial $\mathbf{K}_\rightarrow(\mu_1)$ vector of the atom. This in turn shortens the $\mathbf{K}_\leftarrow(\mu_0)$ vector to 3rd base by inverse factor $b^{-1}=e^{-\rho}$ leaving a larger deficit $\omega_\gamma\sqrt{2}$ between the length $\mu_1/\sqrt{2}$ of $\mathbf{K}_\leftarrow(\mu_1)$ and the new 3rd baseline $e^{-\rho}\mu_0/\sqrt{2}$. That ω_γ is the exact *photoemission frequency*.

$$\mu_1/\sqrt{2}=e^\rho\mu_0/\sqrt{2}\ \text{ or: }\ \mu_1/\mu_0=e^\rho \qquad (5.2.22a)$$

$$\omega_\gamma=\frac{\mu_1-e^{-\rho}\mu_0}{2}=\mu_0\frac{e^\rho-e^{-\rho}}{2}=\mu_0\sinh\rho \qquad (5.2.22b)$$

We relate ω_γ to the non-relativistic beat frequency $\Delta=\mu_1-\mu_0$, and the recoil shift $\delta\omega$ in Fig. 5.2.6(c).

$$\omega_\gamma=\mu_0\frac{e^\rho-e^{-\rho}}{2}=\frac{\mu_0}{2}\left(\frac{\mu_1}{\mu_0}-\frac{\mu_0}{\mu_1}\right)=\frac{(\mu_1-\mu_0)(\mu_1+\mu_0)}{2\mu_1}=\frac{\Delta}{2}\left(1+\frac{\mu_0}{\mu_1}\right) \qquad (5.2.23a)$$

$$\delta\omega=\Delta-\omega=\frac{\Delta}{2}\left(1-\frac{\mu_0}{\mu_1}\right)=\frac{\Delta^2}{2\mu_1} \qquad (5.2.23b)$$

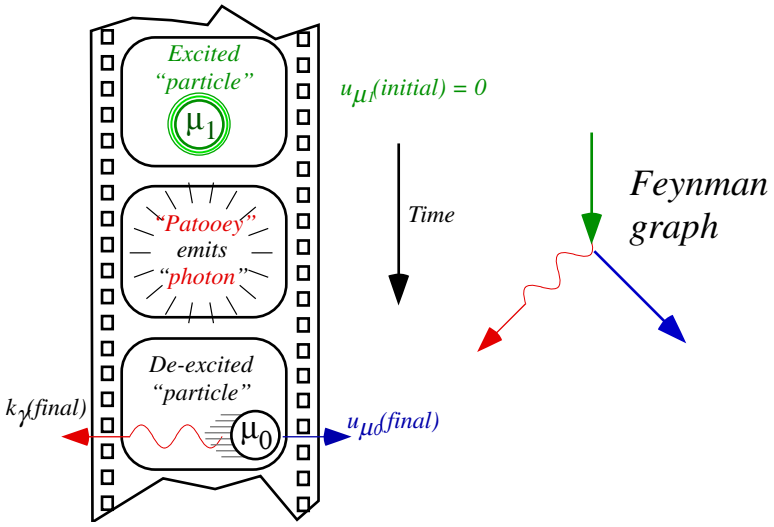

Fig. 5.2.5 Photoemission process

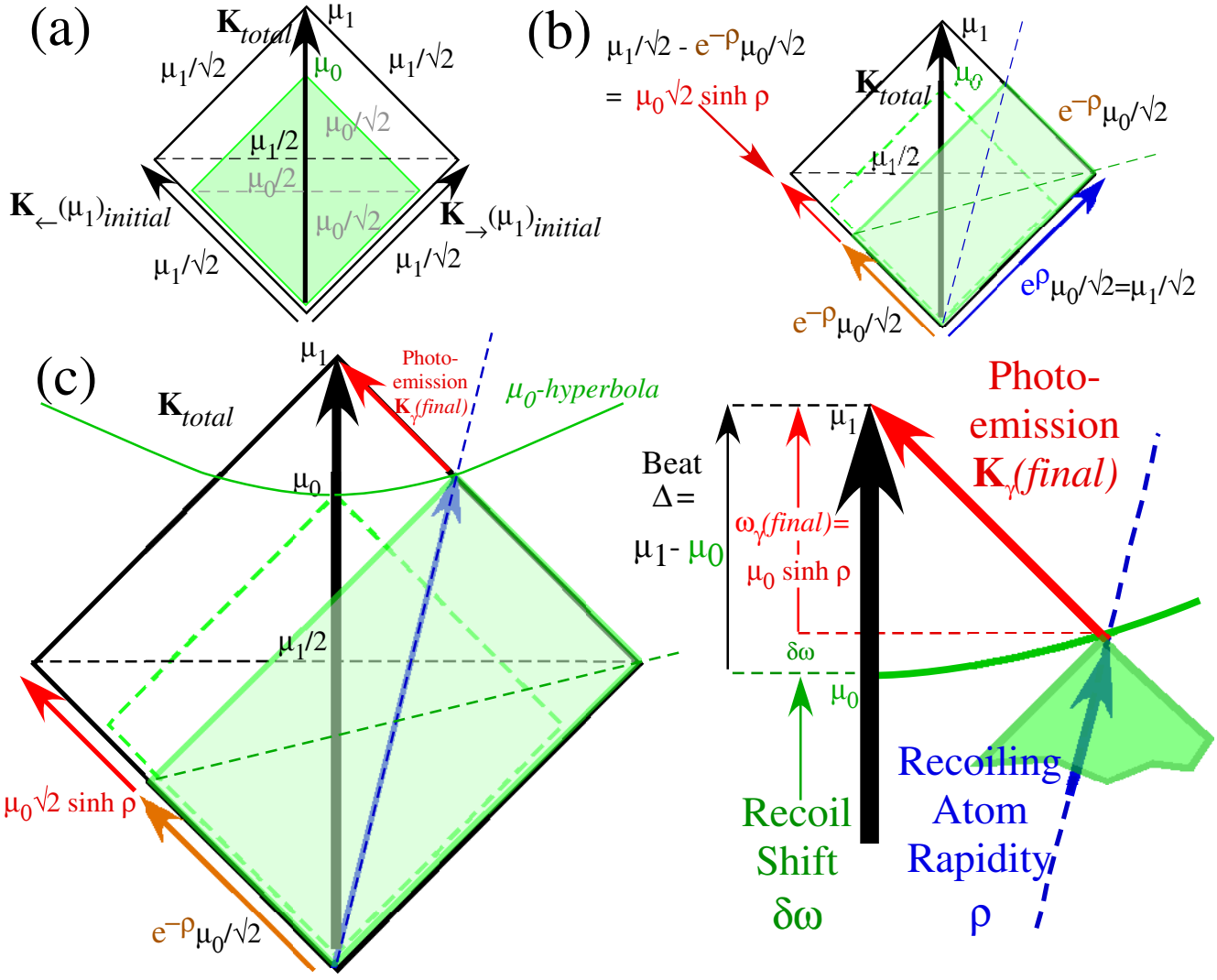

Fig. 5.2.6 Diamond geometry of photoemission **K**-*vectors derives recoil shift and atomic recoil velocity.*

5.3. Pulse Wave (PW) Dynamics :Wave-Particle Duality

The continuous wave (CW) approach to relativity and quantum theory used so far in this Chapter 5 and the preceding Chapter 4 takes full advantage of all parts including the "inside" and "outside" of a simple two-component wave interference first sketched in Fig. 4.2.4. Experimentalists rarely get such an ideal and coherent view. If they did, this CW theoretical approach would have been noticed long before.

Instead, we are usually restricted to an "outside only" view of waves made of many spectral components that are often incoherent. This is simply the usual classical world; a big incoherent mess! The book and pencil you may be holding now, and you, too, are combinations of unimaginably enormous numbers of so many insanely tiny waves that the wave nature of it all is about *last* thing you'd notice.

Now let us add up some number *2, 3, 4,..., N* waves to make pulse waves (PW) with "bumps" that resemble a classical "particles." We imagining a Newtonian "corpuscle spitter" in Fig. 5.2.2 and analyze pulses alluded to in discussing Fig. 4.2.11 and Fig. 4.3.5. (*"patooey..patooey..patooey..."*)

(a) Taming the phase: Wavepackets and pulse trains

In graphs like Fig. 4.6.1 a real wave $\mathrm{Re}\Psi(x,t)$ is plotted in spacetime. If the intensity $\Psi^*\Psi$ or envelope $|\Psi|$ is plotted, the part of the wave having the fast and wild phase velocity disappears leaving only its envelope moving constantly at the slower and more "tame" group velocity.

For example, the complicated dynamics of the (SWR=-1/8) switchback of Fig. 4.6.1(d) is reduced to parallel grooves by a $|\Psi|$-plot in Fig. 5.3.1(a). The grooves follow the group envelope motion that has only a steady group velocity . The lower part of Fig. 4.6.1 is thus tamed. Pure plane wave states Fig. 4.6.1 (a) and Fig. 4.6.1(f) are tamed even more in a $|\Psi|$-plot to become featureless and flat like their envelopes.

One gets a glimpse of phase behavior in an envelope or $\Phi^*\Phi$ plot by adding the lowest scalar DC fundamental *(m=0)*-wave $\Psi_0=1$ to a galloping combination wave such as $\Psi = a\,\Psi_{+4} + b\,\Psi_{-1}$. The result

$$\Phi^*\Phi = \left(1 + a\Psi_{+4} + b\Psi_{-1}\right)^* \left(1 + a\Psi_{+4} + b\Psi_{-1}\right) = \left(1 + a\Psi_{+4} + b\Psi_{-1} + a^*\Psi^*_{+4} + b^*\Psi^*_{-1} + \Psi^*\Psi\right) \qquad (5.3.1)$$
$$= 1 + 2\,\mathrm{Re}\,\Psi + \Psi^*\Psi$$

is plotted in the upper part of Fig. 5.3.1(b). The DC bias keeps the phase part from canceling itself, and the probability distribution shows signs of, at least half-heartedly, following the fast phase motion of the $\mathrm{Re}\Psi$ wave plotted underneath it. (Dashed lines showing phase and group paths are sketched onto $\Phi^*\Phi$.)

Indeed, (5.3.1) shows that if the $(1+\Psi^*\Psi)$ background could be subtracted, then the real wave $\mathrm{Re}\Psi$ plots of Fig. 4.4.4 would emerge double-strength! However, such a subtraction, while easy for the theorist, is more problematic for the experimentalist. Usually we must be content with results more like the upper than the lower portions of Fig. 5.3.1. It's a bit like watching an orgy ensuing beneath a thick rug.

However, such censorship can be a welcome feature. As more participating Fourier components enter the fray, a simpler view can help to sort out important classical effects that might otherwise be hidden in a cacophonous milieu. We next consider examples of this with regard to sharper wavepackets such as spikey pulse trains as well as the more graceful Gaussian wavepackets.

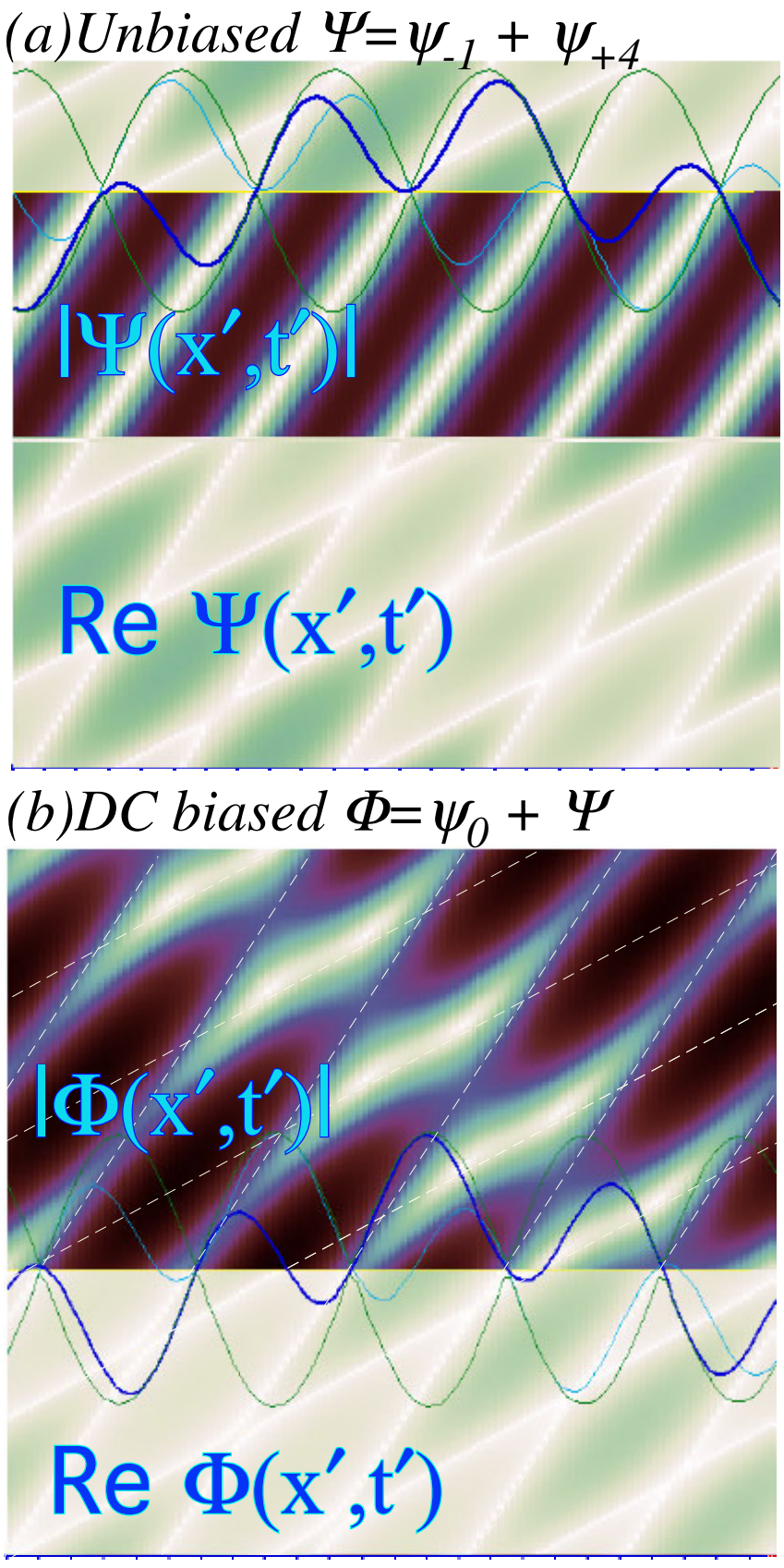

Fig. 5.3.1 Examples of group envelope plots of galloping waves (a) Unbiased. (b) DC biased.

(b) Continuous Wave (CW) vs. Pulsed Wave (PW): colorful versus colorless

Counter-propagating pulsed waves (PW) or Optical pulse trains (OPT), such as are imagined in Fig. 5.2.2, may be written as Fourier series of N continuous wave (CW) ω_1-harmonics.

$$\begin{aligned}\Phi_N(x,t) &= 1 + e^{i(k_1x-\omega_1t)} + e^{i(-k_1x-\omega_1t)} + e^{i(k_2x-\omega_2t)} + e^{i(-k_2x-\omega_2t)} + \ldots + e^{i(k_Nx-\omega_Nt)} + e^{i(-k_Nx-\omega_Nt)} \\ &= 1 + \quad 2e^{-i\omega_1t}\cos k_1x \quad + \quad 2e^{-i\omega_2t}\cos k_2x \quad + \ldots + \quad 2e^{-i\omega_Nt}\cos k_Nx\end{aligned} \tag{5.3.2}$$

The fundamental OPT or *(N=0-1)* beat wave in Fig. 5.3.2(b) is a rest-frame view of Fig. 5.3.1(b)

$$\Phi_1(x,t) = 1 + \quad 2e^{-i\omega_1t}\cos k_1x \tag{5.3.3}$$

Φ_1 should be compared to the pure or unbiased fundamental *(m=±1)*-standing wave Ψ_1 in Fig. 5.3.2(a).

$$\Psi_1(x,t) = 2e^{-i\omega_1t}\cos k_1x \tag{5.3.4}$$

The real part Re Ψ_1 is discussed in connection with the Cartesian spacetime wave grid in Fig. 4.3.3(a). The modulus $|\Psi_1|$, unlike $|\Phi_1|$, is constant in time as indicated by the vertical time-grooves at the extreme upper right of Fig. 5.3.2(a). In contrast, the magnitude $|\Phi_1|$ of the DC-biased beat wave makes an "H" or "X" in its spacetime plot of Fig. 5.3.2(b) thereby showing the beats. The width of the fundamental *(0-1)* beat is one fundamental wavelength $\Delta x = 2\pi/k_0$ of space and one fundamental period $\Delta t = 2\pi/\omega_0$ of time. Including $N=2,3,\ldots$ terms in (5.3.2) reduces the pulse width by a factor of $1/N$ as seen in Fig. 5.3.2 (c-e) below. The spatial $^{\sin Nx}/_{x}$ wave shape is the same as is had by adding $N=2,3,\ldots$ slits to an elementary optical diffraction experiment. Adding more frequency harmonics makes the pulse narrower in time, as well as space. Using *12* terms with *11* harmonics reduces the pulse width to *1/11* of a fundamental period. A pico-period pulse would be a sum of a trillion harmonics!

Reducing pulse width or spatial uncertainty Δx and temporal duration Δt of each pulse requires increased wavevector and frequency bandwidth Δk and $\Delta\omega$. The widths obey *Heisenberg relations* $\Delta x\Delta k \sim 2\pi$ or $\Delta t\Delta\omega \sim 2\pi$. The sharper the pulses the more white or colorless they become. Finally, the spacetime plots will simplify to simple equilateral diamonds or *45°*-tipped squares shown in the *N=11* plots of Fig. 5.3.2(e). Each resembles the baseball diamond of Fig. 5.1.1 or PW paths of Fig. 4.3.5(b).

For *N=11* there is less distinction between the Re Φ and $|\Phi|$ plots than there is for the cases of *N=1,2*, or *3* shown in the preceding plots of Fig. 5.3.2(a-c). However, as in Fig. 5.3.1, there is a still a noticeable distinction between Re Φ and $|\Phi|$ plots with all Re Φ plots being sharper than $|\Phi|$ plots in all cases including the high-N cases. Having phase information increases precision particularly for low N. The sharpest set of zeros, somewhat paradoxically, are found in the *N=1* case of Fig. 5.3.2(a) and for the unbiased Re Ψ plot of the Cartesian wave grid. However, plotting zeros by graphics shading is one thing. Finding experimental phase zeros using $\Psi^*\Psi$, that is, $|\Psi|$ *squared*, is quite another thing.

A close look at the center of the Re Φ plot for *N=11* in Fig. 5.3.2(e) reveals a tiny Cartesian spacetime grid. It is surrounded by "gallop-scallops" similar to the faster-and-slower-than-light paths shown in Fig. 4.5.1. It is due to the interference of counter-propagating ringing wavelets that surround each counter propagating $^{\sin Nx}/_{x}$ –pulse. In contrast note the $|\Phi|$ plots for which the ringing leaves only vertical grooves like those that occupy the entire *N=1* plot of $|\Psi|$ in Fig. 5.3.2(a).

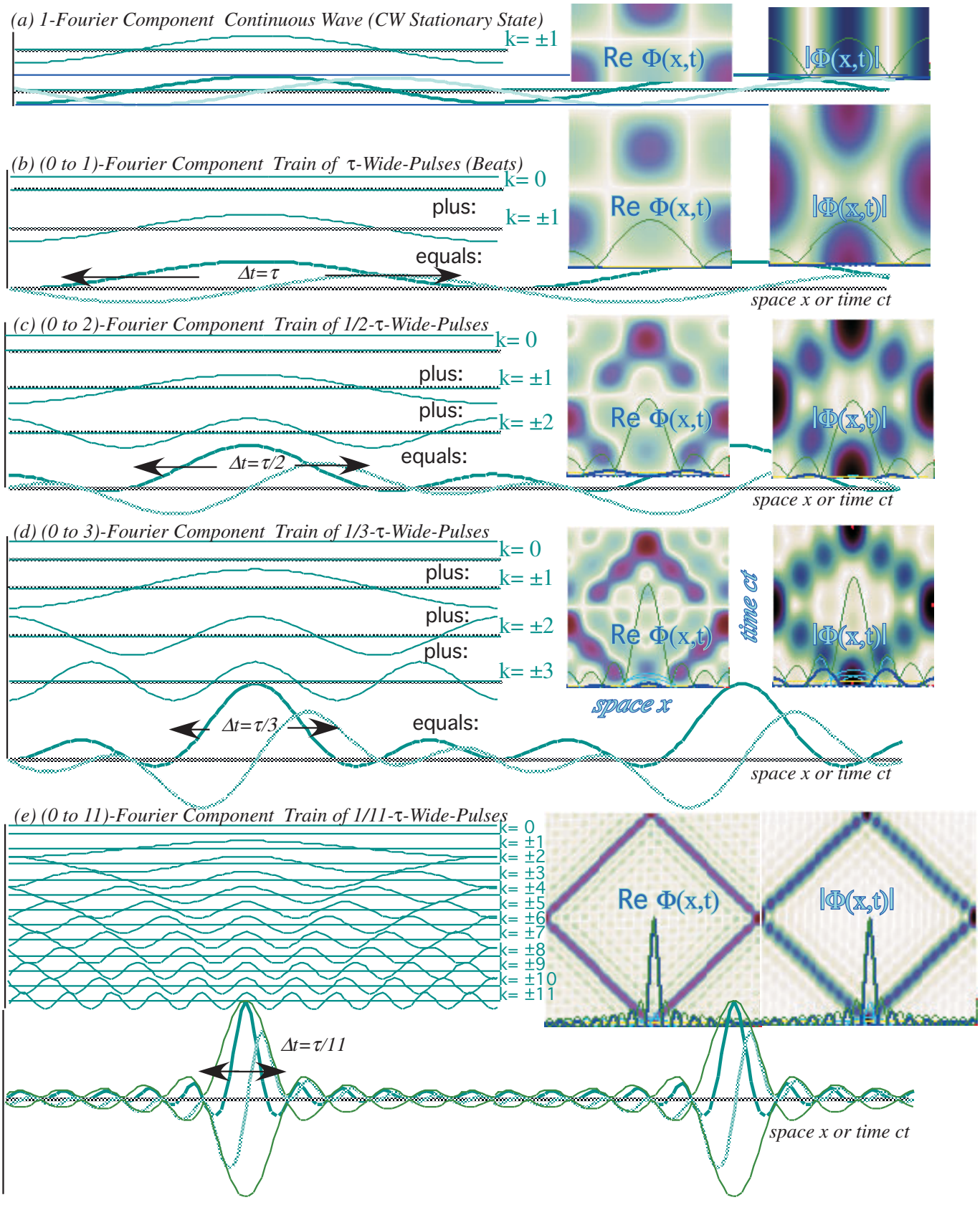

Fig. 5.3.2 Pulse Wave (PW) or Optical Pulse Trains (OPT) and Continuous Wave (CW) Fourier components

Wave ringing: m_{Max}-term cutoff effects

An analysis of wave pulse ringing reveals it may be blamed on the last Fourier component added. There are *11* zeros in the ringing wave envelope in Fig. 5.3.2(e), the same number as in the *11th* and last Fourier component. An integral over $k = m2\pi/N$ approximates a Fourier sum $S(m_{Max})$ up to a maximum $m_{Max}=11$. The unit sum interval $\Delta m=1$ is replaced by a smaller *k*-differential *dk* multiplied by $\frac{\Delta m}{dk} = \frac{N}{2\pi}$.

$$S(m_{Max}) = \sum_{m=-m_{Max}}^{m_{Max}} e^{im(\phi-\alpha)} = \sum_{m=-m_{Max}}^{m_{Max}} \Delta m\, e^{im(\phi-\alpha)} \cong \int_{-k_{Max}}^{k_{Max}} dk \frac{\Delta m}{dk} e^{ik\frac{N}{2\pi}(\phi-\alpha)}$$
$$\cong \frac{e^{i\frac{k_{Max}N}{2\pi}(\phi-\alpha)} - e^{-i\frac{k_{Max}N}{2\pi}(\phi-\alpha)}}{i(\phi-\alpha)} = 2\frac{\sin\frac{k_{Max}N(\phi-\alpha)}{2\pi}}{(\phi-\alpha)} = 2\frac{\sin m_{Max}(\phi-\alpha)}{\phi-\alpha} \qquad (5.3.5)$$

This geometric sum verifies our suspect's culpability. The sum rings according to the highest m_{Max}-terms while lesser *m*-terms seem to experience an interference cancellation. The *last-one-in* is what shows!

Ringing suppressed: m_{Max}-term Gaussian packets

Ringing is reduced by *tapering* higher-*m* waves so they tend to cancel each other's ringing and no single wave dominates. A Gaussian $e^{-(m/\Delta m)^2}$ taper makes cleaner "particle-like" pulses in Fig. 5.3.3.

$$S_{Guass}(m_{Max}) = \frac{1}{2\pi}\sum_{m=-\infty}^{\infty} e^{-\frac{m^2}{\Delta m^2}} e^{im\phi} = \frac{1}{2\pi}\sum_{m=-\infty}^{\infty} e^{-\pi\left(\frac{m}{m_{Max}}\right)^2} e^{im\phi}, \text{ where: } \Delta m = \frac{m_{Max}}{\sqrt{\pi}} \qquad (5.3.6a)$$

Completing the square of the exponents extracts a Gaussian ϕ-angle wavefunction $e^{-(\Delta m\phi/2)^2}$ with an angular uncertainty Δϕ that is twice the inverse of the momentum quanta uncertainty Δm. $(\Delta\phi = 2/\Delta m)$.

$$S_{Guass}(m_{Max}) = \frac{1}{2\pi}\sum_{m=-\infty}^{\infty} e^{-\left(\frac{m}{\Delta m}-i\frac{\Delta m}{2}\phi\right)^2 - \left(\frac{\Delta m}{2}\phi\right)^2} = \frac{A(\Delta m,\phi)}{2\pi} e^{-\left(\frac{\Delta m}{2}\phi\right)^2} \qquad (5.3.6b)$$

Definition $\Delta m = m_{Max}/\sqrt{\pi}$ of momentum uncertainty relates *half-width-($1/e$)th-maximum* Δm to the value $m=m_{Max}$ for which the taper $e^{-(m/\Delta m)^2}$ is $e^{-\pi}$. ($e^{-\pi} = 0.04321$ is an easy-to-recall number near *4%*. Waves $e^{im\phi}$ beyond $e^{im_{Max}\phi}$ have $e^{-(m/\Delta m)^2}$ amplitudes below $e^{-\pi}$.) Amplitude $A(\Delta m,\phi)$ becomes an integral for large m_{Max} as does (5.3.5). Then $A(\Delta m,\phi)$ approaches a Gaussian integral whose value itself is m_{Max}.

$$A(\Delta m,\phi) = \sum_{m=-\infty}^{\infty} e^{-\left(\frac{m}{\Delta m}-i\frac{\Delta m}{2}\phi\right)^2} \xrightarrow[\Delta m>>1]{} \int_{-\infty}^{\infty} dk\, e^{-\left(\frac{k}{\Delta m}\right)^2} = \sqrt{\pi}\Delta m = m_{Max} \qquad (5.3.6c)$$

The resulting Gaussian wave $e^{-(\phi/\Delta\phi)^2}$ has angular uncertainty $\Delta\phi = \phi_{Max}/\sqrt{\pi}$ defined analogously to Δm.

$$S_{Guass}(m_{Max}) \cong \frac{1}{2\pi}\sum_{m=-m_{Max}}^{m_{Max}} e^{-\left(\frac{m}{\Delta m}\right)^2} e^{im\phi} = \frac{m_{Max}}{2\pi} e^{-\left(\frac{\Delta m}{2}\phi\right)^2} = \frac{m_{Max}}{2\pi} e^{-\left(\frac{\phi}{\Delta\phi}\right)^2} \text{ where: } \Delta\phi = \frac{\phi_{Max}}{\sqrt{\pi}} \qquad (5.3.6d)$$

Uncertainty relations in Fig. 5.3.3 are stated using Δm and Δϕ or in terms of *4%* limits m_{Max} and ϕ_{Max}.

$$\Delta m \cdot \Delta\phi = 2 \qquad (5.3.7a) \qquad\qquad m_{Max} \cdot \phi_{Max} = 2\pi \qquad (5.3.7b)$$

In Fig. 5.3.2, the number of pulse widths in interval 2π is the number m_{Max} of *(>4%)*-Fourier terms.

Are these pulses photons?

No! But each pulse would appear to have photons in them if counters were put in the beams. However, it is *highly* unlikely that you would ever hear a counter tick *"click…click…click…"* with one count for each pulse! Newton's mythical *"patooey…patooey…"* becomes a random distribution of clicks *within* each pulse.

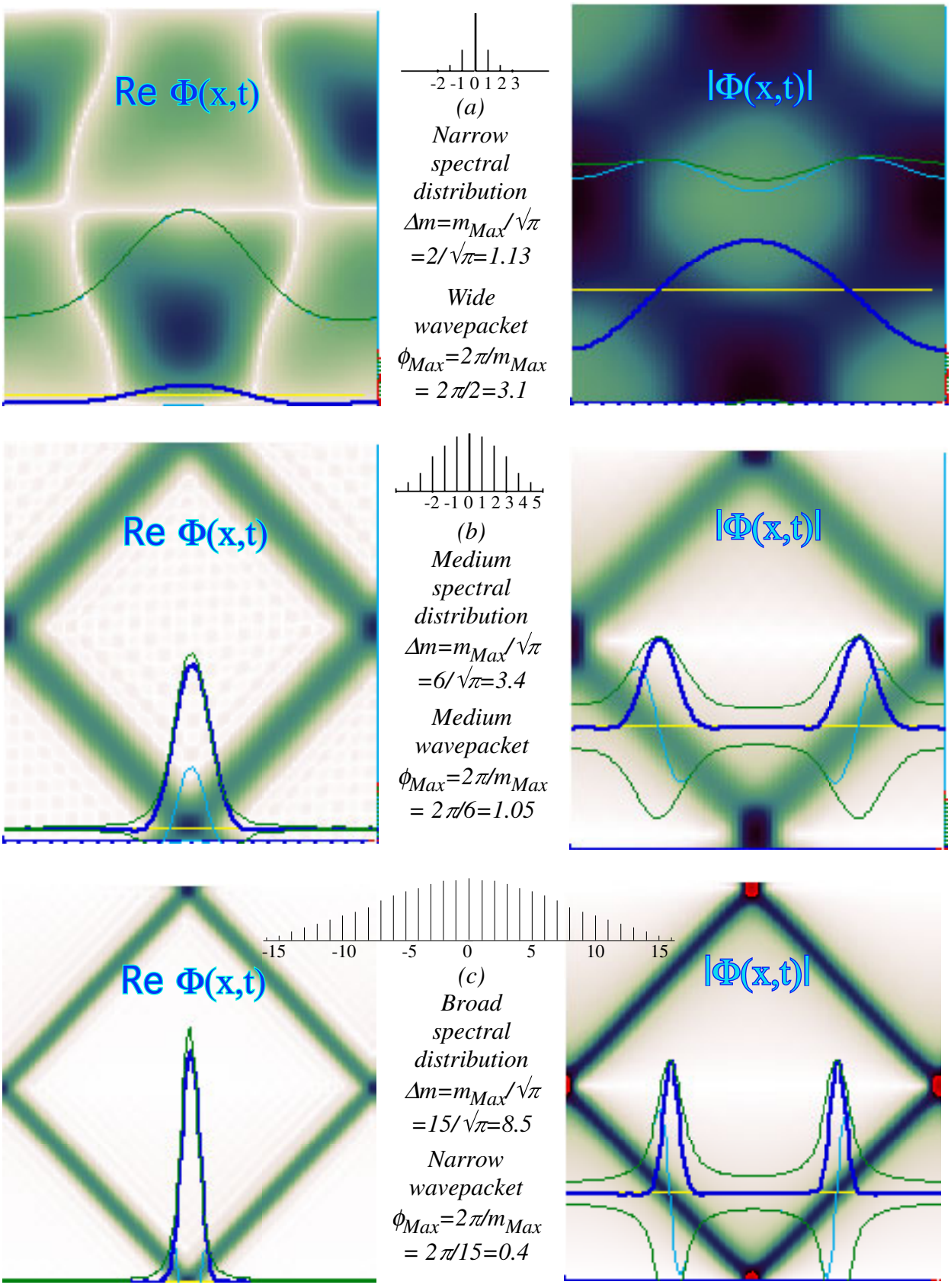

Fig. 5.3.3 Gaussian wavepackets. (Ringing is reduced compared to Fig. 5.3.2.)

(c) PW switchbacks and "anomalous" dispersion

An interesting exercise involves the dynamics associated with *anomalous* or "abnormal" dispersion functions. Often, the term anomalous applies to any dispersion function beyond the elementary optical linear dispersion $\omega=ck$ or quadratic Bohr-Schrodinger dispersion $\omega=Bk^2$. Here, we might so disparage any dispersion that does not fit the relativistic invariant form $\omega^2-(ck)^2=\mu^2$ of (5.1.5) or (5.2.7).

What we are looking for here is abnormal wave behavior like that of the galloping and switchback waves displayed in Fig. 4.5.1 and Fig. 4.6.1, but with an important difference. The extraordinary dances in Fig. 4.5.1 and Fig. 4.6.1 involved phase velocity of *phase* waves Re Ψ or Im Ψ and here we ask if such super luminal behavior is possible for *group* velocity and group envelopes |Ψ| or Ψ*Ψ.

Abnormal relativistic dispersion

Faster-than-light group velocity is not possible on the normal positive branch ($\mu>0$) or positive light cone in Fig. 5.2.1 since no two points on the ($\mu>0$) hyperbola make a line of slope greater than one. Branches of imaginary-μ have the opposite problem; their group velocity is never *less* than c. This led Gerald Feinberg to suggest *tachyonic matter* in 1970. No evidence for it was found. Perhaps, it's not so surprising since a time factor $e^{-i\omega t}$ with imaginary frequency $\omega=i\mu$ is a decaying exponential $e^{-\mu t}$.

This leaves the negative frequency branches ($\mu<0$) or negative light cone branches that are hiding behind the inset Bohr dispersion graph in Fig. 5.2.1. For these branches group velocity $d\omega/dk$ is negative and so is the effective mass $h/(d^2\omega/dk^2)$. This is the domain of Dirac's *anti-matter* as discussed in Sec. 5.7.

Abnormal laboratory dispersion

As described in later chapters, there are no end of abnormal dispersion in waves that involve combination of light and matter. Gases and solids break the Lorentz symmetry of the vacuum by being their own "absolute" frame of reference, and so they are not restricted to the invariant form. The earliest examples of anomalous dispersion involve above-resonance polaron light whose index of refraction n is less than one. (Velocity is defined as c/n so $n<1$ is faster-than-light.)

Still it was not until recently that dispersion control in laser-pumped matter became so powerful that an index could be made zero or negative with phase or group velocities of virtually arbitrary sign and magnitude. This includes "backward waves" whose envelope travels oppositely to the wave phase.

Fig. 5.3.4 sketches dispersion cases of *normal* ($n>1$ and $V<c$), *vacuum* ($n=1$ and $V=c$), *anomalous* ($n<1$ and $V>c$), *evanescent* ($n=0$ and $V=\infty$), and *negative-backward* ($n<0$ and $V<0$). The latter has the peculiar property of emitting a pulse before it arrives! As shown in Fig. 5.3.5, this is an example of a spacetime switchback analogous to the phase switchbacks in Fig. 4.6.1. It plays out like the zeros in Fig. 4.6.1(d) only now it is a whole pulse and envelope instead of a zero that cruises toward its annihilation by its "anti-pulse" or "back-in-time-traveling" part that was produced in an earlier "pair-creation" event.

These hyper-anomalous pulses are set-up-jobs like any Fourier system. Pulses look like they go back in time but they don't "cause" anything before they're sent because they were never really "sent" at all! Wave interference dynamics makes the classical rules we are used to, and on the average, obeys them.

However, that which giveth also taketh away. For quantum waves, classical rules are made to be broken! When matter waves get left alone, as will be shown later in Sec. 5.6, they party like mad!

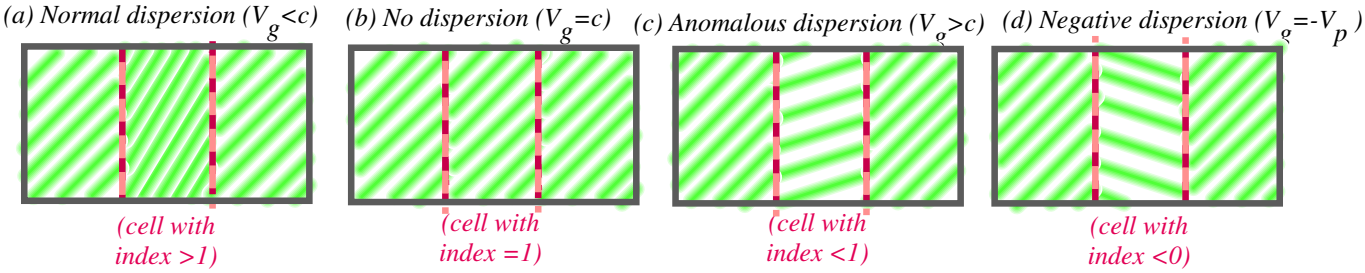

Fig. 5.3.4 Spacetime tracks of wave pulse group envelopes for various dispersion cases

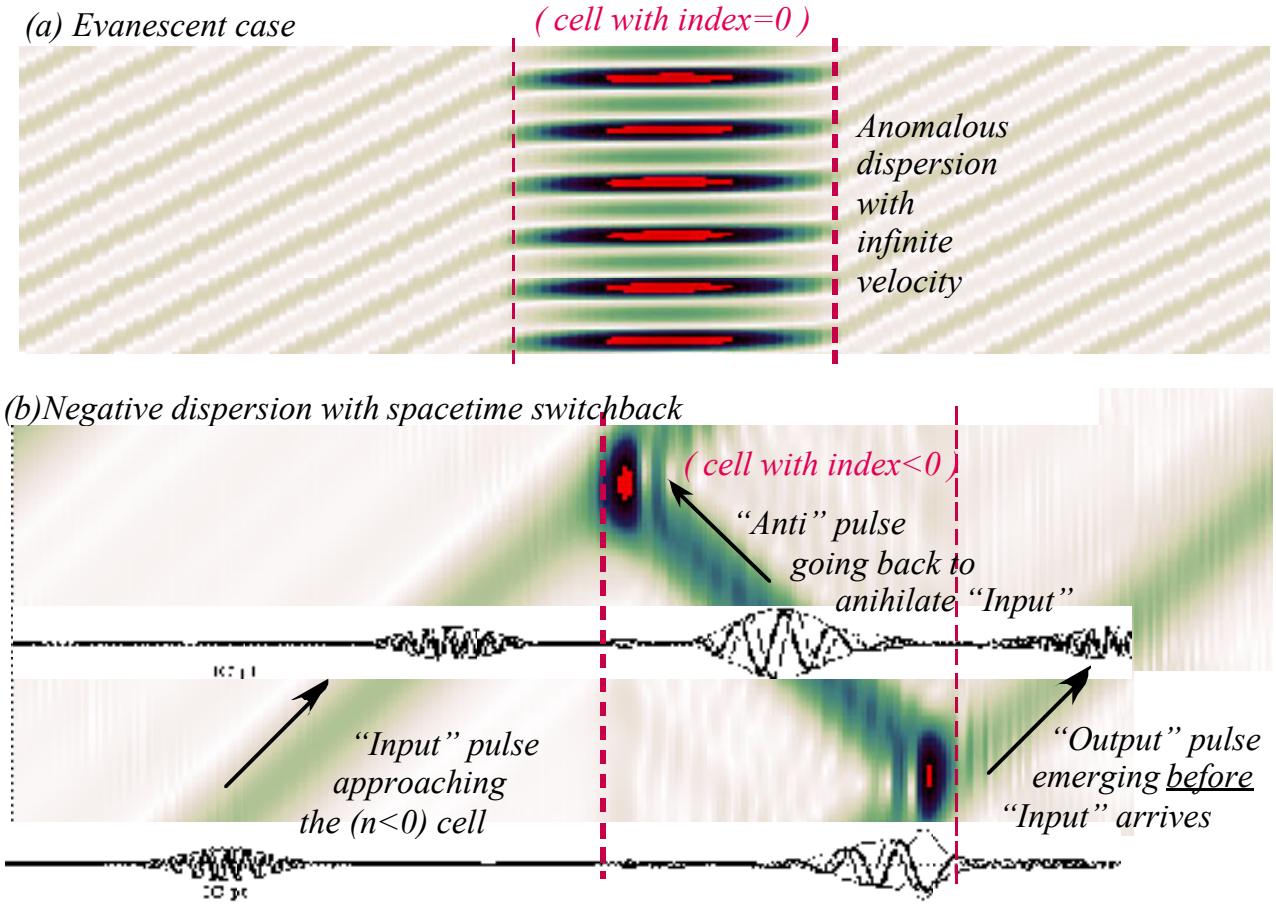

Fig. 5.3.5 Simulations of optical pulse group envelopes for hyper-anomalous dispersion cases

5.4. Quantum-Classical Relationships

Deriving classical mechanical phenomena from quantum mechanics is probably a reasonable strategy given that quantum theory is supposed to supersede the classical. Yet we seem compelled to do the reverse by explaining and even deriving quantum mechanical effects using classical or semi-classical arguments. Such a reverse engineering strategy is most certainly doomed at the most fundamental level.

Nevertheless, it often seemed the only recourse available, particularly in atomic and molecular physics. Also, we often teach quantum theory by saying, " the particle does this...," and relativity pedagogy is still based on old-fashioned classical meter sticks, particles, pulses, and clocks.

The continuous wave (CW) approach of this unit has shown that quantum theory and relativity really need each other. It is possible to learn both with far less effort than struggling with even one of the many apparent paradoxes posed by either one of these subjects taken alone. The only price is an abandonment of a classical "bang-bang-particle" Newtonian paradigm, much as Newtonian physics required disabusing oneself of an Aristotelian one.

(a) Deep classical mechanics: Poincare's invariant

The unified CW approach of Chapters 4-5 is based upon wave mechanics. It appears at first sight to "short-circuit" classical mechanics. However, we will here argue that the CW approach actually brings quantum development closer to the very deepest levels of classical mechanics including the earliest ideas of wave phase due to Christian Huygens and the related invariance principles of Poincare'. These ideas are embodied in the classical *Legendre transformation* that expresses a Lagrangian function L in terms of a Hamiltonian function H.

$$L = p\dot{x} - H \tag{5.4.1}$$

This is rewritten as the *Poincare' differential invariant* which is also called the *differential of action S*.

$$dS = L\,dt = p\,dx - H\,dt \tag{5.4.2}$$

Assuming action $S=\int L\,dt$ is an integrable function leads directly to the *Hamilton-Jacobi equations*, that is, the coefficient of each differential dx and dt must be the respective derivative of action S.

$$p = \frac{\partial S}{\partial x}\,, \qquad (5.4.3a) \qquad\qquad -H = \frac{\partial S}{\partial t} \qquad (5.4.3b)$$

Dirac and Feynman showed that the action is essentially the *quantum phase* Φ in units of $\hbar$.

$$\Psi \approx e^{iS/\hbar} = e^{i\int L\,dt/\hbar} \tag{5.4.4}$$

Quantum relations (5.2.5) for momentum $p= \hbar k$ and energy $H=E= \hbar\omega$ give action-phase differential

$$dS=\hbar d\Phi=\hbar k dx - \hbar\omega dt, \tag{5.4.5a}$$

and a *Hamilton-Dirac-Feynman action-phase equivalence*. For free space-time it is a plane wave phase

$$S/\hbar=\Phi=kx - \omega t. \tag{5.4.5b}$$

So, the notion in Sec. 5.2 of phase invariance actually appears much earlier in the history of classical physics. Unfortunately, it has been quite well disguised by unnecessarily complex formalism.

(b) Classical versus quantum dynamics

Time behavior has similar classical or semi-classical roots. The Hamilton velocity equation

$$\dot{x} = \frac{\partial H}{\partial p} \tag{5.4.6a}$$

is related to the definition (5.2.9b) of group velocity by derivative of the dispersion function.

$$u = \frac{\partial \omega}{\partial k} \tag{5.4.6b}$$

The Hamilton change-of-momentum or "force" equation has a relativistic example discussed later.

$$\dot{p} = -\frac{\partial H}{\partial x} \tag{5.4.7a}$$

It is related to the wave refraction due to spatial gradient of frequency dispersion.

$$\dot{k} = -\frac{\partial \omega}{\partial x} \tag{5.4.7b}$$

As we will see in Sec. 5.5, this is the wave theoretical counterpart of Newton's *(F=ma)*-Law.

A crummy (but quick!) derivation of Schrodinger's equation

We can pretend to derive quantum theory using the ancient classical stuff. As stated previously, this bass-ackwards approach is just a trick. It is by no means an equal to proper Dirac derivations of quantum energy and momentum operators that will be given in *Unit 4 (Wave Equations)*. It is included mainly for historical and pedagogical mnemonics. A slightly improved derivation follows here in Sec. (c).

The reverse-engineering approach takes the x-derivative of the wave (5.4.4) using (5.4.3a).

$$\frac{\partial}{\partial x}\Psi \approx \frac{\partial}{\partial x}e^{iS/\hbar} = \frac{i}{\hbar}\frac{\partial S}{\partial x}e^{iS/\hbar} = \frac{i}{\hbar}p\Psi \tag{5.4.8a}$$

This resembles the *momentum-p-operator* definition that we will derive more clearly in Unit 4.

$$\frac{\hbar}{i}\frac{\partial}{\partial x}\Psi = p\Psi \tag{5.4.8b}$$

The time derivative is similarly related to an "energy-operator" or Hamiltonian operator.

$$\frac{\partial}{\partial t}\Psi \approx \frac{\partial}{\partial t}e^{iS/\hbar} = \frac{i}{\hbar}\frac{\partial S}{\partial t}e^{iS/\hbar} = -\frac{i}{\hbar}H\Psi \tag{5.4.9a}$$

The famous H-J-equation (5.4.3b) makes this into the more famous *Schrodinger time equation*.

$$i\hbar\frac{\partial}{\partial t}\Psi = H\Psi \tag{5.4.9b}$$

Again, a more rigorous development of this awaits a few chapters ahead.

If you now put in a generic off-the-shelf Hamiltonian function $H=p^2/2M+V(x)$ you get

$$i\hbar\frac{\partial}{\partial t}\Psi = \left[\frac{p^2}{2M} + V(x)\right]\Psi = \frac{-\hbar^2}{2M}\frac{\partial^2\Psi}{\partial x^2} + V(x)\Psi \tag{5.4.10}$$

which is the *non-relativistic Schrodinger wave equation*. By non-relativistic we mean it has a potential energy $V(x)$ with no momentum part to balance. Also, it treats time as a parameter that cannot mix with spatial coordinate x, and so it cannot manifest the intimate relation of relativity and quantum theory.

The derivation above obtains a famous result using less than rigorous steps. Most notable is the wavy equals sign in (5.4.9a) which indicates that a variable amplitude factor has been left out. When this is fixed the result is Bob Wyatt's useful semi-classical approach to non-relativistic quantum mechanics. It should be noted that substituting $\Psi = e^{iS/h}$ into Schrodinger's equation (5.4.10) does not quite return us to Hamilton-Jacobi equations (5.4.3). Instead the result is a wave equation of the *Riccati* form.

$$-\psi\frac{\partial S}{\partial t} = -\psi\frac{\hbar i}{2m}\nabla^2 S + \psi\left[\frac{1}{2m}\left(\frac{\partial S}{\partial \mathbf{r}}\right)^2 + V(r)\right]$$
$$\frac{\hbar i}{2m}\nabla^2 S = \frac{\partial S}{\partial t} + \left[\frac{1}{2m}\left(\frac{\partial S}{\partial \mathbf{r}}\right)^2 + V(r)\right] = \frac{\partial S}{\partial t} + H\left(\frac{\partial S}{\partial \mathbf{r}}, \mathbf{r}\right) \qquad (5.4.11)$$

In the limit that the left hand double (Laplacian) derivative vanishes, the full quantum Schrodinger equation reduces to the classical H-J equations (5.4.3). This is sometimes called a *semi-classical limit*.

$$\hbar\left|\nabla^2 S\right| << \left(\frac{\partial S}{\partial \mathbf{r}}\right)^2, \text{ or: } \hbar\left|\frac{d^2 S}{dx^2}\right| = \hbar\left|\frac{dp_x}{dx}\right| << p_x^2, \text{ or: } \hbar\left|\frac{dp_x}{dx}\right| / \left|p_x\right| << \left|p_x\right| = \hbar\left|k_x\right| \qquad (5.4.12a)$$

For this to hold, DeBroglie wavelength $\lambda_x/h = 1/\hbar k_x = 1/p_x$ must be small compared to its variation in the space of a wavelength. Equivalently wavevector k_x is large compared to relative rate of change of k_x.

$$\left|\frac{dk_x}{dx}\right| / \left|k_x\right| << \left|k_x\right|, \text{ or: } \left|\frac{d\lambda_x}{dx}\right| << 1 \qquad (5.4.12b)$$

(c) A slightly improved derivation of Schrodinger's equation

A μ-wave dispersion function (5.2.8) *sans* its *($\hbar\mu = Mc^2$)* term gives a Newtonian approximation.

$$KE = \hbar\omega - \hbar\mu \Rightarrow KE_{NR} = \hbar\omega \cong \frac{(\hbar ck)^2}{2\hbar\mu} = \frac{p^2}{2M} \quad \text{where:} \begin{cases} \hbar k = p \\ \hbar\mu = Mc^2 \end{cases}$$

An approximate classical Hamiltonian is a sum of the Newtonian kinetic energy *KE* and a potential **V**.

$$\mathbf{H} = \frac{\mathbf{p}^2}{2M} + \mathbf{V} = KE_{NR} + PE_{NR}$$

Presumably, **V** is an interaction energy of the μ-wave with whatever else might occupy its vacuum. Fourier plane waves $\psi_{k,\omega}(x,t) = \langle x,t|k,\omega\rangle = e^{i(kx-\omega t)}/\sqrt{N}$ are eigenfunctions of momentum **p** or *KE* only.

$$\langle x,t|\mathbf{p}|k,\omega\rangle = \hbar k\langle x,t|k,\omega\rangle = \frac{\hbar}{i}\frac{\partial}{\partial x}\psi_{k,\omega}(x,t) \qquad (3.4.13a)$$

$$\langle x,t|KE|k,\omega\rangle = \hbar\omega\langle x,t|k,\omega\rangle = \hbar i\frac{\partial}{\partial t}\psi_{k,\omega}(x,t) \qquad (5.4.13a)$$

A wave $\langle x,t|\Psi\rangle$ with Fourier coefficients $\alpha_{k,\omega} = \langle k,\omega|\Psi\rangle$ satisfies a Schrodinger time equation.

$$\sum_{k,\omega}\alpha_{k,\omega}\langle x,t|KE|k,\omega\rangle = \sum_{k,\omega}\alpha_{k,\omega}\langle x,t|H-V|k,\omega\rangle = i\hbar\sum_{k,\omega}\alpha_{k,\omega}\frac{\partial}{\partial t}\psi_{k,\omega}(x,t) \qquad (5.4.14a)$$

$$\langle x,t|KE|\Psi\rangle = \langle x,t|H-V|\Psi\rangle = i\hbar\frac{\partial\Psi(x,t)}{\partial t} \text{ where: } \Psi(x,t) = \sum_{k,\omega}\alpha_{k,\omega}\langle x,t|k,\omega\rangle = \langle x,t|\Psi\rangle \qquad (5.4.14b)$$

But, only certain waves $\langle x,t|\Phi_E\rangle$ satisfy a *Schrodinger energy eigen-equation* $\mathbf{H}|\Phi_E\rangle = E|\Phi_E\rangle$.

$$\langle x,t|KE|\Phi_E\rangle = -\frac{\hbar^2}{2M}\frac{\partial^2}{\partial x^2}\Phi_E(x,t) = (E-V)\Phi_E(x,t) \qquad (5.4.15a)$$

Eigenvalue E is used to define non-relativistic time and frequency relations for stationary state $|\Phi_E\rangle$.

$$i\hbar\frac{\partial}{\partial t}\Phi_E(x,t) = E\Phi_E(x,t) \text{ where: } \Phi_E(x,t) = \Phi_E(x,0)e^{-iEt/\hbar} \qquad (5.4.15a)$$

This restatement of Planck's (E=ħν)-axiom is an "improved" derivation of Schrodinger theory, but every step of it further erodes relativity of spacetime. To arrive at (5.4.15) we must *(1)* discard proper frequency *($\hbar\mu=Mc^2$)*, *(2)* consider only non-relativistic low-*(ω,ck)* approximations, *(3)* introduce a scalar potential *V(x)* without a relativistic vector potential companion (in QED this is an E•r approximation) , and *(4)* define energy eigenstates by single-frequency time dependence. The last step precludes the first example in Fig. 4.3.3 from being viewed as an energy state in any but the one frame of Fig. 4.3.3(a) that is monochromatic $E_0=\hbar\omega_0$. Again, the proper Dirac derivation of (5.4.15) and solutions are in Unit 4. But, proper or not, Schrodinger theories all have difficulties due to their ignoring relativity.

Schrodinger difficulties

Failure to treat time, frequency, and energy on the same footing as, respectively, space, *k*-vector, and momentum leads to a logically tangled web. Repair of Schrodinger theory with perturbative patching is difficult, misleading, and lacking physical insight. This leads to many longstanding difficulties that go untreated since Schrodinger's equation has for so long been so successful in its realm of approximation.

A key Schrodinger difficulty involves the concepts of inertia and mass. The *wave effective inertial mass M_{eff}* (5.2.20a) is inversely proportional to the curvature of the dispersion function (5.2.8) and *not* a constant except for the quadratic case $\omega=B\,k^2$. For low velocity ($\beta=u/c<<1$) M_{eff} approaches the *rest mass $M=\hbar\mu/c^2$* given by (5.2.5b), a constant $\hbar/c^2$ times proper-frequency μ.

$$M_{eff}=\frac{F}{a}=\frac{1}{\left(\frac{d^2E}{dp^2}\right)}=\frac{M}{\left(1-\beta^2\right)^{3/2}}\xrightarrow[\beta\approx 0]{}M \qquad (5.4.16)$$

At high β , M_{eff} differs from the *momentum mass M_{rel}* of relation (5.2.5c). M_{rel} also is M at slow u.

$$M_{rel}=\frac{M}{\left(1-\beta^2\right)^{1/2}}\xrightarrow[\beta\approx 0]{}M \qquad (5.4.17)$$

Photon dispersion is linear *($\omega=c|k|$)* so (5.4.16) does not apply. Indeed, photon effective mass is *infinite* since its group and phase velocity are invariant. But, effective mass of any wave at *k=0* is its *invariant rest mass M*. Higher $M=\hbar\mu/c^2$ makes waves harder to accelerate (unless M is zero as for photons). Then the optical dispersion function ($\omega=c|k|$) in Fig. 5.1.1 has a kink with infinite curvature at the origin *k=0*. So, by equation (5.4.16a), photon rest mass is indeed zero but photon M_{eff} is infinite everywhere else!

The standard Schrodinger equation (5.4.15) is ill equipped to handle variable effective mass, and it literally falls apart for problems involving *negative energy states* with *negative dispersion ($\mu<0$)* or *tachyon states (imaginary μ)*. It might seem that the Newtonian $k^2/_{2M}$ dispersion plot in Fig. 5.2.1(b) is a strategically placed "fig-leaf" covering an embarrassment of Dirac negative-μ (anti-particle) bands for which (5.4.16a) gives negative M_{eff}. The negative-energy or negative-μ bands are states whose phasors run in reverse, that is, counter-clockwise and a world going back in time! Some of the seemingly bizarre wave behavior due to abnormal or anomalous dispersion has been shown in Fig. 5.3.5. The behavior of high-energy matter-anti-matter reactions has to involve similarly bizarre wave dynamics. So will exciton states involving combinations of conduction-band "carriers" and valence-band "holes" in semiconductors.

Classical relativistic Lagrangian derived by quantum theory

The classical Hamiltonian H is derived from the Lagrangian L (5.4.1) so action $S=\int L\,dt$ is arguably a more fundamental quantity than energy. The quantum energy or frequency $\omega=E/\hbar$ is a negative time derivative (5.4.3b) of the phase $\Phi=S/\hbar$, which arguably is the most fundamental quantity of all.

The preceding discussions of these quantities give some idea why classical mechanics could seem to be so prescient about concepts that only make sense in light of quantum wave mechanics. Perhaps, the key link is when Poincare's invariant (5.4.2) is related to the phase invariance axiom (4.3.6). One may view families of classical trajectories fanning out like rays from each spacetime point. Normal to the classical momentum $\mathbf{p}=\nabla S$ (5.4.3a) of each ray are the wavefronts of constant phase Φ or action S. Then, according to a "matter-wave" form of Huygen's principle, new wavefronts are continuously built as in Fig. 5.4.1 through interference from "the best" of all the little wavelets emanating from a multitude of source points.

The "best" are the ones that are extremes in phase, so-called *stationary-phase* rays, who thereby satisfy *Hamilton's Least-Action Principle* requiring that $\int L dt$ is minimum for "true" classical trajectories. This in turn enforces Poincare' invariance by eliminating, through destructive interference, any "false" or non-classical paths because they do not have an invariant (and thereby stationary) phase, and therefore cancel each other in a cacophonous mish-mash of mismatched phases.

The idea of phase invariance that began this chapter may be restated using the classical ideas of action and Lagrangian functions. Plane phase $\Phi = kx-\omega t$, in the mass rest frame where $x=0=k$, is a product $-\mu\tau$, of minus the proper frequency $-\omega=-\mu$ multiplying the proper time $t=\tau$. The differential of this phase by Einstein-Planck mass-energy-frequency equivalence relation (5.2.5b) is

$$d\Phi = kdx-\omega dt=-\mu\, d\tau = -(Mc^2/\hbar)\, d\tau. \qquad (5.4.18)$$

τ-Invariance (5.1.4) (or Einstein time dilation (4.4.1a)) gives $d\tau$ in terms of velocity $u=\frac{dx}{dt}$.

$$d\tau = dt\,\sqrt{(1-u^2/c^2)} \qquad (5.4.19)$$

Combining definitions for action $dS=Ldt$ (5.4.2) and phase $dS = \hbar d\Phi$ (5.4.5) gives

$$L = -\hbar\mu\tau = -Mc^2\sqrt{(1-u^2/c^2)}. \qquad (5.4.20)$$

This is a *relativistic matter Lagrangian* whose action integral $S=\int Ldt$, says Hamilton, must be *minimized*.

Feynman's clever interpretation of the S minimization as sketched in Fig. 4.5.2 is that a massive projectile flies in such a way that its "clock" τ is *maximized*. Since proper frequency μ is constant for a given type of matter, this is the same as minimizing $-\mu\tau$ or maximizing $+\mu\tau$. What *does* minimize τ? Answer: Huygen's wave interference demands stationary and extreme phase, that is, the fastest clock!

So, the mechanically ordered Newtonian "clockwork-world" appears then to be the perennial "cosmic gambling house winner" in a kind of wave dynamical lottery occurring in an underlying quantum wave fabric. Since it seems to be such a winner for so long, many physicists find it difficult to say good-bye to a purely classical paradigm even as it becomes more and more clear that it's all "faked" by interfering waves. The classical period of physics was made a huge success by Newton and others who began the great enlightenment period of the 18th century and proceeded through the 20th. We only hope the 21st century will be at least as enlightening as we move on to examining a very wavy universe.

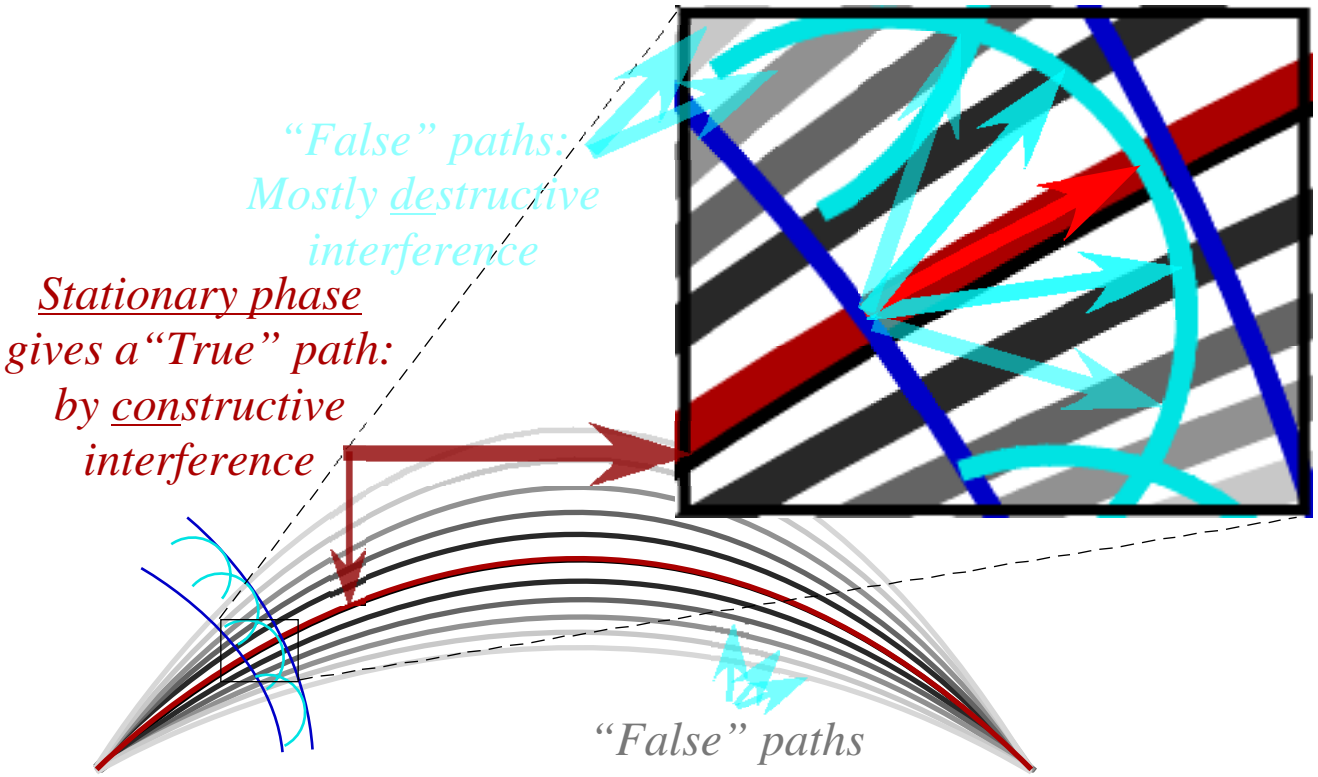

Fig. 5.4.1 Quantum waves interfere constructively near "True" path. Waves mostly cancel elsewhere.

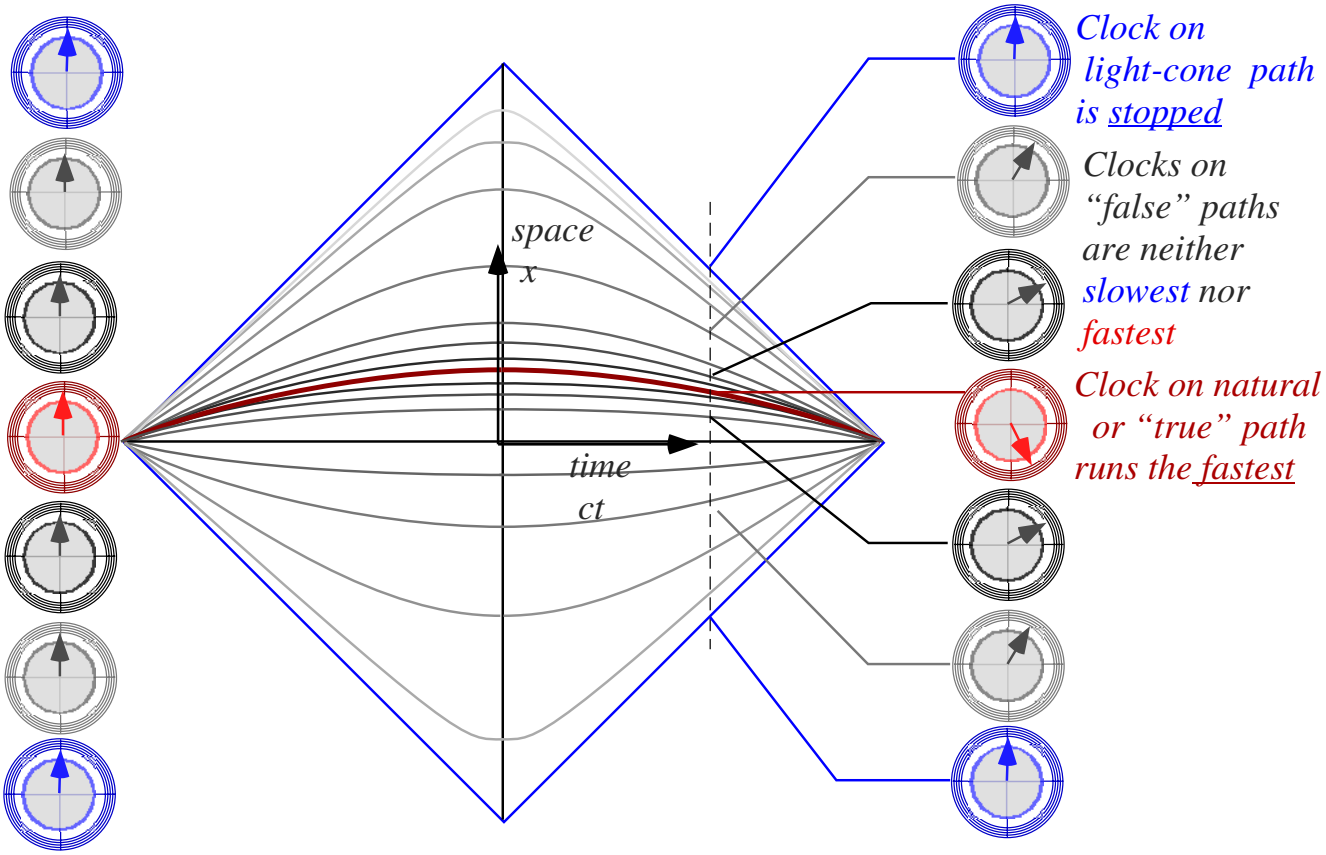

Fig. 5.4.2 "True" paths carry extreme phase and fastest clocks. Light-cone paths carry stopped clocks.

5.5 Relativistic acceleration: Newton's invariants

The theory of special relativity is one of inertial frames and constant velocity. At first this might seem to preclude discussion of frames with non-constant velocity such as linear acceleration (changing inclination in space and time) or rotating frames (changing inclination in space).

Linear accelerated Lorentz frames in just one-space dimension provide a glimpse of some of the issues of Einstein's general theory for curved spacetime and gravity. Einstein's *equivalence principle* claims that a *g*-accelerated frame or "Einstein elevator" has the same *local* physics as a frame fixed in a uniform *g*-field. We now consider accelerated frames by classical theory and then by wave mechanics.

(a) Classical particle and PW theory of acceleration

A classical theory of an accelerating particle must deal with its mass, which involves rest mass M (5.2.5a), relativistic mass M_{rel} (4.5.16), and effective mass M_{eff} (5.4.17). Definition of mass depends on which time derivatives we use, proper time differentials $d\tau$ or coordinate time differential dt. Ordinary u velocity is a ratio of coordinate x and coordinate time t. Equation (5.2.5c) for momentum p involves a ratio of coordinate x and *proper* time τ. (p also has rest mass M multiplying the *proper velocity* $\upsilon=dx/d\tau$.)

$$u=\frac{dx}{dt} \qquad (5.5.1a) \qquad\qquad p=M\upsilon=M\frac{dx}{d\tau} \quad (5.5.1b)$$

The ratio of t and τ differentials follows from (5.4.19) or from definition (5.1.4) of proper time τ.

$$d\tau=dt\sqrt{1-u^2/c^2} \qquad (5.5.1c)$$

The ratio of proper time derivatives of momentum and velocity is the effective mass in equation (5.4.17).

$$\frac{dp}{d\tau}=\frac{d}{d\tau}\frac{Mu}{\sqrt{1-u^2/c^2}}=\frac{M\dfrac{du}{d\tau}}{\sqrt{1-u^2/c^2}}+\frac{\dfrac{Mu^2}{c^2}\dfrac{du}{d\tau}}{\left[1-u^2/c^2\right]^{\frac{3}{2}}} \qquad (5.5.2)$$

$$=\frac{M}{\left[1-u^2/c^2\right]^{\frac{3}{2}}}\frac{du}{d\tau}=M_{eff}\frac{du}{d\tau}$$

In quantum dynamics and related Newtonian sub-relativistic classical dynamics, wavevector k (that is, momentum $p=\hbar k$) in (5.2.5c) grows linearly with boost velocity u from its zero-k resting value, while frequency ω (that is, energy $E=\hbar\omega$) in (5.2.5b) grows quadratically with u from its resting value of proper frequency μ (that is, rest energy $\hbar\mu=Mc^2$). If u grows linearly with time $\tau\sim t$, as it would at first with constant acceleration g, then wavevector (momentum) varies initially as $g\tau$ while frequency (energy) varies initially as $g\tau^2/2$. All this recapitulates elementary classical mechanics, as it must. At time $\tau=0$, the τ-derivative of u is g, the τ-derivative of p is Mg, but the τ-derivative of E is zero.

$$\left.\frac{dp}{d\tau}\right|_0=Mg\,, \qquad \left.\frac{dE}{d\tau}\right|_0=0\,. \qquad (5.5.3)$$

Consider a rocket frame *(x",ct")* where $dp"/d\tau$ is *always* a constant Mg. This is an Einstein elevator model of uniformly accelerating gravity. The lab value p at each speed u is a Lorentz boost (5.2.10a).

$$p = \frac{p'' + u\,E''/c^2}{\sqrt{1-(u/c)^2}} \tag{5.5.4}$$

The τ-derivative of p has the same boost since proper time τ is invariant. τ=0 values (5.5.3) are used.

$$\frac{dp}{d\tau} = \frac{\frac{dp''}{d\tau} + \frac{u}{c^2}\frac{dE''}{d\tau}}{\sqrt{1-(u/c)^2}} = \frac{Mg + \frac{u}{c^2}0}{\sqrt{1-(u/c)^2}} = \frac{Mg}{\sqrt{1-(u/c)^2}} \tag{5.5.5a}$$

This reduces to an elementary *pre*-relativistic constant-g Newtonian equation by using t/τ-ratio (5.5.1c).

$$\frac{dp}{dt} = Mg \tag{5.5.5b}$$

The velocity is not Newtonian since u cannot grow indefinitely or it will exceed c, but, the momentum p (and wavevector k) as well as energy E (and frequency ω) do grow indefinitely as u approaches c.

Equating (5.5.5a) and (5.5.2) gives an easily integrated equation for velocity u.

$$\frac{dp}{d\tau} = \frac{M\frac{du}{d\tau}}{\left[1-\frac{u^2}{c^2}\right]^{\frac{3}{2}}} = \frac{Mg}{\left[1-\frac{u^2}{c^2}\right]^{\frac{1}{2}}}, \qquad M\frac{du}{d\tau} = Mg\left[1-\frac{u^2}{c^2}\right], \qquad g\tau = \int \frac{du}{\left[1-\frac{u^2}{c^2}\right]} \tag{5.5.6}$$

The integral yields the boost velocity u/c as a hyperbolic tangent of a product of proper time τ and g/c.

$$\frac{u}{c} = \tanh(g\tau/c) = \sinh(g\tau/c)/\cosh(g\tau/c) \tag{5.5.7a}$$

So, hyperbolic rapidity $\rho = \tanh^{-1}u/c = g\tau/c$ increases linearly with proper time τ while velocity u approaches c. Time dilation factor $\cosh\rho$ is a hyper-cosine of proper time $g\tau/c$ consistent with (4.3.7).

$$\frac{dt}{d\tau} = \frac{1}{\sqrt{1-\frac{u^2}{c^2}}} = \frac{1}{\sqrt{1-\tanh^2(g\tau/c)}} = \cosh(g\tau/c) \tag{5.5.7b}$$

Coordinate velocity u (5.5.1a) and proper velocity $v=p/M$ from (5.5.1b) are also hyper-functions.

$$u = \frac{dx}{dt} = \frac{\frac{dx}{d\tau}}{\frac{dt}{d\tau}} = \frac{\frac{dx}{d\tau}}{\cosh(g\tau/c)} = c\tanh(g\tau/c) \qquad \text{where:} \qquad v = \frac{p}{M} = \frac{dx}{d\tau} = c\sinh(g\tau/c)$$

(5.5.7c) (5.5.7d)

This is no accident. Integrating equations (5.5.7) shows a constant acceleration trajectory is a hyperbola.

$$x = \frac{c^2}{g}\cosh(g\tau/c) \tag{5.5.8a}$$

$$ct = \frac{c^2}{g}\sinh(g\tau/c) \tag{5.5.8b}$$

These are not just any hyperbolas, but *invariant hyperbolas* such as traced by rockets in Fig. 5.5.1.

$$x^2 - (ct)^2 = \left(c^2/g\right)^2 \tag{5.5.8c}$$

A constant-g trajectory is invariant since all must agree on the shape of a given constant proper acceleration curve. A ship with a big "g" stamped on its tail doesn't look like a 2g-ship to someone else who happens to moving by outside it. The g-number is an intrinsic proper invariant.

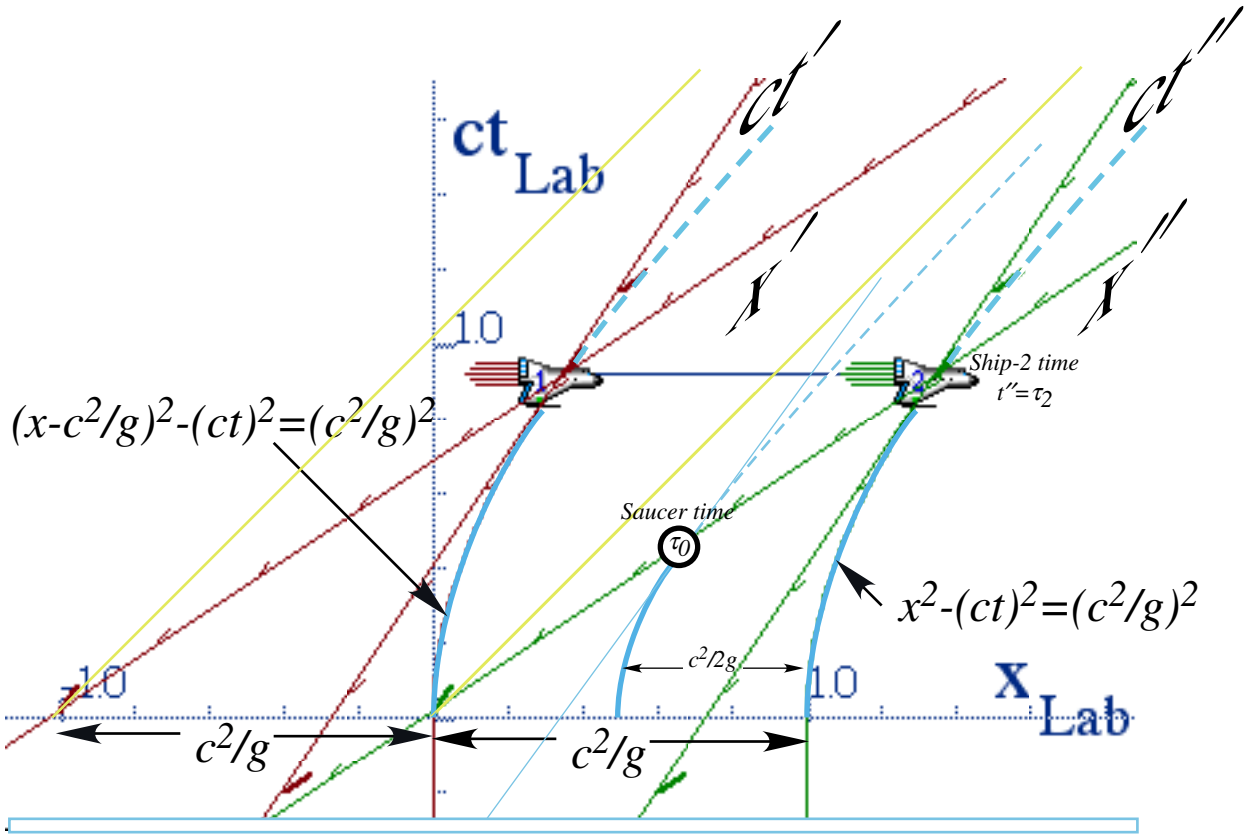

Fig. 5.5.1 Examples of constant acceleration space-time trajectories of ships (g) and saucer (2g).

The relativistic momentum $p=Mv$ is growing as a hyper-sine of proper time in (5.5.7d) and so is lab coordinate time t (5.5.8b). Constant (local) acceleration yields constantly growing (lab) momentum (5.5.5b) just as Newton had claimed all along! So we call the trajectories in Fig. 5.5.1 *Newton's invariants*.

Proper length: Gentlemen start your engines!

Still, there was little to prepare Newton for the modern consequences of his second law in relativistic form (5.5.5). To show this, Fig. 5.5.1 has two identical ships fire their engines at $t=0$ lab time to begin a constant g journey in parallel. What happens next from the point of view of their instantaneous Lorentz frames seems so bizarre that it boggles the mind. If you like paradox, this is a race to watch, a cosmic NASCAR!. The idea of fielding such an event originates with John. E. Heighway around 1967.

The acceleration $g=c^2$ imagined here is astronomical; from zero to half the speed of light in less than a second! Also, there is a "flying saucer" (A circle in Fig. 5.5.1) with *twice* the acceleration located a distance $c^2/2g$ behind ship-2 and the same distance ahead of ship-1 who starts the race at lab origin $x=0$.

Since ship-2 starts at lab $x=c^2/g$ from origin it will trace a hyperbolic invariant trajectory in the lab according to (5.5.8c). So will the alien saucer which starts at $x=c^2/2g$ with acceleration $2g$. You might think that the $2g$ saucer would rapidly catch up with the $1g$ ship-2 it is chasing, and it does appear to do so to the lab observers. As always in relativity, the word we need to question here is "appear."

According to observers at rest in any ship-2 frame, the distance between the saucer and ship-2 *remains fixed at* $x'=c^2/2g$ for as long as both continue their respective acceleration $2g$ and g. And, the lab observers might note that the saucer, in spite of its superior acceleration, never *passes* ship-2. In fact, all they are seeing is gradual Lorentz contraction (4.4.1) of saucer, ship-2, and the distance separating them, while, meantime, the distance separating ship-1 and ship-2 does not shrink at all.

The key idea here is that the saucer and ship-2 are on *concentric* hyperbolic invariants of *proper length* ℓ from the origin. *Proper length* ℓ-curves defined by $x^2-(ct)^2 = \ell^2 = x''^2-(ct'')^2$ are just the $i\tau$-curves in Fig. 5.1.2(a), that is, the imaginary proper-time $i\tau$-curves that serve as space-axis grid markers. The x''-axis tips for the ship-2 and saucer as they accelerate, but each stays put at the $x''=c^2/g$ and $x''=c^2/2g$ grid marker, respectively. In other words, their proper separation $\Delta x''=c^2/2g$ does not change; it is as though the saucer and ship-2 *were connected by a rigid beam of constant proper length*. Ship-2 has a saucer-trailer! (It is always puzzling that alien flying saucers or other UFO's always visit trailer camps in Alabama, Arkansas, and such places. Perhaps, they just want to *be* trailers.)

Meanwhile, ship-1 follows a hyperbola that is identical to (but not concentric to) that of ship-2. The origin for ship-1 is also fixed a distance c^2/g behind it according to (5.5.8c) and as shown in Fig. 5.5.1. The ship-1 space x'-axis tips just as fast in the lab frame as the x''-axis of ship-2 and its trailing saucer. Along the x'-axis, ship-1 could find ship-2 and its saucer way up in the upper right hand corner of Fig. 5.5.1. He'd better be quick about it because ship-2 and saucer are receding rapidly from ship-1 in its x'-frame. This *Lorentz expansion* is the necessary flipside of Lorentz contraction because the separation Δx of ship-1 and ship-2 is constant in the lab x-frame where their kinetic behavior is identical.

You might think that ship-2 and its saucer-trailer would see ship-1 falling behind them on their x''-axis, and that their view of the Lorentz expansion would equal that of ship-1. But, as indicated in Fig. 5.5.1, the behavior of ship-1 seen by ship-2 is quite extraordinary. In the x''-frame of the trailer-saucer and ship-2, they would see (if they could) ship-1 *stuck at time-zero*. Ship-1's engines won't start, and neither do any of its clocks! Ship-1, in the ship-2 x''-frame, appears to be pretty much a dead parrot.

In spite of this, ship-1 manages to keep up with the very-much-alive ship-2 as does the saucer! Indeed, the Lorentz space-expansion makes the x''-distance from ship-1 and ship-2 stay put at the invariant value $x''=c^2/g$ with the saucer always halfway between at $x''=c^2/2g$. The saucer-trailer acceleration of $2g$ must be twice the rate g of the ship-2 just to remain at $x''=c^2/2g$ behind it.

One key to this strange behavior is in the proper time values of the participants. The instantaneous lab-relative velocity u_2 of ship-2 in Fig. 5.5.2 is equal to the velocity u_0 of its saucer-trailer. Along the x''-axis line, each concentric hyperbolic trajectory has the same tangent slope or velocity but not the same curvature or acceleration. The velocity equation (5.5.7a) gives

$$\frac{u_2}{c} = \tanh\left(g\tau_2 / c\right) = \frac{u_0}{c} = \tanh\left(2g\tau_0 / c\right) \qquad (5.5.9a)$$

This means that the proper time τ_2 on board ship-2 is twice the proper time τ_0 on its saucer trailer.

$$g\tau_2 / c = 2g\tau_0 / c \quad \text{implies:} \quad \tau_2 = 2\tau_0 \qquad (5.5.9b)$$

This means that the ship-2, which is loafing along with *1g* acceleration, is aging twice as fast as its attached saucer-trailer that has to do a 2g acceleration just to keep up. (Exercise keeps us younger!) Also, lab time coordinates t_2 and t_0 (indicated by vertical arrows pointing at ship-2 and saucer, respectively, in Fig. 5.5.2) have the same *2:1* ratio according to (5.5.8b) and (5.5.9b).

$$\frac{t_2}{t_0}=\frac{\frac{c^2}{g}\sinh(g\tau_2/c)}{\frac{c^2}{2g}\sinh(2g\tau_0/c)}=\frac{2\sinh(g\tau_2/c)}{\sinh(2g\tau_0/c)}=2 \qquad (5.5.10)$$

This checks with the geometry of Fig. 5.5.2. Readings on co-moving clocks along x'' are proportional to distance x'' while the acceleration each one needs to keep up the same velocity is inverse to x''.

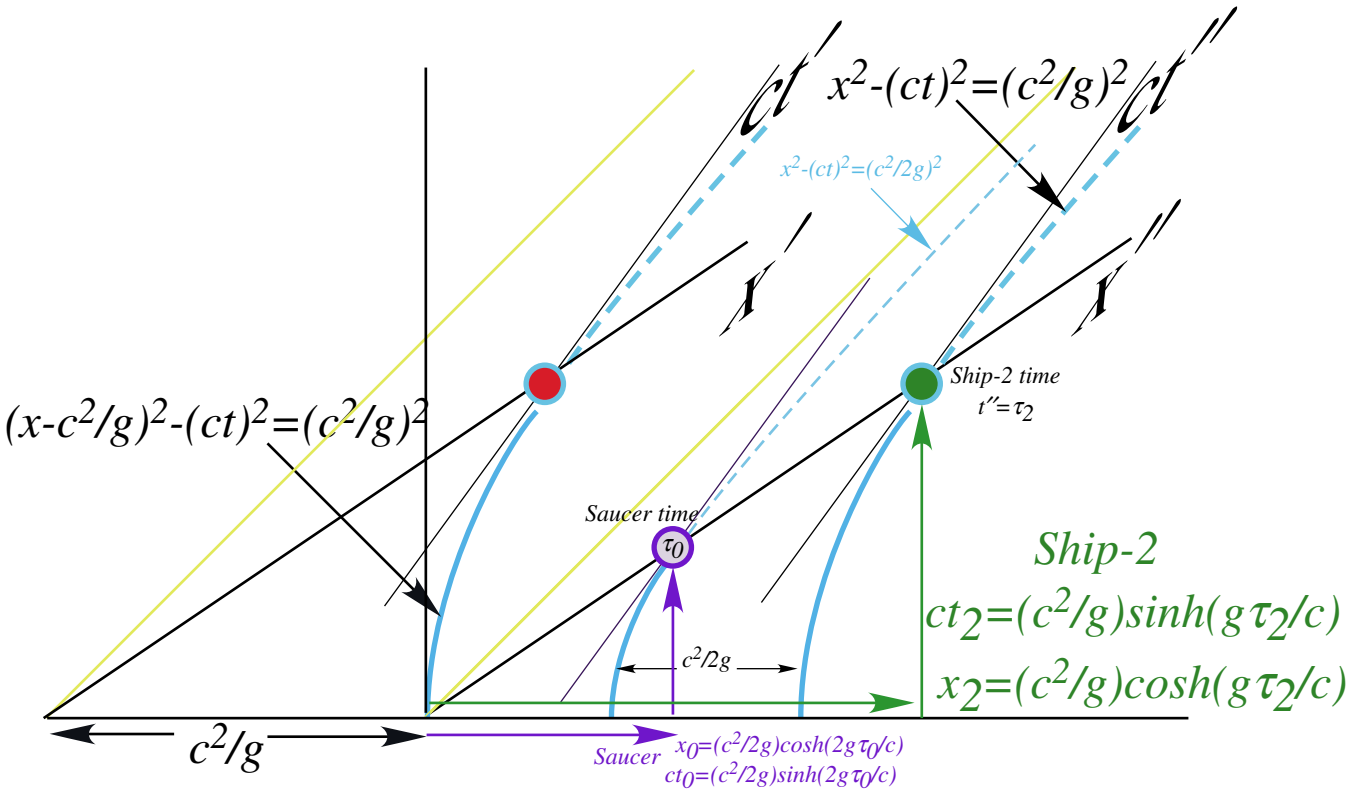

Fig. 5.5.2 Coordinates and proper time relations for ship-1 (one-g) and saucer-trailer (two-g).

Some of the paradox concerning the ship and its length-invariant extension to the saucer-trailer can be resolved by using optical pulse trains bouncing back and forth between ship-2 and its saucer trailer. If the length $x''=c^2/2g$ separating these two objects never changes as long as their accelerations are constant (*1g* for the ship and *2g* for the saucer) then that length can be used as a timing device by bouncing pulses between mirrors held by each of them. The space-time paths of these pulses are shown in Fig. 5.5.3.

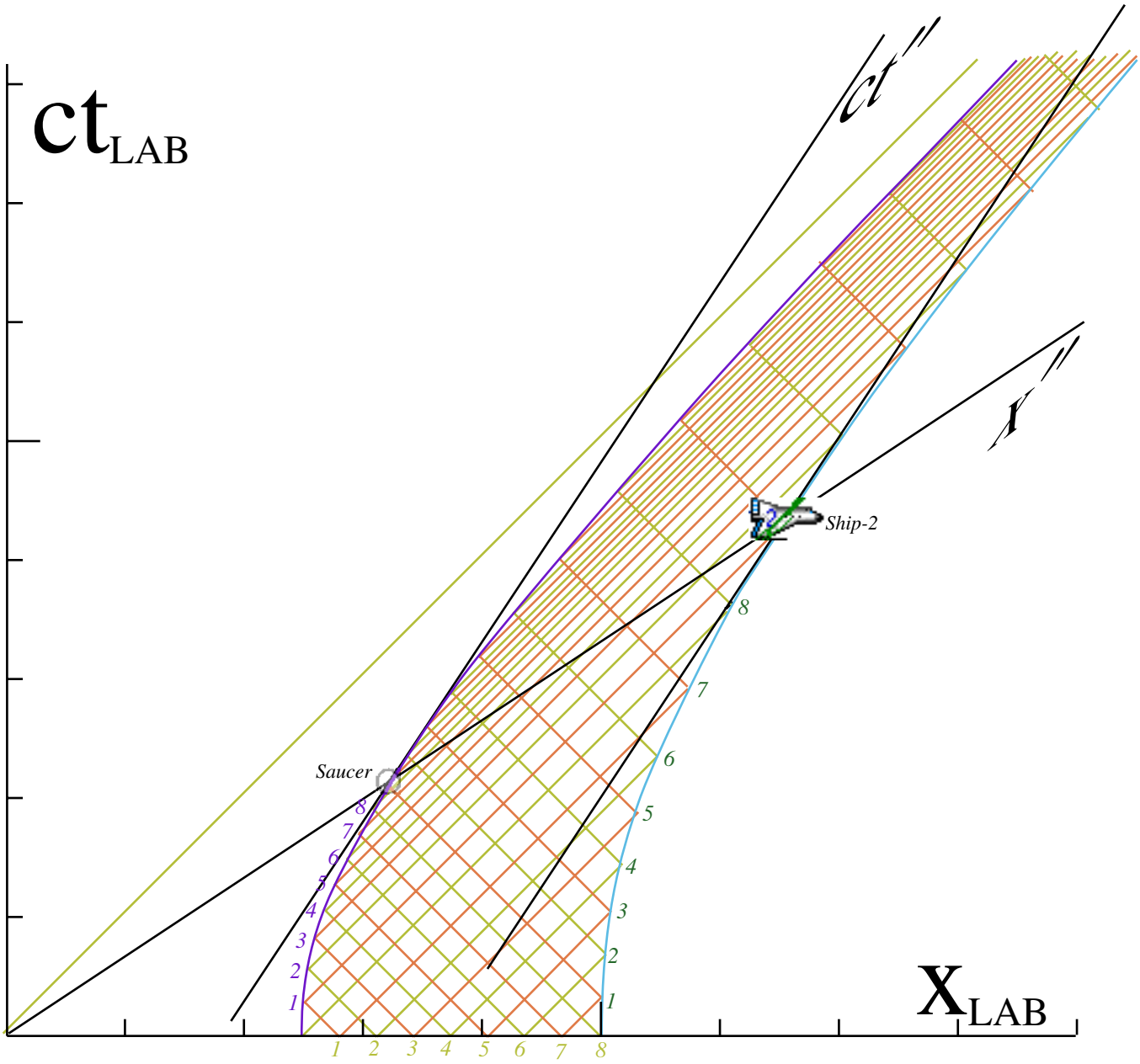

Fig. 5.5.3 Optical pulse wave paths between ship-2 (one-g) and saucer-trailer (two-g) trajectories.

A total of eight pulses are running in each direction along the x''-axis between ship-2 and saucer. At the lab moment when the x''-axis is pictured in Fig. 5.5.3, both the ship and the saucer have bounced eight pulses since departure and are in the process of bouncing a ninth. The *45°* lines in Fig. 5.5.3 could also be paths of continuous wave (CW) ReΨ zeros of moving waves. Interfering wave combinations give local standing wave Minkowski grids (Recall Fig. 4.3.3). The grids start out Cartesian at the bottom of Fig. 5.5.3. (Recall Fig. 4.3.2) Then acceleration makes local Minkowski grids of increasing velocity u. Next we study some detailed properties of accelerated waves. In so doing, we rederive the classical results easily.

(b) Wave interference and CW theory of acceleration

Accelerating Minkowski grids can be made using counter-propagating CW laser beams like the ones making constant-u grids in Fig. 4.3.3. A group velocity u may be achieved by detuning to $\omega_{\leftarrow}=(1/b)\omega'_0$ the laser pointing against u while up-tuning the forward laser $\omega_{\rightarrow}=(b)\omega'_0$, by the same Doppler factor $b=e^{\rho}$ given by (4.3.5b). The exponent ρ is the *rapidity* argument in hyperbolic definitions (4.3.7) of velocity u.

$$b=e^{\rho} \qquad (5.5.11a) \qquad\qquad u/c=\tanh\rho \qquad (5.5.11b)$$

In Fig. 4.3.3(b) frequency shifting is due to the laser's Doppler b-shifts from motion relative to the atom (or ship) frame. In Fig. 5.5.4 we propose to use *tunable* fixed lasers to accelerate an atom frame (and maybe an atom, too), but now the atom will see a *Cartesian* spacetime grid like Fig. 4.3.3(a) made by *one* green ω'_0 frequency from *either* laser due to its perceived Doppler shifts of $\omega_{\rightarrow}$ and $\omega_{\leftarrow}$.

$$\omega_{\rightarrow}=(b)\,\omega'_0=e^{\rho}\omega'_0 \qquad \text{and} \qquad \omega_{\leftarrow}=(1/b)\,\omega'_0=e^{-\rho}\omega'_0 \qquad (5.5.12)$$

To the atom, both the blue laser $\omega_{\rightarrow}$ off to the left and a red laser $\omega_{\leftarrow}$ off to the right always look green!

This uses tunable versions of grid broadcasting schemes wherein both frequency (5.2.11) and amplitude (5.2.12) would vary in order to achieve a desired instantaneous rapidity ρ at a particular position $(x(t),ct)$ of the atomic (x',ct')-grid-origin in the laser-lab. The trick is to schedule the location and timing of pair(s) of counter-propagating laser beam sources so their beams intersect at the precise spacetime point $(x(t),ct)$ where they can interfere and make the desired local instantaneous atomic (x',ct')-grid of rapidity ρ. In other words, the laser pair on the lightcone of each trajectory point $x(t)$ "paints" a local grid having rapidity ρ so that the specified trajectory $x(t)$ is a continuous spacetime curve.

$$u=\frac{dx}{dt}=c\tanh\rho \qquad (5.5.13)$$

One scheme, shown in Fig. 5.5.4, uses a line of n laser pairs strung out along the lab x-axis. The n^{th} blue-red pair $(\omega_{n\rightarrow},\omega_{n\leftarrow})$ of lasers has the left-hand laser located at $x_{n\rightarrow}$ and the right-hand one at $x_{n\leftarrow}$.

$$x_{n\rightarrow}=x(t_n)-ct_n \qquad (5.5.14a) \qquad\qquad x_{n\leftarrow}=x(t_n)+ct_n \qquad (5.5.14b)$$

They are set to turn on at lab time $t=t_0=0$ with frequencies $(\omega_{n\rightarrow},\omega_{n\leftarrow})$ given by (5.5.12) so as to produce a desired rapidity ρ_n or velocity u_n (5.5.13) at the n^{th} trajectory point $x_n=x(t_n)$.

Another scheme has just two fixed lasers on the left at $x=a_{\rightarrow}$ and $x=a_{\leftarrow}$ on the right, respectively, but requires each to "chirp" its frequency long *before* $t=0$. As in Fig. 5.5.4(b), the atom accelerates left-to-right if the left-hand laser up-chirps (red to blue) while the right-hand laser down-chirps, and vice-versa.

Invariant atomic proper time τ may be used in time derivatives instead of lab coordinate time t.

$$p\equiv\frac{dx}{d\tau}=\frac{dx}{dt}\frac{dt}{d\tau}=c\tanh\rho\cosh\rho=c\sinh\rho \qquad (5.5.15a) \qquad \frac{dt}{d\tau}=\frac{1}{\sqrt{1-u^2/c^2}}=\cosh\rho \qquad (5.5.15b)$$

We use (5.4.19) or definition (5.1.4) of proper time τ. Relations for laser scheduling of (5.5.14) follow.

$$\frac{d(x+ct)}{d\tau}=c(\cosh\rho+\sinh\rho)=ce^{\rho} \qquad (5.5.15c) \qquad \frac{d(x-ct)}{d\tau}=c(\cosh\rho-\sinh\rho)=ce^{-\rho} \qquad (5.5.15d)$$

$$x+ct=c\int d\tau\; e^{\rho} \qquad (5.5.15e) \qquad\qquad x-ct=c\int d\tau\; e^{-\rho} \qquad (5.5.15f)$$

$$x=c\int\sinh\rho\; d\tau \qquad (5.5.15g) \qquad\qquad ct=c\int\cosh\rho\; d\tau \qquad (5.5.15h)$$

This gives the trajectory $x(t)$ given a "local schedule" of rapidity $\rho(\tau)$ as a function of proper time.

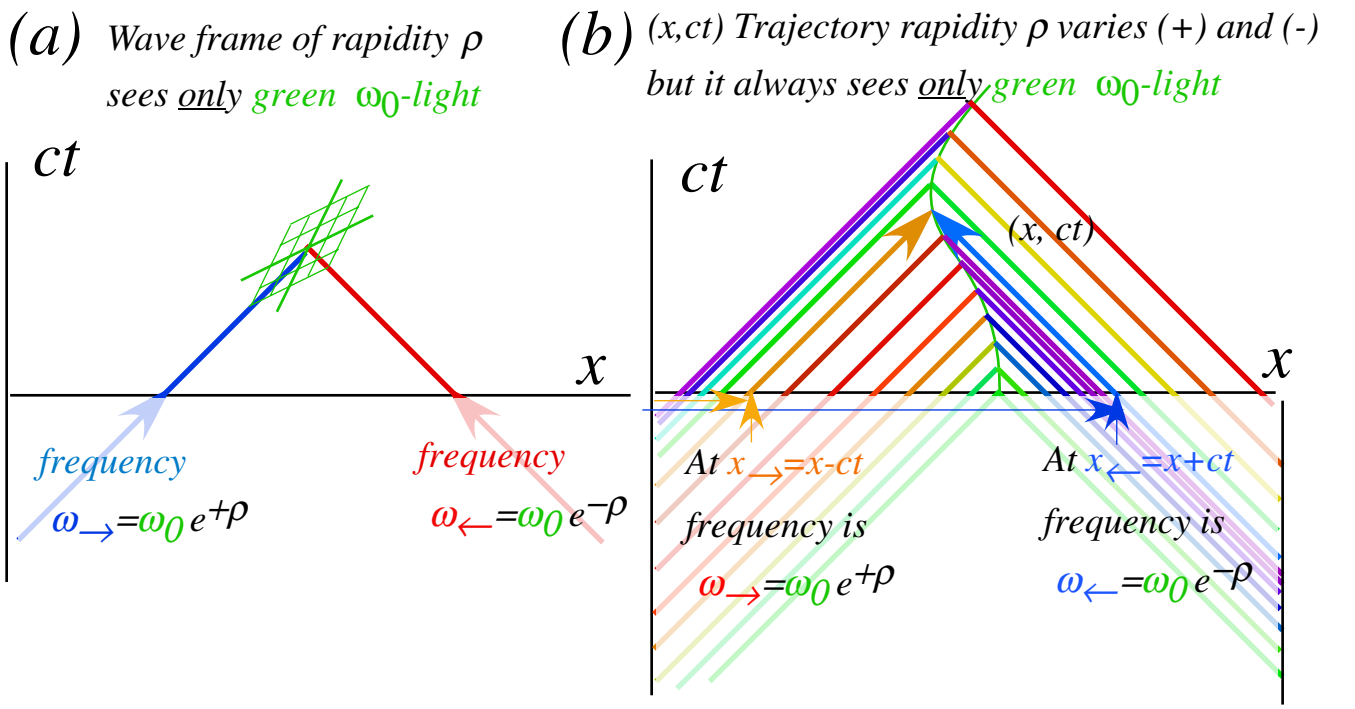

Fig. 5.5.4 Accelerating frames by laser Doppler. (a) Single laser pair. (b) Laser pairs "paint" trajectory.

The simplest choices for a rapidity schedule are *case(a)* $\rho=\rho_0$ (constant) or *case(b)* $\rho=g\tau/c$ (linear). The constant *case(a)* gives a straight line trajectory and the usual Minkowski grid in Fig. 5.5.5(a) below. The linear *case(b)* gives the hyperbolic trajectory in Fig. 5.5.5(b). This agrees with (5.5.8) in Sec. (a).

$$x = c\int \sinh\rho_0 \; d\tau = c\tau\sinh\rho_0 \qquad (5.5.16a)$$

$$x = c\int \sinh\left(\frac{g\tau}{c}\right) d\tau = \frac{c^2}{g}\cosh\left(\frac{g\tau}{c}\right) \qquad (5.5.16b)$$

$$ct = c\int \cosh\rho_0 \; d\tau = c\tau\cosh\rho_0 \qquad (5.5.17a)$$

$$ct = c\int \cosh\left(\frac{g\tau}{c}\right) d\tau = \frac{c^2}{g}\sinh\left(\frac{g\tau}{c}\right) \qquad (5.5.17b)$$

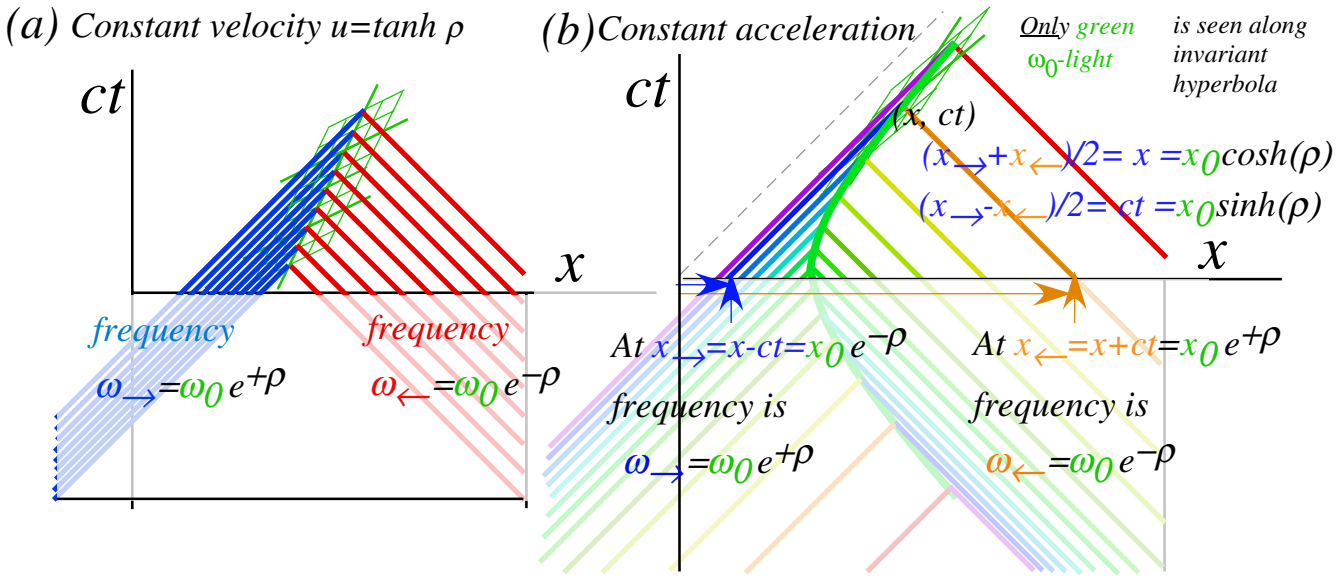

Fig. 5.5.5 Wave paths. (b) Constant velocity and frequency (b) Constant acceleration by exponential chirp.

Describing accelerated frames by CW laser waves leads to a simpler derivation of a trajectory (5.5.16b) than the classical approach that gave (5.5.8) and does so without introducing a massive particle. However, mass-like invariants are hiding in this CW derivation as are the PW rays shown in Fig. 5.5.3.

If the color-varying CW laser beams come from far right and left hand sources as in Fig. 5.5.5(b) they cover the spacetime region as shown in Fig. 5.5.6(a) and generate a curved spacetime manifold of nested constant-acceleration paths as shown in Fig. 5.5.6(b). Among these hyperbolas are the paths of the ship and saucer trailer of Fig. 5.5.3. Fig. 5.5.6(b) is a whole manifold of Newton's invariants.

Atoms (or ships), following the hyperbolic trajectory in Fig. 5.5.5(b), see an invariant green frequency ω'_0 as they run head-on into an ever more red laser beams and run away from ever more blue ones. Each hyperbolic path of Fig. 5.5.6(b) experiences some *single* invariant color. As shown in Fig. 5.5.6(a), each path crosses a variety of red and blue beams but Doppler shifts them all to one fixed hue.

Each path's invariant color is that of whichever laser beams cross the x-axis where that path starts out at $t=0$. The saucer-trailer starts out at the intersection of two blue-green beams. Thereafter, the saucer-trailer sees only the same blue-green color during its trip up its hyperbola just as the ship always lives in the same green light it saw starting further out along the lab x-axis.

Besides invariant frequency $\omega_0=\omega'_0$ for a path starting at lab position x_0 when $t=0$, each path has other constants of motion such as *radius* $x_0=\ell=x'_0$ to origin. The distance between any two paths such as ship-to-saucer-trailer separation $\ell_{-1}-\ell_0$ is *rigid*. By (5.5.12), (5.5.17b) and (5.5.16b), products of frequency and radius *are equal to each other for all paths* in Fig. 5.5.6. The constant P sets the plot scale.

$$\ell_{-2}\,\omega_{-2}=\ell_{-1}\,\omega_{-1}=\ell_0\,\omega_0=\ell_1\,\omega_1=\ell_2\,\omega_2=P \quad (5.5.18a) \qquad c^2/g_n=\ell_n=\sqrt{x_n^2-c^2t_n^2} \quad (5.5.18b)$$

Invariant frequency $\omega=P/\ell$ at radius ℓ must go to zero at large ℓ and approach infinity near origin. Origin in Fig. 5.5.6 is a remarkable singularity, as we'll see. All accelerated frames have singularities. Perhaps, we are a little *too* familiar with the singularity of a rotating frame: its *center of rotation*.

The center of spacetime "rotation" in Fig. 5.5.6 is certainly less familiar. It's an *event horizon*. You cannot communicate with the ship, saucer-trailer, or any of their friends after the *45°* line through origin (or to the left of it). As long as they continue to accelerate they will outrun your messages! (However, their frame's continued acceleration depends on your left lab laser chirping out an infinite amount of energy *before* the $t=0$ singularity and on having an infinite number of low-ν lasers off to the right.)

Other physical constants of motion for Fig. 5.5.6 are related to the invariant frequency and radius ℓ of each path and have singular behavior, too. One is acceleration g, which by (5.5.16b) blows up at $\ell=0$.

$$g=c^2/\ell=\omega\,c^2/P \quad (5.5.19)$$

An important invariant is the rate for "aging" or proper time evolution. (This was called proper frequency μ in (5.1.5).) Judging a μ or ω requires *frequency standards* such as an Argon atom that rings for green frequency ω_0 or a Krypton atom that rings for a (very) blue frequency $\omega_{-2}=2\omega_0$. Suppose the ship uses Argon to measure time by the green light it's seeing while a saucer-trailer at $x_{-2}=x_0/2$ uses Krypton to measure time by its local blue-light standard. Then on each *NOW* line between them in Fig. 5.5.6, the ship has counted the same number of green-standard ticks as the trailer has counted blue-standard ticks.

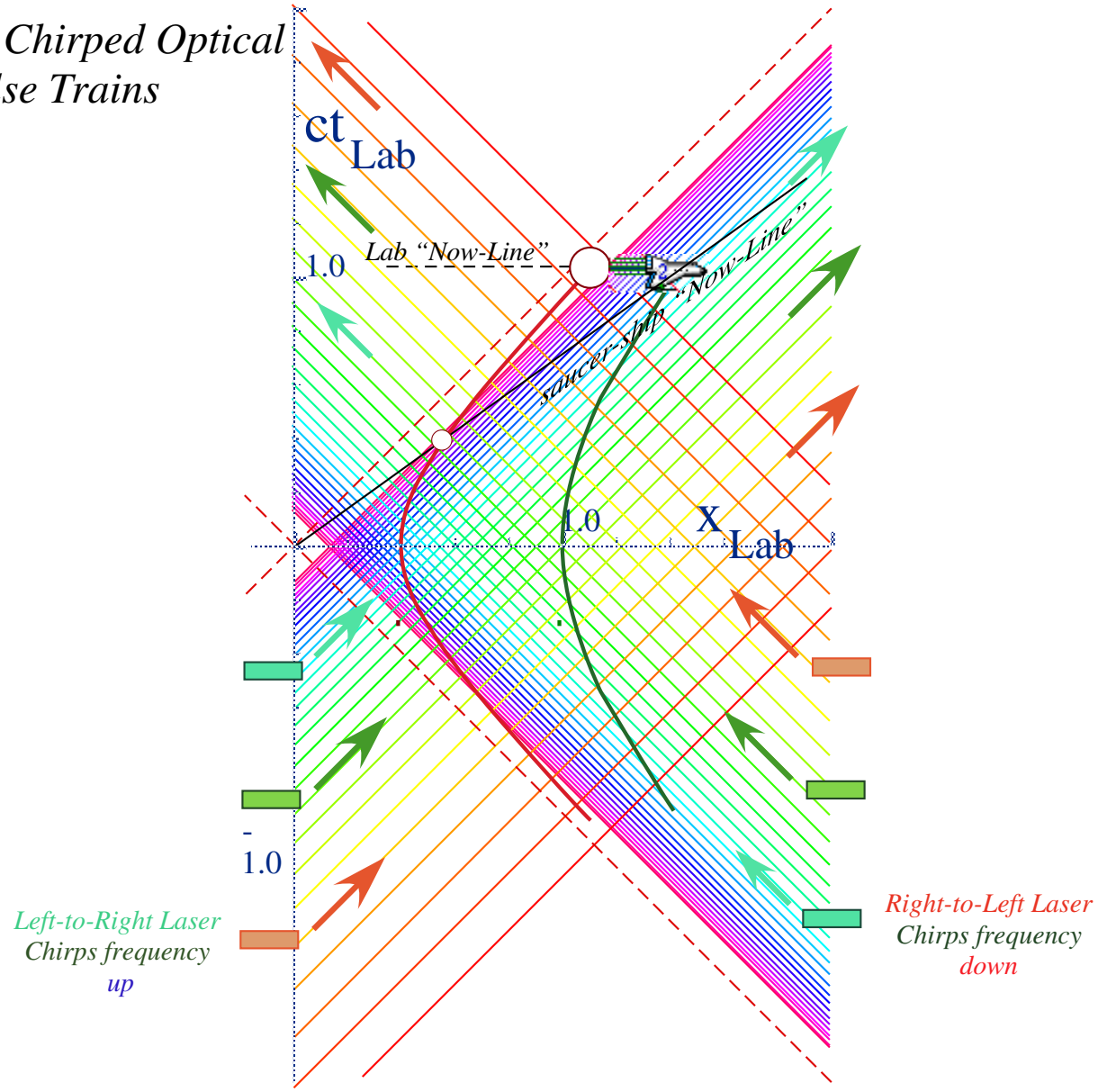

Fig. 5.5.6 Constant-acceleration spacetime (a) Pair(s) of lasers make grid for accelerating paths.

Fig. 5.5.6(b) shows that idea of *NOW* does not imply equal *proper time*. The ship's *NOW* of *10* green ticks includes a trailer who has also seen 10 ticks, just as we noticed in the earlier Fig. 5.5.3 based on pulse waves or in Fig. 5.5.6(a). But that trailer uses blue ticks, and two blue ticks equals one green tick. So the trailer has only "lived" 5 green ticks while the ship has "lived" 20 blue ticks yet they're both on the same *NOW* line. Some *NOW!* Clearly a single frequency standard is needed to properly gauge proper time.

A ship and trailer bouncing the same light wave in a rigid tube would notice it is blue shifted at the bottom but red-shifted (green here) at the high end. A similar effect is present in the equivalent constant gravitational field and is called the *gravitational red (blue) shift*. As long as the constant acceleration *g* of this system persists, its occupants see a fixed blue-to-red "rainbow" color distribution up an optical tube as in Fig. 5.5.6(b), yet, the entire tube is always (*NOW)* going the same speed relative to the lab!

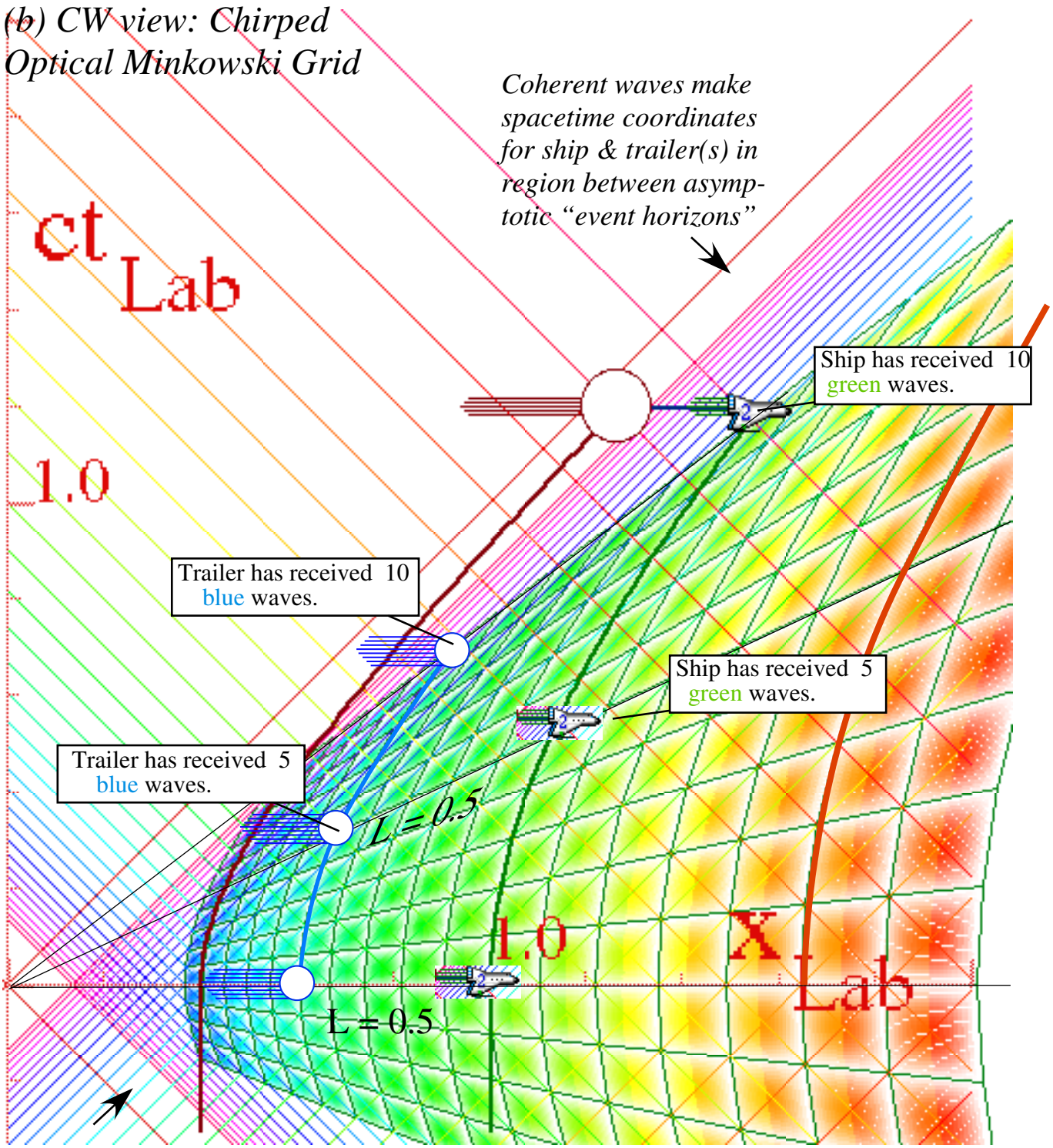

Fig. 5.5.6 Contd. (b) Interfering pair(s) of CW lasers make curved Minkowski grid for accelerating paths.

Fig. 5.5.6(b) shows hyperbolic-polar coordinates (ℓ,ρ) where (5.5.16b) gives rapidity "angle" $\rho = g\tau/c$ to accompany the hyperbolic "radius" ℓ. So proper time τ is a hyperbolic "arc-length" as Fig. 5.5.6 suggests.

$$\rho = \frac{g\,\tau}{c} = \frac{\omega\, c\tau}{P} = \frac{c\tau}{\ell} \qquad (5.5.20a) \qquad\qquad c\tau = \ell\,\rho \qquad (5.5.20b)$$

Per-spacetime diamond geometry

It is remarkable that proper time τ-evolution or "aging" is in direct proportion to one's hyperbolic radius or distance "up-field" from the singular origin. Spacetime is mirrored in per-spacetime as described in Sec. 4.2. Spacetime "particle" path vectors $\mathbf{X}=(x,ct)$ match per-spacetime-vectors $\mathbf{K}=(ck,\omega)$ that define local energy-momentum grids according to the baseball diamond wave geometry of Fig. 5.1.1.

$$\mathrm{X}_{particle}: \begin{matrix} x_p = \ell \cosh\rho \\ ct_p = \ell \sinh\rho \end{matrix} \quad (5.5.21a) \qquad \mathrm{K}_{group}: \begin{matrix} \omega_g = \omega_0 \sinh\rho \\ ck_g = \omega_0 \cosh\rho \end{matrix} \quad (5.5.21b) \qquad \mathrm{K}_{phase}: \begin{matrix} \omega_p = \omega_0 \cosh\rho \\ ck_p = \omega_0 \sinh\rho \end{matrix} \quad (5.5.21c)$$

This geometry is sketched in Fig. 5.5.7 for two different speeds or rapidity values *u/c=1/5* and *3/5* using laser ray lines excerpted from Fig. 5.5.6. The geometric growth of wavelength for increasing radius in spacetime is shown by a series of diamonds made by echoing rays off each *NOW* line of fixed rapidity. A similar diagram in per-spacetime would mirror a growth in wave*vector* or frequency, that is, the inverse of Fig. 5.5.7 as in (5.5.18). Having each echo give a constant $\delta\lambda/\delta\ell$ yields an exponential chirp (5.5.12).

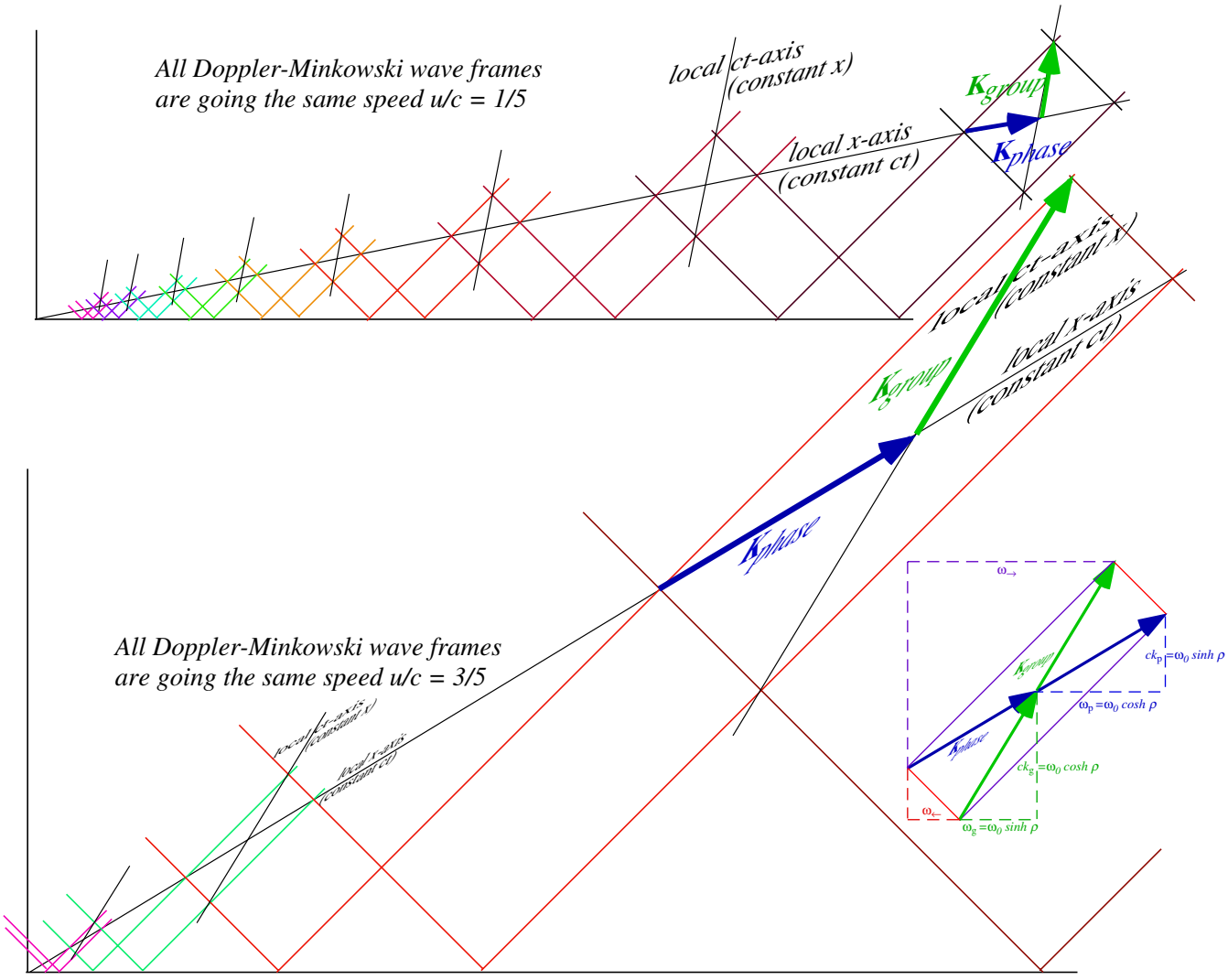

Fig. 5.5.7 Geometric growth of PW ray spacing or CW wavelength or wave vectors.

Acceleration by Compton scattering

The basic parameters of an elementary Compton scattering process in Fig. 5.5.8(a) are sketched in a right hand inset. The *IN* parameters are a fixed mass M_0, or wave proper frequency $\mu_0 = M_0c^2/\hbar$ with zero rapidity $(\rho_0=0)$ and a colliding photon frequency ω_1 or energy $E_\gamma(initial)=\hbar\omega_1$. The *OUT* parameters are a Compton scattered photon frequency ω_2 or energy $E_2(final)=\hbar\omega_2$ and the final velocity u_2 of mass M_0 or else its final rapidity ρ_2 by the usual definition $u_2=\tanh\rho_2$. Geometry helps relate the parameters.

The small μ_0-diamond is stretched by the *IN* photon ω_1 vector $\mathbf{K}_{\rightarrow}(\omega_1)_{intial}$ going from the 2nd-base point μ_0 to point *I* on the 1st-2nd baseline of a larger μ_2-diamond. By emitting an *OUT* photon with vector $\mathbf{K}_{\leftarrow}(\omega_2)_{final}$ going from point *F* to point *I*, the mass returns to its μ_0-hyperbola. But it's boosted to a final rapidity ρ_2, as its $\mu_0/\sqrt{2}$-by-$\mu_0/\sqrt{2}$ diamond shifts to the narrow $\mu_0 e^{(\rho_2)}/\sqrt{2}$-by-$\mu_0 e^{(-\rho_2)}/\sqrt{2}$ rectangle of the same area. Its length $\mu_0 e^{(\rho_2)}/\sqrt{2}$ equals $\mu_2/\sqrt{2}$ in Fig. 5.5.8(a).

$$\mu_2 = \mu_0\, e^{(+\rho_2)} \quad , \qquad \text{or,} \qquad \rho_2 = \ln\,(\mu_2 / \mu_0) \tag{5.5.22}$$

The diagonal length $\sqrt{2}\omega_1$ of the *IN* photon vector $\mathbf{K}_{\rightarrow}(\omega_1)_{intial}$ is the difference between the μ_2-diamond baseline $\mu_2/\sqrt{2}$ (or length $\mu_0 e^{(+\rho_2)}/\sqrt{2}$ of the rectangle) and $\mu_0/\sqrt{2}$. This gives ω_1 in terms of μ_0 and ρ_2.

$$2\omega_1 = \mu_2 - \mu_0 = \mu_0 e^{(+\rho_2)} - \mu_0 \tag{5.5.23}$$

The diagonal length $\sqrt{2}\omega_2$ of the *OUT* photon vector $\mathbf{K}_{\leftarrow}(\omega_2)_{final}$ is the difference between the μ_0-diamond baseline $\mu_0/\sqrt{2}$ and the width $\mu_0 e^{(-\rho_2)}/\sqrt{2}$ of the rectangle. This gives ω_2 in terms of μ_0 and ρ_2.

$$2\omega_2 = \mu_0 - \mu_0 e^{(-\rho_2)} = 2\omega_1\, e^{(-\rho_2)} \tag{5.5.24}$$

Inverting (5.5.24) and taking $e^{(+\rho_2)}$ with $\mu_0 = M_0c^2/\hbar$ in (5.5.22) gives a famous Compton relation.

$$1/\omega_2 = 1/\omega_1\, e^{(+\rho_2)} = 1/\omega_1\,(\mu_2 / \mu_0) = 1/\omega_1\,((2\omega_1 + \mu_0) / \mu_0) = 2/\mu_0 + 1/\omega_1 \tag{5.5.25a}$$

$$\lambda_2 = 2\pi c/\omega_2 = 4\pi c/\mu_0 + \lambda_1 = 2\lambda_{Compton} + \lambda_1\,, \quad \text{where: } \lambda_{Compton} = 2\pi\hbar/M_0c = h/M_0c \tag{5.5.25b}$$

Photon wavelength jumps by twice a *Compton wavelength h/Mc* in back-scattering from mass *M*. That represents a momentum "kick" given by the photon to mass *M*. A photon thus acts "like a particle."

Suppose the *IN* ω_1 photon excites a state of higher proper energy $\hbar\mu_1 = M_1c^2$. To do this, the μ_0 particle must have an existent μ_1–excited state and ω_1 must be tuned to satisfy its recoil equations.

$$\mu_2 = \mu_1\, e^{(+\rho_1)} = \mu_0\, e^{(+\rho_2)} \tag{5.5.26a}$$

$$\mu_1 = \mu_0\, e^{(+\rho_1)} \tag{5.5.26b}$$

$$\omega_1 = \mu_1 \sinh(\rho_1) \tag{5.5.26c}$$

The $\mathbf{K}_{\rightarrow}(\omega_1)_{intial}$ jump goes from point μ_0 to point *I* and "sticks" at intermediate recoil ρ_1 without emitting ω_2 and recoiling further to $\rho_2 = 2\rho_1$. Photo *absorption* or "gulp" of photon ω_1 is the reverse of photo *emission* "patooey" discussed earlier. Here, the required *IN* frequency ω_1 is *greater* than the gap $\Delta=\mu_1-\mu_0$ whereas the *OUT* frequency ω_1 in (5.2.22) is *less* than Δ as is ω_2 in (5.2.24) above. However, the recoil $\rho_1=\rho_2/2$ rapidity of the *IN* process equals that of the *OUT*. Each is *half* of the Compton recoil ρ_2 by (5.5.26).

Fig. 5.5.8(b) shows back-to-back Compton processes with the ρ_2–moving particle hit by a second photon of lab frequency $\omega_3 = \omega_1\, e^{(+\rho_2)}$ so Doppler-blue-shifted to appear as a ω_1–photon. The second scattering yields another ω_2 photon, but it appears as a red-shifted frequency $\omega_4 = \omega_2\, e^{(-\rho_2)}$ in the lab. Continued bombardment by geometric progression of up-chirped light gives a quantum version of constant acceleration pictured in Fig. 5.5.7 wherein the particle "feels" the same Compton kick from each chirp.

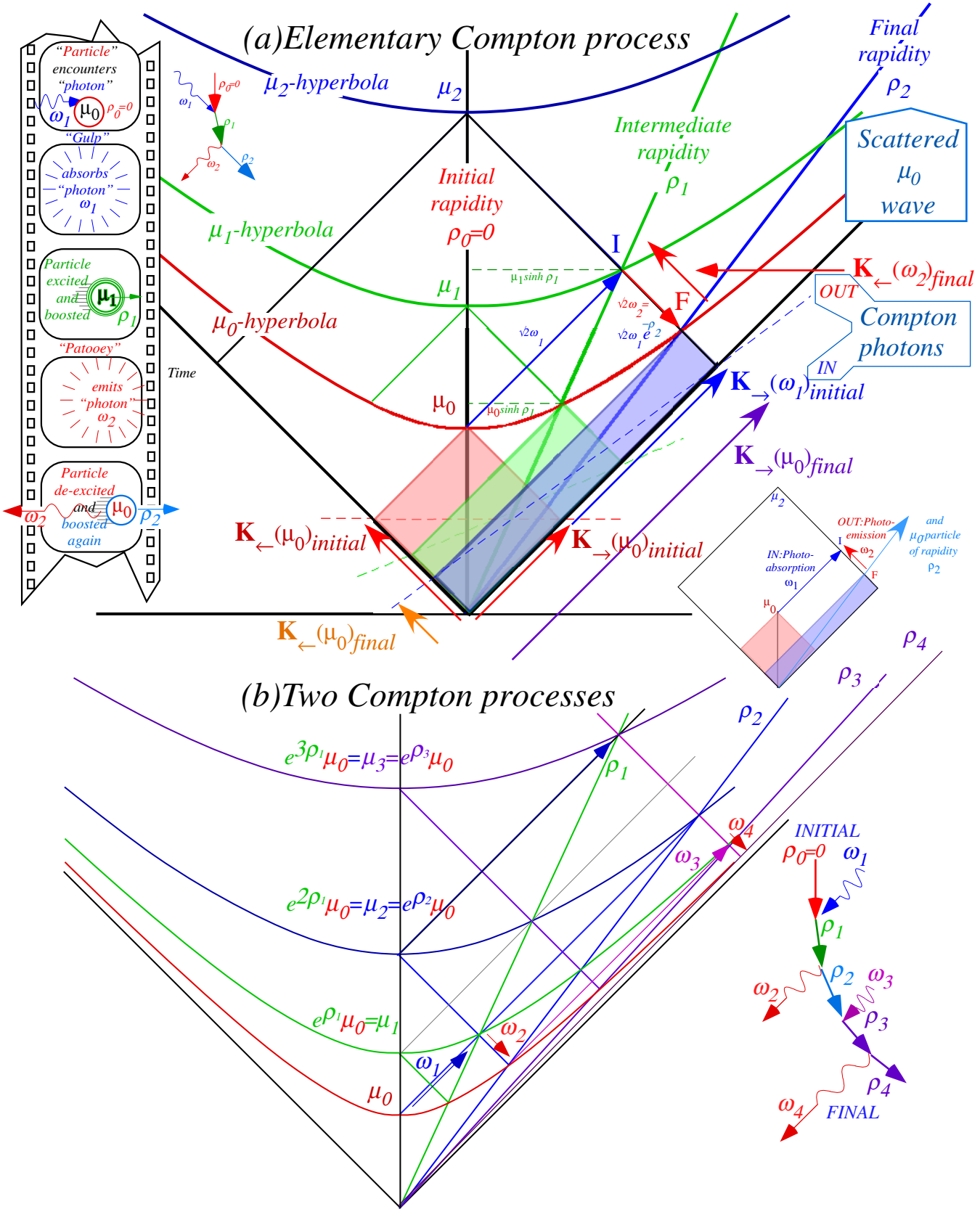

Fig. 5.5.8 Compton scattering (a) Elementary geometry. (a) Geometry of quantum acceleration

5.6 Bohr-Orbitals and Higher Energy Physics

Most of atomic, molecular, and optical physics is concerned with energy on the order of a few *electron Volts* or *eV*. One *eV* is *e*-Joules or *1.6E-19 J*, the energy acquired by an electron falling through one *Volt* of electric potential. Here we introduce atomic Bohr orbitals and some high(er) energy physics.

(a) Dirac's anti-matter

The square root in energy dispersion $E = \sqrt{[(cp)^2+(mc^2)^2]}$ should have ±signs. At least P.A.M. Dirac thought so. He is credited with recognizing the negative energy terms as the representation of *anti-matter* that follows an up-side-down hyperbolic dispersion relation. Examples involving the photon and electron are shown in Fig. 5.6.1 below. Dirac made the extraordinary suggestion that the empty space vacuum is actually a sea of electrons (and other Fermions) occupying the negative energy states in a kind of cosmic valence band. Only when we come along with energy of a little over *1MeV* do we actually see a pair creation of an electron popping out of the sea and leaving behind a "hole" or *positron*, the anti-electron. (Actually, two photons of *0.511MeV* each are needed because of symmetry and conservation requirements.)

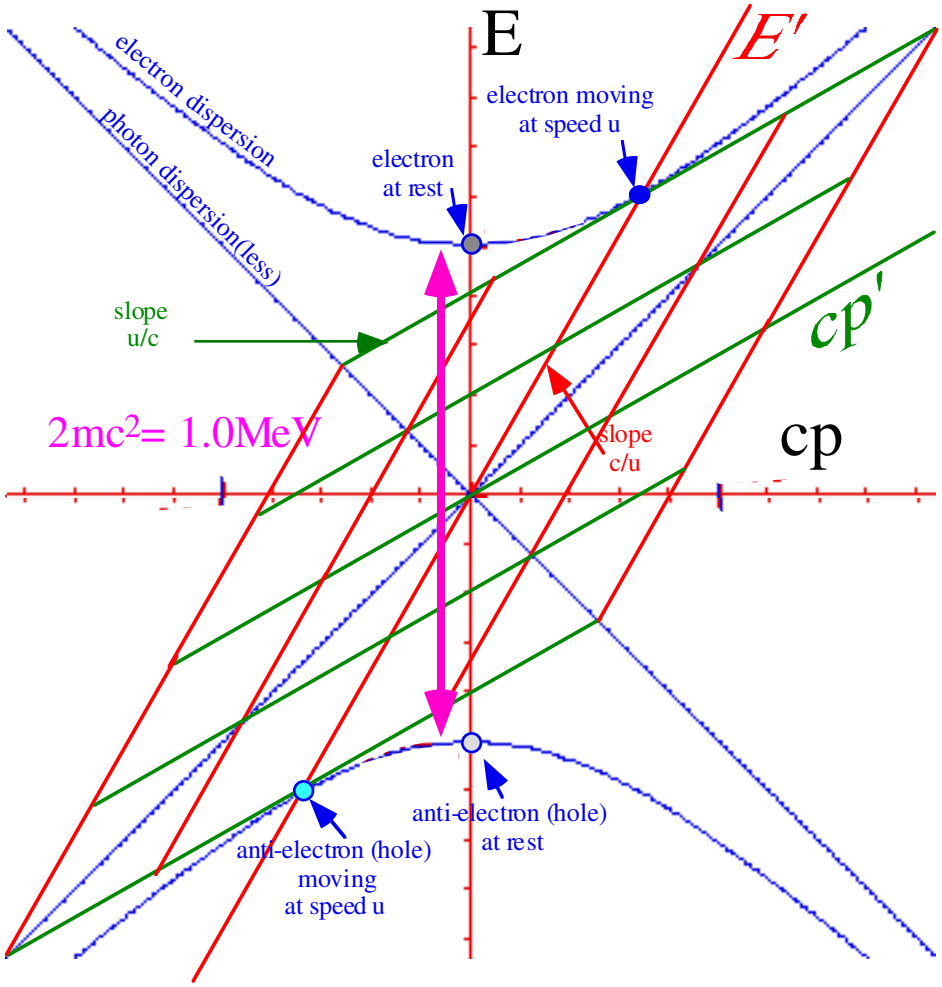

Fig.5.6.1 Relativistic dispersion relations for a photon and an electron and their anti-particles

Dirac's relativistic electron theory is wonderful but mysterious one.As we will see (much later) it shows that the electron is made of something zipping around in its "belly" with an average speed of c. If we identify this "ticking" frequency (It's called "Zwitterbegung" which sounds impressive until hearing the German translation for "trembling motion.") with a beat frequency equal to the band-gap difference $2mc^2$ between the positive and negative energy bands we get *1.5 thousand ExaHertz*.

$$\omega_{\text{zwitterbegung}} = 2\mu_\varepsilon = 2mc^2/\hbar = 1.56E21(\text{radian})Hz \qquad (5.6.1)$$

An electron has a pretty fast "ticker" and its "heartbeat" is observable!

(b) Numerology: Bohr electron radii and Compton wavelength

Since the advent of the Bohr model of the hydrogen atom, the idea of particles being composites of other particles zipping around has been used a lot in the development of quantum theory. Briefly, the Bohr model imagined an electron orbiting in a circle of radius r so that the centrifugal force just balanced the Coulomb attraction to the opposite charged proton.

$$\frac{mv^2}{r} = \frac{e^2}{4\pi\varepsilon_0 r^2} \qquad (5.6.2a)$$

This combined with the Bohr hypothesis that orbital momentum ℓ was a multiple N of $\hbar$ or

$$\ell = m\,v\,r = N\,\hbar \qquad (N = 1, 2,...) \qquad (5.6.2b)$$

gives the *atomic Bohr radius* a_0

$$r = \frac{4\pi\varepsilon_0\hbar^2}{me^2}N^2 \left(= r_{Bohr} = 5.28E-11\ m.\ = 0.528\ \text{Å for } N=1\right) \qquad (5.6.3a)$$

and quasi-relativistic electron speed of

$$\frac{v}{c} = \frac{\ell}{mrc} = \frac{1}{N}\frac{e^2}{4\pi\varepsilon_0\hbar c} \quad \left(= 7.31\text{E-}3 = \frac{1}{137.} \text{ for } N=1\right) \qquad (5.6.3b)$$

The ratio $\alpha = e^2/(4\pi\varepsilon_0\hbar c) = 1/137.036$ is called the *fine-structure constant* α. It shows up a lot in atomic physics. Dirac was concerned with working out the relativistic corrections to the energy of atoms. While a hydrogen electron goes less than 1% of the speed of light, a heavily charged atomic ion would increase (5.6.3b) in proportion to its charge and make relativistic effects large.

If we imagine that whatever Dirac said was going c inside an electron is going around in a circle of radius r at speed c and "ticking" or orbiting at the zwitterbegung frequency then

$$\omega_{\text{zwitterbegung}}\, r = c \qquad (5.6.4a)$$

or

$$r_{Dirac} = c\ /\ \omega_{\text{zwitterbegung}} = \hbar\ /2mc = 1.93\ E\text{-}13\ m. \qquad (5.6.4b)$$

Now, it needs to be said that most of the preceding calculations are what is known as *numerology*; simple estimation exercises done to get a rough order of magnitude for the size of things. Occasionally, as in the case of (5.6.3), these rough estimates hit right on, but one shouldn't expect such luck. There is no immediately obvious reason for us to expect that Dirac's "thing" is oscillating on a circle, and there was little reason for Bohr to expect the right answer by just considering circular orbits. Indeed, the lowest atomic H-orbital is a "diving" orbit of maximal unit eccentricity and zero angular momentum.

But still we ask, "How big would it be if it were a circle?" This gives some idea about the relative size of an electron in these two situations. The Dirac answer is about one-hundredth that of the Bohr radius (5.6.3a), but about one hundred times that of a nucleus (Nuclear radii are typically a few Fermi: *1 Fm = 1 Fermi = 1.0E-15 m. = 1 femto meter = 1 fm*; this is one case where a unit abbreviation is correct in lower and upper case!) Being more precise, and this may be a silly numerological exercise, it is interesting to note that the ratio of the Dirac radius to the Bohr radius is

$$\frac{r_{Dirac}}{r_{Bohr}} = \frac{\hbar\ /2mc}{4\pi\varepsilon_0\hbar^2\ /\ me^2} = \frac{1}{2}\cdot\frac{e^2}{4\pi\varepsilon_0\hbar c} = \frac{1}{2}\cdot\frac{1}{137.} = \frac{\alpha}{2} \qquad (5.6.5)$$

This is exactly one-half the fine-structure constant $\alpha=1/137$.

The preceding quantum numerology can be compared to some older classical numerology. The *classical radius of the electron* is defined as the radius an electron would have to have in order to have its electrostatic energy $e^2/(4\pi e_0\, r_{classical})$ equal to its rest energy mc^2. (Remember, this is numerology, not physics. Electrostatic energy depends sensitively on charge distribution. Nevertheless, the classical radius appears more legitimately in the theory of Rayleigh scattering.) Here is the classical radius.

$$e^2/(4\pi e_0\, r_{classical}) = mc^2 \quad \text{or} \quad r_{classical} = e^2/(4\pi e_0\, mc^2) = 2.8\text{E-}15 \text{ m.} \qquad (5.6.6)$$

Now this is about the size of a nucleus and about a hundred times smaller than the "quantum" electron Dirac-radius estimated in (5.6.4b). In fact it is exactly another fine-structure ratio to r_{Bohr}.

$$\frac{r_{Classical}}{r_{Bohr}} = \frac{e^2\ /\ 4\pi\varepsilon_0 mc^2}{4\pi\varepsilon_0\hbar^2\ /\ me^2} = \left(\frac{e^2}{4\pi\varepsilon_0\hbar c}\right)^2 = \left(\frac{1}{137.}\right)^2 \qquad (5.6.7a)$$

It happens that the "quantum electron diameter", that is ($2r_{Dirac}$), relates to a legitimate experimental constant; $2r_{Dirac}$ happens to be the *Compton (angular) wavelength* ($\lambda\!\!\!^{-}_{Compton}$)

$$2r_{Dirac} = \lambda\!\!\!^{-}_{\text{Compton}} = \hbar/mc = 3.86\ E\text{-}13\ m. \qquad (5.6.7b)$$

The "straight" *Compton wavelength* $\lambda_{Compton}$

$$2\pi\cdot 2r_{Dirac} = \lambda_{\text{Compton}} = h/mc = 2.43\ E\text{-}12\ m. \qquad (5.6.7c)$$

is the wave length of the γ-radiation needed to excite pair-creation of electron and anti-electron from the vacuum. (Recall we mentioned that this is a two-photon process.) The quantity $2\lambda_{\text{Compton}}$ is the change in wavelength that a photon suffers in a head-on collision with an electron. λ_{Compton} is less than 1% of a typical X-ray wavelength but it is 100% of the wavelength of the photons needed to create an electron-positron pair.

As a final numerological exercise, we derive the angular momentum $\ell = m\,v\,r$ of the fictitious "zwitterbegung" orbit inside the electron. With $v=c$ and r = r_{Dirac} the following is obtained.

$$\ell = m\,c\ r_{Dirac} = m\,c\,\hbar\ /\ 2mc$$
$$= \hbar\ /\ 2$$

We did mention that numerology occasionally gives the correct answer, in this case, the spin angular momentum of an electron! We won't give this equation a number since it is not (yet) legitimate physics. As we said, numerology is just that, estimating some numbers and their orders of magnitude, and that's all we should expect at first.

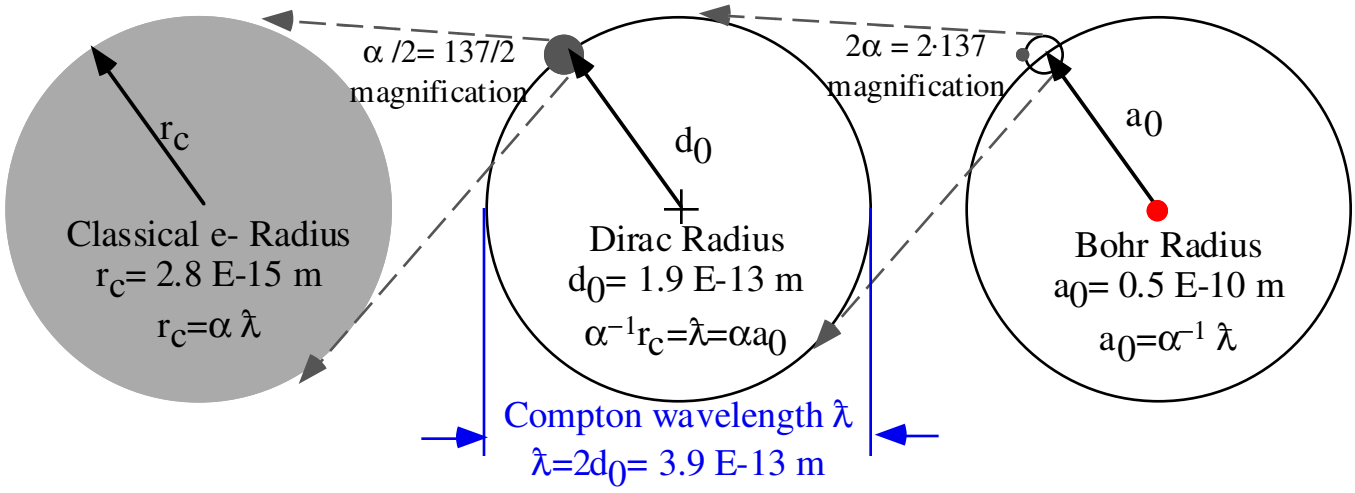

Fig.5.6.2 Various electron radii and their relative sizes related by fine-structure constant α = 1/137.

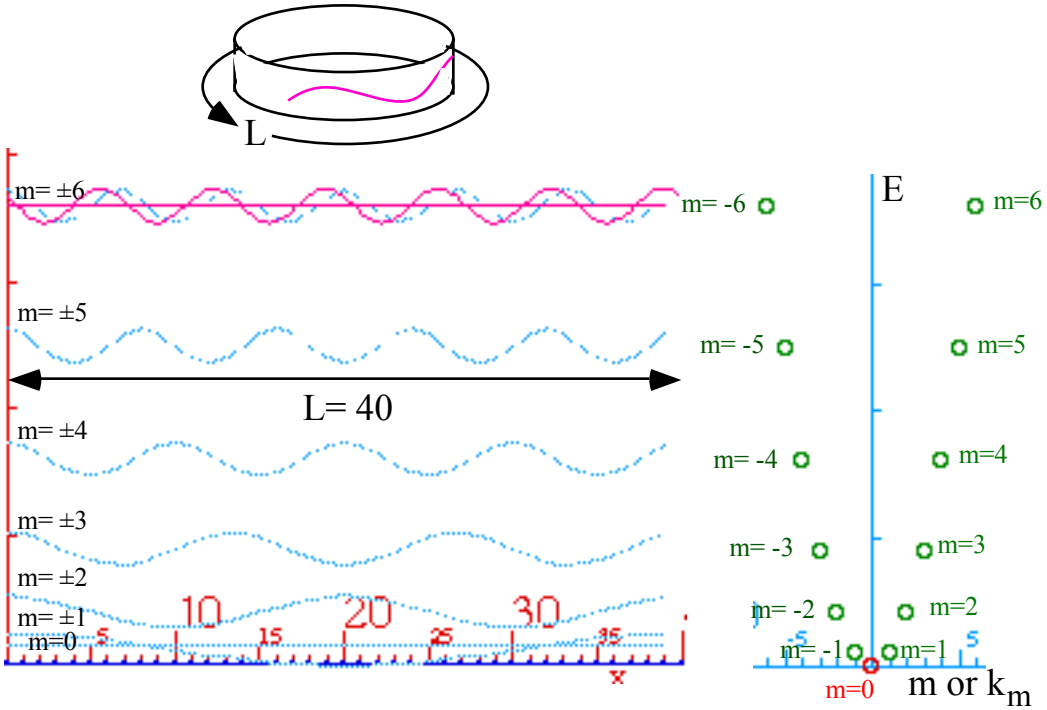

Fig. 5.6.3 Sketches of Bohr waves confined to 1-D L-interval and quantum energies (for m=0 to 6).

(c) Bohr matter-wave PW revivals: When μ-waves party!

Bohr's simplest model is called the *quantum rotor* and consists of a μ-wave wrapped around a ring of fixed radius *r*. The Bohr atomic model contains rings having Bohr radii r_N (5.6.3) for all radial quantum numbers $N=1,2,3\ldots\infty$. Here we will study just one such ring with large *N* and circumference $L=L_N=2\pi r_N$ as sketched at the top of Fig. 5.6.3. As sketched in the lower part of Fig. 3.6.3, the waves on this ring must have an integral number *m* of wavelengths within its circumference *L*.

$$m\,\lambda_m = L \quad \text{or:} \quad k_m = 2\pi/\lambda_m = m\,2\pi/L = m/r \;(m=0,\ 1,\ \pm2,\ \pm3,\ldots) \tag{5.6.8}$$

This *m* is called the *magnetic* or *angular momentum quantum number* and quantizes the amount of *angular momentum* circulating the ring. Quantization is necessary to have phase matching at each 2π turn.

As we will see, even this simple quantum rotor model is capable of extraordinary wave dynamics. Wrapping waves onto a ring, along with their spacetime or per-spacetime, introduces some big problems, only a few of which we can deal with here. While this ring wave is on a one-dimensional path, it is really a wave in two or three-dimensional space and time, the subject of the following Chapter 6.

Bohr-Schrodinger dispersion and group velocity

Here we use the Bohr-Schrodinger approximation to the dispersion function in (5.2.8).

$$E_m = \hbar\omega_m = \frac{p_m^2}{2M} = \frac{\hbar^2 k_m^2}{2M} \tag{5.6.9}$$

The quantized k_m values in (5.6.8) gives quantized energy or frequency values plotted in Fig. 5.6.3.

$$\omega_m = \frac{\hbar k_m^2}{2M} = \left(\frac{\hbar(2\pi)^2}{2ML^2}\right)m^2 = \left(\frac{\hbar}{2Mr^2}\right)m^2 \equiv \omega_1 m^2 \tag{5.6.10a}$$

From this dispersion we get group velocity values by (4.7.8), one for each line between quantum points in Fig. 5.6.4. With $L=2\pi r$ and $k_m=m/r$ it gives $V_g(m,n)$ as multiples of *fundamental velocity* $V_1=\omega_1 r$.

$$V_{group}(m,n) = \frac{\omega_m-\omega_n}{k_m-k_n} = \frac{h}{2Mr}\left(\frac{m^2-n^2}{m-n}\right) = \omega_1 r(m+n) \tag{5.6.10b}$$

V_1 is the lowest quantum orbit speed and ω_1 is the *fundamental transition* or lowest *beat frequency*.

$$V_1 = \omega_1 r = \left(\frac{h}{2Mr}\right) \tag{5.6.10c}$$

So, if a Bohr quantum rotor has, say, range of *m*-wave states excited from $m=0$ to $m=\pm4$, then the possible velocity values given by (5.6.10b) range from *0* to *but not including* $\pm8V_1$. Because the $m=4$ state cannot interfere with itself, the maximum slope in Fig. 5.6.4 is 7 V_1, just shy of tangent-slope derivative $d\omega/dk=8$ at $m=4$. This shows why the conventional $d\omega/dk$–formula for group velocity should not be used in most quantum mechanical applications.

In the wave business, it's generally considered "impolite" to just cut-off the wave *m*-distribution at, say, $m=\pm4$ as imagined in Fig. 5.6.4. Doing so leads unnecessary complications of "ringing" shown in Fig. 5.3.2. Better is a tapered distribution such as a Gaussian (5.3.6) that yields unwrinkled waves like Fig. 5.3.3. This will be applied to the Bohr waves below.

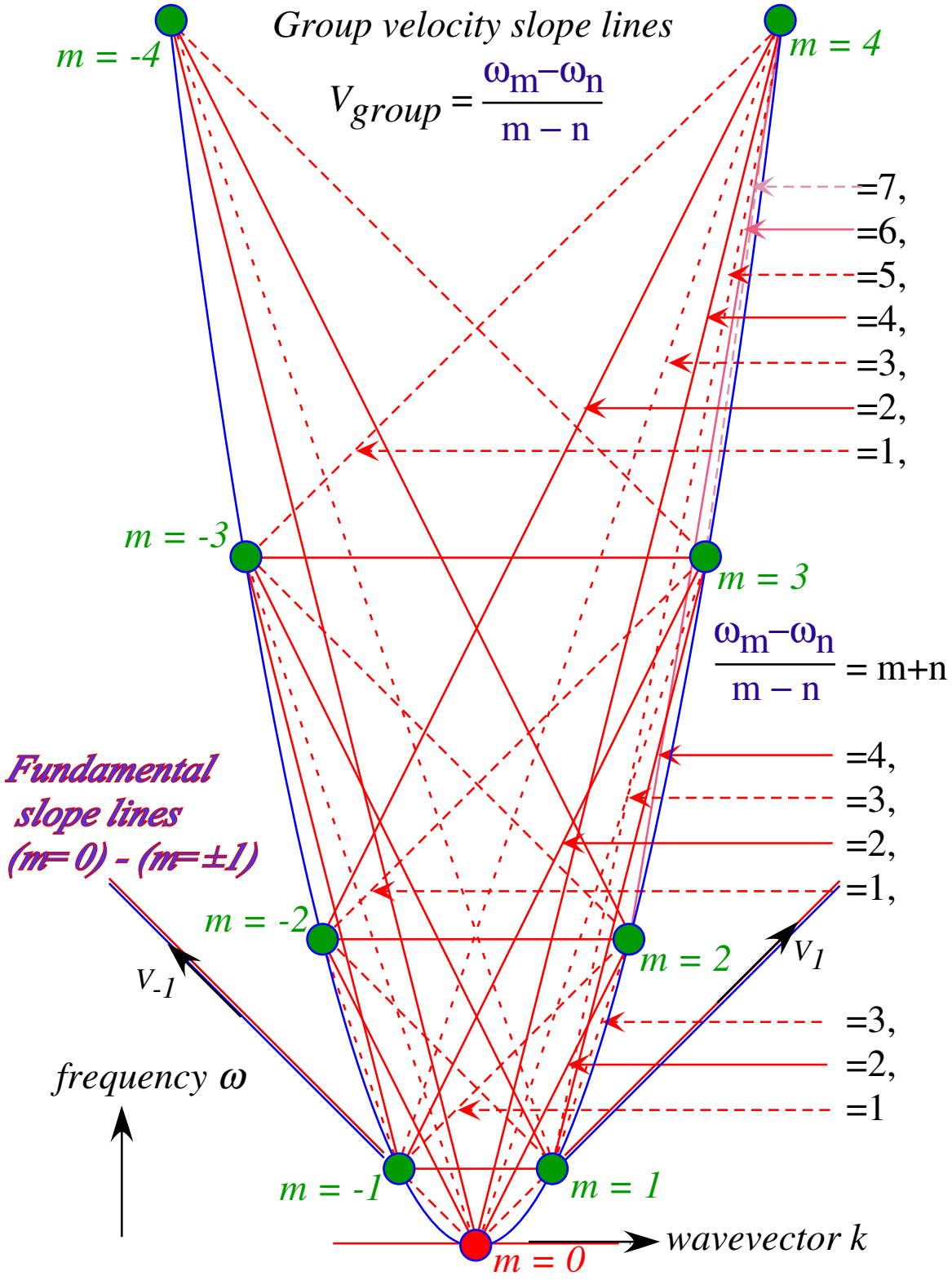

Fig. 5.6.4 Bohr per-spacetime plot and group velocity lines for combinations of m=0 to m=±4.

Bohr μ-wave quantum speed limits

Instead of $d\omega/dk$, one needs to consider a *lattice* of per-spacetime **K**-vectors such as Fig. 5.6.4 or an *array* $V_g(m,n)$ of velocity values given in (5.6.10b). Here, the $V_g(m,n)$ array given by (5.6.10d) is a simple one.

$$V_{group}(m,n)_{\le 4} = \begin{array}{c|c|cccccccccc} E_m & m/n & \cdots & -4 & -3 & -2 & -1 & 0 & 1 & 2 & 3 & 4 \\ & \cdots & & & & & & & & & & \\ 16 & -4 & & -8 & -7 & -6 & -5 & -4 & -3 & -2 & -1 & 0 \\ 9 & -3 & & -7 & -6 & -5 & -4 & -3 & -2 & -1 & 0 & 1 \\ 4 & -2 & & -6 & -5 & -4 & -3 & -2 & -1 & 0 & 1 & 2 \\ 1 & -1 & & -5 & -4 & -3 & -2 & -1 & 0 & 1 & 2 & 3 \\ 0 & 0 & & -4 & -3 & -2 & -1 & 0 & 1 & 2 & 3 & 4 \\ 1 & 1 & & -3 & -2 & -1 & 0 & 1 & 2 & 3 & 4 & 5 \\ 4 & 2 & & -2 & -1 & 0 & 1 & 2 & 3 & 4 & 5 & 6 \\ 9 & 3 & & -1 & 0 & 1 & 2 & 3 & 4 & 5 & 6 & 7 \\ 16 & 4 & & 0 & 1 & 2 & 3 & 4 & 5 & 6 & 7 & 8 \end{array} \qquad (5.6.10d)$$

Even so, the array gives a clear picture of the number of each type of *(m,n)-beat* or *(m-n)-transition* giving rise to equal group velocity $(m+n)\ V_1$. Apart from the zero velocity entries (standing waves) it is clear that the greatest number $2N$ of contributors are for *fundamental* $(m+n)=\pm 1$ transitions giving group velocity $V_{\pm 1} = \pm\omega_1 r$ of (5.6.10c). Next in line is double-group-speed $V_2 = 2\omega_1 r$, then triple-group-speed $V_3 = 3\omega_1 r$, and so on, each with one less contributing *(m-n)*-pair, up to $V_{2N} = 2N\omega_1 r$, the *quantum speed limit* for a $m=(-N^{th})$-to-$(+N^{th})$ harmonic wave combination. But, Gaussian distributions "spill over" their N-limits.

An $(N=4)$-Gaussian distribution of Bohr-μ-wave harmonics is plotted in Fig. 5.6.5. Waves up to the 4^{th} or 5^{th} harmonic dominate while 6^{th} and 7^{th} m-values lie in the distribution tail ends. Compare the Bohr μ-wave to an optical pulse train (OPT) γ-wave having a similar Gaussian in Fig. 5.3.3(b).

What a difference! While the spacetime picture of the γ-wave OPT makes a single "baseball diamond" path, the μ-wave harmonics plotted in Fig. 5.6.5 show many overlapping diamonds. The m^{th}-group speed V_m is m-times the fundamental V_1, so the m^{th}-harmonic diamond takes a fraction $(1/m)$ of the fundamental diamond time period τ_1 and then repeats m times in that period. The result is more than N overlapping diamonds made of wave nodes or anti-nodes, most squashed by some fraction $1/m>1/N$.

Follow the zeros!

If there is one rule for learning wave theory, it is, *"Follow the zeros!"* Zeros of ReΨ are spacetime coordinate grids in Chapter 4, beginning with Fig. 4.2.11 and Fig. 4.3.3. Here the zeros of probability or group wave magnitude |Ψ| show prominently in Fig. 5.6.5. The |Ψ|-zeros (white-regions) stand out more clearly than the fainter and more broken diamonds that emanate from the original Gaussian pulse wave at the bottom center of the Fig. 5.6.5. In contrast, just one centered diamond is clearly visible in the γ-wave OPT plots of Fig. 5.3.2 and Fig. 5.3.3 while near-zero gallop-scallops fill the rest of those figures.

A |Ψ|-plot like Fig. 5.6.5 shows mainly group-wave |Ψ|-zeros or *nodes*. Phase wave (ReΨ)-zeros are more complicated and require some more theory and technology that will be introduced in Unit 3.

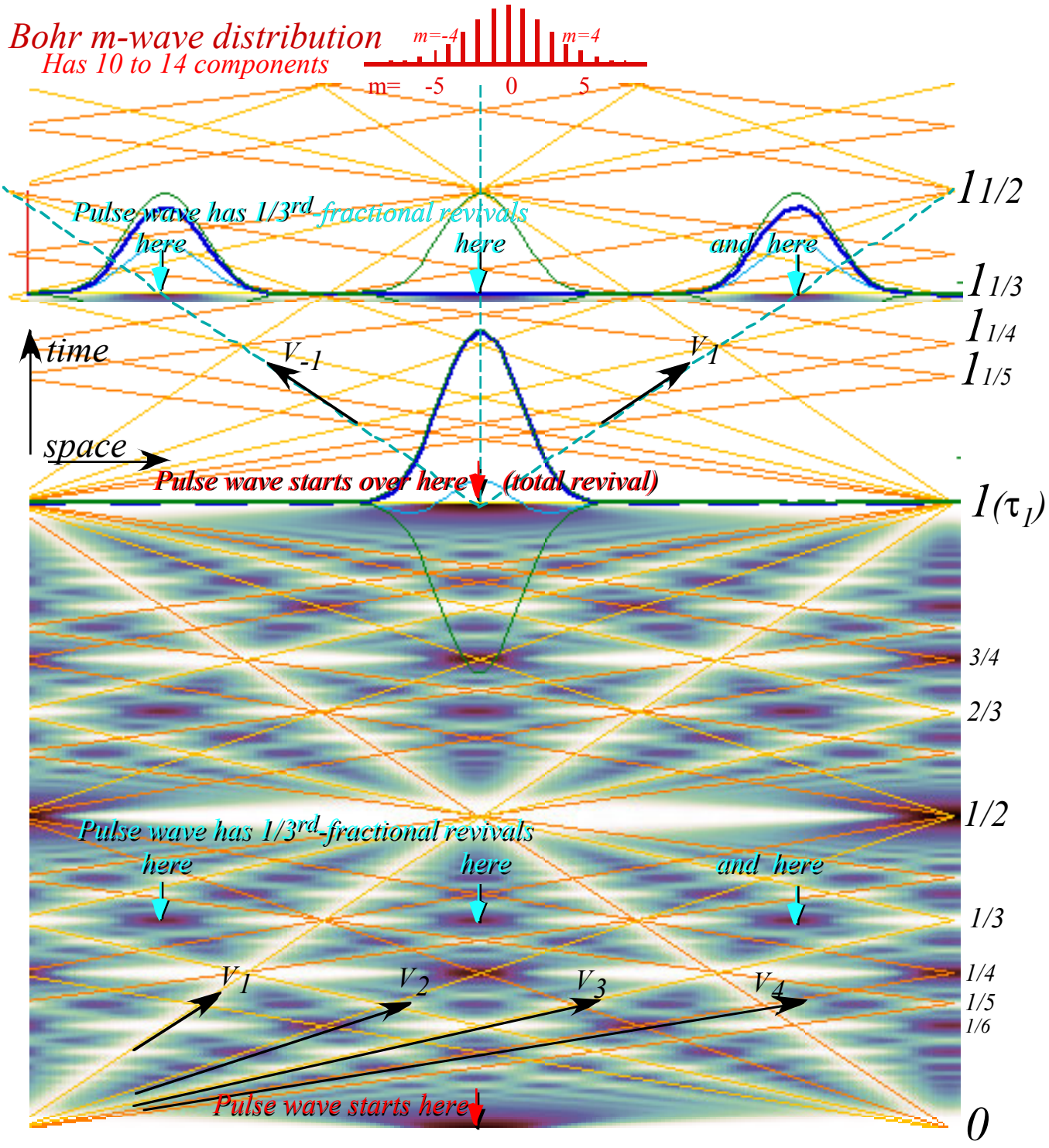

Fig. 5.6.5 (N=4)-Gaussian Bohr μ-wave pulse in spacetime |Ψ|-plot shows multiple group velocities.

Nodes tell a primary story of quantum wave interference. Instead of first asking the question of why and where a physical system or "particle" *IS*, we should first ask a more Zen-like question, that is, "*Where is it NOT!* As Holmes remarked, it was the dogs that *didn't* bark who first revealed the truth.

One reason for such a nihilistic philosophy is a simple emerging fact. There *ARE NO* Newtonian "particles" or corpuscles, only waves that often masquerade as particles. More to the point, |Ψ|-zeros are robust indicators of interference because, by being completely zero, they are not as sensitive as their still-breathing neighbors who, so being, are tossed up and down with each passing wavelet. In other words, if you're already dead, who can hurt you anymore? Nodes (|Ψ|-zeros) cut clear and contiguous paths in the spacetime plots while the anti-nodes (|Ψ|-peaks) leave fuzzy and broken paths.

Bohr μ-wave pulse train dephasing and revival

The initial pulse wave at the bottom of Fig. 5.6.5 starts out with an "expansion" phase before its quantum diamond paths can be seen emerging sometime between $1/12^{th}$ or $1/14^{th}$ of the fundamental period τ_1. That is just enough time for the fastest components, who travel above the quantum speed limit of $2NV_1 = 8V_1$, to make one trip around the ring. The $m=\pm5$, $m=\pm6$, and $m=\pm7$ harmonics are in the "tails" of the $(N=4)$-Gaussian distribution plotted at the top of Fig. 5.6.5. A $(6+7)$-combination has group velocity $13\ V_1$ and exceeds the quantum speed limit of $5V_1$. That's a quantum *50 mph* over the speed limit. Off to jail!

When these "outlaws" first run into each other coming around the ring, they make the very finest gallop-scallops near the bottom of Fig. 5.6.5. These scallops are part of the very finest group velocity zero-lines emanating from the initial antipodal node (at the point on the Bohr ring opposite to the initial anti-node), that is, from either side of the *x*-axis in Fig. 5.6.5. The pulse wave then begins to *dephase* as a dozen or so velocity components spread out while literally cutting the pulse into ribbons of nodes!

However, after a whole period τ_1, the whole bloody mess reassembles or *revives* into a perfect reconstruction of the original pulse as plotted just above the center of Fig. 5.6.5. The concept of *rephasing* or *revival* was pointed out relatively recently by Joseph E. Eberly in a much more complicated system, the Jaynes-Cummings quantum electrodynamic model of an atom in a cavity.

For the Bohr model plotted in Fig. 5.6.5, a *total revival* is possible after each period τ_1, because all Bohr frequencies ω_m (5.6.10a) are an integral multiple m^2 of the fundamental transition frequency ω_1. Also, there are *(1/m)-fractional revivals* in which the initial pulse appears to be "cloned" into *m* or *m/2* copies that pop-up at uniform intervals of space and time between that of the main revivals. Their node or anti-node spacing depends on intersections of the group-velocity diamonds as do *(1/3)*-fractional revivals indicated in Fig. 5.6.5. One could argue that the *(1/3)*-clones in the upper part of Fig. 5.6.5 are due to the "particle" traveling at V_1 from its initial pulse origin. However, such a Newtonian picture is misleading. (Just look what happened to that clone on its way to the forum!)

If only the fundamental $(m=0)$-to-$(m=\pm1)$ transitions are excited, only speed V_1 is possible as in Fig. 5.6.6 . Now the resulting spacetime plot resembles a 2-component γ-wave pulse plot in Fig. 5.3.2(b) or Fig. 5.3.3(a). Again, one could argue for a "particle" going velocity $\pm V_1$ from its initial pulse origin, but here wave interference or beat makes a Newtonian theory laughable. Less laughable are the quite clearly defined "X" nodal paths having velocity $\pm V_1$ in Fig. 5.6.6. It *is* more difficult to laugh at the deceased!

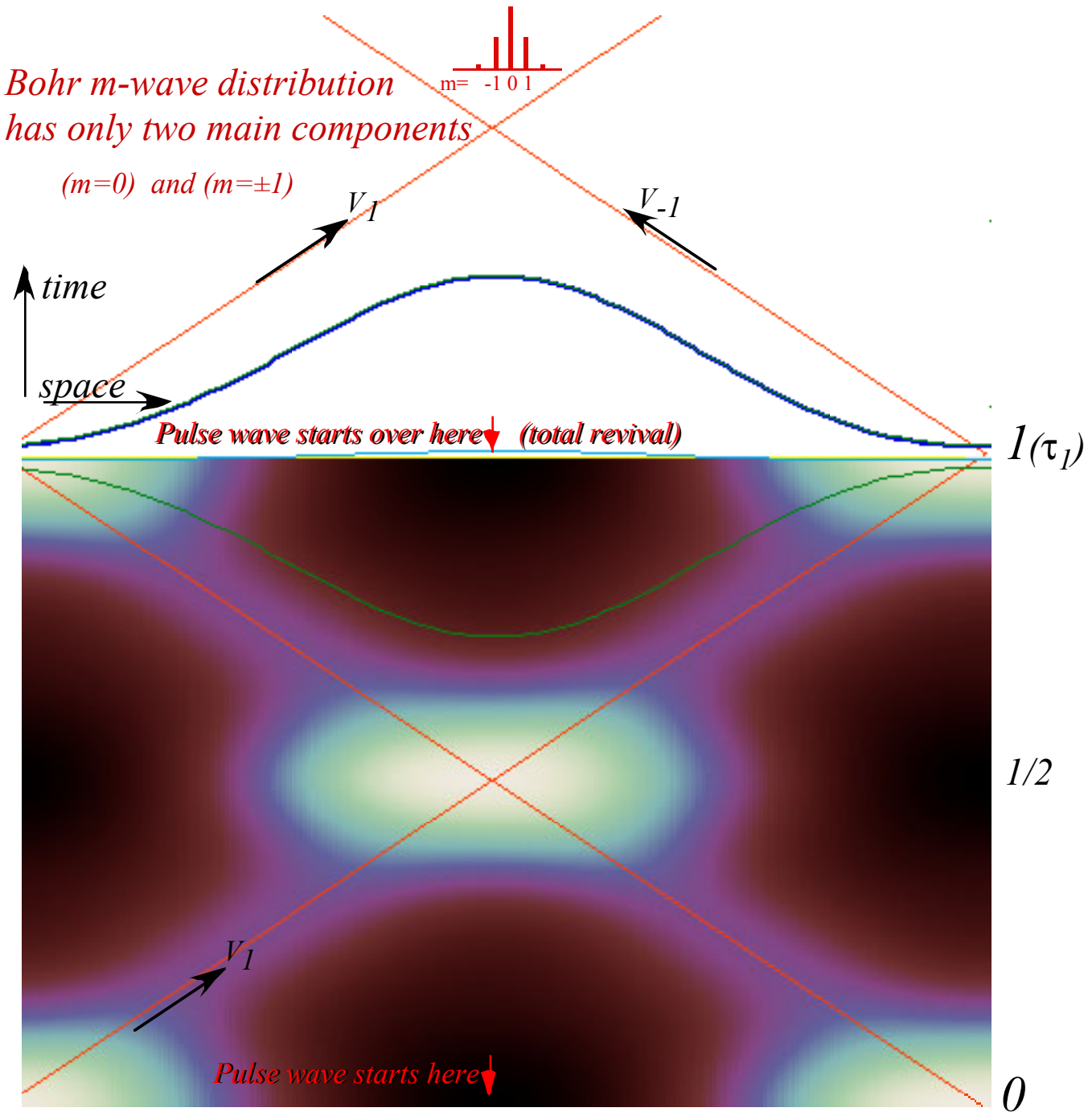

Fig. 5.6.6 (N=4)-Gaussian Bohr m-wave pulse in spacetime |Ψ|-plot shows multiple group velocities.

Ignored in all the |Ψ|-plots above are the wave phase, phase velocity, and ReΨ-zeros which, even for the simplest non-trivial 2-state case above in Fig. 5.6.6, have much more detailed structure than do the group waves and probability distributions plotted so far. To tell a comprehensible story about phase requires some symmetry group algebra of Fourier theory and its number-theoretic ancestry as given in Unit 3. In our wave-world, phase is the key, and the devil is definitely in its details.

Problems for Chapter 5.

Aquatic Dispersion *(revised 10.15.03)*

5.1.1 Suppose a dispersion function $\omega_{Aqua}(k)=ak^{1/2}$ describes water waves. (It does approximately.)

(a) Find phase and group velocity as a function of wavelength λ and wavevector k. Find V_{phase}/V_{group}.

(b) Water waves are peculiar by being both transverse and longitudinal. Suppose each surface point follows both the ReΨ and ImΨ parts of its phasor instead of just ReΨ (transverse wave) or just ImΨ (longitudinal wave), that is, goes around in a circle. Will the surface shape still be a sine wave?
If not, tell what sort of curve it might be under different conditions. (What amplitude "breaks" a wave)

(c) Does $\omega_{Aqua}(k)$ have Lorentz invariance?.,.i.e., is same for ship and any moving observer?
Compare $\omega_{Aqua}(k)$ to $\omega_{Newton}(k)$ below by comparing V_{phase}/V_{group}. for each.

Holiday Dispersion

5.1.2 Suppose that no matter what amplitudes or phase you attached to each wave point, the wave phasors would all rotate at exactly 1 Hz without any change of amplitude. (Call this a "Movie Marquis" or "Christmas Tree" system after the string of uncoupled blinking lights in it.)

(a) Derive and plot a dispersion function $\omega_{Xmas}(k)$ that would describe this system.

(b) Tell what V_{phas} and V_{group} you expect to see as a function of wavelength λ and wavevector k.

(c) Does $\omega_{Xmas}(k)$ have Lorentz invariance.i.e., is same for all observers? . approximately… sometimes?

Fig-Newton Dispersion

5.1.3 Suppose a dispersion function $\omega_{Newton}(k)=ak^2$ describes matter waves. (It does approximately.)

(a) Give V_{phas} and V_{group} velocity as a function of wavelength λ and wavevector k. Find V_{phase}/V_{group}.

(b) Does $\omega_{Newton}(k)$ have Lorentz invariance?. approximately… sometimes?

Deer in the headlights

5.1.4--Imagine a deer crosses the East bound lane of a superhighway on which all cars have the same source frequency ω_0 for headlights and tailights. The deer sees frequency ω_W to the West and ω_E off in the East.

(a) If the deer knows all cars go the same speed u, can it find u and ω_0 from ω_W and ω_E? How or why not?

(b) Now, what if the headlight source frequency ω_{0Head} and tailight source frequency ω_{0Tail} are different?

(c) If cars go different speeds u_1 and u_2, can deer find the speeds and source frequencies from ω_W and ω_E? How or why not? What if $\omega_{0Head} = \omega_{0Tail}$? Would knowing source frequency(s) help? Explain.

(d) Suppose instead each car has head-matter-asers putting out kinkless wave (ω_H , $ck_H=0$) and tail-matter-asers putting out (ω_T , $ck_T=0$), and the deer (crafty doe) can measure (ω_W , ck_W) in the west and (ω_E , ck_E) in the East. Is this enough for the deer to determine both cars' speed and frequency? How or why not?

Really-really fast

5.2.1.At ultra-relativistic speeds it may be useful to use the parameter $\delta=1-\beta$ instead of $\beta=\tanh(\theta)$ since the latter gets so close to unity that numerical underflow problems may arise. Find approximate and exact expressions relating δ to (and from): (a) Rapidity θ, (b) Doppler red/blue shift b. (c) Lorentz contraction (d) Time dilation.

How long does it take to get to α-Centauri in 6 months?

5.2.2. Suppose we define a velocity we will call $v_{ignorant}$ as that speed that someone ignorant of relativity would say a spaceship had to go to get to a distant star in a given time. For example, if we ask how fast a ship would have to go to get to α-Centauri (~4 light years away) in 6 months then the "ignorant" person would say it had to go $v_{ignorant} = 8c$, that is, eight times the speed of light, so if super-luminal travel is prohibited 6 months is too short.

But the relativity expert says that there is a speed v_{expert} which will get the ship to α-Centauri in 6 months according to the ship's passengers, who, after all, are the ones counting.

(a) Compute v_{expert} for this 6-month α-Centauri trip and derive general algebraic relations giving v_{expert} in terms of $v_{ignorant}$ and vice-versa.

(b) How long does it really take to get to α-Centauri in 6 months? (Lighthouse time.)

The cost of ignorance::NASA goes for broke

5.2.3 Use the velocity $v_{ignorant}$ defined in the preceding problem and results concerning the *α-Centaur* voyage.

(a) Relativistic momentum of particle m can be expressed nicely in terms of $v_{ignorant}$. Do so.

(b) Given the proposed journey to α-Centauri in 6 months work up a budget estimate. How many GNPU (1 GNPUnit = $\$10^{12}$=\$1 Trillion) will it cost to get a ship of mass 10^6 kg (1,100 tons) up to speed at the prevailing rate of power: \$0.10/kWHr. ? (1 kWHr = $3600\text{x}10^3$ J) Note: Don't count the rest mass energy of the ship in your cost...assume NASA (i.e. you the taxpayer) has already bought that.

` Bottom line: Cost=_____

A Long Way to Go for a Beer

5.5.1 Suppose you have been accelerating at 9.8m/sec^2 since birth. (You have been!) By the time you are 21 and can legally order a drink you have traveled a long way relative to the inertial "birth" frame in which you were born. How long? Let's see!

All this is derived using a relativistic Newton's law in your (proper) local time τ. Recall (5.5.3)

$$\frac{dp_x''}{d\tau} = mg, \qquad \frac{dE''}{d\tau} = 0$$

Since all observers should agree that you are experiencing constant 1 g acceleration they will all see your trajectory as a single invariant curve. You should plot this curve in (x,ct) and (cp,E) graphs.

(a) At 1 year of age what is your hyperbolic rapidity angle relative to the inertial frame? ρ_u=_____

(b) At 1 year of age what is your speed relative to that frame? u/c=_____

(c) When you are 1 year old how much time has passed in that "birth" frame? _____sec. and_____yr.

(d) When you are 1 year old how far have you gone in that frame? _____m.

(e) At 21 years of age what is your hyperbolic rapidity angle relative to the inertial frame? ρ_u=_____

(f) At 21 years of age what is your speed relative to that frame? 1-u/c=_____ (Use δ in *Really-really fast*.)

(g) When you are 21 years old how much time has passed in that frame? _____sec. and _____yr.

(h) When you are 21 years old how far have you gone in that frame? _____m.

Homecoming or Born again!

(i) At what age do you have enough kinetic energy relative to the birth frame to recreate all your mass there?

Boom and BOOO-OOM!

5.6.1 Suppose your job is to estimate and compare the energy yields per kilogram of conventional chemical explosives and of nuclear fission devices. You have at your disposal only the topics of this chapter, particularly the famous $E=Mc^2$ result of (5.2.5b), the Bohr radius of (5.6.3), the Coulomb energy $V(r)=q^2/4\pi\varepsilon_0 r$ from (5.6.2), approximate nuclear size of 5 Fermi, and Avagodro's number of *6.02e23* nuclei per mole.

(a) Estimate the yield of a kg of $^{92}U_{235}$ assuming it splits roughly in half. (First, do you follow the suggestions of the popular literature and use the Mc^2 formula? Why, how, or why not?)

(b) Estimate the yield of a kg of Lead Azide PbN_6 assuming it splits completely. (Is Mc^2 formula at all applicable here? Why, how, or why not?) For lead and Nitrogen you may assume 2 Bohr radii each and that all electrons disappear. (This maximum energy estimate exceeds true yield. By roughly how much?)

Bleep the phase, maybe

5.6.2 Details of wave phase dynamics have been such nebulous and complicated subjects that some physicists have simply said, "(Bleep) the (bleeping) phase!" Can you help this situation?

(a) Consider the possible phase velocity or velocities for an Bohr matter wave excited as it was in Fig. 5.6.5 and Fig. 5.6.6. Give formulas and construct tables as was done for the group velocity in (5.6.10).

(b) Give a geometric construction of Bohr-Schrodinger phase velocity that relates to the group velocity construction of Fig. 5.6.4. Does Schrodinger's ignorance of Mc^2 for his quantum theory affect this? Discuss why or why not.

3's Company

5.6.3 Find what group velocity values would show up for a 3-level excitation of m=0,±1, and ±2, only. Sketch the reulting wave-probaility-zero paths or nodal lines and anti-nodal lines in space time for one fundamental period. (Optional: Compare to a plot of (Δm~±2)-range $^{\sin x}/_x$ and Gaussian packets by BohrIt or equivalent.)

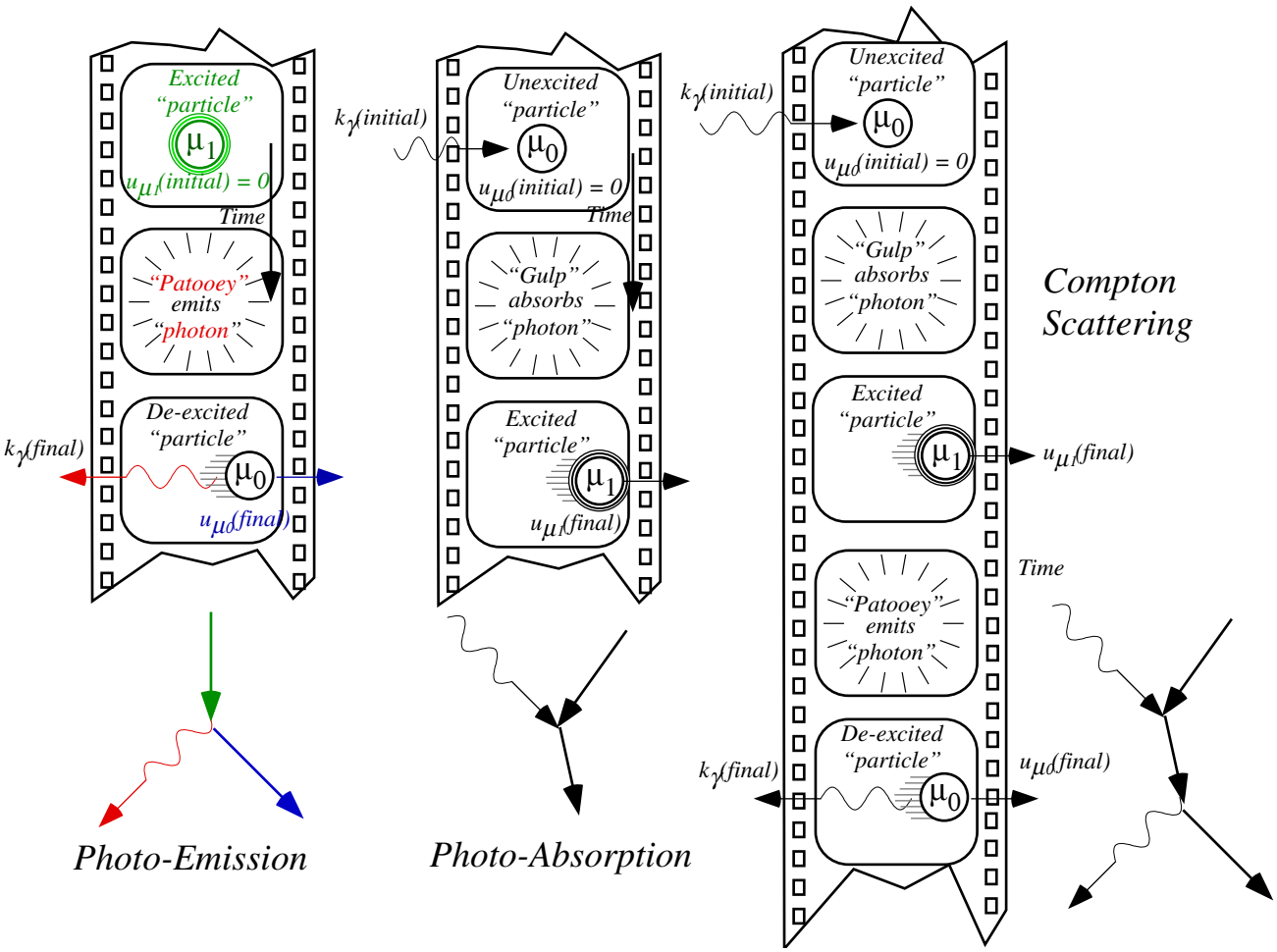

"Patooey"- Compton emission recoil

5.6.4 When an excited stationary molecule, atom, or nucleus emits a photon (γ-wave) during a quantum transition, it ends up on a lower μ-hyperbola, that is, it gets lighter by starting out at k_1=0 on a μ_1-hyperbola and ends up with a non-zero k_0 on a lower μ_0-hyperbola. This is called a *Compton recoil* process.

Suppose that the recoil process conserves the sum $\mathbf{K}_\gamma + \mathbf{K}_\mu = \mathbf{K}_{Total}$ of the μ-wave and γ-wave **K**-vectors $\mathbf{K}_\gamma$=(ck(γ), ω(γ)) and $\mathbf{K}_\mu$=(ck(μ), ω(μ)). Given the initial and final μ-levels μ_1 and μ_0 derive equations for the final momenta and energies of the μ-wave and γ-wave. Solve by geometry or algebra in terms of μ_1 and μ_0.

(a) Graph the transition on a per-spacetime graph for the case $\mu_1 = 2$ and $\mu_0 = 1$. (High energy physics)

(b) Graph the transition on a per-spacetime graph for the case $\mu_1 = 2$ and $\mu_0 = 1.8$. (Lower energy physics)

(c) Consider an H atom state or level whose μ_1 value is 10 eV higher than μ_0. (Way low energy physics) (Recall that its ground energy is ~Mc^2 where $M=m_{proton}$.) Give recoil momenta and velocity in mks units but energy in eV. Compare the shift in energy to 10eV? Is it big enough to be observed easily?

"Gulp"- Compton absorption recoil

5.6.5 The quantum absorption process is essentially the reverse of the emission process in Prob. 5.6.4 but as shown in the middle figure the μ_0 particle is initially stationary. For cases (a-c) work out the corresponding algebra, graphs, and numerical results (for (c)). For part (c) let a stationary H atom be excited from its ground state to a state or level whose μ_1 value is 10 eV higher than μ_0.

"Gulp & patooey"- Compton scattering

5.6.6 A photon backscattering (180°) off of a particle is the most extreme form of *Compton scattering*. As shown in the 3rd figure, this process is equivalent to absorption followed by emisssion. While this is the key to analyzing scattering crossections, it is not necessary for deriving final recoil and frequency shift values. These may be found using the techniques sketched in Sec. 5.2(g) and should depend only on initial light frequency and ground state paricle mass or proper frequency μ_0 . Derive formulas using geometry as in Fig. 5.2.6 wherever possible.

Fast company (Based on Lab booklet for RelativIt)

5.RelativIt.1. Consider *Relativit* Fig. 2a showing an elastic collision between identical m=1MeV particles with equal but opposite momenta in the Lighthouse frame. (It is called a center-of-momentum (CM) frame.)
(a)Given Fig. 2a compute correct relativistic momentum components for the same identical particle collision seen by the ship in Fig. 2b. Is this momentum conserved?
(b) Suppose instead that the particles scattered at $\Theta_{CM}=180°$ instead of $\Theta_{CM}=90°$ as in the figure, that is both come in and go out with the same speeds $u=\pm c/2$ in the Lighthouse frame along the ship's path. Derive the final velocities and momenta according to the ship going $v=-c/2$ (RLH).
(c) Plot the initial and final (cp, E) vectors of the two particles in (b) for the Lighthouse frame.
(d) Plot the initial and final (cp', E') vectors of the two particles in (b) for the Ship frame.
(e) If the collision is totally inelastic, that is, results in one big "Glunkon" particle, show momentum energy of the resulting Glunkon in both plots (c) and (d).
(In each plot show the vector sum of the (cp, E) vectors before collision and the sum after collision. Should this sum be conserved? Use the mass shell hyperbolas.)

Relativistic decadence (Based on Lab booklet for RelativIt)

5.RelativIt.2. Suppose a 2MeV "Slobon" particle sitting in Lighthouse frame decays into a rest mass 1MeV "Skinon" particle and a photon which is emitted in the direction of the ship's travel. (Ship goes $v=-c/2$ (RLH).)
(a) Compute all final energies and momenta and plot this event according to the Lighthouse.
(b) Compute all final energies and momenta and plot this event according to the Ship.
(You should do plots on (cp, E) and (cp', E') graphs first, but also sketch results on (x, ct) plot.)

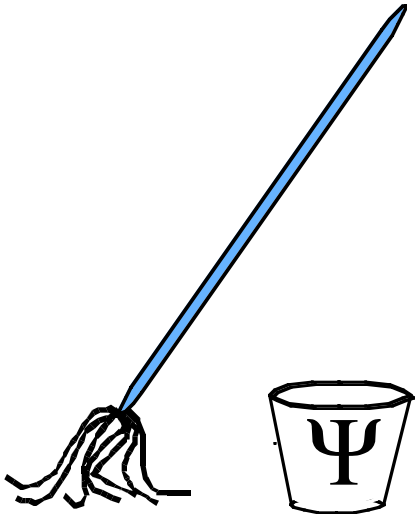

QM for AMOP

Chapter 6
Multidimensional Waves And Modes

W. G. Harter

CHAPTER 6. MULTIDIMENSIONAL WAVES AND MODES 1

6.1. Wavevector Geometry and Transformation 1
(a) 3-Dimensional waves and 4-vectors 1
(b) Transverse vs. longitudinal Doppler: Stellar aberration 3
(c) Graphical wave 4-vector transformation 6

6.2. Laser Wave 4-Vector Coordinate Frames 7
(a) Counter propagating waves in space-time 7
(b) Cosmic positioning system 8
(c) Wavevector defined coordinate planes 9

6.3. Wave Guide Dispersion and Cavity Eigenfrequencies 11
(a) 2-Dimensional wave mechanics: guided waves and dispersion 11
(b). Rays and wavefronts: Phase and group velocity 13
Group waves and "messages":(How do I send one?) 17
(c). Evanescent waves 17
(d). Trapped waves and cavity modes: discrete frequencies 18

Problems for Chapter 6. 20

REVIEW TOPICS & FORMULAS FOR UNIT 2 22

Continuous wave dynamics in 3-dimensional space is determined by its wavevector components and the frequencies associated with each. This chapter introduces the geometry, relativity, and physics of wave 4-vectors that contain wavevector **k** and frequency ω. The various kinds of Doppler effects associated with optical and matter waves are derived. 3D-relativistic wave coordinates are introduced and an example involving a simple wave-guide model is worked out. Optical wave-guides have the same form of dispersion as a quantum matter wave.

Chapter 6. Multidimensional Waves and Modes

6.1. Wavevector Geometry and Transformation

Chapters 4 and 5 introduced the key ideas of wave mechanics using waves in one spatial dimension, usually labeled as the x-axis. The introduction in Ch. 4 of space-time relativity is then reduced to a study of spacetime "2-vectors" $\mathbf{X}=(x,ct)$. Per-spacetime "2-vectors" $\mathbf{K}=(ck,\omega)$ were related to $\mathbf{X}=(x,ct)$ by (4.2.11) as sketched in Fig. 4.2.11. The $\mathbf{K}$ satisfy optical dispersion $\omega=ck$ or else relativistic matter-wave dispersion $\omega^2=(\hbar Mc^2)^2+(ck)^2$ that is the key to quantum theory. Here 3D wave mechanics is discussed using 4-dimesional spacetime "4-vectors" $X^\mu=(\mathbf{r}, ct)$ and per-spacetime 4-vectors $K^\mu=(c\mathbf{k}, \omega)$.

(a) 3-Dimensional waves and 4-vectors

(ck,ω)-transformation formulas like (4.3.10) simplify Doppler analysis. Now we generalize the wavevector k to a three dimensional vector $\mathbf{k}$ and, for relativity, a *per-spacetime 4-vector* $k^\mu=(\mathbf{k}, \omega/c)$. This is matched by a *space-time 4-vector* $x^\mu=(\mathbf{r}, ct)$. The general plane wave function is the following.

$$\Psi(\mathbf{r}, ct) = A\, exp\, i\,(\mathbf{k}\bullet\mathbf{r} - \omega t) = A\, e^{\,i\,(\mathbf{k}\bullet\mathbf{r} - \omega t)} \qquad (6.1.1)$$

Transformation equations that preserve the phase $(\mathbf{k}\bullet\mathbf{r} - \omega t)$ are obvious generalizations of (4.3.10).

$$\begin{pmatrix} x' \\ y' \\ z' \\ ct' \end{pmatrix} = \begin{pmatrix} \cosh\rho_x & 0 & 0 & -\sinh\rho_x \\ 0 & 1 & 0 & 0 \\ 0 & 0 & 1 & 0 \\ -\sinh\rho_x & 0 & 0 & \cosh\rho_x \end{pmatrix} \begin{pmatrix} x \\ y \\ z \\ ct \end{pmatrix} \qquad (6.1.2a)$$

$$\begin{pmatrix} ck_x' \\ ck_y' \\ ck_z' \\ \omega' \end{pmatrix} = \begin{pmatrix} \cosh\rho_x & 0 & 0 & -\sinh\rho_x \\ 0 & 1 & 0 & 0 \\ 0 & 0 & 1 & 0 \\ -\sinh\rho_x & 0 & 0 & \cosh\rho_x \end{pmatrix} \begin{pmatrix} ck_x \\ ck_y \\ ck_z \\ \omega \end{pmatrix} \qquad (6.1.2b)$$

Phase invariance axiom (4.3.6) for the 4-vectors is consistent with such a Lorentz transformation.

$$\Phi = -\mu\tau = \mathbf{k}\bullet\mathbf{r} - \omega t = \mathbf{k}\bullet\mathbf{r} - (\omega/c)(ct) = \mathbf{k}'\bullet\mathbf{r}' - (\omega'/c)(ct'). \qquad (6.1.2c)$$

(6.1.2a) preserves the individual $(\mathbf{r}, ct)$-invariant of *proper time* τ. (Recall (5.1.4).)

$$(c\tau)^2 = (ct)^2 - r^2 = (ct')^2 - r'^2 \text{ where: } r = |\,\mathbf{r}\,| = \sqrt{(\mathbf{r}\bullet\mathbf{r})} = (x^2 + y^2 + z^2\ )^{1/2}. \qquad (6.1.2d)$$

(6.1.2b) preserve the individual $(\mathbf{k}, \omega/c)$-invariant of *proper frequency* μ. (Recall (5.1.5).)

$$(\mu)^2 = (\omega)^2 - (ck)^2 = (\omega')^2 - (ck')^2 \text{ where: } k = |\,\mathbf{k}\,| = \sqrt{(\mathbf{k}\bullet\mathbf{k})} = (k_x^2 + k_y^2 + k_z^2\ )^{1/2}. \qquad (6.1.2e)$$

Multiplying four-vector $(\mathbf{k},\omega/c)$ by c gives a more conventional $(c\mathbf{k},\omega)$ and avoids fractions $1/c$.

There is economy in (6.1.2); one transformation matrix does both wavevector-frequency $(c\mathbf{k},\omega)$ and space-time $(\mathbf{r}, ct)$. It gives the observed direction $\mathbf{k}'$ of a $(c\mathbf{k},\omega)$ light ray or any wave that was sent in a certain direction $\mathbf{k}$ from moving source. It gives the observed frequency ω', too. Both $\mathbf{k}$ and ω are linear functions of $\mathbf{k}'$ and ω'. The inverse is found by simply flipping the rapidity $+\rho_x$ to $-\rho_x$.

To visualize the $\mathbf{k}$-vector one may imagine (as in Fig. 6.1.1) parallel stacked phase planes normal to $\mathbf{k}$ all marching lockstep in the $\mathbf{k}$ direction at phase velocity $\mathbf{v}_{phase} = (\omega/k)\mathbf{e}_\mathbf{k}$, where k is the length of $\mathbf{k}$, and $\mathbf{e}_\mathbf{k}$ is a unit vector normal to the phase planes and in the direction of propagation. The distance between planes of phase Φ and $\Phi+2\pi$ is the wavelength $\lambda = 2\pi/k$ as given by the usual formulas in Fig. 4.2.10. The period $\tau = 2\pi/\omega$ is time between phase planes Φ and $\Phi+2\pi$ passing a point $\mathbf{r}$. Relations (6.1.2) hold whether or not V_{phase} is equal to the speed of light c and apply to all vacuum waves (6.1.1).

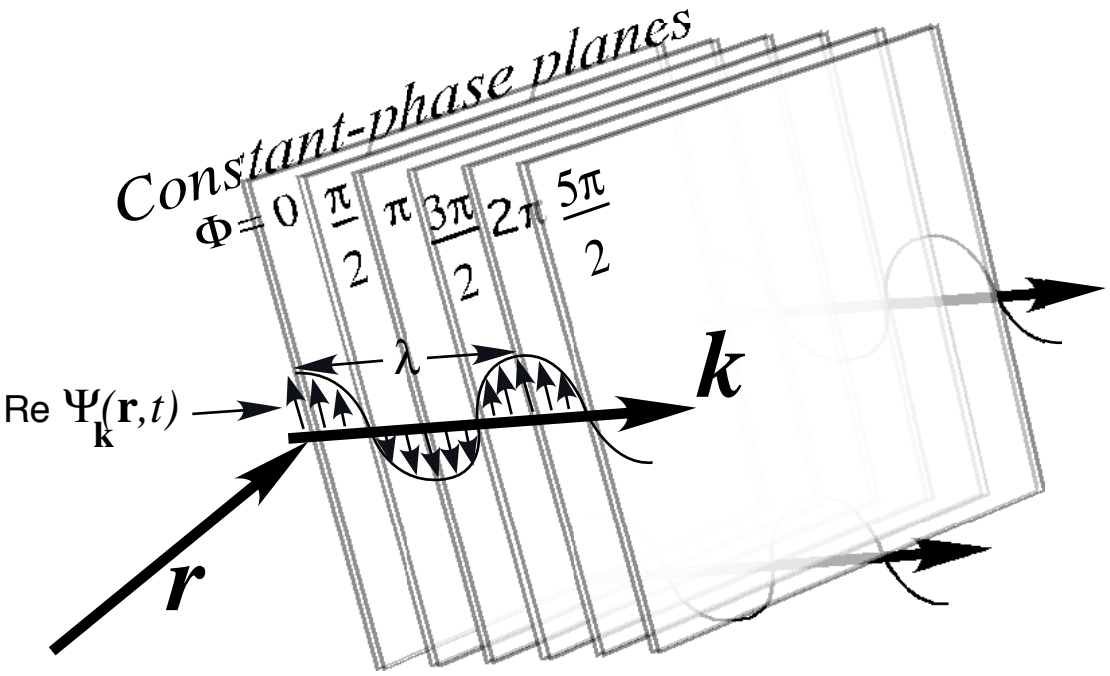

Fig. 6.1.1 Anatomy of a plane wavefunction $\Psi_k(\mathbf{r},t) = A\exp i(\mathbf{k}\bullet\mathbf{r} - \omega t)$ *with wavevector* **k**.

Use caution in interpreting the wavy arrows depicting $Re\,\Psi(\mathbf{r},t)$ in Fig. 6.1.1. For light waves the arrows could be actual **E**-field vectors as discussed in Ch. 1. (Recall (1.2.8-11).) Otherwise $\Psi(\mathbf{r},t)$ is a scalar wave or probability density wave that points in any (or no particular) direction. Vector waves have a polarization direction **E**. For vacuum em waves **E** is always normal to **k**, as indicated in Fig. 6.1.1.

For light waves or "photons" the *proper time* τ along its spacetime path $r=ct$ is zero by (5.1.4).

$$(c\tau)^2 = (ct)^2 - r^2 \quad (=0 \text{ for light or "photons"}) \tag{6.1.3}$$

A proper frame of a particle is one it drags with it so its r'-coordinate is origin ($r'=0$). Since light travels at c (Its position in the lab frame is $r=ct$.) it's impossible for it to "age" in its own (proper) frame. Hence its *proper frequency* μ is zero, too, by (5.1.5b). Optical phasors stop at $k=0$ since $\omega=ck$ is invariant.

$$(\mu)^2 = (\omega)^2 - (ck)^2 \quad (=0 \text{ for light or "photons"}) \tag{6.1.4}$$

The phase velocity of light is only $c=\omega/k$. Chapter 5 introduced matter waves with non-zero $\mu = Mc^2/\hbar$ that do age and only have speeds *other than* c. For real μ, V_{group} is less than c but $V_{phase} > c$. Motion of light "trapped" by waveguides and cavity walls occupies Sec. 6.3. Such imprisonment causes a non-zero "aging" rate μ for light and makes its waves "heavy" as seen already in discussion of Fig. 5.2.3.

Besides allowing a 3D range of **k**, (6.1.2) allows 3D Lorentz frame velocity **u**. Here $\mathbf{u} = u_z\mathbf{e}_z$.

$$\begin{pmatrix} x' \\ y' \\ z' \\ ct' \end{pmatrix} = \begin{pmatrix} 1 & 0 & 0 & 0 \\ 0 & 1 & 0 & 0 \\ 0 & 0 & \cosh\rho_z & -\sinh\rho_z \\ 0 & 0 & -\sinh\rho_z & \cosh\rho_z \end{pmatrix} \begin{pmatrix} x \\ y \\ z \\ ct \end{pmatrix} \tag{6.1.5a}$$

$$\begin{pmatrix} ck_x' \\ ck_y' \\ ck_z' \\ \omega' \end{pmatrix} = \begin{pmatrix} 1 & 0 & 0 & 0 \\ 0 & 1 & 0 & 0 \\ 0 & 0 & \cosh\rho_z & -\sinh\rho_z \\ 0 & 0 & -\sinh\rho_z & \cosh\rho_z \end{pmatrix} \begin{pmatrix} ck_x \\ ck_y \\ ck_z \\ \omega \end{pmatrix} \tag{6.1.5b}$$

In this case the prime frame is moving at velocity $u_z = c\cdot\tanh\rho_z$ up the unprimed z-axis. (Set $z'=0$ in (6.1.5a). Then solve for $z = u_z t$.) Let us try to visualize $(c\mathbf{k}, \omega)$ transformations like (6.1.2b) or (6.1.5b).

(b) Transverse vs. longitudinal Doppler: Stellar aberration

A novel description of relativity by L. C. Epstein introduces a "cosmic speedometer" consisting of a telescope tube tipped to catch falling light pulses from a distant overhead star. A stationary telescope points straight up the *x*-axis at the apparent position *S* of the star. (Fig. 6.1.2a) But, for a velocity $\mathbf{u}=u_z\mathbf{e}_z$ across the star beam *x*-axis, the telescope must tip to catch the starlight, so the apparent position *S'* tips toward **u**. (Fig. 6.1.2b). The telescope tips by the *stellar aberration angle* σ. The sine of the tipping angle σ is velocity ratio $\beta= u_z/c$ which is the hyper-tangent of relativistic rapidity ρ_z (or θ in (4.4.4).)

$$\beta= u_z/c = \sin\sigma = \tanh\rho_z \qquad (6.1.6)$$

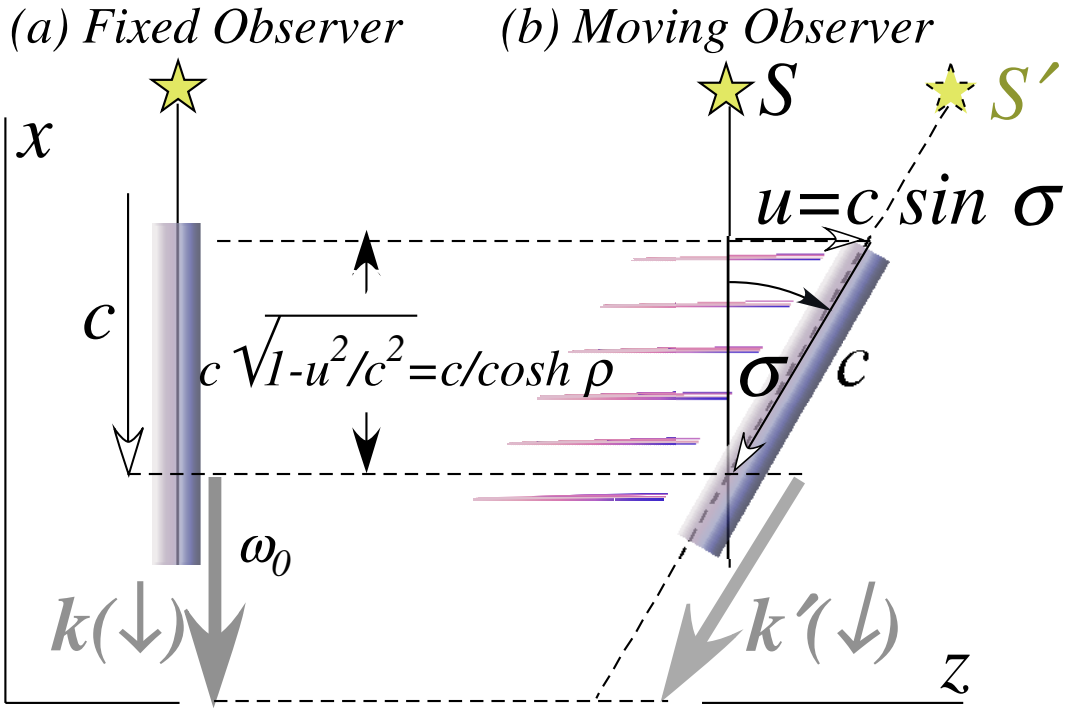

Fig. 6.1.2 Cosmic speedometer visualization of aberration angle σ and transverse Doppler shift coshρ.

Proper time τ and frequency μ invariance (6.1.2d-e) implies that 4-vector components normal to velocity **u** of a boost are unchanged. That is, a boost along *z* of *(ct,z)* to *(ct',z')* (or (ω,ck_z) to (ω',ck_z')) must preserve both *(x,y)=(x',y')* and $(ck_x,ck_y)=(ck_x',ck_y')$ just as a rotation in the *xy*-plane of *(x,y)* to *(x',y')* leaves unaffected the components *(ct,z)=(ct',z')* and $(\omega,ck_z)=(\omega',ck_z')$ transverse to the rotation.

Invariant (6.1.3) also demands light-speed conservation as sketched in Fig. 6.1.2b. Starlight speed down the σ-tipped telescope is *c*, so the *x*-component of starlight velocity reduces from *c* to

$$c_x'=c\cos\sigma=c\sqrt{(1-u_z^2/c^2)} = c/\cosh\rho_z\ . \qquad (6.1.7)$$

Transformation (6.1.5b) assures that *x*-or-*y*-components of $\mathbf{k}\downarrow$ are unchanged by u_z-boost.

$$(ck_x,ck_y)=(ck_x',ck_y') \qquad (6.1.8)$$

So the length of $\mathbf{k}\downarrow$ increases by a factor *cosh* ρ as shown in Fig. 6.1.3 as does the frequency $\omega'\downarrow$.

$$c|k'\downarrow| = c|k\downarrow|\cosh\upsilon_z = \omega_0\cosh\upsilon_z = \omega_0/\sqrt{(1-u^2/c^2)} \qquad (6.1.9)$$

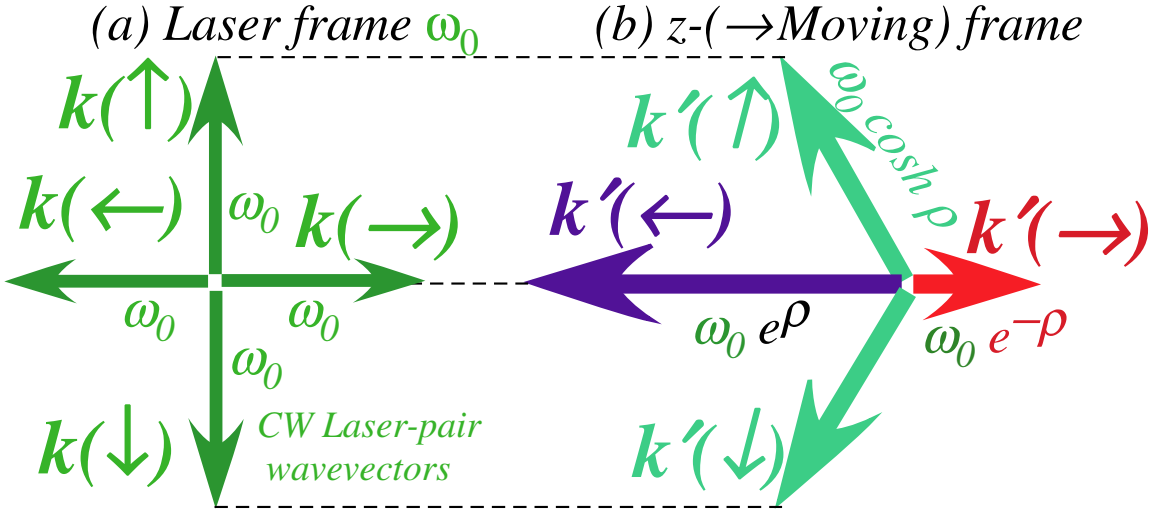

Fig. 6.1.3 CW version of cosmic speedometer showing transverse and longitudinal k-vectors.

If the observer crosses a star ray at very large velocity, that is, lets u_z approach c, then the star angle σ approaches $90°$ and the frequency increases until the observer sees an X-ray or γ-ray star coming almost head on! The $\cosh\rho_z$ factor is a *transverse Doppler shift*. For large ρ_z, it approaches e^{ρ_z}, which is the ordinary *longitudinal Doppler shift* upon which the CW relativity derivations of Ch. 4 are based. Relations (6.1.6-9) are summarized in a 4-vector transformation: ω_0 has a *transverse Doppler shift* to $\omega_0 \cosh\rho_z$, $ck_z=0$ becomes $ck_z' = -\omega_0 \sinh\rho_z$, but the x-component is unchanged: $ck_x' = \omega_0 = ck_x$.

$$\begin{pmatrix} \omega'_\downarrow \\ ck'_{x\downarrow} \\ ck'_{y\downarrow} \\ ck'_{z\downarrow} \end{pmatrix} = \begin{pmatrix} \cosh\rho_z & \cdot & \cdot & -\sinh\rho_z \\ \cdot & 1 & \cdot & \cdot \\ \cdot & \cdot & 1 & \cdot \\ -\sinh\rho_z & \cdot & \cdot & \cosh\rho_z \end{pmatrix} \begin{pmatrix} \omega_\downarrow \\ ck_{x\downarrow} \\ ck_{y\downarrow} \\ ck_{z\downarrow} \end{pmatrix} = \begin{pmatrix} \cosh\rho_z & \cdot & \cdot & -\sinh\rho_z \\ \cdot & 1 & \cdot & \cdot \\ \cdot & \cdot & 1 & \cdot \\ -\sinh\rho_z & \cdot & \cdot & \cosh\rho_z \end{pmatrix} \begin{pmatrix} \omega_0 \\ -\omega_0 \\ 0 \\ 0 \end{pmatrix} = \omega_0 \begin{pmatrix} \cosh\rho_z \\ -1 \\ 0 \\ \sinh\rho_z \end{pmatrix} \tag{6.1.10a}$$

If starlight had been $\mathbf{k}_\leftarrow$ or $\mathbf{k}_\rightarrow$ waves going along **u** and z-axis, the usual longitudinal Doppler blue shifts $e^{+\rho_z}$ or red shifts $e^{-\rho_z}$ would appear on both the k-vector and the frequency, as stated by the following.

$$\begin{pmatrix} \omega'_\rightarrow \\ ck'_{x\rightarrow} \\ ck'_{y\rightarrow} \\ ck'_{z\rightarrow} \end{pmatrix} = \begin{pmatrix} \cosh\rho_z & \cdot & \cdot & -\sinh\rho_z \\ \cdot & 1 & \cdot & \cdot \\ \cdot & \cdot & 1 & \cdot \\ -\sinh\rho_z & \cdot & \cdot & \cosh\rho_z \end{pmatrix} \begin{pmatrix} \omega_0 \\ 0 \\ 0 \\ \pm\omega_0 \end{pmatrix} = \omega_0 \begin{pmatrix} \cosh\rho_z \mp \sinh\rho_z \\ 0 \\ 0 \\ -\sinh\rho_z \pm \cosh\rho_z \end{pmatrix} = \omega_0 \begin{pmatrix} e^{\mp\rho_z} \\ 0 \\ 0 \\ \pm e^{\mp\rho_z} \end{pmatrix} \tag{6.1.10b}$$

The Epstein speedometer tracks light pulses and particles in space and time. Instead of space-x and time-ct coordinates of a Minkowski graph, he plots space coordinate-x against *proper* time-$c\tau$. This view has all things, light γ and particle P included, moving at the speed of light as shown in Fig. 6.1.4. Light never ages, so its "speedometer" is tipped to the maximum along x-*axis*. (See *RelativIt* for animations, and Lewis Epstein's *Relativity Visualized*, (Insight Press San Francisco 1978) for details.)

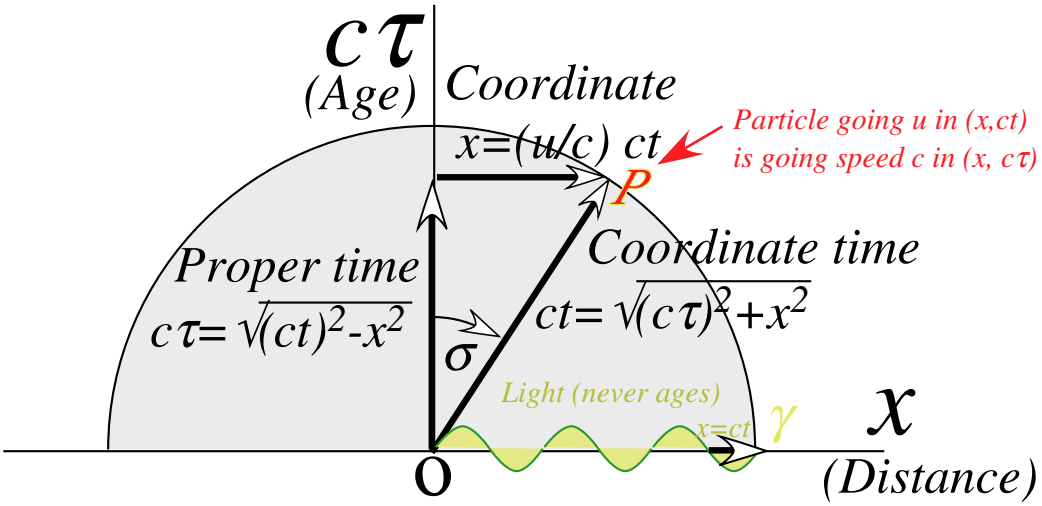

Fig. 6.1.4 Space-proper-time plot makes all objects move at speed c along their cosmic speedometer.

One nice feature of the Epstein space-proper-time view is its take of the Lorentz-Fitzgerald contraction of a proper length L to $L'=L\sqrt{1-u^2/c^2}$. (Recall discussion around (4.3.8).) As shown in Fig. 6.1.5 below, L' is simply the projection onto the x-axis of a length L tipped by σ.

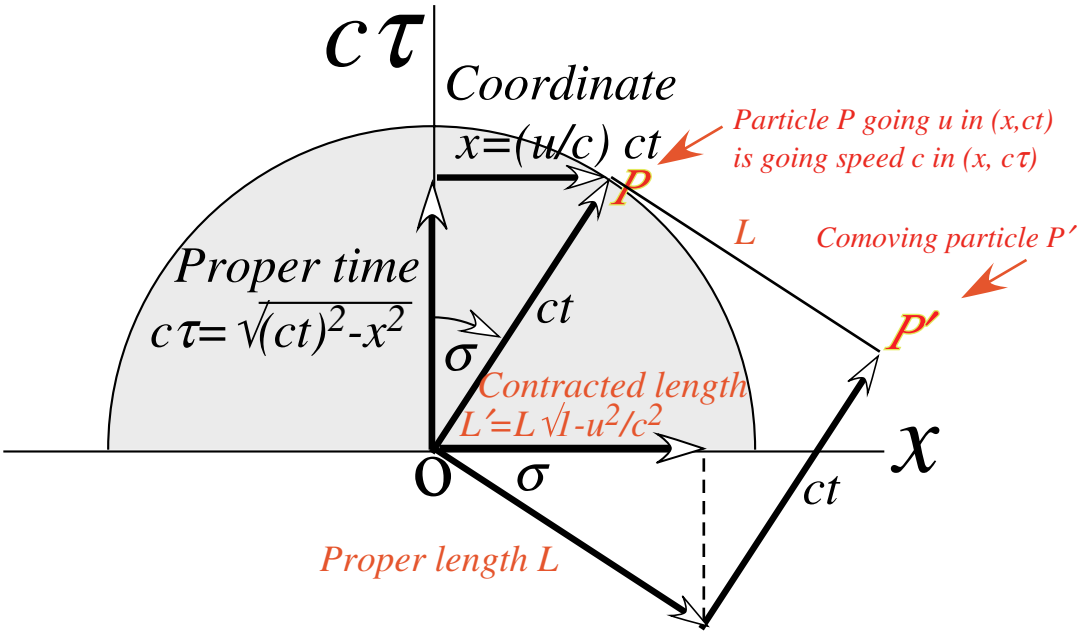

Fig. 6.1.5 Space-proper-time plot of Lorentz contraction as geometric projection of rotated line L.

The problem with the *(x,cτ)* view is that a space-time event is not plotted as a single point for all observers. Since the time parameter τ is an invariant quantity, the *(x,cτ)* graph it is not a metric space.

(c) Graphical wave 4-vector transformation

Geometric constructions combining Fig. 6.1.2 and Fig. 6.1.3 help to quantitatively visualize 4-wavevector transformations. One is shown in Fig. 6.2.1. The *c*-dial of the "speedometer" is first set to the desired **u**-speed which determines angle σ. The top of the *c*-dial (which may also represent a transverse $c\mathbf{k}\uparrow$-vector in units of Lab frequency ω_0) is projected parallel to the velocity axis until it intersects the *c*-dial vertical axis. A transformed $c\mathbf{k'}\uparrow$-vector of length $\omega'\uparrow=\omega_0 \cosh \rho$ results, similar to $c\mathbf{k'}\downarrow$ in (6.1.10a). Both $c\mathbf{k'}\uparrow$ and $c\mathbf{k'}\downarrow$ have a projection on the velocity axis of $\omega_0 \sinh \rho$ while maintaining their transverse components ω_0 and $-\omega_0$, respectively, in order to stay on the light cone. A dashed circle of radius $\cosh \rho$ is drawn concentric to the *c*-dial and determines the longitudinal vectors $c\mathbf{k'}_{\rightarrow}$ and $c\mathbf{k'}_{\leftarrow}$ of Doppler shifted length and frequency $\omega_0 e^{-\rho}$ and $\omega_0 e^{\rho}$, respectively, as required by transformation (6.1.10b).

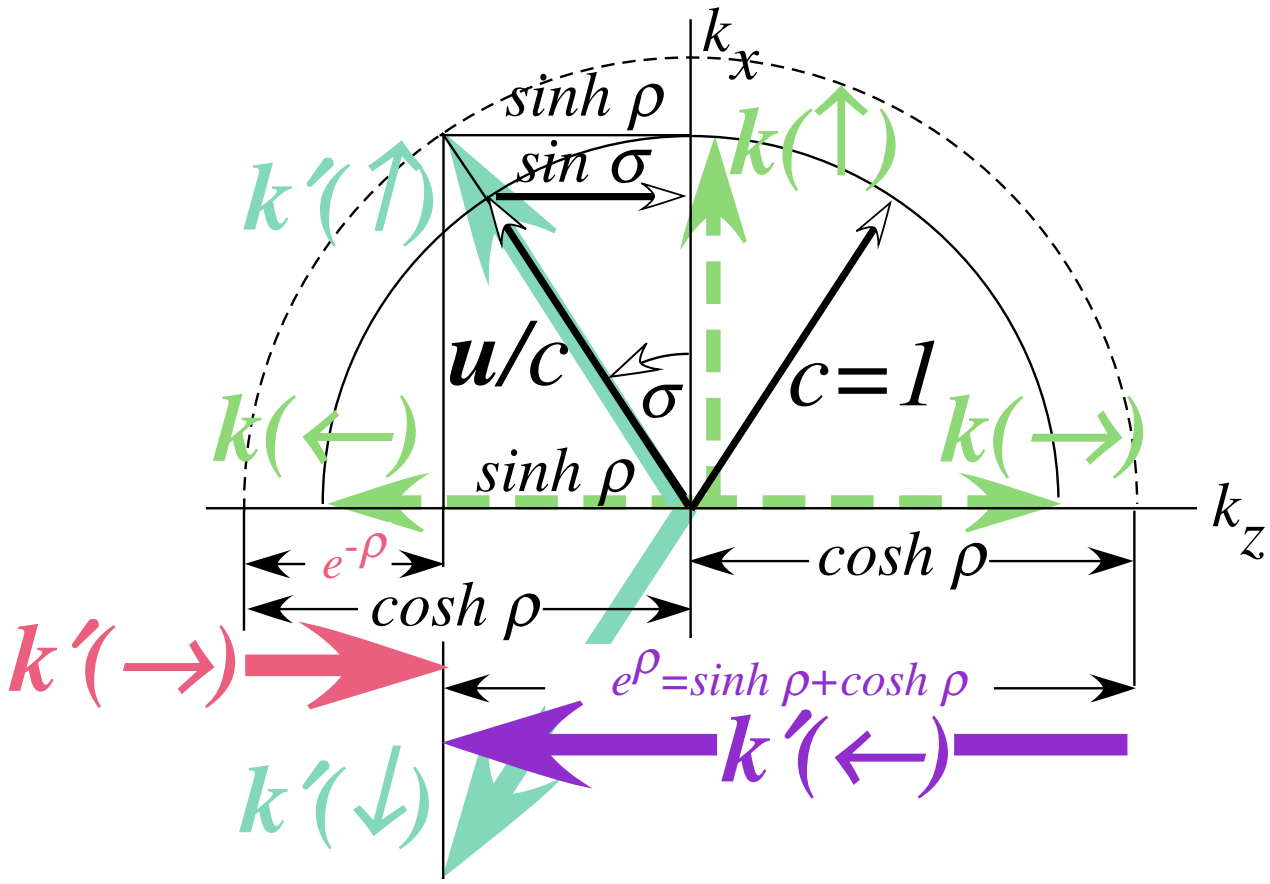

Fig. 6.1.6 CW cosmic speedometer. Geometry of Lorentz boost of counter-propagating waves.

There is similarity between the 2D per-spatial (k_x *versus* k_z) CW cosmic speedometer construction above in Fig. 6.1.6 and the one-dimensional (ω *versus* k) construction in Fig. 4.4.2(c). This is because optical invariance relation for *(μ=0)*-γ-waves demands that the *c***k**-vector length be frequency ω.

$$\omega = ck = \sqrt{k_x^2 + k_y^2 + k_z^2}$$

That is the radius of the circle in both Fig. 4.4.2 and Fig. 6.1.6.

6.2. Laser Wave 4-Vector Coordinate Frames

Chapter 4 introduced the idea of a two-dimensional space-time *(x,ct)* coordinate system generated by a pair of continuous wave (CW) lasers. (Fig. 4.2.3) The result is the Lorentz-Einstein-Minkowski coordinates shown in Fig. 4.2.9 and labeled in Fig. 4.2.10. Now we discuss 3-dimensional problems involving 4-dimesional space-time $x^\mu = (\mathbf{r}, ct)$ coordinate systems made by counter-propagating CW lasers generating waves of 4-dimensional wavevector-frequency $k^\mu = (c\mathbf{k}, \omega)$.

(a) Counter propagating waves in space-time

One-(space) dimensional plane waves $\Psi(z,t)$ are now generalized to ones for which the word "plane" aptly describes constant phase wavefronts in Fig. 6.1.1. The general 1D wavefunction (4.2.6) is generalized to the following $\Psi_{\{\mu\}}(\mathbf{r},t)$.

$$\Psi_{A_\rightarrow,\omega_\rightarrow,\mathbf{k}_\rightarrow;A_\leftarrow,\omega_\leftarrow,\mathbf{k}_\leftarrow}(\mathbf{r},t) = A_\rightarrow e^{i(\mathbf{k}_\rightarrow\bullet\mathbf{r} - \omega_\rightarrow t)} + A_\leftarrow e^{i(\mathbf{k}_\leftarrow\bullet\mathbf{r} - \omega_\leftarrow t)} \tag{6.2.1}$$

Again, waves $\Psi_\mathbf{k}(\mathbf{r},t)$ with zero *SWR* have the simplest phase properties and transformation rules.

$$\Psi_\mathbf{k}(\mathbf{r},t) = \left(e^{i(\mathbf{k}_\rightarrow\bullet\mathbf{r} - \omega_\rightarrow t)} + e^{i(\mathbf{k}_\leftarrow\bullet\mathbf{r} - \omega_\leftarrow t)} \right)/2 \tag{6.2.2}$$

An expo-cosine identity generalizing (4.3.1) defines 3-D phase and group-envelope waves.

$$\Psi(\mathbf{r},t) = \Psi_\mathbf{k}(\mathbf{r},t) = \frac{1}{2}e^{i(\mathbf{k}_\rightarrow\bullet\mathbf{r}-\omega_\rightarrow t)} + \frac{1}{2}e^{i(\mathbf{k}_\leftarrow\bullet\mathbf{r}-\omega_\leftarrow t)}$$

$$= e^{i\frac{(\mathbf{k}_\rightarrow+\mathbf{k}_\leftarrow)\bullet\mathbf{r}-(\omega_\rightarrow+\omega_\leftarrow)t}{2}} \cos\frac{(\mathbf{k}_\rightarrow-\mathbf{k}_\leftarrow)\bullet\mathbf{r}-(\omega_\rightarrow-\omega_\leftarrow)t}{2} \tag{6.2.3a}$$

$$= e^{i(\overline{\mathbf{K}}\bullet\mathbf{r}-\overline{\Omega}t)}\cos(\overline{\mathbf{k}}\bullet\mathbf{r}-\overline{\omega}t) \quad \text{where:} \tag{6.2.3b}$$

$$\overline{\mathbf{K}} = \frac{(\mathbf{k}_\rightarrow+\mathbf{k}_\leftarrow)}{2}, \qquad \overline{\mathbf{k}} = \frac{(\mathbf{k}_\rightarrow-\mathbf{k}_\leftarrow)}{2},$$

$$\overline{\Omega} = \frac{(\omega_\rightarrow+\omega_\leftarrow)}{2}, \qquad \overline{\omega} = \frac{(\omega_\rightarrow-\omega_\leftarrow)}{2}. \tag{6.2.3c}$$

The Lab frame is defined by stationary phase planes separated by $\lambda_0 = 2\pi c/\omega_0$ normal to the beam axis-z between the two lasers of the same frequency ω_0 and equal but opposite wavevectors.

$$\Psi_{\mathbf{k}_0}(\mathbf{r},t) = e^{-i(\omega_0 t)}\cos(\mathbf{k}_0\bullet\mathbf{r}) \tag{6.2.4a}$$

where: $\overline{\mathbf{k}} = \mathbf{k}_\rightarrow = -\mathbf{k}_\leftarrow = \mathbf{k}_0$, and $\overline{\Omega} = \omega_\rightarrow = \omega_\leftarrow = \omega_0$ (6.2.4b)

The group planes of zero ReΨ are fixed normal to $\mathbf{k}_0$.

$$\mathbf{k}_0 \bullet \mathbf{r} = \pm\pi/2, \pm 3\pi/2, \ldots \tag{6.2.4c}$$

The phase zeros periodically go infinitely fast in the $\mathbf{k}_0$-direction at certain times.

$$\ldots\omega_0 t = \pm\pi/2, \pm 3\pi/2, \ldots \tag{6.2.4d}$$

This is the same situation described before in Fig. 4.2.3a where the only boost allowed was along the beam z-axis as in the squared-off lasers in Fig. 4.2.3b but no 3-dimensional boosting or rotation was considered.

However, three dimensions presents a much more complicated range of possible symmetry transformations involving the six *Lorentz group* parameters for x, y, and z boosts and rotations or,

including translations, nine parameters of the *Poincare' group*. Nevertheless, by appealing to continuous-wave optical thought experiments it is possible to simplify the derivation and visualization of this enormous symmetry of locally flat space-time for both classical and quantum theory. This, in spite of the fact that real lab experiments would be dicey at best. Squared-off laser waves of Fig. 4.2.3 would have difficulty achieving planarity over more than a few microns unless a great distance separated them.

(b) CW Cosmic positioning system

By replacing the pulsing star with orthogonal pairs of CW lasers as in Fig. 6.1.3, one might make a cosmic positioning system (CPS) similar to the Earth global positioning system (GPS) in that coherent em waves are used instead of rigid meter sticks. The wave dynamics associated with each pair automatically broadcasts a set of relativistic **k**-vectors and coordinate planes for any observer; the laser waves already "know" relativity! From the wavevectors, an observer can ascertain orientation and velocity relative to the Lab CPS system, and by coordinate plane integration, the translation position, as well. The key axiom, again, is phase invariance (6.1.2c), which for photons is (6.1.3) or for CW lasers (6.1.4).

First is individual laser phase invariance. Pairs $(ct_0,\mathbf{r}_0)$ and $(\omega_0,c\mathbf{k}_0)$ are in Lab CPS frame.

$$\Phi_{\rightarrow}=\mathbf{k}'_{\rightarrow}\bullet\mathbf{r}'-\omega'_{\rightarrow}t'=\mathbf{k}_{\rightarrow}\bullet\mathbf{r}-\omega_{\rightarrow}t=\ \mathbf{k}_0\bullet\mathbf{r}_0-\omega_0t_0 \qquad (6.2.5a)$$

$$\Phi_{\leftarrow}=\mathbf{k}'_{\leftarrow}\bullet\mathbf{r}'-\omega'_{\leftarrow}t'=\mathbf{k}_{\leftarrow}\bullet\mathbf{r}-\omega_{\leftarrow}t=-\mathbf{k}_0\bullet\mathbf{r}_0-\omega_0t_0 \qquad (6.2.5b)$$

Individual laser 4-vectors are, by definition, located on the light cone or null-invariant.

$$c^2\mathbf{k}'_{\rightarrow}\bullet\mathbf{k}'_{\rightarrow}-\omega'^2_{\rightarrow}=c^2\mathbf{k}_{\rightarrow}\bullet\mathbf{k}_{\rightarrow}-\omega^2_{\rightarrow}=\ c^2k_0^2-\omega_0^2=0 \qquad (6.2.6a)$$

$$c^2\mathbf{k}'_{\leftarrow}\bullet\mathbf{k}'_{\leftarrow}-\omega'^2_{\leftarrow}=c^2\mathbf{k}_{\leftarrow}\bullet\mathbf{k}_{\leftarrow}-\omega^2_{\leftarrow}=\ c^2k_0^2-\omega_0^2=0 \qquad (6.2.6b)$$

If any pair of 4-vectors $(\alpha,\mathbf{a})$ and $(\beta,\mathbf{b})$ are Lorentz covariant, then so is any linear combination of them.

$$(\gamma,\mathbf{c})=A(\alpha,\mathbf{a})+B(\beta,\mathbf{b})=(A\alpha+B\beta,A\mathbf{a}+B\mathbf{b})$$

In other words, invariance of α^2-$\mathbf{a}\bullet\mathbf{a}=\alpha'^2$-$\mathbf{a}'\bullet\mathbf{a}'$ and β^2-$\mathbf{b}\bullet\mathbf{b}=\beta'^2$-$\mathbf{b}'\bullet\mathbf{b}'$ implies invariance for the combination γ^2-$\mathbf{c}\bullet\mathbf{c}=\gamma'^2$-$\mathbf{c}'\bullet\mathbf{c}'$, as well. So, phase invariance (6.1.2c) applies to sum $\overline{\mathbf{K}}=(\mathbf{k}_{\rightarrow}+\mathbf{k}_{\leftarrow})/2$ and difference $\overline{\mathbf{k}}=(\mathbf{k}_{\rightarrow}-\mathbf{k}_{\leftarrow})/2$ wavevectors attached to corresponding sum $\overline{\Omega}=(\omega_{\rightarrow}+\omega_{\leftarrow})/2$ and difference $\overline{\omega}=(\omega_{\rightarrow}-\omega_{\leftarrow})/2$ frequencies. However, the new invariants have different values.

$$\overline{\mathbf{K}}'\bullet\mathbf{r}'-\overline{\Omega}'t'=\overline{\mathbf{K}}\bullet\mathbf{r}-\overline{\Omega}t=\ \ 0-\omega_0t_0 \qquad (6.2.7a)$$

$$\overline{\mathbf{k}}'\bullet\mathbf{r}'-\overline{\omega}'t'=\overline{\mathbf{k}}\bullet\mathbf{r}-\overline{\omega}t=\ \ \mathbf{k}_0\bullet\mathbf{r}_0-0 \qquad (6.2.7b)$$

In fact, sum and difference vectors are not on the light cone like their laser components (6.2.6).

$$\overline{\Omega}'^2-c^2\overline{\mathbf{K}}'\bullet\overline{\mathbf{K}}'=\overline{\Omega}^2-c^2\overline{\mathbf{K}}\bullet\overline{\mathbf{K}}=\ \ \omega_0^{\ 2}-0\qquad=c^2k_0^2 \qquad (6.2.8a)$$

$$\overline{\omega}'^2-c^2\overline{\mathbf{k}}'\bullet\overline{\mathbf{k}}'\ \ =\overline{\omega}^2-c^2\overline{\mathbf{k}}\bullet\overline{\mathbf{k}}\ \ =0-\ c^2\mathbf{k}_0\bullet\mathbf{k}_0\ =-c^2k_0^2 \qquad (6.2.8b)$$

The sum vector $(\overline{\Omega},c\overline{\mathbf{K}})$ in (6.2.8a) has a proper frequency $\mu=\omega_0=ck_0$ and behaves like a massive particle. Because of this, uniform wave guide modes have the dispersion of a massive particle which is a *mass-shell M-hyperboloid*(6.2.8a) such as was plotted in Fig. 5.2.1a. This will be shown in Sec. 6.3

The difference vector $(\overline{\omega},c\overline{\mathbf{k}})$ has an extraordinary imaginary proper frequency $\mu=ick_0$. Such an object is called a *Feinberg τ-Tachyon*, and is quite unlike ordinary matter. A real mass starts out at zero wavevector $(k=0)$ with real (proper) frequency $\mu=\omega_0$, zero group velocity $d\omega/dk$, and infinite phase

velocity ω/k. In contrast, tachyons start out at zero frequency $(\omega=0)$ with a real wavevector k_0 , zero phase velocity $(\omega/k=0)$ and infinite group velocity $(d\omega/dk=\infty)$. A tachyon dispersion curve is a vertical τ-hyperbola given by (6.2.8b) and drawn below the photon asymptote in Fig. 5.2.1a. Such a τ-wave is also known as an "instanton" since it everywhere at the instant it has infinite group velocity. Our name for the τ-wave is less poetic: it is simply the group cosine envelope which is static in the Lab CPS frame. (It *defines* Lab-frame's coordinate planes.)

As the observer's rest frame changes velocity **u**, the sum vector $\left(\overline{\Omega},c\overline{\mathbf{K}}\right)$ follows an *M*-hyperbola (6.2.8a) while difference vector $\left(\overline{\omega},c\overline{\mathbf{k}}\right)$ follows a tachyon hyperbola (6.2.8b). Meanwhile, pairs of laser 4-wavevectors $(\omega_{\rightarrow},c\mathbf{k}_{\rightarrow})$ or $(\omega_{\leftarrow},c\mathbf{k}_{\leftarrow})$ (for light moving along the *x*-axis) and $(\omega_{\uparrow},c\mathbf{k}_{\uparrow})$ and $(\omega_{\downarrow},c\mathbf{k}_{\downarrow})$ (for light moving along the vertical *z*-axis) each follow null light-cone-invariants (6.2.6). The details of how $(\omega_{\rightarrow},c\mathbf{k}_{\rightarrow})$, $(\omega_{\leftarrow},c\mathbf{k}_{\leftarrow})$, $(\omega_{\uparrow},c\mathbf{k}_{\uparrow})$, and $(\omega_{\downarrow},c\mathbf{k}_{\downarrow})$ transform is sketched in Fig. 6.1.6.

(c) Wavevector defined coordinate planes

Examples of the effects of *x*-boosts, *z*-boosts and combinations of them on the CPS wavevector pairs are plotted in Fig. 6.2.1 where the relative velocity is *3c/5*. Fig. 6.2.1b is identical to the pair of wavevectors shown in the preceding Fig. 6.1.6, and Fig. 6.2.1c is the same thing rotated by *90°*.

Also shown are the CPS coordinate grid planes as seen in the observer's frame at a particular instant of the observer's time. These are planes that are the group *phase=0 mod* π planes in the CPS frame and fixed to it, so they are moving rigidly in any boosted observer's frame opposite to the boost. They are obtained from the wavevector differences such as $(\mathbf{k}_{\rightarrow} - \mathbf{k}_{\leftarrow})$ by solving (6.2.7b) as repeated below.

$$\overline{\mathbf{k}} \bullet \mathbf{r} - \overline{\omega} t = \mathbf{k}_0 \bullet \mathbf{r}_0 = 0,\pm\pi,\pm 2\pi,... \qquad (6.2.9)$$

At the observer instant *t=0* one simply obtains a plane through origin and normal to $(\mathbf{k}_{\rightarrow} - \mathbf{k}_{\leftarrow})/2$.

This wave based solution is simpler than trying to use a Lorentz coordinate transformation to find observer coordinates *(ct, x, y, z)* in terms of CPS coordinates (ct_0, x_0, y_0, z_0). The latter would be easy if one desired observer values of CPS planes at a fixed CPS time t_0, but it is quite inconvenient if, as is the case, we desire their location as the observer sees them at his instant *t*.

The effect of doing $u_x/c=3/5$ and $u_z/c=3/5$ boosts singly and in sequence of different orders is shown in Fig. 6.2.1. A single boost induces an 80% Lorentz contraction $(1/\cosh \upsilon = 0.8)$ in the direction of the boost. Two Lorentz boosts also induce a rotation, in fact, rotation group R(3) is a subgroup of the Lorentz group. The spectroscopic equivalent of the rotation is called *Thomas precession*. This important effect will be discussed later.

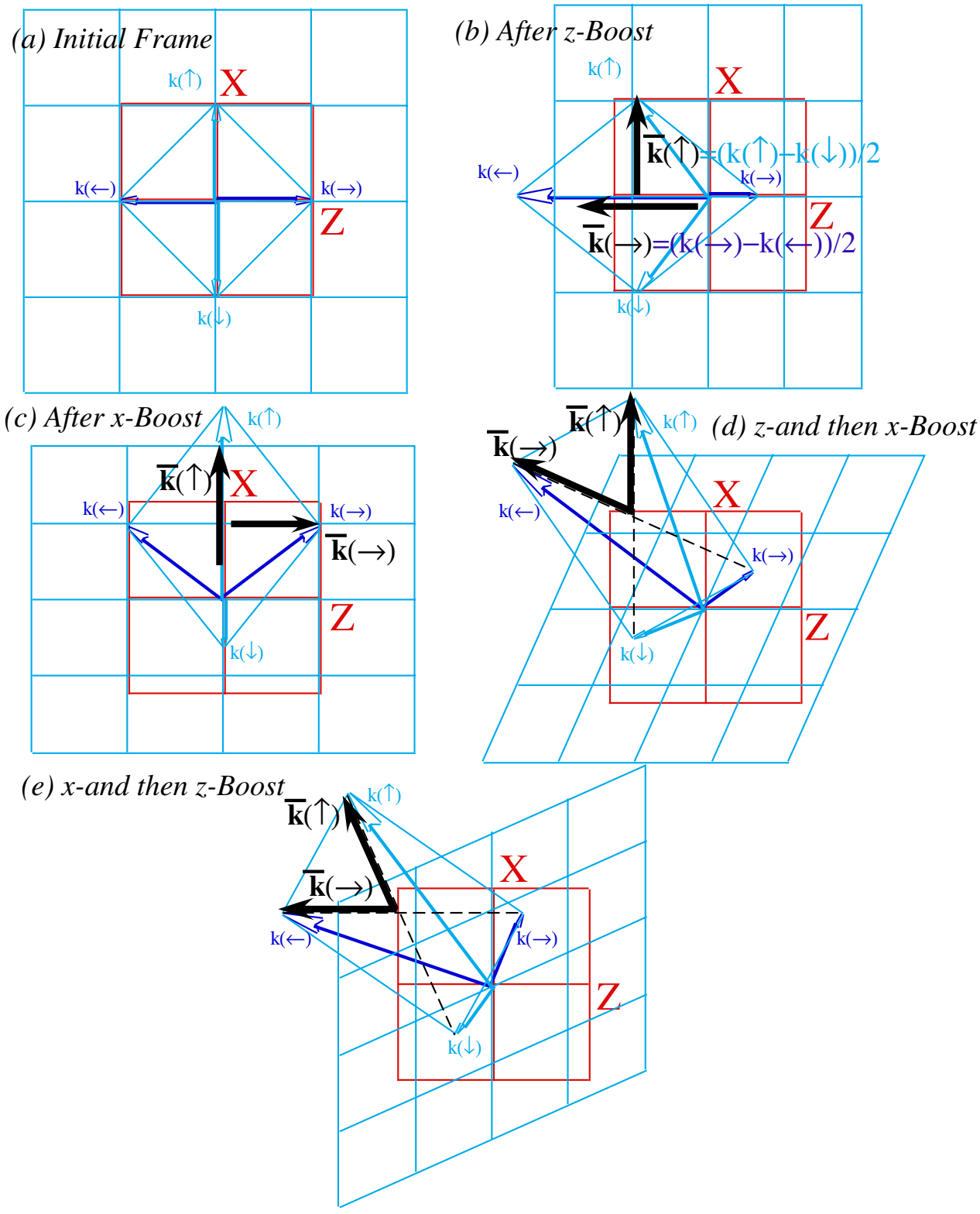

Fig. 6.2.1 Examples of sequential relativistic transformations of a tetrad of light wavevectors.

6.3. Wave Guide Dispersion and Cavity Eigenfrequencies

A wave guide confines 3-dimensional *(c***k**, *ω)* light waves to propagate in one dimension. The result is a dispersion function that is of the same form as (5.2.8) for quantum matter waves.

$$\omega^2=\mu^2-(ck)^2 \qquad (6.3.1)$$

Putting end plates on a guide further confines the wave to a cavity mode and restricts its frequency dispersion to discrete or "quantized" frequency eigenvalues ω_m. This is discussed below.

(a) 2-Dimensional wave mechanics: guided waves and dispersion

A two or three-dimensional wave will be seen to exceed the *c*-limit when it approaches an axis obliquely. It happens for plane waves. The phase velocities along coordinate axes are given by

$$v_x = \omega /k_x , \qquad v_y = \omega /k_y , \qquad v_z = \omega /k_z . \qquad (6.3.2)$$

Each of the components (k_x , k_y , k_z) must be less than or equal to magnitude *k*. Thus, all the component phase velocities equal or exceed the phase velocity ω /k which is *c* for light! In fact, water waves can exceed *c* ; if a wave breaks parallel to shore the 'break-line" moves infinitely fast since k_x is zero.

This has application to the basic wave mechanics of a wave guide consisting of a 'Hall of Mirrors" along the *x*-axis shown in Fig. 6.3.1. Let two parallel mirrors on either side of the *x*-axis be separated by a distance *y=W*. The South wall will be at *y=-W/2* and the North wall at *y=W/2*. (*z*-axis or "up" is into the page of Fig. 6.3.1.) The Hall should have a floor and ceiling at *z=±H/2*, but its position doesn't matter as long as we consider only waves moving in the *xy*-plane direction. The effect of *H* is discussed later.

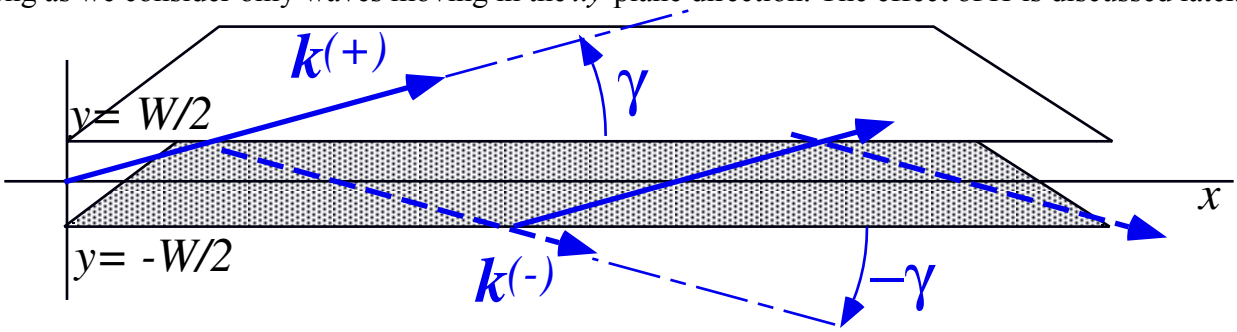

Fig. 6.3.1 A "hall of mirrors" model for an optical wave guide of width W.

Now consider what would happen if you shine a laser or maser down this hall. (In quantum jargon, "we propagate a photon beam.") Let the beam be at an angle γ to the *x*-axis in the plane of the Fig. 6.3.1. Two waves will result as indicated in Fig. 6.3.1; one you sent in with its **k**-vector $\mathbf{k}^{(+)}$ pointing at angle +γ

$$\mathbf{k}^{(+)} = (k^{(+)}_x, k^{(+)}_y, 0) = (k \cos \gamma , k \sin \gamma , 0)$$

and its *y*-reflected mirror image with its **k**-vector $\mathbf{k}^{(-)}$ pointing at angle -γ.

$$\mathbf{k}^{(-)} = (k^{(-)}_x, k^{(-)}_y, 0) = (k \cos \gamma , -k \sin \gamma , 0).$$

By adding the two waves with $\mathbf{k}^{(+)}$ and $\mathbf{k}^{(-)}$ you can make a wave function inside the Hall of Mirrors that vanishes at the mirror surface boundaries.

$$\Psi(\mathbf{r},t)= exp\, i(\mathbf{k}^{(+)}\bullet\mathbf{r} - \omega t) + exp\, i(\mathbf{k}^{(-)}\bullet\mathbf{r} - \omega t)$$
$$= exp\, i(k\, x \cos \gamma + k\, y \sin \gamma - \omega t) + exp\, i(k\, x \cos \gamma - k\, y \sin \gamma - \omega t)$$
$$= exp\, i(k\, x \cos \gamma - \omega t) [\, exp\, i(k\, y \sin \gamma) + exp\, i(- k\, y \sin \gamma)]$$

$$= e^{i(k\,x\cos\gamma\ -\ \omega\,t)}\,[\ 2\cos(\ k\,y\sin\gamma\ )\ ] \qquad (6.3.3)$$

The only requirement is that the wave function vanish on the mirror surfaces *(y=±W/2)* since we're assuming E-fields cannot penetrate these walls. This boundary condition is easily solved for the angle γ.

$$0=2\cos(\ k\,(W/2)\sin\gamma\ )\ ,\ \ or:\ k\,(W/2)\sin\gamma=\pi/2\ ,\ or:\ \sin\gamma=\pi/(\ k\,W) \qquad (6.3.4a)$$

The wavevector magnitude is related to angular frequency by the usual $k = \omega/c$. Stated another way we fix the *y*-component of the $\mathbf{k}^{(+)}$ or $\mathbf{k}^{(-)}$ vectors to just fit a half-wave in the width *W* of the Hall of Mirrors.

$$k^{(+)}_y = k\sin\gamma = \pi/W \qquad (6.3.4b)$$

These conditions lead to what is called a *dispersion function* $\omega(k_x)$ or ω *vs.* k_x *relation*.

$$\omega = kc = c(k_x^2 + k_y^2 + k_z^2\ )^{1/2} = c(k_x^2 + \pi^2/W^2\ )^{1/2} \qquad (6.3.5a)$$

$$\omega = \sqrt{(c^2k_x^2 + \omega_{cut}^2)}\ \ \text{where:}\qquad \omega_{cut} = \pi c/W. \qquad (6.3.5b)$$

The minimum or *cut-off frequency* $\omega_{cut} = \pi c/W$ is defined. Solving for k_x gives

$$k_x = (\omega^2/c^2 - \pi^2/W^2\ )^{1/2}. \qquad (6.3.5c)$$

This is the equation for a hyperbola in $(\omega,\ ck_x)$ space which plotted below in Fig. 6.3.2.

$$\omega^2 - c^2k_x^2 = \pi^2c^2/W^2 = \omega_{cut}^2 \qquad (6.3.5d)$$

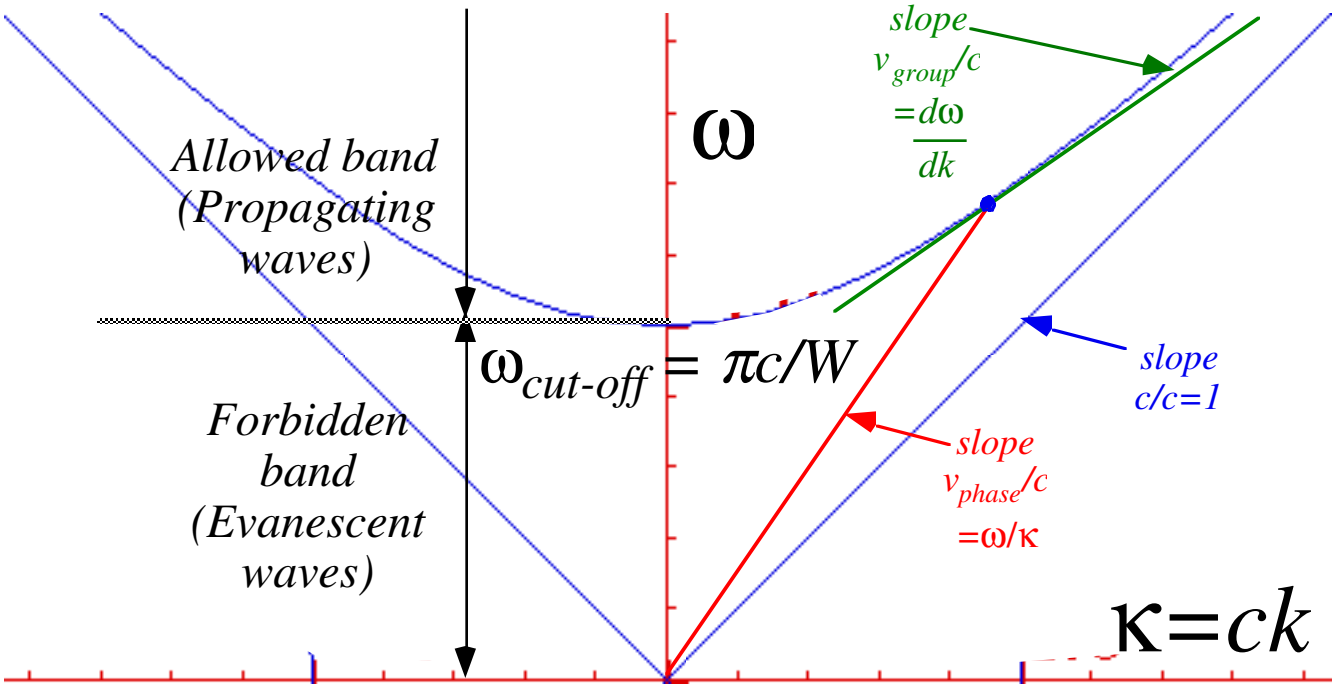

Fig. 6.3.2 Dispersion function for a fundamental TE wave guide mode

The hyperbolic asymptotes are lines of slope equal to the speed of light *c*. (6.3.5d) is a standard relativistic invariant function. All observers, no matter what their relative *x*-velocity, agree on how the light travels through space-time in a Hall of Mirrors. This holds only if the mirrors are "perfect" in that their performance does not depend on their *x*-velocity. You can't tell if a "perfect' mirror was sliding past you! But, if the mirrors' atomic response varies with velocity, as it will when photon frequencies are Doppler

shifted into X-ray values, then the dispersion function will cease to be a relativistic invariant. Polarization wave velocity in solids or liquids is rarely, if ever, invariant to the material velocity.

The dispersion relation $\omega(k_x)$ is used to calculate the Hall wave velocities. From the dispersion relation $\omega(k_x)$ in (6.3.6 a) we obtain the phase velocity from (4.4.7) and group velocity from (4.4.6b) for a mono-chromatic wave propagating down the Hall. (However, a group wave cannot be monochromatic!)

$$v_x\,(phase) = \omega/k_x = c\omega\,/(\omega^2 - \pi^2c^2/W^2)^{1/2} \quad (6.3.7\text{ a}) \qquad v_x\,(group) = d\omega/dk_x = ck_x/(k_x^{\,2} + \pi^2/W^2) = c\,(\omega^2 - \pi^2c^2/W^2)^{1/2}/\omega \quad (6.3.7\text{ b})$$

Using (4.34b) we get the speeds in terms of angle γ and vacuum light speed c.

$$v_x\,(phase) = c/\cos\gamma \quad (6.3.7\text{ c}) \qquad v_x\,(group) = c\cos\gamma \quad (6.3.7\text{ d})$$

As the wavelength is reduced (higher k and ω) $v_x\,(phase)$ and $v_x\,(group)$ approach c which is what light would do anyway if the Hall width W was huge. However, as wavelength grows (lower k and ω) the tipping angle γ grows from zero toward $90°$ in order to match a half wave perfectly to the Hall width W. Then $v_x\,(phase)$ approaches infinity while $v_x\,(group)$ slows to a crawl as the frequency approaches a minimum *cut-off* value $\omega_{cut} = \pi c/W$. This is the *proper frequency* μ of a guided photon, the smallest red-shifted frequency a moving observer could see if he Doppler shifts k_x to zero. The next figures, done by the program *GuideIt* show waves going down a hall at various frequencies.

(b). Rays and wavefronts: Phase and group velocity

Fig. 6.3.3 begins with light entering the Hall of Mirrors at $\gamma = \pm 45°$ to the x-axis. The rays of the $+45°$ wave are being traced as they appear to reflect off the North wall into the $-45°$ wave. Note that the wave amplitude (represented by wavy lines) is maximum in the center of the hallway $(y=0)$ as required by the amplitude factor $[\,2\cos(k\,y\sin\gamma)\,]$ in (6.3.3). The same factor makes the wave identically zero at the North and South walls $(y = \pm W/2)$ according to (6.3.4a).

The wave moves at a speed $v_x\,(phase) = c\sqrt{2}$ according to (6.3.7 c). But, the velocity $v_x\,(group) = c/\sqrt{2}$ is exactly half as fast. This is the velocity of the *rays*. Their progress down the x-axis of the hallway is slower than their actual speed c because they are ricocheting back and forth off the walls as seen in the figures below. This "off-the-wall" explanation of group velocity makes it clear why the group velocity is c times the cosine of the angle γ. It is the x-component of a tipped wave velocity vector. The rays are attached to *wave fronts* of constant phase. On the way up the wave front phase is $2n\pi$ (multiple of 2π) indicated by a thin solid line. The phase changes by π when a ray bounces off a wall, so downward rays are attached to a wave front having a phase of $(2n-1)\pi$, indicated by a thin dotted line. Where solid $(2n\pi)$ fronts meet is a wave *crest.* Where dotted $(n\pi)$ fronts meet is a wave *trough.* A *node* is where fronts of opposite phase meet such as along walls that have a line of nodes.

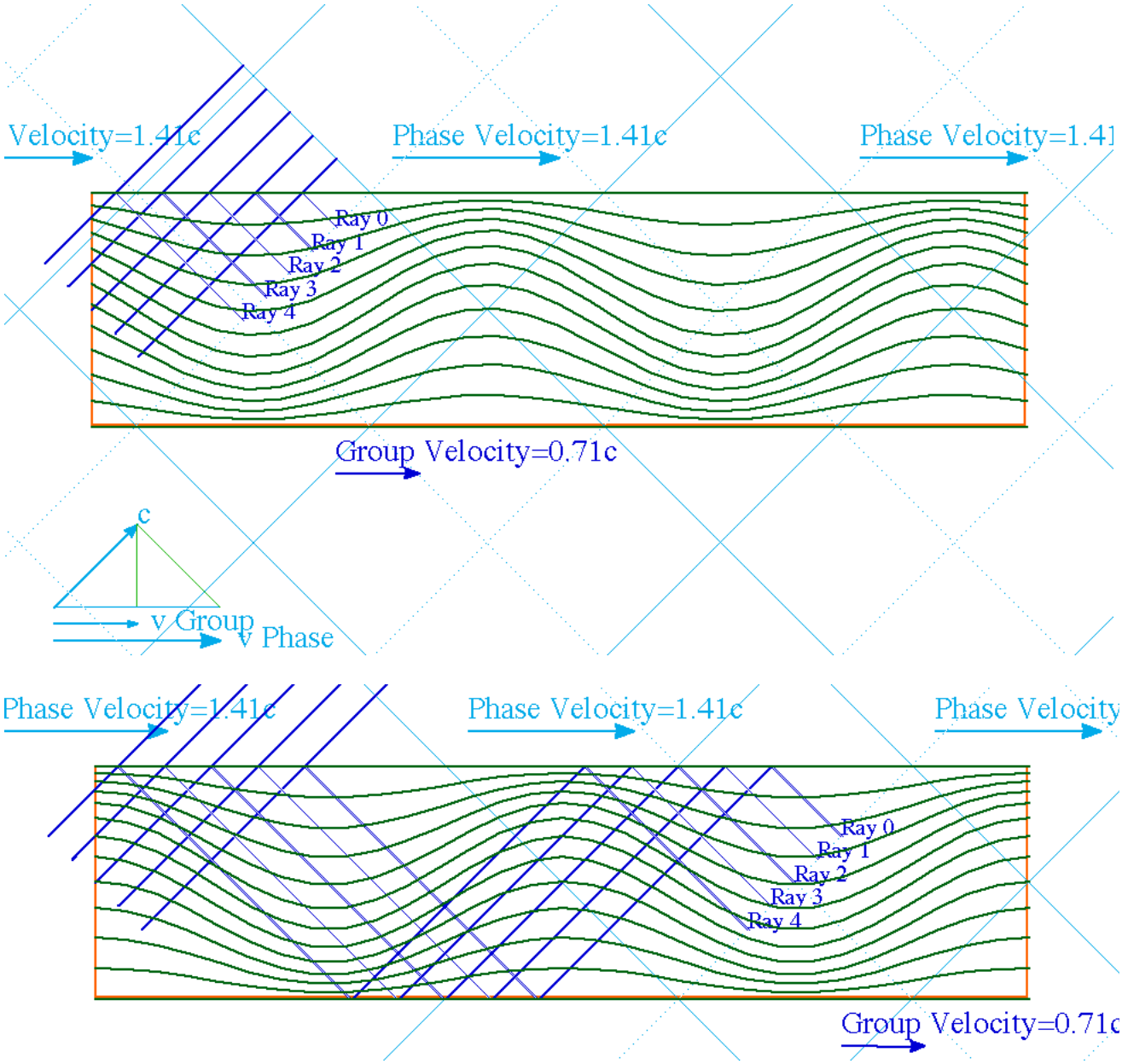

Fig. 6.3.3 Right moving guide wave with $\gamma = 45°$, $V_{phase}=\sqrt{2}c$, $V_{group}=c/\sqrt{2}$.

The *x*-phase velocity v_x *(phase)* is the speed of the *intersection* of wave fronts with the walls (nodes) or the *x*-axis (crests and troughs). In the sequence of frames below, note how much faster crests and troughs move than rays. The wave fronts go at velocity *c* along rays, that is, *perpendicular* to the fronts while rigid diamond-shaped wave patterns go at v_x *(phase)=1.41c* down the *x*-axis as shown in Fig. 6.3.4. Attached to the diamonds are nodal rectangles (actually *squares* in this example) whose borders lie along the top and bottom walls (as required by the *y*-boundary conditions (6.3.4a)) and whose vertical sides lie half-way between the crests and troughs. Unlike the diamonds, the nodal squares are observable borders of the interference minima and maxima. The phase diamonds represent unobservable "artistic license."

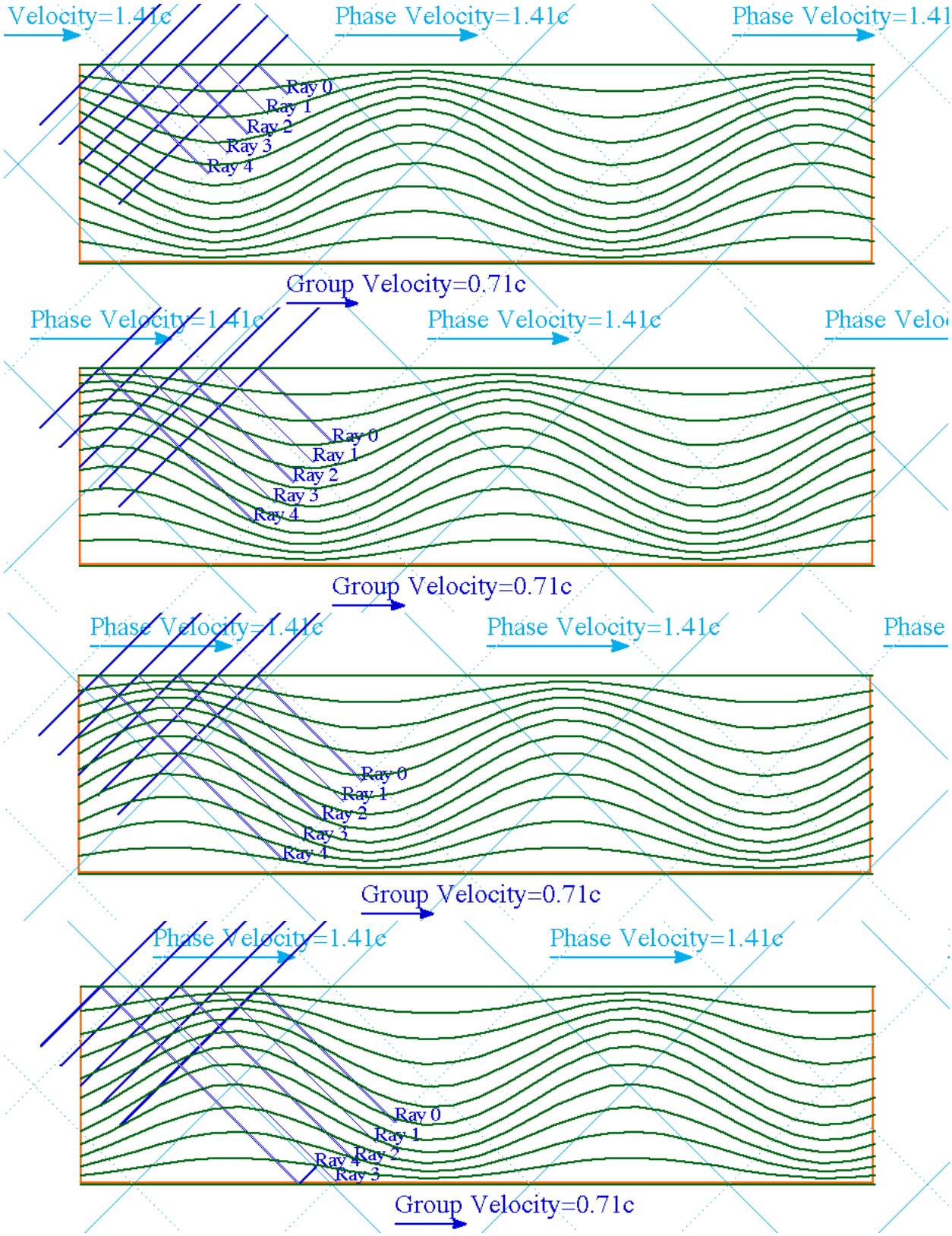

Fig. 6.3.4 Right moving guide wave with $\gamma = 45°$. Rays are half as fast as wave crests.

Higher frequency means a lower γ with two velocities are approaching *c* as shown in Fig. 6.3.5a where $\gamma = 30°$. As a Hall of mirrors gets much wider than the *~0.5 μm* optical wavelength you can simply look down it with no detectable dispersion. In this limit V_{phase} and v_x *(group)* both converge on *c*.

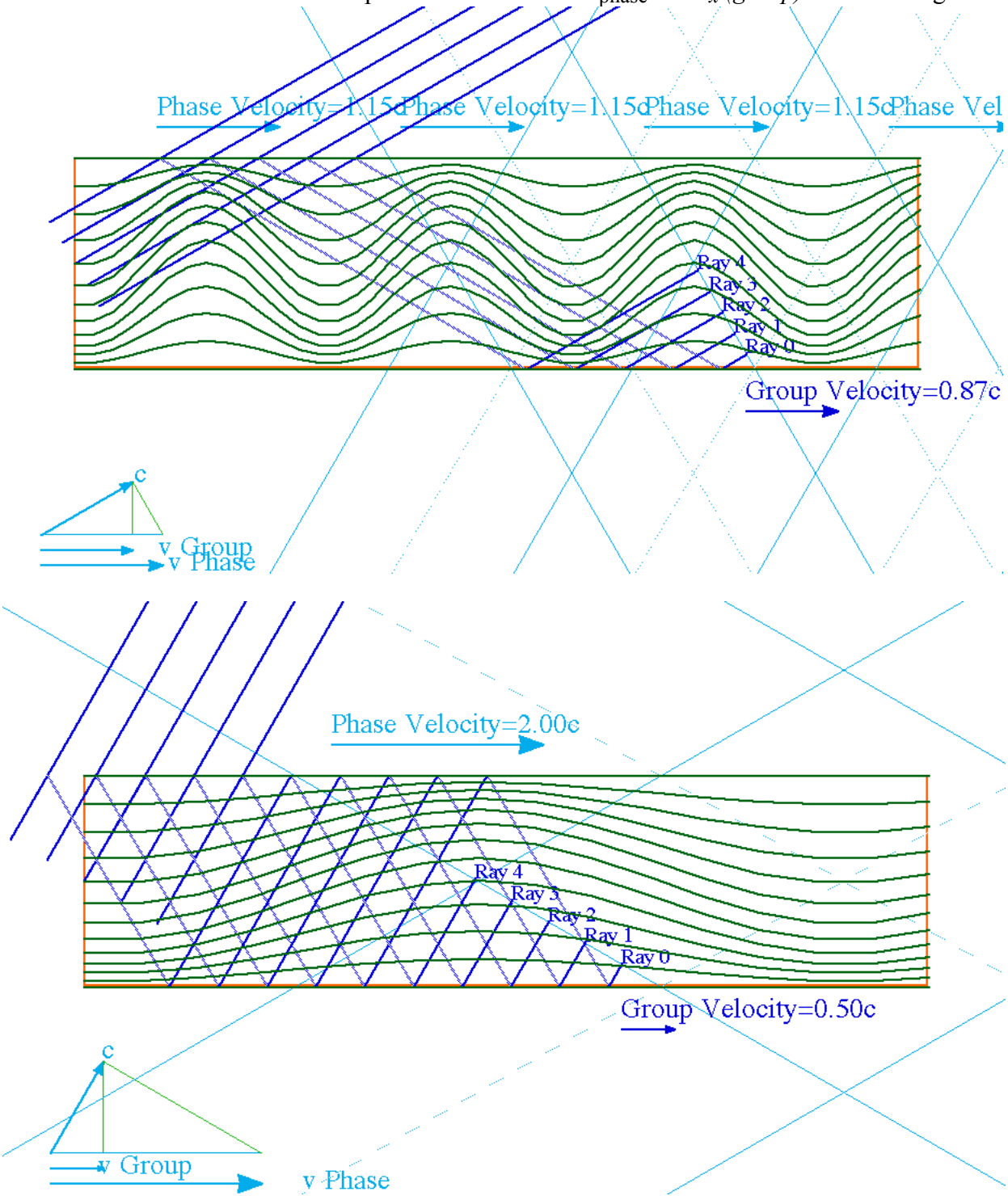

Fig. 6.3.5 Guide waves. *(a)Higher frequency case:* $\gamma = 30°$, $v_{x\,(phase)} = c\sqrt{3}/2c$, $v_{x\,(group)} = c2/\sqrt{3}$. *(b)Lower frequency case:* $\gamma = 60°$, $v_{x\,(phase)} = 2c$, $v_{x\,(group)} = c/2$.

Suppose the light frequency is reduced so the wavelength increases and the angle γ increases to *60°*. Then v_x *(phase)* grows to *2c* while the ray or group velocity reduces to v_x *(group)* = *c cos 60°=c/2*. That is one-half the speed of light and one-fourth v_x *(phase)* =*2c* as shown in Fig. 6.3.5b.

Group waves and "messages":(How do I send one?)

Group waves can carry "messages" as was discussed in Sec. 4.4, but this requires at least two different frequency components. The guide waves pictured so far are mono-chromatic and carry no information except a steady "hum" if they are classical waves, or a steady and uniform rain of random counts if we are describing a quantum wave. There is a $|cos(k\, y \sin \gamma)|^2$ distribution of intensity, but otherwise it's smooth, featureless and motionless. (Quantum mechanics can be really dead, sometimes!)

To send "messages" or "wave-packets" it is necessary to have more than one frequency going in. If the frequencies are close by then AM "lumps" (like Fig. 4.3.3) of increased photon counts will be observed moving down the hall at the velocity v_x *(group)* given by (6.3.7d). As usual, you need many counts to make out even one "lump." (Low-quantum phenomena are elusive, to say the least!)

(c). Evanescent waves

There is an important lower limit to frequency below which waves will not propagate. This happens just when the wave is too big in wavelength to fit even half of it in the wave guide. The limit is indicated in the Fig. 6.3.2 at the bottom of the hyperbolic dispersion function (6.3.5).

For an angular frequency below the so-called *cut-off value*

$$\omega_{cut} = \pi\ c / W \qquad (6.3.8)$$

the wave vector

$$k_x = (\omega^2 - \pi^2 c^2 / W^2\ )^{1/2}$$

goes to zero and then becomes imaginary. Instead of the usual *propagating* wave

$$\Psi = \ exp\ i(k_x\, x\ - \omega\, t) \qquad (6.3.9)$$

we get a so-called *evanescent* wave

$$\Psi = \ exp\ -(\mu_x\, x\,) exp\ i(-\ \omega\, t) \qquad (6.3.10a)$$

that decays exponentially with the distance x along the wave guide. Its decay rate constant is

$$\mu_x = (\pi^2 c^2 / W^2 - \omega^2\ )^{1/2} = ik_x\ , \qquad (6.3.10b)$$

and it gets greater as the frequency ω becomes smaller than ω_{cut} .

The cutoff ω_{cut} in (6.3.8) is the bottom of a band of allowed frequencies, and it is the bottom of the lowest of a series of bands for which the an integral number n_y >1 of half waves fit across the hall. A generalization of (6.3.4b) for n_y half waves is

$$k^{(+)}_y = k \sin \gamma = n_y\, \pi /W \qquad (n_y\ = 1, 2,...) \qquad (6.3.11a)$$

This leads to *multiple overlapping bands of dispersion function* $\omega_{n_y}(k_x)$.

$$\omega_{n_y}(k_x) = kc = c(k_x^2 + k_y^2 + k_z^2\ )^{1/2} = c(k_x^2 + n_y^2\, \pi^2 / W^2\ )^{1/2} \qquad (6.3.11b)$$

The lowest three of these overlapping hyperbolas (for n_y = 1, 2, and 3) are plotted in Fig. 6.3.6.

(d). Trapped waves and cavity modes: discrete frequencies

When a wave is completely trapped in all the directions it can move, then its spectrum ceases to be continuous and becomes discrete or "quantized." This is what happens to the wave guide modes if the Hall of Mirrors is capped by a pair of doors at, say, $x=0$ and $x=L$, so it becomes a *wave cavity* of length L.

The doors demand the wave electric field be zero at x-boundaries as well as along the walls. The new boundary condition to go with (6.3.11a) is the following.

$$k_x = k\cos\gamma = n_x \pi/L \qquad (n_x = 1, 2, ...) \qquad (6.3.12a)$$

Now the frequency bands become broken into discrete "quantized" values $\omega_{n_x n_y}$, one for each pair of integers or "quantum numbers" n_x and n_y.

$$\omega_{n_x n_y} = kc = c(k_x^2 + k_y^2 + k_z^2)^{1/2} = c(n_x^2\pi^2/L^2 + n_y^2\pi^2/W^2)^{1/2} \qquad (6.3.12b)$$

The frequency values fall where the n_y-hyperbola intersects the n_x-value of k_x in (6.3.12a) as shown in Fig. 6.3.6. These correspond to *cavity modes*. Note: no zero or negative n_x or n_y allowed.

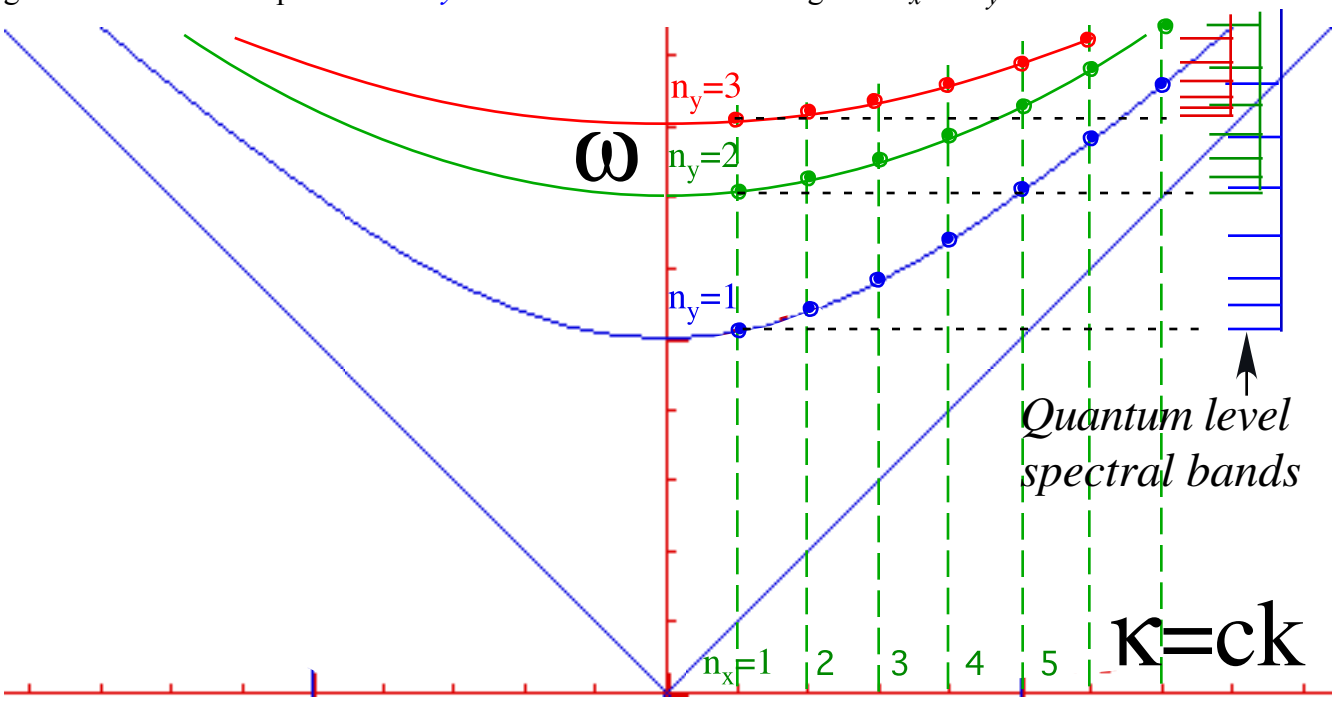

Fig. 6.3.6 Cavity mode dispersion diagram showing overlapping and discrete ω *and k values.*

Three of the lowest cavity modes for the fundamental ($n_y=1$) dispersion curve corresponding to the x-quantum numbers $n_x = 1, 2$, and 3 are plotted in Fig. 6.3.7 below. These are 2D standing waves. They can be thought of as interference patterns of four moving wave fronts, two oppositely moving pairs for each of the two wavefront lines intersecting at an antinode in each of the figures.

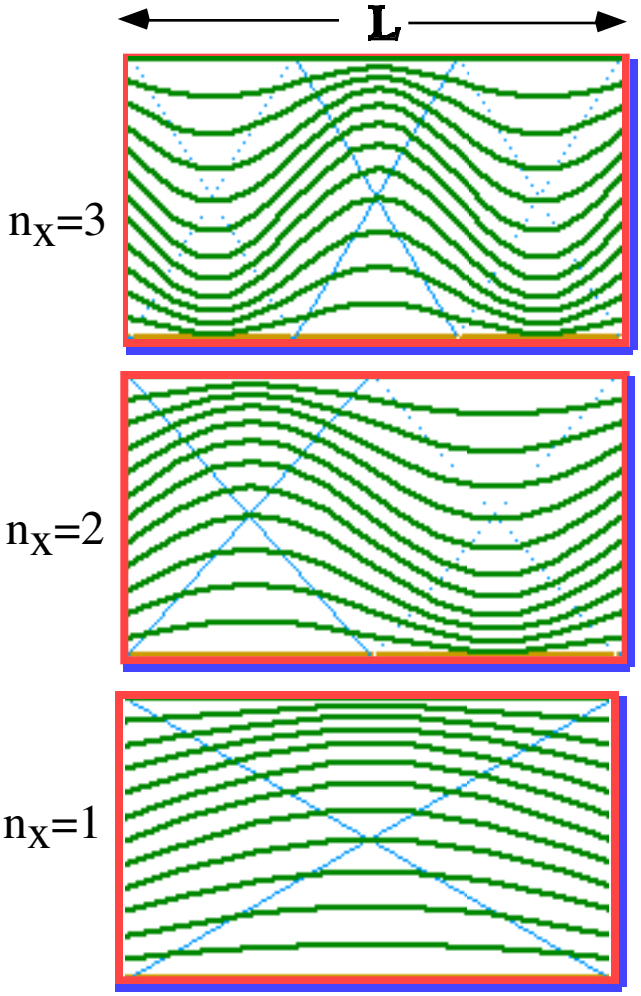

Fig. 6.3.7 Cavity modes for three lowest quantum numbers

It should be noted that the Hall of Mirrors used in the preceding section is a tall hall indeed. It has no floor and no ceiling! Clearly, this is an impractical wave guide with infinite wavelength in the out-of-the-page direction z. The hall needs a floor and a ceiling separated by height H with boundary conditions.

$$k_z = n_z\,\pi/H \quad (n_z = 1, 2,\ldots) \qquad (6.3.13a)$$

This gives new frequency bands corresponding to "quantized" values $\omega_{n_x\,n_y\,n_z}$.

$$\omega_{n_x\,n_y\,n_z} = kc = c(k_x^2 + k_y^2 + k_z^2)^{1/2} = c(n_x^2\pi^2/L^2 + n_y^2\pi^2/W^2 + n_z^2\pi^2/H^2)^{1/2} \qquad (6.3.13b)$$

Also, z-confinement has the effect of up-shifting the spectrum in (5.1.6) due to the addition of the extra term $n_z^2\pi^2/H^2$ in (6.3.13b). Since the lowest possible quantum number is $n_z = 1$, we cannot ever ignore it. However, for a tall hall *(H>>W or H>>L)* the resulting shift is small.

Problems for Chapter 6.

Happy Medium

6.1.1 (a) In counter propagating γ-rays of frequency ω_A and ω_B, what speed observer sees a single ω?
(b) In γ-rays of fixed $\mathbf{k}_A$ and $\mathbf{k}_B$, can observer of speed $\mathbf{u}$ see a single ω? If so, find $\mathbf{u}(\mathbf{k}_A, \mathbf{k}_B)$ and $\omega(\mathbf{k}_A, \mathbf{k}_B)$.

Twin Geeks

6.1.2 Two twins decide to split up with one staying in the lab to watch TV while the other goes down the street at velocity u for a day (lab coordinate time) and then spends the next day returning at the same speed.
(a) Plot the two paths on a space-proper-time graph for $u=c/2$. Indicate their difference in age on the graph.
(b) Compute their age difference for $u=c/2$ and $u=0.99c$ and $u=3x10^3$ m/s.
(c) Derive the stellar aberration angles σ for each of the three velocities above.

Transverslongitudinal

6.1.3 The CW speedometer in Fig. 6.1.3 and Fig. 6.1.6 allow ruler-compass Lorentz transformation of optical wave-**k**-vectors that lie along (longitudinal Doppler) and normal (transverse Doppler) to frame velocity **u**.
(a) Construct an accurate plot of both kinds of Doppler shifts for $u=4/5c$.
(b)What about a **k**-vector that starts out neither longitudinal ($0°$ or $180°$) nor transverse ($\pm 180°$)? Construct or plot the $u=4/5c$ transformed vectors from ones that were originally at $\pm 45°$ and $\pm 135°$.

Improper Frequency

6.1.4 Cosmic speedometers in Fig. 6.1.1 through Fig. 6.1.6 are based on light (photons) or other zero-rest-mass particles and CW lasers. Consider the corresponding plots for particles and matter waves?
(a) Consider a proper-frequency *vs.* ck_z plot for a mass-M matter wave of group velocity $\mathbf{u}=u_z\mathbf{e_z}$. Compare it to a proper-time *vs.* coordinate-z plot of a particle of velocity $\mathbf{u}=u_z\mathbf{e_z}$. Do both for $u_z=4/5c$.
(b). Plot a tetrad of length-$(|c\mathbf{k}|=1)$-matter-wave **k**-vectors of the same proper frequency $\mu=1$ in the xz-plane at $0°$, $90°$, $180°$, and $270°$. (Let $c=1$.) The plot them as viewed by an observer with velocity $u_z=4/5c$.

Warped speed

6.2.1 Fig. 6.1.6e show shows a Cartesian xz-plane grid will appear to warp when viewed by an observer who has been boosted by $3/5c$ in the x-direction and then by the same speed in his z-direction.
(a). Obtain the same plot using $4/5c$ speeds, instead.
(b).Does the lab frame see the observer's second boost go $4/5c$ in the lab z-direction? If not, how fast and what direction?

Add it up (Fast!)

6.2.2 Relativistic velocity addition for 1-dimensional travel is given by formulas (4.3.12). The velocity v'_z of something seen by an observer who is moving u_z in lab is added to u_z as follows to give that velocity v_z as seen by the lab.

$$v_z = (u_z + v'_z)/(1 + u_z v'_z/c^2)$$

(a). Explain and derive this from (4.3.12) and from the momentum transformation (5.2.10).
(b) Derive a 3-dimensional generalization which gives (v_x, v_y, v_z) in terms of (v'_x, v'_y, v'_z) and (u_x, u_y, u_z). (Hint: Recall the distinction between velocity dx/dt and derivative $dx/d\tau$ used in momentum (5.3.14b).)
.

Listening to a Hall of mirrors

6.3.1. Let the 'Hall of Mirrors' be 4m. wide and lined with polished gold. Suppose a 62.5 MHz radio wave is propagating down its positive x-axis. (Assume floorless hall of Fig. 6.3.1.)

(a) First compute the period_____, angular frequency_____, wavenumber_____, angular wave number_____, and wavelength_____ of this radio wave in a boundary-free vacuum. Use conventional notation and give standard mks units.

(b) Plot the dispersion function ω(k) for this Hall. Then compute the period_____, angular frequency_____, wavenumber_____, angular wave number_____, and wavelength_____ of the 62.5 MHz radio wave along the x-axis of the 'Hall' in the fundamental (lowest) TE mode. Indicate ω and k on your plot as in Fig. 6.3.1.

(c) Compute the phase velocity_____c_ and group velocity_____c_ of this wave in the aforementioned tunnel. Indicate these velocities by secant or tangent lines on your plot. How fast could a radio message go from x=0 to x=24m?_____sec.

Traveling in a Hall of Mirrors

6.3.2 Consider the space-time wave of problem 6.3.1.

(a) Sketch ray paths and plane wavecrest-wave trough lines that define the 62.5 MHz wave as well as some wavy curves representing the actual E-field value inside the Hall. Follow form of Figs.6.3.4 in for at least two full wavelengths at times t=0, then 1/4 , 1/2, and 3/4 period later, but also include a set of four phasors per wavelength to represent the complex wavefunction along the hall center (y=0).

(b) Give the frequency and wavelength for the wave seen by a ship going along the x-axis at velocity $v = {}^{4}/_{5}c$ and at $v = -{}^{4}/_{5}c$. Compute the phase and group velocities which the ship would see.

(c) Do the velocity addition formulas (4.3.12) give the right velocities (phase or group) obtained here?

(d) Can the ship go fast enough to see a guide wave Doppler red-shift to below its cutoff? Explain.

Hiding in a Hall of Mirrors

6.3.3 Consider the hall of problem 6.3.1.

(a) Suppose an intense radio (Raser?) of frequency 18.78 MHz is bombarding the end of this tunnel. How far into the tunnel would you have to go so the E-field is less than 5% of what it is at the end?_____ (TE fundamental only) Answer the same for the intensity ($\Psi^*\Psi$) instead of E-field?_____

(b) What if the Raser was tuned right at ω_{cutoff}?

Trapped in a Hall of Mirrors

6.3.4 Consider the hall of problem 6.3.1.

(a) Suppose gold doors at *x=0* and *x=24m*. enclose the Hall. Compute the frequency of the lowest TE wave that can resonate in this cavity._____Give complex wavefunction and sketch crest-trough lines and phasors for this wave.

(b) Compute the cut-off frequency below which radio will not propagate in the tunnel. Give both angular and regular frequency._____

Review Topics & Formulas for Unit 2

Expo-Cosine Identity on 2-Component Counter-propagating Minkowski / Cartesian (standing) wave

Apply: $\frac{e^{ia}+e^{ib}}{2}=e^{i\frac{a+b}{2}}\frac{e^{i\frac{a-b}{2}}+e^{-i\frac{a-b}{2}}}{2}=e^{i\frac{a+b}{2}}\cos\frac{a-b}{2}$ to: $\Psi=\frac{e^{i(k_\rightarrow x-\omega_\rightarrow t)}+e^{i(k_\leftarrow x-\omega_\leftarrow t)}}{2}$

$\Psi_{Minkowski}(x,t)=e^{i\frac{(k_\rightarrow+k_\leftarrow)x-(\omega_\rightarrow+\omega_\leftarrow)t}{2}}\cos\frac{(k_\rightarrow-k_\leftarrow)x-(\omega_\rightarrow-\omega_\leftarrow)t}{2}=e^{-i\omega_0t'}\cos k_0x'=\Psi_{Cartesian}(x',t')$

Blue shifted: $\omega_\rightarrow=f\,\omega_0$, $k_\rightarrow=f\,k_0$, *Red shifted:* $\omega_\leftarrow=(1/f)\omega_0$, $k_\leftarrow=-(1/f)k_0$,

$\Psi_{Minkowski}(x,t)=e^{i\frac{(f-1/f)k_0x-(f+1/f)\omega_0t}{2}}\cos\frac{(f+1/f)k_0x-(f-1/f)\omega_0t}{2}=e^{-i\omega_0t'}\cos k_0x')=\Psi_{Cartesian}(x',t')$

Minkowski Wave velocities and Doppler f- factor using relativity postulate: $c=\omega_0/k_0=\omega_\rightarrow/k_\rightarrow=-\omega_\leftarrow/k_\leftarrow$

$$V_{phase}=\frac{\omega_\rightarrow+\omega_\leftarrow}{k_\rightarrow+k_\leftarrow}=\frac{f+1/f}{f-1/f}\frac{\omega_0}{k_0}\quad V_{group}=u=\frac{\omega_\rightarrow-\omega_\leftarrow}{k_\rightarrow-k_\leftarrow}=\frac{f-1/f}{f+1/f}\frac{\omega_0}{k_0}=\frac{f^2-1}{f^2+1}c$$

Let: $\beta=u/c$ solve for:

$$f=\sqrt{\frac{1+\beta}{1-\beta}},\quad 1/f=\sqrt{\frac{1-\beta}{1+\beta}},\quad f+1/f=\frac{1+\beta+1-\beta}{\sqrt{1-\beta^2}},\ \text{and}\ f-1/f=\frac{1+\beta-1+\beta}{\sqrt{1-\beta^2}},$$
$$=\frac{2}{\sqrt{1-\beta^2}},\qquad =\frac{2\beta}{\sqrt{1-\beta^2}}.$$

$$\Psi_{Minkowski}(x,t)=e^{i\left\{\frac{\beta k_0x}{\sqrt{1-\beta^2}}-\frac{\omega_0t}{\sqrt{1-\beta^2}}\right\}}\cos\left[\frac{k_0x}{\sqrt{1-\beta^2}}-\frac{\beta\omega_0t}{\sqrt{1-\beta^2}}\right]=e^{-i\omega_0t'}\cos k_0x'=\Psi_{Cartesian}(x',t')$$

Equating Standing and Minkowskii wave phases gives Lorentz transformation:

$$\left[\frac{k_0x}{\sqrt{1-\beta^2}}-\frac{\beta\omega_0t}{\sqrt{1-\beta^2}}\right]=k_0x'\quad \textit{(cosines' phases)}\qquad x'=\frac{x-\beta ct}{\sqrt{1-\beta^2}}=x\cosh\theta-ct\sinh\theta$$

$$\left\{\frac{\beta k_0x}{\sqrt{1-\beta^2}}-\frac{\omega_0t}{\sqrt{1-\beta^2}}\right\}=-\omega_0t'=-k_0ct'\quad (e^{i\{\ \}}\ \textit{phases})\qquad ct'=\frac{-\beta x+ct}{\sqrt{1-\beta^2}}=-x\sinh\theta+ct\cosh\theta$$

Einstein dilation factor: $\Delta=1/\sqrt{1-\beta^2}=\cosh\theta=1/$*contraction factor:* $\sqrt{1-\beta^2}=\operatorname{sech}\theta$. *Doppler factor:* $f=e^{\theta}$.

Space-time (x,ct) invariants: $(x+ct)(x-ct)=(x)^2-(ct)^2=(x'+ct')(x'-ct')=(x')^2-(ct')^2$
$(c^2\tau_A\tau_B)=(ct_A)(ct_B)-x_Ax_B=(ct'_A)(ct'_B)-x'_Ax'_B$
$(c\tau)^2=(ct)^2-x^2=(ct')^2-x'^2$

Wavevector-frequency (ck,ω) invariants: $(ck+\omega)(ck-\omega)=(ck)^2-(\omega)^2=(ck'+\omega')(ck'-\omega')=(ck')^2-(\omega')^2$
$(\mu_A\mu_B)=(\omega_A)(\omega_B)-ck_Ack_B=(\omega'_A)(\omega'_B)-ck'_Ack'_B$
$(\mu)^2=(\omega)^2-k^2=(\omega')^2-k'^2$

Mixed (x,ct)-(ck,ω) invariant: Proper phase $= \Phi = kx - \omega t = k'x' - \omega' t'$ or: $c\Phi = ckx - \omega ct = ck'x' - \omega' ct'$

Requires Wavevector-frequency (ck,ω) Lorentz transformation:

$$ck' = \frac{ck - \beta\omega}{\sqrt{1-\beta^2}} = ck\cosh\theta - \omega\sinh\theta$$

$$\omega' = \frac{-\beta ck + \omega}{\sqrt{1-\beta^2}} = -ck\sinh\theta + \omega\cosh\theta$$

Planck Axiom

$$E = \hbar\omega$$

deBroglie Theorem

$$\mathbf{p} = \hbar\mathbf{k}$$

Bohr Quantum Radius r_{Bohr}

$$= a = \frac{4\pi\varepsilon_0}{me^2} = 0.528\text{Å}$$

Dirac Diameter $2r_{Dirac} =$

$$\lambda\!\!\!^{-}_{Compton} = \frac{\hbar}{mc} = 3.68\cdot 10^{-13}$$

Relativisitic Dispersion

$$\hbar\omega = \sqrt{\left(mc^2\right)^2 + c^2(\hbar k)^2}$$

$$= mc^2 + \frac{1}{2m}(\hbar k)^2 + \ldots$$

Classical Radius $r_{Einstein} =$

$$\frac{e^2}{4\pi\varepsilon_0 mc^2} = 2.818\cdot 10^{-15}_{(m.)}$$

Electron Wavelength λ_e

$$\lambda_e(E\quad) = h / \sqrt{2meE(in\ eV)}$$

$$= 1.23nm / \sqrt{E(in\ eV)}$$

Group Velocity: $V_{group} =$

$$\frac{d\omega}{dk} = \frac{c^2(\hbar k)}{\sqrt{\left(mc^2\right)^2 + c^2(\hbar k)^2}}$$

$$= \frac{c^2\hbar k}{\hbar\omega} = \frac{c^2 p}{E} = u = \frac{c^2}{V_{phase}}$$

Fine Structure Constant

$$\alpha = \frac{e^2}{4\pi\varepsilon_0\hbar c} = \frac{1}{137.036}$$

$$= \frac{r_{Einstein}}{\lambda\!\!\!^{-}_{Compton}} = \frac{\lambda\!\!\!^{-}_{Compton}}{r_{Bohr}}$$

Photon Wavelength λ_γ

$$\lambda_\gamma(E\quad) = h / emcE(in\ eV)$$

$$= 1.24\mu m / E(in\ eV)$$